UNI
BASEL

Towards the Optimization of Tumor Targeting Radiolabeled Peptides for Molecular Imaging and Therapy

Inauguraldissertation

zur
Erlangung der Würde eines Doktors der Philosophie

vorgelegt der
Philosophisch-Naturwissenschaftlichen Fakultät
der Universität Basel

von

Christiane Anke Fischer (geb. Kluba)

aus Deutschland

Basel, 2014

Genehmigt von der Philosophisch-Naturwissenschaftlichen Fakultät

auf Antrag von

Prof. Dr. Edwin C. Constable

Prof. Dr. Thomas L. Mindt

Prof. Dr. Roger Schibli

Basel, den 24.06.2014

                                        Prof. Dr. Jörg Schibler (Dekan)

This PhD-Thesis was conducted under the supervision of Prof. Dr. Thomas L. Mindt from December 2009 until July 2014 at the University Hospital Basel, Clinic of Radiology and Nuclear Medicine, Division of Radiopharmaceutical Chemistry, Basel, Switzerland.

Parts of this thesis have been published, presented, and awarded at national and international congresses.

This Ph.D. thesis is based on the following publications:

Peer-reviewed publications:

Fischer C. A., Vomstein S., Mindt T. L.; A Bombesin-Shepherdin Radioconjugate Designed for Combined Extra- and Intracellular Targeting; *Pharmaceuticals*, **2014**, 7, 662-675.

Cordier D., Gerber A., Kluba C., Bauman A., Hutter G., Mindt T. L., Mariani L.; Expression of Different Neurokinin-1 Receptor (NK$_1$R) Isoforms in Glioblastoma Multiforme: Potential Implications for Targeted Therapy; *Cancer Biother. Radio.,* **2014**, 29, 221-226.

Kluba C. A. and Mindt T. L.; Click-to-Chelate: Development of Technetium and Rhenium-Tricarbonyl Labeled Radiopharmaceuticals; *Molecules*, **2013**, 18, 3206-3226.

Valverde I., Bauman A., Kluba C. A., Vomstein S., Walter M. A., Mindt T., L.; 1,2,3-Triazoles as Amide Bond Mimics: Triazole Scan Yields Protease-Resistant Peptidomimetics for Tumor Targeting; *Angew. Chem. Int. Ed.*, **2013**, 52, 8957-8960.

Kluba C. A., Bauman A., Valverde I., Vomstein S., Mindt T. L.; Dual-targeting conjugates designed to improve the efficacy of radiolabeled peptides; *Org. Biomol. Chem.,* **2012**, 10, 7594-7602.

Published abstracts:

Kluba C. A., Vomstein S., Zimmermann M., Valverde I., Bauman A., Mindt T. L.; Dual Targeting bombesin-shepherdin radioconjugate for targeting extracellular GRP-receptor and intracellular Hsp90; *Eur. J. Nucl. Med. Mol. Imaging*, **2013**, 40, S293-S294.

Valverde I., Bauman A., Kluba C. A., Vomstein S., Mindt T., L.; 1,2,3-Triazole Backbone-Modified Peptidomimetics for Improved Tumor Targeting; *Eur. J. Nucl. Med. Mol. Imaging*, **2013**, 40, S294.

Valverde I. E., Bauman A., Kluba C., Mascarin A., Vomstein S., Walter M., Mindt T. L.; Click-Peptides: Novel 1,2,3-Triazole Backbone-Modified Peptidomimetics for Tumor Targeting; *J. Pept. Sci.*, **2012**, 18, S117.

Kluba C. A., Bauman A., Valverde I. E., Vomstein S., Mindt T. L; Dual-Targeting Conjugates Designed to Improve the Efficacy of Radiolabeled Peptides; *Eur. J. Nucl. Med. Mol. Imaging*, **2012**, 39, S380.

Valverde I. E., Bauman A., Kluba C., Mindt T. L.; Click-Peptides: A novel Strategy for the Design of Stabilized Radiopeptides for Tumor Targeting; *J. Labelled Compd. Rad.*, **2011**, 54, S63.

Congresses: oral presentations

"Variation of cellular uptake of ^{177}Lu-DOTA-[Thi^8,Met(O$_2$)^{11}]-Substance P in different glioblastoma cell lines"; C. A. Fischer, D. Cordier, A. Bauman, L. Mariani, T. L. Mindt; *Swiss Congress of Radiology (SGNM)*, **2014**, Montreux, Switzerland

"Click Peptides: A Novel Strategy for the Design of Stabilized Radiolabeled Peptides for Tumor Imaging", I. E. Valverde, A. Bauman, C. Kluba, A. Mascarin, S. Vomstein, M. Walter, T. L. Mindt *18th French Peptide Symposium* **2013**, Lazaret, Séte, France

"Click-Peptides: Novel 1,2,3-Triazole Backbone-Modified Peptides for Tumor Targeting", I. E. Valverde, A. Bauman, C. Kluba, A. Mascarin, S. Vomstein, M. Walter, Thomas. L. Mindt, *Fall Meeting of the Swiss Chemical Society (SCG)* **2012**, Zurich, Switzerland

"Click-peptides - Design of Novel Stabilized Radiopeptides for Tumour Targeting", I. E. Valverde, A. Bauman, C. Kluba, M. Walter, T. L. Mindt *16th European Symposium on Radiopharmacy and Radiopharmaceuticals* **2012**, Nantes, France

"Click-Peptides: A novel Strategy for the Design of Stabilized Radiopeptides for Tumor Targeting", I. E. Valverde, A. Bauman, C. Kluba, T. L. Mindt, *19th International Symposium on Radiopharmaceutical Sciences* **2011**, Amsterdam, The Netherlands

"Optimierung von Radiopeptiden durch den Einsatz von Trifunktionellen Konjugaten", C. A. Kluba, T. L. Mindt, *19. Arbeitstagung der Arbeitsgemeinschaft Radiochemie/-Radiopharmazie (AGRR) der Deutschen Gesellschaft Nuklearmedizin (DGN)*, **2011**, Ochsenfurt, Germany

"Towards the Optimization of Peptidic Radiopharmaceuticals"; C. A. Kluba, T. L. Mindt, *3-Ländertreffen Nuklearmedizin*, **2011**, Bregenz, Austria

Congresses: poster presentations

"Bifunctional Bombesin-Shepherdin Radioconjugate for Targeting Extracellular GRP-receptor and Intracellular Hsp90"; C. A. Fischer, S. Vomstein, T. L. Mindt; *Annual Research Meeting, Department of Pharmaceutical Sciences*, **2014**, University of Basel, Basel, Switzerland

"Dual-targeting bombesin-shepherdin radioconjugate for targeting extracellular GRP-receptor and intracellular Hsp90"; C. A. Kluba, S. Vomstein, M. Zimmermann, I. Valverde, A. Bauman, T. L. Mindt; *Annual Congress of the European Association of Nuclear Medicine* **2013** (poster walk), Lyon, France

"1,2,3-Triazole Backbone-Modified Peptidomimetics for Improved Tumor Targeting", I. E. Valverde, A. Bauman, C. A. Kluba, S. Vomstein, T. L. Mindt; *Annual Congress of the European Association of Nuclear Medicine* (poster walk) **2013** Lyon, France

"Novel dual-targeting BBS-TPP radioconjugate for tumor imaging"; C. A. Kluba; A. Bauman, I. Valverde, S. Vomstein, T. L. Mindt, *Basler Chemistry Symposium, Ph.D. Chemistry Community* **2013**, University of Basel, Basel, Switzerland

"1,2,3-Triazole Backbone-Modified Peptides for Tumor Targeting", I. E. Valverde, T. L. Mindt, *20th International Symposium on Radiopharmaceutical Sciences* **2013**, Jeju, Korea

"Novel dual-targeting BBS-TPP radioconjugate for tumor imaging"; C. A. Kluba; A. Bauman, I. Valverde, S. Vomstein, T. L. Mindt, *Annual Research Meeting, Department of Pharmaceutical Sciences*, **2013**, University of Basel, Basel, Switzerland

"Dual-Targeting Conjugates Designed to Improve the Efficacy of Radiolabeled Peptides"; C. A. Kluba, A. Bauman, I. E. Valverde, S. Vomstein, T. L. Mindt, *Annual Congress of the European Association of Nuclear Medicine* **2012** (poster walk), Milano, Italy

"Click-Stabilized Peptidomimetics for Tumour Targeting", I. E. Valverde, A. Bauman, C. Kluba, A. Mascarin, S. Vomstein, M. Walter, T. L. Mindt, *World Molecular Imaging Congress* **2012**, Dublin, Ireland

"Dual-Targeting Conjugates Designed to Improve the Efficacy of Radiolabeled Peptides"; C. A. Kluba, A. Bauman, I. E. Valverde, S. Vomstein, T. L. Mindt, *Fall Meeting of the Swiss Chemical Society (SCG)* **2012**, ETH Zurich, Zurich, Switzerland

"Click-Peptides: Novel 1,2,3-Triazole Backbone-Modified Peptidomimetics for Tumor Targeting", I. E. Valverde, A. Bauman, C. Kluba, T. L. Mindt, *32nd European Peptide Symposium* **2012**, Athens, Greece

Awards:

SCS-DSM Prize for best poster presentations (Medicinal Chemistry): "Dual-Targeting Conjugates Designed to Improve the Efficacy of Radiolabeled Peptides"; C. A. Kluba, A. Bauman, I. E. Valverde, S. Vomstein, T. L. Mindt, *Fall Meeting of the Swiss Chemical Society (SCG)* **2012**, ETH Zurich, Zurich, Switzerland

Young talent price for the best scientific presentation: "Optimierung von Radiopeptiden durch den Einsatz von Trifunktionellen Konjugaten", C. A. Kluba, T. L. Mindt, *19. Arbeitstagung der Arbeitsgemeinschaft Radiochemie/-Radiopharmazie (AGRR) der Deutschen Gesellschaft Nuklearmedizin (DGN)*, **2011**, Ochsenfurt, Germany

Three travel awards from the Swiss Society of Radiopharmacy/Radiopharmaceutical Chemistry (SGRRC):
Annual Congress of the European Association of Nuclear Medicine **2013**, Lyon, France
Annual Congress of the European Association of Nuclear Medicine **2012**, Milano, Italy
3-Ländertreffen Nuklearmedizin, **2011**, Bregenz, Austria

IV

Contents

V

Summary

Radiopharmaceuticals based on regulatory peptides have become an indispensable tool in nuclear medicine for the diagnosis (molecular imaging) and radionuclide therapy of cancer. The specificity of these radiopeptides towards G-protein-coupled receptors (GPCR), which are overexpressed by various cancer cells and their favorable pharmacological properties make them ideal vectors for the targeted delivery of radioactivity to tumors and metastases. However, there are still challenges to be met in order to develop peptide-based radiopharmaceuticals with ideal properties in terms of imaging quality and therapeutic efficacy where therapeutic radionuclides are employed.

A potential drawback of several radiolabeled peptides under investigation is represented by a rapid washout of radioactivity after receptor-mediated internalization into tumor cells. In certain cases, the washout of radioactivity from cells occurs at a rate comparable to that required for accumulation in cancerous tissues. This not only renders the initial efforts of targeted delivery in part futile but also results in an imaging quality and therapeutic efficiency lower than achievable. To address this issue, novel strategies are needed to improve the cellular retention of the radioactivity. A possible approach may include the employment of multi-targeting radioconjugates made of different moieties specific for extra- and intracellular targets. Towards this goal, we investigated the combination of tumor targeting peptides with an additional moiety specific for an intracellular target and radiolabeled the conjugate with the ^{99m}Tc-tricarbonyl core as a reporter probe for single-photon emission computed tomography (SPECT). We envisioned that enabling interactions of radioconjugates with intracellular targets after receptor-mediated uptake by endocytosis would result in the trapping of radioactivity in tumors.

Specifically, we combined a modified binding sequence of the peptide bombesin, [Nle^{14}]BBS(7-14), for extracellular targeting of the tumor-associated gastrin releasing peptide receptor (GRP-r) with a triphenylphosphonium group for intracellular targeting of the organelle mitochondria or with the peptide shepherdin, an inhibitor of the cytosolic chaperon heat-shock protein 90 (Hsp90). The conjugates were assembled by the "Click-to-Chelate" approach, an efficient synthetic strategy for the preparation of bifunctional ^{99m}Tc-labeled radiopharmaceuticals. The radioconjugates were evaluated *in vitro* using GRP-r-overexpressing PC-3 cells. Our investigations revealed that the additional moiety for intracellular targeting did not impact the tumor-targeting capability of the bombesin-derived conjugates but neither did it result in an improved cellular retention of the radioactivity. Drawing from our experience and considering recent literature data, we conclude that endosomal entrapment or lysosomal degradation of the bifunctional radiopeptide conjugates is likely to impede with intracellular interactions and thus, responsible for the observed unaltered cellular efflux of radioactivity. Future studies will be directed towards the combination of bifunctional radiopeptide conjugates with drug delivery systems designed to facilitate endosomal escape.

A different approach for the optimization of peptidic radiotracers includes the improvement of their metabolic stability since most of them exhibit a very short biological half-life due to rapid degradation by endogenous peptidases. Enhancement of the stability of radiopeptides results in a prolonged circulation time in the blood and, as a consequence, an improved tumor uptake *in vivo*. A number of different strategies have been reported for the stabilization of regulatory peptides, however, with varying degree of success in providing peptidomimetics with retained affinity to the corresponding GPCR. In an effort to probe a novel peptide backbone modification methodology, the use of 1,4-disubstituted 1,2,3-triazoles as metabolically stable *trans* amide bond isosters was investigated. The systematic replacement of amide bonds within the binding sequence of the tumor-affine peptide bombesin, [Nle^{14}]BBS(7-14), by triazoles provided a series of ^{177}Lu-labeled peptidomimetics with both retained affinity towards GRP-r and an increased stability in blood serum. *In vivo* evaluation of a

lead compound in xenografted mice showed that the enhanced stability of the radiopeptidomimetic resulted in a doubling of the uptake of radioactivity in tumors. The described amide-to-triazole substitution methodology is currently being applied to other tumor targeting peptides of medicinal interest.

The specificity and affinity of radiopeptides towards different receptor subtypes is another aspect to consider for optimizations. Inhomogeneous expression of receptor subtypes by tumors may influence the efficiency of a radiotracer. For example, intratumoral administration of radiolabeled substance P (SP) led to significant differences in the clinical response of patients suffering from gliomas despite proven expression of its target, the neurokinin-1 receptor (NK_1R). In an effort to identify factors that may be responsible for the varying therapeutic outcome observed, several SP conjugates were evaluated *in vitro* using four established glioma cell lines differing in their level of RNA expression of the full length and truncated receptor isoforms. Cell binding and internalization of SP-conjugates were only observed with cell lines exhibiting high expression of RNA of the full-length NK_1R. Pre-therapeutic screening for NK_1R isoforms may therefore be advisable for the selection of glioma patients for NK_1R-targeted radionuclide therapy.

Abbreviations

°C	degree Celsius
μ	micro-
^{18}F-FDG	2'-[^{18}F]fluoro-2'-deoxyglucose
5-Ava	5-aminovaleric acid
5-HT	5-hydroxytryptamine (serotonin)
Å	angstrom(s)
AA	amino acid
Ac	acetyl
AC	adenylate cyclase
Ala (A)	alanine
Ala(SO$_3$H)	L-cysteic acid
aq	aqueous
AR	androgen receptor
Arg (R)	arginine
Asn (N)	asparagine
ATPase	adenosine triphosphatase
AZT	azido thymidine
BBS, BBS	bombesin
BFCA	bifunctional chelating agent
Bn	benzyl
Boc	*tert*-butoxycarbonyl
BPAMD	(4-{[bis-(phosphonomethyl))-carbamoyl]methyl}-7,10 bis-(carboxymehtyl)-1,4,7,10-tetra-azacyclododec-1-yl)acetic acid
Bq	bequerel
BSA	bovine serum albumin
bzlg	benzylaminodiglycolic acid
c	centi-; cyclic
calcd	calculated
cAMP	3',5'-cyclic adenosine monophosphate
CB-TE2A	1,4,8,11-tetraazabicyclo[6.6.2]-hexadecane-4,11-diyl-diacetic acid
CCK	cholecystokinin
CCP	clathrin-coated pits
CCV	clathrin-coated vesicles
cGMP	3',5'-cyclic guanosine monophosphate
Cha	cyclohexylalanine
CNS	central nervous system
Cp	cyclopentadienyl
CT	computed tomography
CuAAC	Cu(I)-catalyzed azide-alkyne cycloaddition
Cys (C)	cystein
d	day; doublet; deci-
DADS	diamidedithiols
DADT	diaminedithiols
DAMA	diamidemonoamine-thiols
dd	doublet of doublets
DFO	desferrioxamine B

DFT	density functional theory
DG	diacetylglycerol
DIPEA	*N,N*-Diisopropylethylamine
DMEM	Dulbecco's Modified Eagle's Medium
DMF	*N,N*-dimethylformamide
DNA	deoxyribonucleic acid
DOTA	1,4,7,10,-tetraazacyclododecane-1,4,7,10-tetraacetic acid
DOTAGA	1,4,7,10-tetraazacyclododecane-4,7,10-triacetic acid-1-[2-glutaric acid]
DOTMP	1,4,7,10-tetraazacyclododecane-1,4,7,10-tetramethylene-phosphonate
dpa	bis(pyridine-2-ylmethyl)amine
DSB	double-strand breaks
dT	deoxythymidine
DTPA	diethylentriaminepentaacetic acid
E	energy
e.g.	for example (*exempli gratia*)
EC	electron capture
EDDA	ethylenediamine-*N,N'*-diacetic acid
EDTA	ethylenediaminetetraacetic acid
EDTMP	ethylene diamine tetramethylene phosphonate
eg	ethylene glycol
equiv.	equivalent
ER	endoplasmatic reticulum
ER	estrogen
ESI	electrospray ionization
et al.	and others (*et alia*)
Et	ethyl
eV	electron Volt
FAM	carboxyfluorescein
FBS	fetal bovine serum
FCCP	carbonyl cyanide 4-(trifluoro-methoxy)phenylhydrazone
FDA	Food-and-Drug-Administration
FLT	3-deoxy-3'-[^{18}F]fluorothymidine
Fmoc	9- fluorenylmethoxycarbonyl
G	giga-
g	gram(s)
GABA	γ-aminobutyric acid
GAPDH	glyceraldehyde-3-phosphate dehydrogenase
GBM	glioblastoma multiforme
GDP	guanosine 5'-diphosphate
GI	gastrointestinal
GIST	gastrointestinal stromal tumors
Gln (Q)	glutamine
GLP	glucagon-like peptide-1
Glu (E)	glutamic acid
Gly (G)	glycine
GMP	good manufacturing practices
GPCR	G-protein-coupled receptor

GPER	G-protein-coupled estrogen receptor
G-protein	guanosine triphosphate-hydrolyzing protein
GRK	G-protein-coupled receptor kinase
GRP	gastrin-releasing peptide
GRP-10	neuromedin C
GRP-r	gastrin-releasing peptide receptor
GTP	guanosine 5'-triphosphate
Gy	gray
h	hour(s), human
HATU	N-[(dimethylamino)-1H-1,2,3-triazolo[4,5-b]pyridin-1-yl-methylene]-N-methyl-methanaminium-3- oxide
Hepes	4-(2-hydroxyethyl)-1-piperazineethanesulfonic acid
HEU	high enriched uranium
His (H)	histidine
HOBt	1-hydroxybenzotriazole
HPLC	high-pressure liquid chromatography
HRMS	high-resolution mass spectrometry
Hsp90	heat-shock protein 90
hTK1	human cytosolic thymidine kinase 1
HYNIC	6-hydrazinonicotinamide
Hz	hertz
IgG	immunoglobulin G
IP3	inositol-1,4,5-triphosphate
IR	infrared
IT	isomeric transition
iv	intravenous
J	coupling constant
k	kilo
K_d	dissociation constant
L	liter(s)
LET	linear energy transfer
Leu (L)	leucine
LEU	low enriched uranium
logD	logarithm of partition coefficient (at pH 7.4)
LRMS	low-resolution mass spectrometry
Lys (K)	lysine
m	meter(s), milli-; multiplet
M	molar; mega; metal
m/z	mass-to-charge ratio
M^+	parent molecular ion
MAG3	mercaptoacetyltriglycine
MALDI	matrix-assisted laser desorption ionization
MAMA	monoamide-monoamine-dithiols
max	maximum
MD	molecular dynamics
Me	methyl

Met (M)	methionine
min	minute(s), minimum
mol	mole(s), molecular
MRI	magnet resonance imaging
mRNA	messenger RNA
MS	mass spectrometry
MTC	medullary thyroid carcinomas
MTD	maximum tolerated dose
Mw	molecular weight
n	nano-, number
n.c.a	no carrier added
N_3S	dimethylglycycl-L-seryl-L-cysteinglycinamide
N4	6-carboxy-1,4,7,11-tetraazaundecane
NET	neuroendocrine tumors
NHL	non-Hodgkin's lymphoma
NHS	N-hydroxysuccinimide
NISP	Non-reactor Based Isotope Supply Contribution Program
NK_1R	neurokinin-1 receptor
NK_1R-Fl	full-length isoform of neurokinin-1 receptor
NK_1R-Tr	truncated isoform of neurokinin-1 receptor
NKA	neurokinin A
NKB	neurokinin B
Nle	norleucine
NLS	nuclear localization signal
NMB	neuromedin B
NMR	nuclear magnetic resonance
NOTA	1,4,7-triazacyclononane-1,4,7-triacetic acid
NPY	neuropeptide Y
NRT	non-reverse transcription
NRU	National Research Universal
NT	neurotensin
OC	octreotide
p	pico-; para
PBS	phosphate buffered saline
PC-3	human prostate adenocarcinoma cell line
PCR	polymerase chain reaction
PEG	polyethylene glycol
PEG_4	15-amino-4,7,10,13-tetraoxapentadecanoic acid
PET	positron emission tomography
Phe (F)	phenylalanine
PIP2	phosphatidylinositol 4,5-diphosphate
PLC	phospholipase C
PnAO	propylene amine oxime
ppm	part(s) per million
PR	progesterone receptor
Pro (P)	proline
PRRT	peptide-receptor radionuclide therapy

qRT-PCR	quantitative reverse transcriptase PCR	TETA	1,4,8,11-tetraazacyclotetradecane-1,4,8,11-tetraacetic acid
R, r	receptor; residual entity	tetrofosmin	1,2-bis[bis(2-ethoxyethyl)phosphino]ethan
RCP	radiochemical purity	TFA	trifluoroacetic acid
RCY	radiochemical yield	Thi	thienylalanine
RGD	Arg-Gly-Asp	Thr (T)	threonine
RIP	ribosome inactivating protein	TK	tachykinin
RNA	ribonucleic acid	TLC	thin-layer chromatography
rpm	revolutions per minute	TMS	trimethylsilyl
rt	room temperature	TOF	time of flight
s	singlet, second(s)	TPP	triphenylphosphonium
SAAC	single amino acids chelates	TPPTS	trisodium triphenylphospine-3,3',3"-trisulfonate
SAP	saporin	TRAP	1,4,7-triazacyclononane-1,4,7-tris[methyl(2-carboxyethyl)-phosphinic acid)]
Sar	sarcosine		
sc	subcutaneous		
SCLC	small-cell lung cancer		
Ser (S)	serine	Trp (W)	tryptophane
SP	substance P	Trt	trityl
SPECT	single-photon emission computed tomography	Tyr (Y)	tyrosine
		UV	ultraviolet
SPPS	solid-phase peptide synthesis	Val (V)	valine
SSB	single-strand breaks	VIP	vasoactive intestinal peptide
SST	somatostatin	VIS	visible
Sta	statin ((3S,4S)-4-amino-3-hydroxy-6-methylheptanoic acid)	WHO	world health organization
		wt	weight
T	absolute temperature	α	alpha
t	time; triplet	α-MSH	α-melanocyte-stimulating hormone
$t_{1/2}$	half-life		
tacnR:	1,4,7-triazacyclononan derivatives	β	beta
TAMS	triamide-thiols	β^3hGlu	β^3-homoglutamic acid
TBTA	Tris[(1-benzyl-1H-1,2,3-triazol-4-yl)methyl]amine	β^3hLys	β^3-homolysine
		β^3hSer	β^3-homoserine
TBTU	2-(1H-Benzotriazole-1-yl)-1,1,3,3-tetramethylaminium tetrafluoroborate	γ	gamma
		δ	chemical shift in parts per million
tBu	*tert*-butyl	ψ[Tz]	1,4-disubstituted [1,2,3]-triazole

I.   Introduction

1. Radiopharmaceutical chemistry and nuclear medicine

Radiopharmaceutical chemistry deals with the development and evaluation of pharmaceuticals labeled with radioactive probes for applications in nuclear medicine. The development of radiopharmaceuticals dates back to the Hungarian chemist and Nobel laureate (1943) George de Hevesy's work studying the biochemical processes of animals with radioactive tracers ("tracer principle").[1] Most radiopharmaceuticals or radiotracers consist of a radioactive nuclide and a biological ligand or pharmaceutical. They are classified according to their medical application into diagnostic or therapeutic radiopharmaceuticals. They can be categorized into two classes, compounds that accumulate exclusively by their chemical and physical properties and those whose distribution is targeted, through specific receptor binding or other biological interactions (target-specific radiopharmaceuticals).[1-2] Depending on the nature of the disease-relevant target, the targeting vector can be a macromolecule, for example, an antibody, or a small biomolecule, such as a peptide, peptidomimetic, or non-peptide receptor ligand (Figure 1).[1-2]
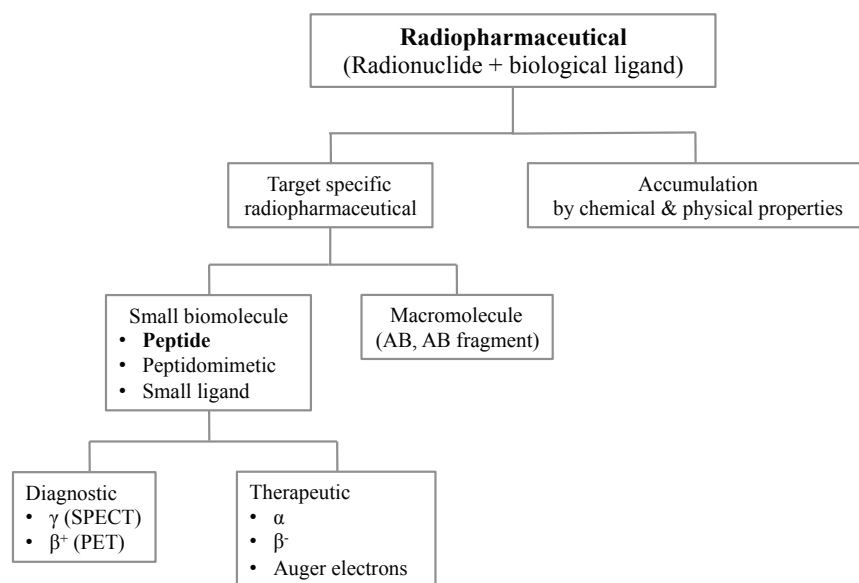
Figure 1. Schematic overview of radiopharmaceuticals.

A diagnostic radiopharmaceutical is labeled with a gamma-emitting (γ) radioisotope for single-photon emission computed tomography (SPECT, section 1.1.1) or a positron-emitting radioisotope (β$^+$) for positron emission tomography (PET, section 1.1.2 and 1.2.2.4).[3] The principle of diagnostic radiopharmaceuticals is to enable visualization of molecular or functional information through accumulation in different organs and tissues.[2] Molecular imaging using radiopharmaceuticals may provide the means for characterization, visualization, and measurement of biological mechanisms at the cellular and molecular level in humans.[2,4] With this non-invasive method, diseases and their status can be assessed. Diagnostic radiopharmaceuticals can also be used to monitor the efficacy of specific therapeutic applications (section 2.3.2).[2]

Therapeutic radiopharmaceuticals are administered in nanomolar, subpharmacological concentrations and are not intended to have any pharmacological effect.[2,5] Instead, radiopharmaceuticals deliver therapeutic doses of ionizing radiation to disease sites that are mainly tumor tissues (section 1.2.2.1).[2,5] Important characteristics of radionuclide therapy are the time of exposure, dose rate, distribution of the

radioactivity, and as a result of those, the absorbed dose of radiation in both the diseased and healthy tissue.[2,6] Thus, the type of radiation, half-life, and energy deposited of the emitting radionuclides are crucial. Radionuclide therapy can be applied using three different administration routes; either *via* external beam radiation (photons), implants (brachytherapy), or systemic application.[2] Brachytherapy, or internal radiotherapy, uses sealed sources of radiation (seeds) that are implanted inside or next to the disease tissue. It is used for treatment of easily accessible tumors and most often in the treatment of prostate cancer patients.[2] Disseminated metastatic tumors can be treated with systemically administrated radiopharmaceuticals that deliver therapeutic radionuclides specifically to tumor sites without damaging the surrounding healthy tissue (e.g., peptide-receptor radionuclide therapy, PRRT, section 2.4.1).[2] Appropriate radionuclides for radionuclide therapy are alpha (α), beta (β⁻), and Auger electron emitters (section 1.2.2.3).[2-3] This thesis focuses on targeted molecular imaging and therapy, using peptide-based radiopharmaceuticals. The principles and general considerations thereof are described in subchapter 2.

1.1   Different imaging modalities in nuclear medicine

SPECT and PET are important modalities in nuclear medicine for non-invasive molecular imaging of (patho)physiological processes *in vivo*.[3] Compared to other imaging modalities, such as computed tomography (CT) and magnetic resonance imaging (MRI), which provide morphological information of tissues and organs with high spatial resolution, the strength of PET and SPECT lies in their ability to visualize biochemical processes on a cellular level.[7] Compared to CT or MRI, the high sensitivity of PET and SPECT allow the administration of imaging compounds in very low concentration (Table 1).[7-8]

Table 1. Comparison of different imaging modalities.[7-8]

Modality	Spatial resolution [mm]	Concentration of imaging agent [M]	Radiation	Information
SPECT	8-20	10^{-6}	yes	functional
PET	3-10	10^{-8}-10^{-10}	yes	functional
CT	1	10^{-4}	yes	morphological
MRI	<1	10^{-5}	no	morphological

1.1.1   *SPECT imaging*

SPECT imaging requires a gamma (scintillation) camera with a detector head that rotates around the long axis of the patient from multiple angles. A three-dimensional dataset can be acquired through a computer-based tomographic reconstruction algorithm. Usually, a full 360-degree rotation is applied to obtain an optimal reconstruction. The acquisition time can be accelerated by using multiple-headed gamma cameras (2-4 detector heads) rotating around the patient. Such a camera head is made up of a collimator, scintillation crystal (usually sodium iodide), photomultiplier, and an amplifier (Figure 2).[3] The collimator is a device used to narrow radiation beams that allows only vertical radiation beams to pass, which results in the high spatial resolution of the detector.[3] Different collimator types can be applied, including parallel hole, pinhole, converging, and diverging collimators.[3] Pinhole collimators are used to image small organs (e.g., thyroid glands). Diverging collimators are used to image organs that are larger than the size of the detector, whereas converging collimators are used to target organs that are smaller than the detector. The most commonly used collimators in nuclear medicine applications are parallel-hole collimators with varying diameter of the holes.[3] Each gamma photon that

reaches the connected scintillation detector results in a light flash, or scintillation. A photo-multiplier is needed to multiply the signal, which is subsequently converted by an amplifier to an electric signal that can be reported.[3] For SPECT imaging, γ-emitting radionuclides (section 1.2.2.4), which have an ideal γ-energy of 70-250 keV are used, such as ^{99m}Tc, ^{111}In, and ^{67}Ga (Table 2 and Figure 6).[1,3,8]
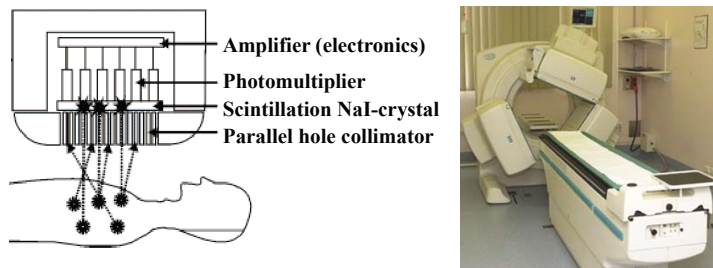

Figure 2. Schematic illustration showing the composition of a scintillation detector and illustration of a SPECT-camera with three detector-heads.[9]

1.1.2   *PET imaging*

PET is based on the coincidence-measurement of two 511 keV γ photons that are emitted in opposite directions (180 ° apart) after annihilation of a positron (obtained from position-emitting radionuclides, section 1.2.2.4 and Figure 7) and an electron. Two oppositely located detectors detect these two photons in coincidence (Figure 3).[3,8] To construct an image of the distribution of radioactivity, data is collected over many angles around the body axis of the patient. Such coincidence measurement obviates the need for a collimator to focus the field of view. The PET-camera consists of circularly arranged γ-detectors (detector ring) where each detector is connected to the opposite detector by a coincidence circuit.[3] Manufacturers use different scintillation detector crystals, such as bismuth germanate, sodium iodide, lutetium oxyorthosilicate, gadolinium oxyorthosilicate, or lutetium yttrium oxyorthosilicate.[3] By measuring coincidence, images can be generated that have less scattered background radiation. Compared to SPECT imaging, better spatial resolution and higher sensitivity can be achieved with PET.[7-8] A selection of some of the relevant β$^+$-emitting radionuclides is listed in Table 2.[1,3]
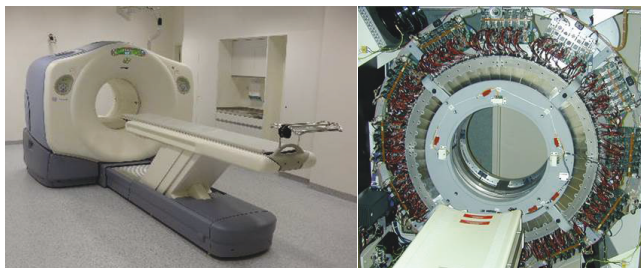
Figure 3. Pictures of a PET-scanner.[9]

1.1.3   *Multimodality imaging*

In the past, single modality instruments were used for SPECT and PET imaging, but nowadays multimodality SPECT/CT and PET/CT instruments are state of the art. This means morphologically imaging of high resolution (CT) is combined with functional information (SPECT, PET) in a fused image that is resulting in higher diagnostic accuracy and localization.[3] A very recent development is using MRI instead of CT for morphological imaging. SPECT/MRI and PET/MRI hybrid imaging reduce the radiation burden on the patient and higher special resolution may be obtained (Table 1).[7,10]

1.2   Radionuclides for medical application

Radionuclides are atoms with an unstable nucleus that transform randomly to a more stable or stable nuclides by undergoing radioactive decay.[3] Radioactive decay may result in either electromagnetic or

particle radiation.[3] Electromagnetic radiation, resulting from emission of gamma- (γ) or x-rays, is applied for diagnostic purposes. Subatomic particle emitting radionuclides (e.g., α, β⁻) are clinically used for therapeutic applications.[1-3] Radionuclides either occur naturally or can be artificially produced.[3] They can be classified further by their decay characteristics or their physico-chemical character (non-metallic: e.g., ^{11}C, ^{13}N, ^{15}O, ^{18}F, ^{32}P, ^{131}I, or metallic: e.g., lanthanides and transition elements).[3]

1.2.1   *Production of radionuclides*

Most radionuclides used in nuclear medicine are artificially produced. Nowadays, more than 2700 radionuclides can be primarily generated in a cyclotron, reactor, or linear accelerator, depending on the target nuclei, the irradiating particle, and its energy.[3]

1.2.1.1   *Cyclotron*

In a cyclotron, charged particles (e.g., protons, deuterons, or α-particles) are accelerated under vacuum in a circular path by an electromagnetic field.[3] Depending on the design and type of the cyclotron, these accelerated particles can obtain very high energies. If targets of stable elements are irradiated by locating them in the beam of the accelerated particles in a cyclotron, the target nuclei get irradiated and a nuclear reaction occurs.[3] Depending on the energy of the beam, a certain number of nucleons (protons, neutrons) are randomly emitted from the irradiated target nucleus, which leads to the formation of the desired radionuclide (Table 2).[3]

1.2.1.2   *Nuclear reactor*

A nuclear reactor is built of fuel rods of fissile materials, such as enriched uranium-235 or plutonium-239 that undergo spontaneous fissions.[3] Nuclear fission is the disruption of a heavy nucleus into two fragments, accompanied by the emission of neutrons.[3] The emitted neutrons cause further fission of other nuclei, initiating a chain reaction. If a target element is introduced into the reactor core, a neutron will interact by fission or reaction of neutron capture with this target nucleus and another (radio)nuclide is produced (Table 2).[3]

Due to their high equipment cost, only few facilities possess cyclotrons or reactors and thus, radionuclides are supplied to distant facilities that are lacking this production equipment.[3] However, very short-lived radionuclides cannot be distributed over long distances and thus, they can only be applied by medical facilities possessing a cyclotron or a reactor.[3]

1.2.1.3   *Radionuclide generator*

A radionuclide generator is based on the principle of the decay-growth relationship of a long-lived parent radionuclide and its short-lived daughter radionuclide. An important requirement is different chemical characteristics of both radionuclides. If this is the case, the parent radionuclide decays constantly and forms the daughter radionuclide that can be easily separated.[3] Radionuclide generators can be easily transported and facilitate the use of short-lived radionuclides in medical institutions that are lacking a cyclotron or reactor for the production of radionuclides.[3] A radionuclide generator is composed of a glass or plastic column that is filled with adsorbent material (e.g., cation-, anion-exchange resin, alumina, or zirconia) on which the mother radionuclide is fixed.[3] Due to the chemical differences, the mother nuclide stays adsorbed and the daughter radionuclide that is produced can be eluted from the generator column with an appropriate solvent (e.g., physiological sodium chloride solution for ^{99}Mo/^{99m}Tc generator).[11] After elution, the amount of daughter nuclide starts to grow again by radioactive decay of the remaining mother nuclide and can repeatedly be obtained by elution

("milking" of the generator).[3] The eluted daughter nuclide should decay to a very long-lived or non-radioactive "grandchild" nuclide to minimize the radiation burden on the patient.[3] A schematic illustration of a radionuclide generator is given in Figure 4. A vial containing the solution of the eluent (A) has to be connected to the generator. Applying vacuum by connecting another evacuated empty vial (B), the daughter nuclide is selectively eluted, while leaving the parent nuclide on the column.[3] Since this radionuclide-eluate is used further for the production of radiopharmaceuticals for parenteral administration, it has to be sterile and pyrogen-free and elution of the generator has to be performed under aseptic conditions.[2-3,11] An ideal radionuclide generator should be convenient to use, give reproducible and repeatedly high yield of the daughter nuclide, is supposed to be free from the parent nuclide (minimal breakthrough) and adsorbent material, and has to be adequately shielded to minimize radiation exposure of the personnel.[3] One of the first and most commonly used radionuclide generator systems is the ^{99}Mo/^{99m}Tc-generator, developed by Tucker and Richards in the late 1950s for the production of technetium-99m.[12] Other commonly used radionuclide generator systems for applications in nuclear medicine are e.g., ^{68}Ge/^{68}Ga, ^{82}Sr/^{82}Rb, and ^{188}W/^{188}Re generators.[1,3]
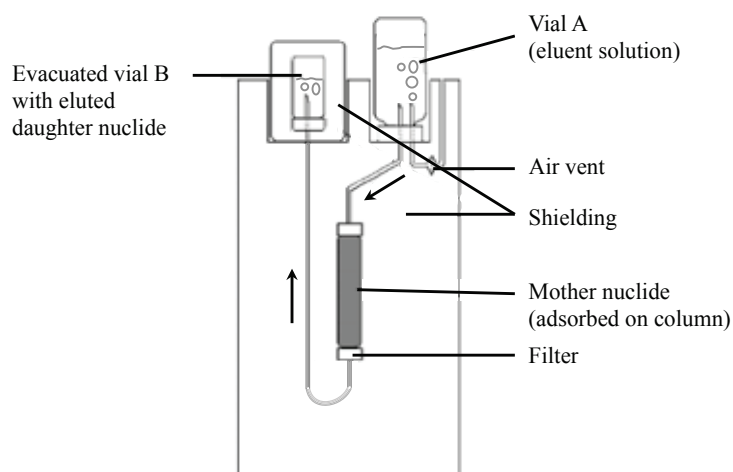

Figure 4. Schematic illustration of the elution of a produced daughter radio-nuclide in a radionuclide generator.[3;9]

1.2.2 *Medical applications of radionuclides*

1.2.2.1 *Radiobiology*

Applying radionuclide therapy, the target of ionizing radiation is the DNA of the cells. Several different lesions are caused by direct ionization of DNA, including single-strand breaks (SSB), double-strand breaks (DSB), damage of base, multiple damaged sites, and cross-links of DNA-bases.[13] These lesions are the result of direct effects (ionization of DNA) or of indirect interaction of free radicals (mainly hydroxyl radicals) with DNA that can be altered by radical scavengers. Distribution of ionizations and the type of lesions depends strongly on the type of radiation and energy.[13] DSB induced by highly specific ionization (α-particles and Auger electrons) are more severe than those caused by more diffuse irradiation.[13] The ability for indefinite cell division declines in mammalian cells as a function of radiation dose and their survival depends on the density of ionization.[13] After irradiation, a delay in progression of cell division in their cell cycle occurs, which is reversible and dose-dependent. This delay depends on the cell cycle phase, whereas cells in pre-mitotic G2 phase exhibit maximum delay, which is altering the mitotic index.[13] After cell irradiation and DNA damage, harm is sensed, several genes are activated, and cells are either awaiting repair of DNA and proceed in the cell cycle, or damages are irreparable and the cells undergo programmed cell death or apoptosis.[13] It has been reported that cells that are adjacent to irradiated cells but have not been irradiated themselves also show increased mutation rates and decreased survival rates. This phenomenon is called "bystander effect".[13]

1.2.2.2   *Radiation dosimetry*

Radiopharmaceuticals are applied in subpharmacological concentrations.[2,5] However, radiation can cause deleterious effects in living organisms.[13] Therefore, it is essential to assess the biological effects in humans for an administered radiopharmaceutical by dosimetric calculations. Dosimetry is the computation of the absorbed dose to different tissues of the body in relation to the total administered radioactivity.[1] Damaging effects caused by irradiation of tissues depend on the administered radioactivity, biological and physical half-lives of the radiopharmaceutical, distribution and metabolism of the radiotracer in the body, individual variations of physiological functions, shape, size, density, relative location, and radiosensitivity of different organs and tissues.[3,13]

1.2.2.3   *Therapeutic applications*

Alpha-decay, the emission of a helium nucleus (α-particle) is common for heavy nuclei (e.g., ^{211}At, $^{212/213}$Bi, ^{225}Ac, Table 2) and is characterized by a high degree of ionization along a linear track with energies of several MeV (5-9 MeV) within a very short range (10-100 µm) and low depth of penetration.[13] Their high linear energy transfer (LET; density of ionization along the path) and micromolar range result in an extremely high-localized dose of radiation and effective killing of single small cells and their clusters, without damaging the surrounding tissue (Figure 5).[3,13] This high-energy radiation is exploited for radionuclide therapy, especially for treatment of small tumors and metastases (section 2.4.1).[1,3,10,13]

Beta-minus (β^-) radiation occurs by the decay of a neutron into a proton, an electron, and electron capture, leading to electron emission.[3] β-particle ionization is infrequent along a linear track and has a short range (0.5-10 mm) with low to medium energy (0.3-2.3 MeV).[13] This radiation can be used for therapeutic applications of small to large size cell clusters (Table 2, Figure 5). A unique advantage of β-particle radiation is their "crossfire effect" (irradiation by decays in distant or neighboring cells, Figure 5).[13] If a sufficient amount of emission occurs in a tissue volume, the probability of lethal hits increases, predominantly from sources bound to other cells.[13] This crossfire killing obviates the necessity for targeting each cancer cell and improves homogeneity of the tumor dose in ensuring sufficient radiation to each cell.[1,3,10,13]
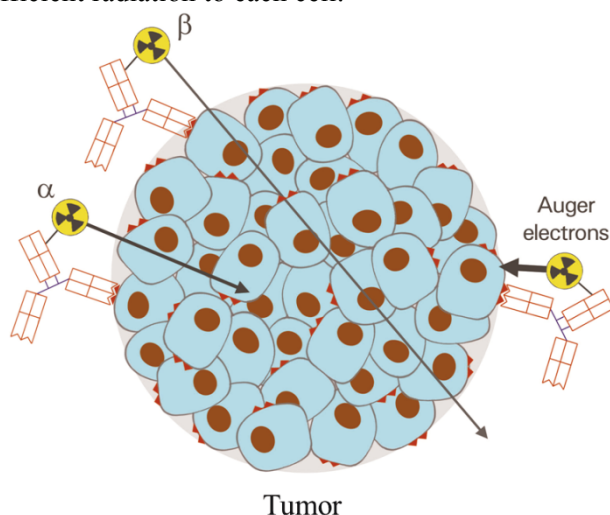
Figure 5. Schematic illustration of crossfire effect, the range of α, β, and Auger electron-emitting radionuclides (length of arrows), and their LET (thickness of arrows).

Auger electrons, first described in the 1920s by Pierre Auger, are concomitantly emitted by radionuclides that are decaying by electron capture or internal convention (almost 50% of the known radioisotopes).[14] Related with these decay processes, inner atomic shell vacancies are formed. To fill these vacancies, cascades of transitions of inner shell electrons take place that result in concomitant emission of several low-energy electrons (Auger, Coster-Kronig, and super-Coster-Kronig transitions).[14] Biological damages caused by this radiation are highly dependent on the location of the

decaying radionuclide within the cell.[13-14] Compared to other particle-emitting radionuclides, the range (nanometer) and also the emitted energy of Auger electrons are extremely low (Figure 5).[13] However, if Auger electrons are in close proximity to the cell nucleus, or even intercalated into DNA of tumor cells, their potential of highly radiotoxic fragmentation and DBS of DNA can be exploited for radionuclide therapy of cancers.[13] Examples of radionuclides that are emitting Auger electrons for potential clinical applications are ^{67}Ga, ^{99m}Tc, ^{111}In, ^{123}I, ^{125}I, and ^{201}Tl (Table 2).[1,3,13-14]

1.2.2.4   *Gamma radiation for molecular imaging*

Gamma rays are emitted alongside other radioactive decay. After radioactive particle decay (α, β), the daughter nucleus is usually left in an excited state.[3] By moving to a lower energy state, residual energy can be emitted by the nucleus in the form of electromagnetic radiation (γ-radiation, Figure 6).[3] Radionuclides emitting γ-radiation (Table 2) are used for SPECT-imaging (section 1.1.1).[1,3,8]
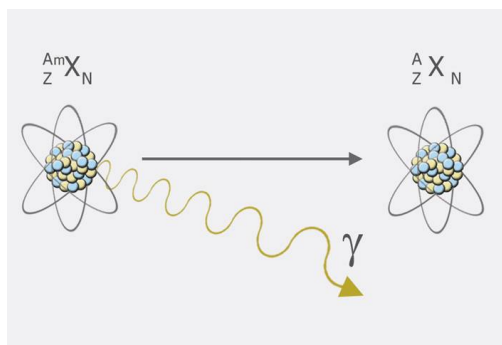
Figure 6. Schematic illustration of gamma decay for SPECT imaging.

Unstable, proton-rich radionuclides decay by positron emission (β^{+}; proton decay). This is a subtype of beta decay, in which a proton of the nucleus is converted into a neutron, a positron (β^{+}), and a neutrino.[3] The positron collates with an electron and the resulting energy is released as annihilation radiation of two diametrically opposed γ-lines of each 511 keV (Figure 7).[1,3,8] This pair of emitted gamma rays is appropriate for detection by PET-cameras (section 1.1.2).[1,3,8]
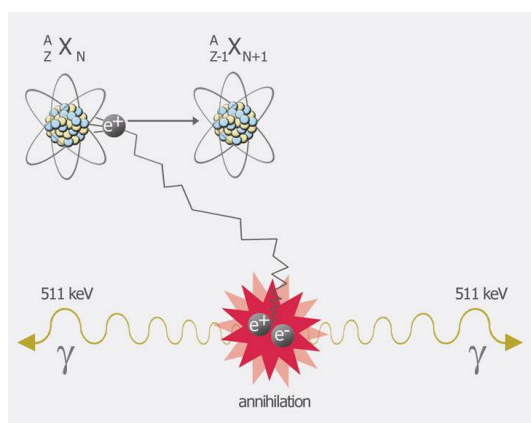
Figure 7. Schematic illustration of proton decay and annihilation radiation for PET imaging.

Relevant radionuclides used in nuclear medicine, for both therapeutic (α, β^{-}, Auger electrons), and diagnostic (γ, β^{+}) applications are summarized in Table 2.

The tracers described in this thesis are radiolabeled with technetium-99m and lutetium-177. Thus, these radiometals will be discussed further in the following sections.

Table 2. Selected radionuclides, their decay properties, and applications in nuclear medicine.[1-2,8,10,15]

| Type	Isotope	$t_{1/2}$ [h]	Decay mode (%), max E, range	Medical application	source
γ -emitter	^{67}Ga	78.3	EC (100), γ, Auger	SPECT	cyclotron
	^{99m}Tc	6.02	IT (100), γ, Auger	SPECT	generator
	^{111}In	67.9	EC (100), γ, Auger	SPECT	cyclotron
	^{123}I	13.3	EC (100), γ, Auger	SPECT	cyclotron
β⁺-emitter	^{11}C	0.34	EC, β⁺ (100)	PET	cyclotron
	^{18}F	1.83	EC, β⁺ (97)	PET	cyclotron
	^{64}Cu	12.9	EC (41), β⁺ (19), β⁻ (40), γ	PET, therapy	cyclotron
	^{68}Ga	1.13	EC (11), β⁺ (89), γ	PET	generator
	^{89}Zr	78.5	EC (77), β⁺ (23)	PET	cyclotron
β⁻-emitter	^{90}Y	64.1	β⁻ (2.28 MeV, 12.0 mm)	therapy	reactor, generator
	^{131}I	193	β⁻ (0.61 MeV, 0.31 mm)	therapy	reactor
	^{177}Lu	161	β⁻ (0.5 MeV, 2.0 mm), γ	therapy	reactor
	^{186}Re	90.5	β⁻ (1.07 MeV, 5.0 mm), γ	therapy	accelerator, reactor
	^{188}Re	16.98	β⁻ (2.12 MeV, 11.0 mm), γ	therapy	reactor, generator
α -emitter	^{211}At	7.2	α (6.79 MeV), 0.06 mm), EC, γ	therapy	cyclotron
	^{213}Bi	0.76	α (8.38 MeV, 0.08 mm), β⁻, γ	therapy	generator

EC: electron capture, IT: isomeric transition

1.2.3   *Technetium-99m*

Technetium-99m (^{99m}Tc, m= metastable) is of particular interest for SPECT imaging, due to its ideal nuclear properties. ^{99m}Tc is the most widely used (> 80%) diagnostic radionuclide in nuclear medicine because of its easy and cost efficient on-site production with a readily available commercial ^{99}Mo/^{99m}Tc-generator system.[2-3,8,11,16] The energy of gamma radiation emitted by ^{99m}Tc (140 keV) is sufficient to penetrate human tissue and enables external detection by SPECT scanners.[3,11,17] The comparatively long half-life (6.02 h, Table 2) conveniently allows for the production of radiopharmaceuticals, administration to the patient, *in vivo* accumulation in the target tissue, and subsequent scintigraphic imaging.[3] In addition, ^{99m}Tc-radiopharmaceuticals could also be administered for radiation therapy, exploiting their concomitant emitted Auger electrons.[14] The decay scheme of ^{99}Mo *via* ^{99m}Tc to stable ^{99}Ru is summarized in Figure 8.[3,11,17]
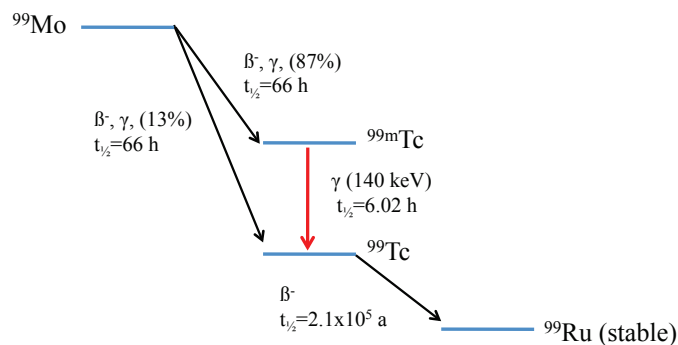
Figure 8. Decay scheme of ^{99}Mo to ^{99}Ru.[3,11,17]

Ready to use pertechnetate (^{99m}TcO$_4^-$) can be obtained by eluting the generator column with sterile saline. The specific activity (amount of radioactivity per amount of radionuclide)[3] of the ^{99m}Tc-eluate

depends on the time interval between the performed elutions.[11,16-17] [99mTc]-radiopharmaceuticals are intravenously administered and hence, radiosynthesis has to be accomplished under sterile and pyrogen-free conditions.[2,11] Synthesis of established [99mTc]-radiopharmaceuticals can be simply performed by adding pertechnetate to a kit formulation.[2,11,15c,16] Kit formulations are used for the sake of convenience, consistency, and reproducibility of the radiochemical purity during radiolabeling. Kits are sterile, pyrogen-free, and lyophilized mixtures of all the required ingredients, including a reducing agent.[1-2,11,16] The most commonly used reducing agent in commercial kits is stannous chloride. But many other reducing agents are also used, such as borohydride, dithionate, dithionite, and phosphines.[2,16] To improve the radiolabeling yield and stability of [99mTc]-radiopharmaceutical, different components can be included, such as solubilizing agents, antioxidants, or weak transferring ligands.[2,16] Many ready-to-use kit-formulations for a huge variety of [99mTc]-radiopharmaceuticals are commercially available for imaging of different organ functions, bone scanning, imaging of myocardial perfusion, and immunoscintigraphy.[11,16-18] The majority of [99mTc]-based radiopharmaceuticals currently used in the clinic are complexes with low molecular weight, whose biological distribution is determined by blood flow and accumulation in organs and tissues due to their chemical and physical properties (Figure 1).[11] Nowadays, efforts in the development of radiotracers are focused on the design of specific (receptor-)targeting radiopharmaceuticals.[2,11,15a,16-17,18b,19]

Based on their periodic relationship, the coordination chemistry of technetium is similar to that of its group VII transition metal congener rhenium ("matched pair").[2,18b,19a] Thus, the strategies developed for technetium labeling of molecular imaging agents can also be adapted to the β⁻-emitting radionuclides [186/188]Re for the development of therapeutic radiopharmaceuticals, using the same biomolecule ("theranostics", section 2.3.2).[2,8,18b,19a] However, there are also significant differences between [99mTc] and [186/188]Re. For instance, they show different redox potential, the reduction of perrhenate ($[Re(VII)O_4]^-$) is slower, and a stronger reducing agent is required. Furthermore, it can be challenging to achieve high *in vivo* stability because of oxidation reactions occurring *in vivo*.[1-2,11,15a,16]

$[^{99m}TcO_4]^-$ cannot be used for direct attachment to biomolecules because it does not form stable complexes. Thus, [99mTc(VII)] of pertechnetate has to be reduced to a lower oxidation state. Technetium exhibits diverse redox chemistry with various oxidation states (-I to +VII).[2,11,16-17,18b,20] The resulting oxidation state depends on the reducing agent, reaction condition, and the chelating system used. The rich redox chemistry offers the possibility of modifying structures and characteristics of technetium complexes developed, by the choice of chelators that possess high affinity for a certain oxidation state.[2,11,16,18b] It goes far beyond the scope of this thesis to discuss the diverse coordination chemistry of technetium, various chelating agents, [99mTc] cores, labeling strategies, and the enormous amount of developed [99mTc]-radiopharmaceuticals. All of this is described in many excellent reviews, for example, those by Liu and others.[2,10-11,16-17,18b,19-20] In the context of this thesis, some selected technetium cores, including Tc(V)-oxo, Tc(V)-dioxo, Tc(V)-nitrido, Tc(III)-hydrazino, and Tc(I)-tricarbonyl (Figure 9) that are used for [99mTc]-labelings of biomolecules will be discussed in the following sections.
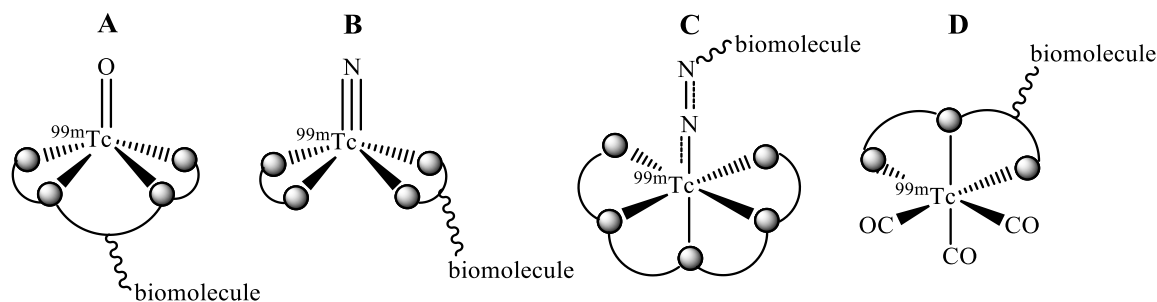
Figure 9. Common ^{99m}Tc cores and schematic complexes thereof with chelating agents used for the radiolabeling of targeted biomolecules; A) Tc(V)-oxo, B) Tc(V)-nitrido, C) Tc(III)-hydrazino and D) Tc(I)-tricarbonyl core (spheres represent coordinating ligands).[16]

1.2.3.1 $[^{99m}Tc=O]^{3+}$ and $[O=Tc=O]^{+}$ cores

The Tc(V)-oxo core, $[^{99m}Tc=O]^{3+}$, is one of the most frequently used cores for ^{99m}Tc-labeling of biomolecules. It forms square pyramidal complexes, in which the π-bonding oxo-group occupies the apical position and stabilizing σ- or π-donating amino, amido, or thiolate ligands form the basal plane.[2,10,16,18b,19a] A wide range of ligand systems for the chelation of the $[^{99m}Tc=O]^{3+}$ core are reported with tetradentate chelators, such as N$_4$ tetraamine type propylene amine oxime (PnAO), N$_3$S triamidethiols (TAMS), N$_3$S diamide-monoamine-thiols (DAMA), N$_2$S$_2$ diaminedithiols (DADT), N$_2$S$_2$ diamidedithiols (DADS), N$_2$S$_2$ monoamide-monoamine-dithiols (MAMA), or N$_2$S$_4$ diaminetetrathiol (for examples thereof, Figure 10 A).[2,16] Tripeptide sequences (e.g., Gly-Ser-Cys) are mimicking an N$_2$S$_2$ or N$_3$S type chelating systems and also form stable Tc(V)-oxo complexes.[2,16] The most prominent example of N$_3$S type chelators for conjugation to biomolecules is mercaptoacetyltriglycine (MAG$_3$).[2,16,18b] The MAG$_3$ chelator itself, radiolabeled with ^{99m}Tc (^{99m}Tc-MAG$_3$) is also commonly administered in nuclear medicine as radiopharmaceutical for imaging of renal perfusion.[2,10,16,18b,19a]

The Tc(V)-dioxo core forms octahedral Tc(V)-complexes with macrocyclic (e.g., cyclam) or acyclic tetraamines that have been used for radiolabeling of antibodies or peptides (Figure 10 B).[16,19a,21] Bidentate phosphines can also form stable complexes with the Tc(V)-dioxo core.[16] An example of a Tc(V)-dioxo-radiopharmaceutical, chelated to bidentate phosphines is $[^{99m}TcO_2(tetrofosmin)_2]^{+}$ (tetrofosmin: 1,2-bis[bis(2-ethoxyethyl)phosphino]ethan) that is commonly administered in nuclear medicine for myocardial imaging.[11,16-17,18b]
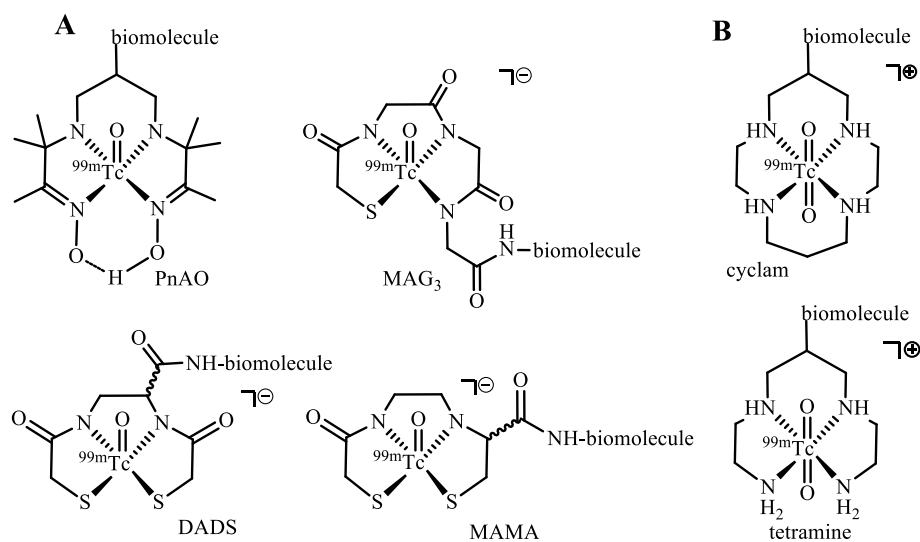

Figure 10. Examples of A) technetium(V)-oxo and B) technetium(V)-dioxo complexes with N$_x$S$_{4-x}$ type chelators.[16]

1.2.3.2 $[^{99m}Tc\equiv N]^{2+}$ core

The technetium-nitrido core, $[^{99m}Tc\equiv N]^{2+}$ is isoelectronic with the technetium-oxo core and forms stable Tc(V)-complexes (square pyramidal, nitrido-group in apical position) with various chelators (e.g., thiolate-S, amine-N, and carboxylic-O donors) for radiolabeling of small molecules with ^{99m}Tc.[2,18b] Compared to the technetium-oxo core, the strong π-electron donating nitrido ligand enables the high stabilization of the Tc(V) oxidation state.[2,16,18b] Among other ligand systems, cysteine and dithiocarbamates in combination with co-ligands (e.g., biphosphines) have been shown to be particularly suitable chelating systems for the radiolabeling of targeted (bio)molecules with the $[^{99m}TcN]^{2+}$ core (Figure 11).[2,11,16,18b]
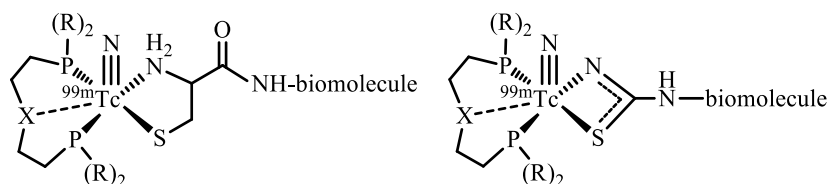

Figure 11. Examples of cysteine- and dithiocarbamato-based chelating ligands for the nitrido core $[^{99m}TcN]^{2+}$; R: alkyl or aromatic residues.[2]

1.2.3.3 $[^{99m}Tc]HYNIC$ core

Hydrazine groups of organic molecules react with metal-oxo species by a condensation reaction to form chemically robust metal-organohydrazine entities, offering an alternative method for the synthesis of ^{99m}Tc-radiopharmaceuticals.[18b] Using the HYNIC (6-hydrazinonicotinamide) core, coligands, such as ethylenediamine-N,N'-diacetic acid (EDDA), tricine, or glucoheptonate are required to complete the square pyramidal or octahedral complexes, because HYNIC occupies only one or two coordination sites of the metal, the pyridyl and/or hydrazine nitrogen (Figure 12).[2,10,16,18b,22] High labeling efficacies can be achieved with the $[^{99m}Tc]HYNIC$ core and the use of coligands also enables pharmacokinetic or hydrophilic modifications.[2,10,16,18b,22] There are also ternary ligand systems with water-soluble phosphines described for ^{99m}Tc labeling of different biomolecules in very high yield and specific activity, e.g., $[^{99m}Tc(HYNIC\text{-}biomolecule)(tricine)(phosphine)]$.[2,16,22] However, formations of product mixtures are possible, depending on the coligands and reaction conditions that are used.[2,10,16,18b,22] The HYNIC core has been reported for ^{99m}Tc-labeling of various biomolecules, such as peptides, antibody fragments, antisense oligonucleotides, and liposomes.[2,16] However, the lack of identity of species present on the tracer level has impeded the general utility of the HYNIC core for the development of ^{99m}Tc-radiotracers.[2,10,16,18b,22]
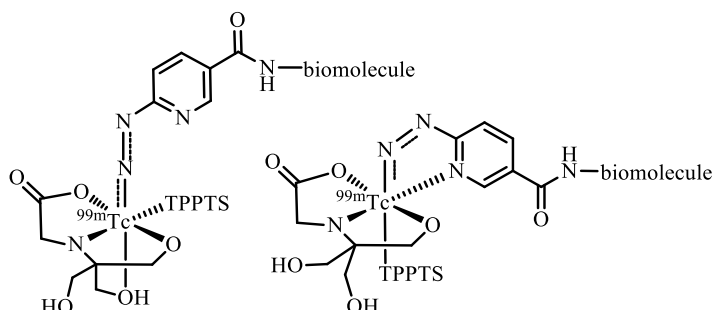

Figure 12. Two possible isomers of $[^{99m}Tc(tricineH_2)HYNIC]$ complexes as the result of mono- or bidentate coordination modes of the HYNIC ligand. TPPTS = trisodium triphenylphospine-3,3',3"-trisulfonate.[22]

1.2.3.4 $[^{99m}Tc(CO)_3]^+$ core

The stable and water-soluble organometallic *fac*-tricarbonyl core, $[M(CO)_3(H_2O)_3]^+$ ($M=^{99m}Tc(I)$, $^{186/188}Re(I)$) was introduced by Alberto, Schibli, and coworkers in 1998.[23] The complex was first formed by direct reduction of pertechnetate or perrhenate with sodium borohydride in the presence of carbon monoxide.[23] In pioneering work by the Schubiger group, the breakthrough for a convenient kit utilization of the tricarbonyl core was the application of solid, stable, and non-toxic potassium boranocarbonate, $K_2[H_3BCO_2]$.[24] Boranocarbonate provides CO release upon hydrolysis, and reduction of Tc/Re(VII) to Tc/Re(I) in a ready to use kit-formulation (IsoLink[TM] kit, "CRS IsoLink kit for tricarbonyl") for the synthesis of ^{99m}Tc and $^{186/188}Re$-tricarbonyl complexes.[19b,24] To use the ^{99m}Tc-tricarbonyl core for the radiolabeling of biomolecules, several bifunctional chelating agents were developed. The three labile water molecules are easily substituted with S, O, or N atoms of various chelating ligands (Figure 13).[17,18b,19,25] Numerous mono-, bi-, or tridentate ligand systems, of e.g., amines, amides, carboxylic acids, imidazoles, pyrazoles, pyridines, thioethers, thiols, phosphines, and combinations thereof lead to stable complexes of ^{99m}Tc and $^{186/188}Re$-tricarbonyl.[17,18b,19,25] Among the possible ligand systems, aromatic amines provide fast complexation, high thermodynamic stability, and kinetic inertness. Combining an aromatic amine with aliphatic amines and/or carboxylates has proven to be advantageous in aqueous solutions.[18b,19b,25a] The amino acid histidine (His) has ideal characteristics for facile and stable complexation of the tricarbonyl core in low ligand concentration (10^{-6} M).[19b,25a] In addition, histidine as a chelating system (e.g., N_α-Ac-His-chelator) can be easily coupled to the N-terminus of peptides for the preparation of targeting radiopharmaceuticals with very high specific activity.[18b,19b,25a] Furthermore, the octahedral *fac*-$[^{99m}Tc(CO)_3(H_2O)_3]^+$ core is generally smaller than octahedral or square-pyramidal complexes of technetium in higher oxidation states and thus, the organometallic tricarbonyl core is the preferred metal core for labeling small biomolecules with technetium or rhenium.[18b,19b,25a] Technetium and rhenium tricarbonyl cores have been widely used for the development of radiolabeled biomolecules, such as peptides (e.g., somatostatin, bombesin, neurotensin, and neuropeptide Y analogs),[25d,26] proteins, and small molecules (e.g., tropane, serotonin, and steroid derivatives).[19b,25b,d] ^{99m}Tc-tricarbonyl complexes with mono- and bidentate chelators suffer from low stability and adverse biodistribution profiles. They display high aggregation of plasma proteins and are retained in the blood pool and the excreting organs (liver, kidneys).[19b,27] Tridentate chelating systems form more stable ^{99m}Tc-tricarbonyl complexes with superior pharmacokinetics *in vivo*.[19b,25b-d,27] Another example of a tridentate ligand is bis(pyridine-2-ylmethyl)amine (dpa), which rapidly forms very stable complexes with ^{99m}Tc-tricarbonyl.[18b,25b] The dpa ligand provides the structural basis for a bifunctional chelate in the single amino acid chelates (SAAC).[18b,28] In this approach, natural or synthetic amino acids are modified by incorporation of a tridentate chelate terminus and a terminus for attachment to small biomolecules.[28] Functionalized η^5 cyclopentadienes (Cp, Figure 13) and carboranes have been used for stable complexation of the *fac*-$[^{99m}Tc(CO)_3(H_2O)_3]^+$ core as well.[18b,19b,25b,d] The tricarbonyl core also enables the production of isostructural $^{186/188}Re$-radiopharmaceuticals as therapeutic analogues, which cannot always be achieved for Tc(V)/Re(V)-complexes.[18b,19,25a] For applications in radiopharmacy, the rather lipophilic character of the *fac*-$[^{99m}Tc(CO)_3(H_2O)_3]^+$ core can be a limiting factor, causing an unfavorable alteration of the hydrophilicity of the radiometal (peptide)conjugate.[18b,19,25b]
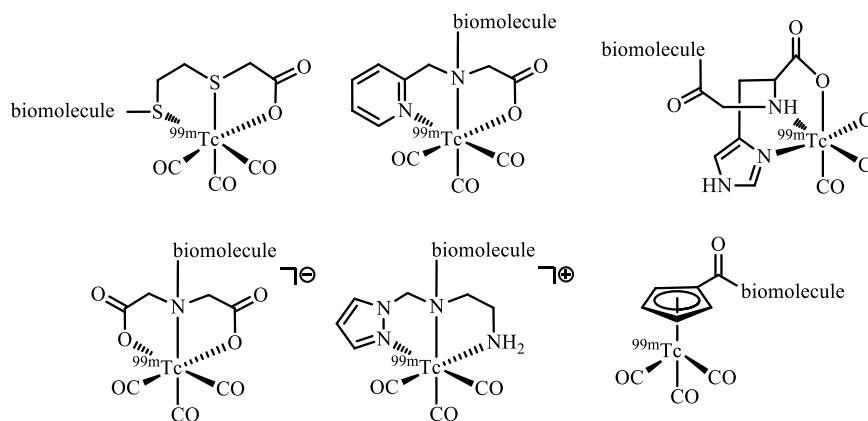
Figure 13. Representative examples of structurally diverse chelating systems for complexation of *fac*-[^{99m}Tc(CO)$_3$(H$_2$O)$_3$]$^+$.[2,18b,19b,25b,d]

An elegant synthetic approach for the formation of chelating systems for the *fac*-[^{99m}Tc(CO)$_3$(H$_2$O)$_3$]$^+$ core and simultaneous conjugation to a biomolecule was reported by Mindt *et al.* in 2006.[29] This approach employs the versatile Cu(I)-catalyzed azide-alkyne cycloaddition (CuAAC, click chemistry)[30] and was termed "Click-to-Chelate".[29] The strategy is shown in Figure 14.
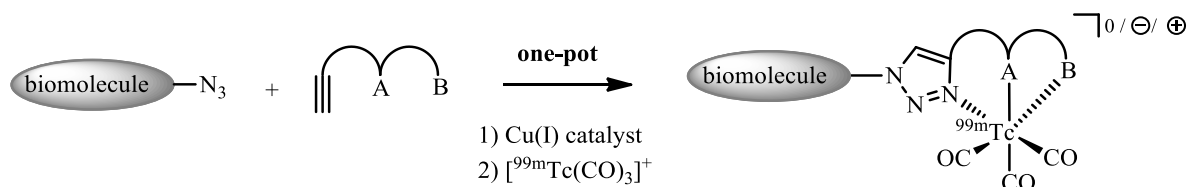
Figure 14. The "Click-to-Chelate" approach enables the labeling with ^{99m}Tc-tricarbonyl and simultaneous assembly with azide-functionalized biomolecules by efficient and convenient one-pot procedures.

The final radioconjugate can be obtained directly by a convenient and efficient one-pot procedure. The "Click-to-Chelate" methodology has proven useful for the assembly and radiolabeling of a broad variety of biomolecules, such as peptides, vitamins, nucleosides, carbohydrates, and phospholipids.[29,31] This promising strategy for the development of ^{99m}Tc-based radiotracers will be discussed in more detail in chapter II of this thesis, since the bifunctional radioconjugates (chapter III and IV) are assembled using an "extended Click-to-Chelate" methodology.[31c]

1.2.3.5 [^{99m}TcO$_3$]$^+$ core

A Tc metal core recently developed is the *fac*-[TcO$_3$]$^+$ core, which is stabilized by tripodal ligands to form a core of approximately the size of an iodide ion.[32] Two synthetic approaches are possible for the formation of [TcO$_3$]$^+$ cores; direct activation of pertechnetate or oxidation of stable Tc complexes containing the metal atom in a lower oxidation state.[32] In contrast to synthetic strategies for bifunctional ^{99m}Tc-complexes based on ligand replacement reactions at the metal core, bifunctional *fac*-[TcO$_3$]$^+$ complexes can be formed conveniently using a ligand-based strategy.[32] Tc-trioxo complexes react with alkenes *via* a metal-mediated vicinal cis-dihydroxylation reaction ((3+2)-cycloaddition).[33] This approach enables the preparation of novel molecular imaging agents and may overcome some of the limitations previously experienced with the coordination chemistry of technetium.[32] In 2009 the group of Alberto reported the synthesis of stable [^{99m}TcO$_3$(tacnR)]$^+$ (tacnR: 1,4,7-triazacyclononan derivatives) complexes from pertechnetate, using phosphines as reagents and called this approach "clack chemistry" (an analogy to established "click chemistry").[34] This methodology was applied to synthesize conveniently bifunctional bioconjugates containing either a hypoxia targeting pharmacophore, a glucose derivative, or an artificial amino acid to demonstrate the

suitability and flexibility of this new labeling approach.[35] Compared to the ^{99m}Tc-tricarbonyl core, advantageous hydrophilicity was confirmed for the $[^{99m}TcO_3(tacnR)]^+$ core and further *in vivo* studies are currently ongoing.[35-36] However, more detailed kinetic investigations are needed and the stereochemistry of the (3+2) cycloaddition has to be controlled to optimize this labeling strategy for routine radiolabeling of biomolecules.[35]

1.2.3.6   General considerations

Due to the central role of technetium-99m in nuclear medicine, a large number of radiopharmaceuticals, based on the various, previously described technetium cores have been developed and evaluated in (pre)clinical studies and some are routinely administered in the clinic.[2,11,16,19a,25b] Examples range from radiolabeled large proteins to medium-size peptides[19a,37] and small compounds, including vitamins (biotin, vitamin B12, and folic acid),[19a] steroid hormones, and neurotransmitters (dopamine and serotonin).[2,11,16,25b]

Because of its ideal nuclear characteristics, ^{99m}Tc remains the most widely used radionuclide in nuclear medicine and radiopharmaceutical sciences. Thus, ^{99m}Tc will continue to be important for the future development of novel targeting radiotracers for diagnosis, assessment of diseases, and monitoring of therapy outcomes.[18b,19a,25b]

However, it has to be critically acknowledged that the continuing global shortage of ^{99m}Tc is a challenge.[19a] Aging nuclear reactors that are important for the world's supply require frequent maintenance and repair.[19a] Less than ten reactors worldwide supply radionuclides for medical applications.[38] Half of the world's supply of radionuclide raw material is produced in the National Research Universal (NRU) reactor at Chalk River (Canada).[38] Unforeseen maintenance at the NRU reactor and coincidental shutdowns of other international reactors led to a global shortage of medical radionuclides (especially ^{99m}Tc) in 2009.[38-39] The NRU reactor is several decades old and although it has since restarted its production, it is planned to cease the production of isotopes in 2016.[39] Thus, consistent and reliable methods for the production of ^{99}Mo or direct production routes of ^{99m}Tc have to be established in order to fulfil the world's demand of ^{99m}Tc.[38] Possible production routes for ^{99}Mo include production from less security-critical low-enriched uranium (LEU) rather than high-enriched uranium (HEU) targets, reactor production by neutron activation (^{98}Mo(n,γ)^{99}Mo reaction), or production by accelerators.[38] However, all of these methods result in ^{99}Mo with lower specific activity, requiring, for example, adapted kit formulations and ^{99}Mo/^{99m}Tc separation techniques.[38] Another potential approach is using cyclotron bombarding of enriched ^{100}Mo targets as an alternative for the direct production of ^{99m}Tc (^{100}Mo(p,2n)^{99m}Tc reaction).[38,40] The Canadian government's "Non-reactor Based Isotope Supply Contribution Program" (NISP) is evaluating the use of linear electron accelerators (LINAC) for the production of ^{99}Mo *via* the ^{100}Mo(γ,n) reaction.[39] LINAC-produced ^{99m}Tc appear to be clinically equivalent to the current fission-produced ^{99m}Tc. In addition, this "green" production route reduces radioactive waste and ^{100}Mo left after processing can be reused and recycled.[39]

1.2.4   Lutetium-177

The radiometal lutetium-177 (^{177}Lu) belongs to the lanthanide group. Its common occurring oxidation state is +3.[1,15c] ^{177}Lu can be produced in a cyclotron, but most commonly this radiometal is produced by neutron bombardment of purified target materials in medium flux nuclear reactors *via* direct or indirect methods.[1-2] Direct neutron activation of enriched ^{176}Lu (^{176}Lu(n,γ)^{177}Lu reaction) in a medium flux reactor leads to production yields of 20-30%.[1,8] Higher specific activities can be reached in higher flux reactors. Disadvantages of this direct production technique are high costs and impurities of long-lived ^{177m}Lu (half-life of 160 d).[1] The indirect production route is realized *via* neutron capture and subsequent β⁻ decay of the parent radioisotope to the desired ^{177}Lu.[1] Neutron activation of enriched ^{176}Yb leads to the production of ^{177}Yb, which decays (half-life of 1.9 h) by β⁻ decay to ^{177}Lu (^{176}Yb(n,γ)^{177}Yb(β-)^{177}Lu reaction).[1] This indirect production route circumvents the formation of the ^{177m}Lu impurity, since β⁻ decay of ^{177}Yb has no branching through the metastable radioactive ^{177m}Lu isotope.[1] Compared to the direct production route, the indirect method provides carrier-free ^{177}Lu at very high specific activity.[1] ^{177}Lu has a physical half-life of 6.7 days.[1-2,15c] The half-life is long enough to allow distribution to hospitals in remote regions and is best suited for radiolabeling of biomolecules with medium to long biological half-lives.[1,8] ^{177}Lu has three low energy β⁻-emissions (0.498 MeV (79%), 0.385 MeV (9%), 0.177 MeV (12%)) with a relatively short range of 1.5 mm (Figure 15).[1-2,8,15c] Owing to its weak energy and short range of β⁻-emission, ^{177}Lu is considered a promising radionuclide for targeted radiotherapy of small tumors and metastases while sparing normal tissue.[1,8,10,41] ^{177}Lu also emits two low energetic γ-rays (0.208 MeV (11%) and 0.113 MeV (6%)), enabling simultaneous imaging with a gamma camera, to determine the extent of disease, calculation and prediction of dosimetry, as well as monitoring of therapeutic efficacy.[1-2,8,15c] The chemistry of ^{177}Lu is similar to other lanthanide radiometals. ^{177}Lu mainly forms highly stable octadentate chelates with cyclic or acyclic polyaminopolycarboxylates.[1-2,8,11,15c] A variety of bifunctional chelating systems suitable for radiolabeling with ^{177}Lu and other lanthanides will be discussed in section 2.3.3.

^{177}Lu

β⁻ (177, 385, **498 keV**)
γ, (113, 208 keV)
$t_{1/2}$=6.647 d
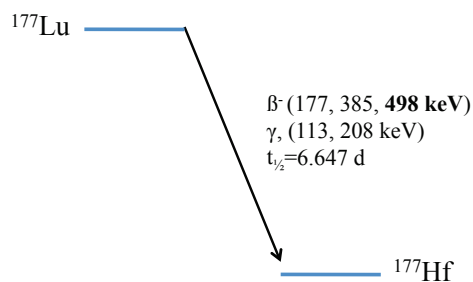
^{177}Hf   Figure 15. Simplified decay scheme of ^{177}Lu to ^{177}Hf.[42]

^{177}Lu has gained interest for targeted radionuclide therapy and many ^{177}Lu-radiolabeled antibodies or small peptides have been (pre)clinically evaluated.[1,15c,43] ^{177}Lu-radiolabeled peptides were developed in particular for targeted radionuclide therapy of neuroendocrine tumors, using somatostatin analogs, e.g., DOTA-TOC and DOTA-TATE (section 2.5.2).[1,15c,43] Administration of these targeting radiopharmaceuticals results in an average survival benefit of several years and markedly improves the quality of life of patients suffering from neuroendocrine tumors.[43] In addition, analogs of the bombesin peptide (section 2.6.1) were radiolabeled with ^{177}Lu.[1,15c] ^{177}Lu-AMBA was clinically evaluated for therapy of prostate cancer. However, severe side effects were reported.[1,44]

Another medical application of ^{177}Lu is the treatment of lymphoma. Malignant lymphoma cells often diffusely infiltrate normal tissue. Because of the advantageous short range of tissue penetration, ^{177}Lu-DOTA-rituximab, a chimeric anti-CD20 antibody was evaluated in a clinical phase I/II study for treatment of patients with indolent lymphomas.[45] High rate of tumor response in all dose levels and in

all entities of lymphoma were reported and hematologic toxicity was only temporary and controllable.[45]

[177]Lu was also clinically evaluated as a palliative therapy for bone metastases, which occur in 60-75% of patients as a corollary of breast and prostate cancer.[1] Its emission of low β^--energy is ideal to minimize unwanted ablation of bone marrow.[1] [177]Lu was conjugated to both 1,4,7,10-tetraazacyclododecane-1,4,7,10-tetramethylene-phosphonate (DOTMP) and ethylene diamine tetramethylene phosphonate (EDTMP) and administered for palliation of bone metastases.[1] Compared to similar [153]Sm-EDTMP, ^{177}Lu-DOTMP was revealed to be superior and may result in longer intervals of remission.[1] Clinical trials evaluating ^{177}Lu-EDTMP are ongoing.[1]

[177]Lu was also conjugated to J591, an antibody targeting the antiprostate membrane antigen (PSMA) and evaluated as treatment in androgen-independent prostate cancer (Phase II clinical trials).[1] ^{177}Lu-J591 showed very promising results and phase III clinical trials are planned.[1] Another clinical trial is underway to evaluate ^{177}Lu-J591 in combination with the chemotherapeutic drug ketoconazole.[1]

2. Peptide-based, targeting radiopharmaceuticals for cancer applications

2.1   Regulatory peptides

Peptides typically contain between two to fifty amino acids (AA) linked by amide bonds.[5] An enormous number of peptides occur physiologically. This thesis focuses on regulatory peptides, such as neuropeptides, gut peptide hormones, vasoactive peptides, and endocrine peptides. Regulatory peptides occur in many different organs and their targets may be present in the gastrointestinal (GI) tract, brain, kidneys, lungs, or in the lymphatic, endocrine, immune, vascular, and peripheral systems.[5] The biological function and metabolic processes of almost all organs are modulated and controlled by regulatory peptides through interaction with specific membrane-bound receptors, most commonly G-protein-coupled receptors (GPCR).[5] Regulatory peptides and their receptors are important for not only physiological processes, but also pathological conditions, such as inflammation and cancer.[5,26,46]

2.2   GPCRs as targets for tumor diagnosis and treatment

2.2.1   GPCR, signal transduction, and signaling pathways

GPCRs belong to the largest and most diverse family of signaling receptors. Nearly half of the drugs currently applied target this receptor family and show enormous success in the development of treatments for a wide range of human diseases.[47] GPCRs are integral membrane proteins that are comprised of a single polypeptide chain with seven transmembrane domains, an intracellular domain that is linked to G-proteins and arrestin for activation of secondary messengers, and an extracellular domain for ligand binding. GPCRs recognize ligands outside of the cell to activate intracellular signal transduction pathways and cellular responses.[47-48] Usually, GPCRs conjugate to heterotrimeric (α, β, γ subunits) guanosine 5'-triphosphate (GTP)-hydrolyzing proteins (G-proteins) at the plasma membrane. In the inactivated state, guanosine 5'-diphosphate (GDP) is bound to G-proteins.[48] Upon ligand binding, GPCRs undergo conformational changes leading to the interaction with G-proteins.[48] Activation of GPCRs promotes the exchange of GDP to GTP on the α-subunit. This leads to dissociation into the G_α-GTP and the $G_{\beta,\gamma}$-subunits that independently signal several membrane bound effectors, for example, phospholipases, ion channels, mitogen-activated protein kinases, guanine nucleotide exchange factors, and many other enzymes.[47-48] They also activate a second intracellular signal and the synthesis of secondary messengers, including 3'-5'-cyclic adenosine monophosphate (cAMP), 3',5'-cyclic guanosine monophosphate (cGMP), diacetylglycerol (DG), inositol-1,4,5-triphosphate (IP$_3$).[48] GTPase activity of the G_α-subunits hydrolyzes GTP to GDP and the $G_{\beta,\gamma}$-subunit reassociates with the G_a-GDP subunit, to inactivate the signal transduction.[48] Depending on the type of the G_α-subunit (e.g., $G\alpha_t$, $G\alpha_{olf}$, $G\alpha_i$, $G\alpha_s$, $G\alpha_q$), different intracellular signaling proteins are affected.[48] $G\alpha_s$ stimulates adenylate cyclase (AC), leading to increased cAMP concentration and activation of various ion channels as well as cAMP dependent ser/thr-specific protein kinases A; whereas $G\alpha_i$ inhibits AC.[48] The $G\alpha_q$ pathway activates phospholipase C-β (PLC), catalyzing cleavage of membrane-bound phosphatidylinositol 4,5-diphosphate (PIP2) into the secondary messengers DG and IP$_3$. IP$_3$ binds to IP$_3$ receptors in the membrane of the endoplasmatic reticulum (ER) to trigger calcium release from the ER.[48] $G_{\beta,\gamma}$ subunit effects several ion channels, including $K^+_{(Ach)}$-channels, and Ca^{2+}-channels, and activates PLC-β-isoenzymes, which lead to the IP$_3$ and DG pathways mentioned above.[47-48] Endogenous ligands that cause physiological changes after binding to the receptor and internalize are called agonists. Ligands that lead to inhibition of the binding of the agonist and do not activate

physiological changes are described as antagonists.[5,10,16,37,41] Binding of agonistic peptide ligands to their corresponding membrane-bound GPCR leads to activation of different effectors and signaling pathways described above that are regulated by temporal membrane trafficking of GPCRs from the cell membrane surface. Excess ligand binding induces acute signal termination or receptor desensitization of G-protein signaling by rapid internalization of the receptor-ligand complex by clathrin-mediated endocytosis.[47-48]

All radiopeptides described in this thesis are agonists and they internalize into tumor cells *via* clathrin-mediated endocytosis.[49] Especially in the case of dual-targeting bombesin derivatives, internalization is a crucial requirement to facilitate intracellular targeting of organelles or cytosolic enzymes. Thus, the mechanism of clathrin-mediated endocytosis will be described in the following section.

2.2.2   *Internalization of the receptor-ligand complex via clathrin-mediated endocytosis*

The steps leading to GPCR endocytotic internalization are the functional uncoupling of the G-proteins from the receptor and the subsequent receptor phosphorylation (PP) by G-protein-coupled receptor kinases (GRKs), which lead to binding of β-arrestin (βarr) to the receptor.[48,50] β-arrestin stabilizes the association with clathrin-coated pits (CCPs) that progressively invaginate the formed pits.[49,52] Finally, through GTPase activity of dynamin (d), the pits are pinched off from the plasma membrane and free clathrin-coated vesicles (CCV) of the receptor-ligand complex are released into the cytosol.[49,52] The CCV fuses with an early endosome, where the receptor-ligand complex dissociates. Either the receptor is directed to recycling endosomes, resensitized and recycled back to the surface of the cell membrane, or the receptor is directed to late endosomes and lysosomes for its terminal degradation (Figure 16).[49,52] The agonistic ligand is either released to the cytosol or degraded within lysosomes, and is finally externalized *via* exocytosis.[48-51]
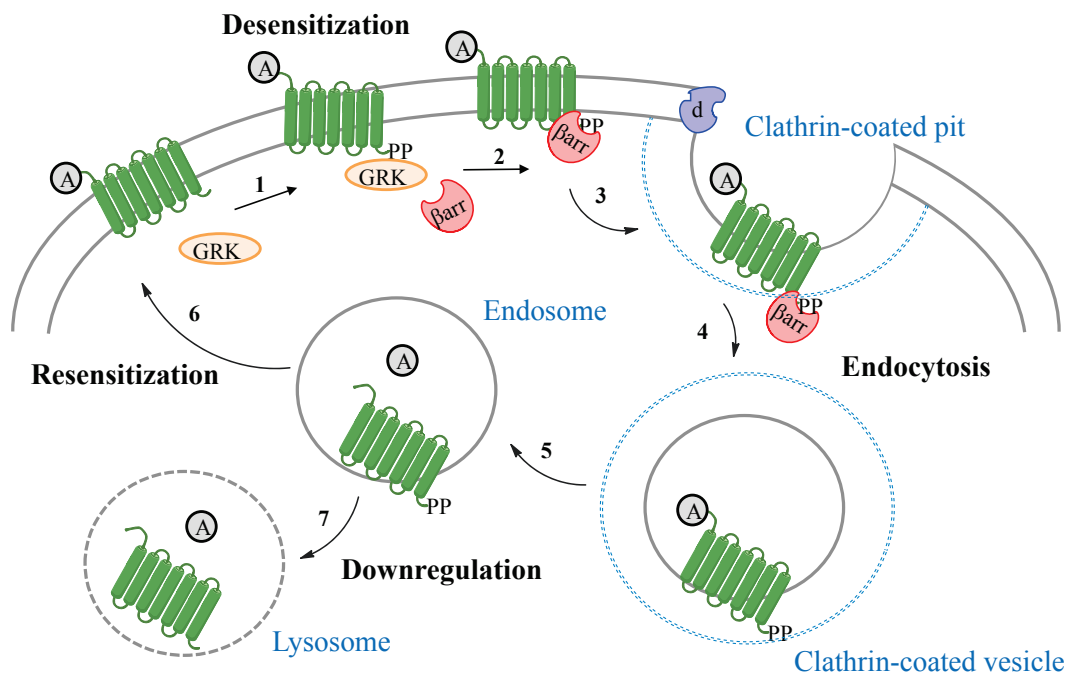
Figure 16. Steps of receptor-ligand internalization by clathrin-mediated endocytosis. Agonist (A) binding, receptor phosphorylation through GRK, and receptor desensitization (1); binding to β-arrestin (βarr) (2) targets the receptor-arrestin-complex to CCP (3) that are pinched-off by the GTPase dynamin (d) (3) to CCV (4) that internalize the receptor-agonist complex into endosomes (5); finally, receptor resensitization and recycling to the cell membrane (6) or downregulation and degradation of the receptor in lysosomes (7) take place.[50b]

2.2.3   Medical application of GPCR-targeting peptides

Due to their internalization, ligands of agonistic peptides can be exploited for specific delivery of cargo (e.g., radioactivity) into cells of interest.[5,52] To identify potentially interesting receptor targets for medical applications, several *in vitro* techniques are available that are based on biochemical (radioligand binding and quantitative receptor autoradiography), immunological (immunoblotting, immunoprecipitation, and immunohistochemistry), and molecular biological methods (northern blotting, reverse transcription/polymerase chain reaction, and RT-PCR).[5,46,53] Amongst them, quantitative receptor autoradiography is most advantageous for the identification of regulatory peptide receptors in pathologic tissue.[5,46,53] For more detailed information concerning the different *in vitro* receptor identification techniques, it is referred to some excellent reviews of Reubi and coworkers, who contributed enormously in this field.[5,46,53] Based on these techniques, the group of Reubi identified several GPCRs of different regulatory peptides to be overexpressed and specifically located in various cancer tissues but not in healthy tissues. They also identified several receptor subtypes of each GPCRs and discovered differences in the receptor binding affinities towards the various ligands.[5,46,52-53] Because of these findings, regulatory peptides are interesting vectors for specific delivery of cargo and can be utilized for targeted imaging and therapy of different cancers (section 2.6, Table 4).[5,37,41,46,53-54] Compared to the relatively low density of peptide receptors in physiological organs, the overexpression of GPCRs of regulatory peptides in numerous cancers is the molecular basis and most important requirement for imaging and targeted therapy with radiopeptides.[15c] If this requirement if fulfilled, regulatory peptides can be used in general in two different ways; either for targeting the mediated functional response of the overexpressed receptors, or to utilize them as binding sites for cytotoxic ligands.[5] In the first case, unlabeled, non-toxic peptide analogs can be used for long-term treatment of cancers to induce a particular biological response, such as growth regulation of cancer cells.[5] Successful clinical utilization of the second application type are targeted molecular imaging or therapy with cytotoxic peptides, carrying cytotoxic drugs or radionuclides.[5]

This thesis is focused on tumor targeting, radiometal-labeled peptides for molecular imaging and peptide-receptor radionuclide therapy of different cancers. The composition, principles of their administration, pharmacodynamics, pharmacokinetics, steps towards their optimization, and selected examples of radiolabeled, tumor targeting conjugates based on regulatory peptides are discussed in the following sections.

2.3   Composition of target-specific, radiometal-labeled peptides

Target-specific, radiometal-labeled peptides are schematically composed of four parts; a targeting peptide, a linker moiety, a bifunctional chelating agent (BFCA), and a radionuclide for imaging and/or therapy (Figure 17).[2,8,15c,16] The targeting peptide serves as a vehicle for specific delivery of the radionuclide to receptors that are overexpressed by the tumor tissue. The BFCA provides both stable complexation of the radiometal and covalent conjugation of it to the targeting peptide. A linker/spacer entity is often incorporated between the peptide and the BFCA. This keeps the chelated radiometal at a reasonable distance from the receptor binding sequence of the peptide and minimizes possible interferences to maintain high binding affinity towards the targeted receptor. A pharmacokinetic modifier may also be built into the linker. The *in vivo* metabolism, binding to the receptor, the biodistribution profile, and the tumor uptake of radiopharmaceuticals can be affected by all four components.[2,8,15c,16] All building blocks will be discussed in more detail in the following sections.
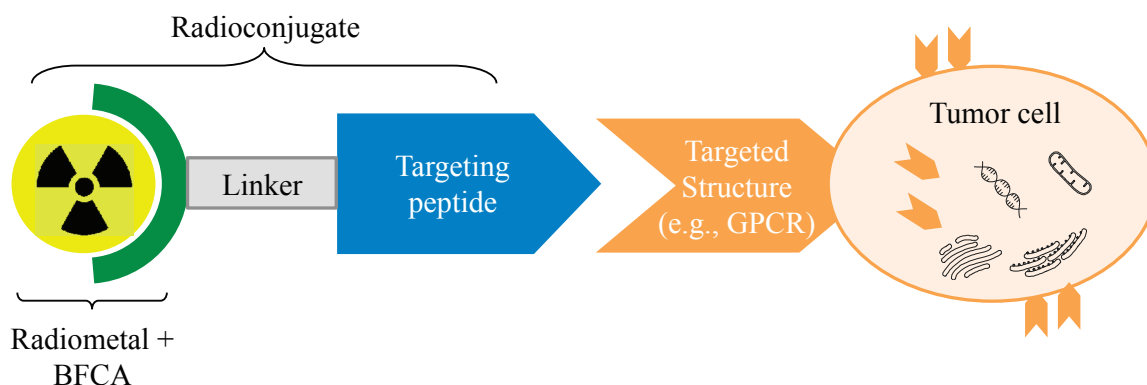
Figure 17. Schematic composition of a targeting radiometal conjugate and targeted GPCRs overexpressed on the plasma membrane of tumor cells.

2.3.1   *Peptides as targeting vectors*

There are several advantages of using regulatory peptides as targeting vectors. The sequences of regulatory peptides can be easily synthesized by solid-phase peptide synthesis (SPPS).[5,26,41] This well established synthetic technique allows easy scale-up, reproducible preparation of chemically well-defined peptides, and facilitates modifications of the peptide sequence in order to optimize their pharmacodynamics (e.g., target affinity and specificity, agonistic or antagonistic effect) and pharmacokinetics (e.g., metabolic stability or clearance pathways).[5,26,41] Chemical modifications, such as incorporation of chelating agents, prosthetic groups, or spacer moieties can be easily realized by SPPS and other bioconjugation techniques.[26] In addition, peptides have high chemical stability, withstanding the harsh conditions that may occur during synthesis or radiolabeling processes.[5,26,41] Compared to other targeting vehicles, such as antibodies, peptides are relatively small in size. Peptides diffuse readily, permitting easy and rapid accessibility to the tumor site after systemic applications and they are usually rapidly cleared from the body, which minimizes the radiation burden on the patient.[5,26,41,55] The favored elimination route is renal clearance but hepatobiliary excretion may also occur, depending on the receptor expression and physicochemical characteristics of the peptide.[5,26,41] In comparison to cytostatic drugs, regulatory peptides are physiologically-occurring and hence, are usually non-toxic.[5] Potential side effects due to their physiological action would only be expected after application of pharmacological doses, as e.g., administration of high doses of non-radioactive compounds for long-term cancer treatments.[5] Radiolabeled peptides for tumor imaging or therapy are administered in very low, subpharmacological concentrations (tracer principle) and thus, pharmacological side effects are usually negligible.[2,5] In contrast to other targeting vectors, such as antibodies, small-sized peptides do usually not lead to antigenicity.[5,41,53,55]

However, there are also limitations. For example, regulatory peptides suffer from poor metabolic stability *in vivo*. They can be rapidly degraded in biological systems by several peptidases present in the serum and most tissues.[5,26,41,55] Increased metabolic stability is important to extend the blood circulation time and enables higher tumor uptake. Thus, metabolic stabilization of the radiopeptide against proteolytic degradation is critical for enhanced accumulation in the targeted tissue.

Internalization and thereby active accumulation and retention of the radioligand in tumor cells have always been considered prerequisites for successful molecular imaging and therapy.[5,52] Interestingly, compared to peptide agonists that internalize, high-affinity peptide antagonists that poorly internalize into tumor cells have recently shown superior tumor binding, tumor uptake, and higher retention rates in preclinical studies.[56] These findings led to a change of paradigm and antagonistic derivatives of

regulatory peptides are now justified as equal or even preferable as potential target-specific radiopharmaceuticals.[19a,37,41,52,57]

The development of targeting peptides can be achieved by rational design and the use of screening libraries.[58] Peptides as targeting vectors can be identified and selected by modifying established endogenous peptides, screening combinatorial peptide libraries, or molecular modeling of peptide-receptor structures.[58d] Established approaches to identify novel targeting peptides include phage display peptide library methods, synthetic library methods requiring deconvolution, the one-bead one-compound combinatorial library methods, and affinity selection methods.[58d] The application of phage display libraries is an especially widely used technique.[58a] This method allows convenient screening of an enormously high number of different phages for the isolation of novel targeting peptides.[58a,d] Detailed information on rational approaches for the discovery of targeting peptides is reviewed in the literature.[58] Examples of different targeting peptides that are applied in nuclear medicine for molecular imaging and therapy of various cancers will be discussed in section 2.6.

2.3.2   *Radiometals as imaging probe or therapeutics*

The choice of the radiometal depends on the medical application of interest, nuclear emission properties, decay mode, radiation type and its energy, physical half-life, stability of any daughter nuclides formed, likely *in vivo* pharmacokinetics of the radio-conjugate, radionuclide production route, cost, and availability. Radiolabeling efficacy, radiochemical yield (RCY), as well as the radiochemical purity (RCP) of the chosen radionuclide and its achievable specific activity are also important considerations when choosing a radiometal for clinical applications.[1-3,6,8,10-11,13,15c]

For imaging, the physical half–life of the radionuclide should complement the pharmacokinetics and be comparable to the biological half-life of the targeting peptide. If the targeting ligand exhibits fast uptake and rapid clearance from the body, a radionuclide with short half-life is ideal. However, the half-life of the radiometal must be long enough to allow convenient preparation of the targeting radiopharmaceutical and application to the patient.[2,6,10-11] The half-life of gamma-emitting radionuclides for imaging applications should allow convenient measurement, dosimetric calculations, and scintigraphy. The radiation burden on the patient is also an important selection criterion for the choice of the radionuclide for molecular imaging.[2,6,10-11]

For radionuclide therapy, most effective tumor cell destruction is achieved by radionuclides that emit high LET radiation in close proximity to the targeted tumor tissue. A physical half-life between 10 hours to 10 days of longer lived radionuclides is appropriate to increase the radiation dose deposited.[6] Additionally, radiometals with stable or very long-lived daughter nuclides should be utilized for radionuclide therapy. This is to prevent uncontrollable irradiation of non-targeted tissue by unstable daughter nuclides should the radiometal become dissociated from the targeting peptide.[2,6,10-11]

Molecular targeting vectors that can be used for both diagnosis and therapy are described as "theranostics".[59] Theranostic agents have recently become of interest in the field of nuclear medicine as they have the potential to be used in patient-individualized treatments, which improve efficacy and cost effectiveness.[60] The theranostic approach is realized by using an identical strategy to radiolabel a targeting vector (e.g., regulatory peptide) with either a diagnostic or therapeutic radiometal.[59] The diagnostic agent enables detection of primary and metastatic diseases by determining the specific phenotype on the molecular level, and assessing the heterogeneity of the tumor tissue. Initial low-dose imaging allows the biodistribution, dosimetry, maximum tolerated dose (MTD, not causing undesired side effects), receptor expression, and clearance to be evaluated.[59] This is then followed by

personalized treatment using the analogous targeting vector labeled with a therapeutic radiometal.[1] In principle, the theranostic approach can predict toxicity and guarantee optimal balance between therapeutic risk and benefit for each individual patient.[60a] Successful clinical examples of the theranostic approach include PET/CT imaging with ^{68}Ga-DOTA-TOC/DOTA-TATE and targeted radionuclide therapy with ^{177}Lu/^{90}Y-DOTA-TOC/DOTA-TATE for the treatments of neuroendocrine tumors (section 2.5.2).[60b] Theranostic bombesin analogs (e.g., AMBA), radiolabeled with ^{68}Ga and ^{177}Lu have been evaluated in humans for the imaging and therapy of metastatic breast, lung, and prostate cancers (section 2.6.1).[44b,60b] Another example is the application of the bisphosphonate-based agent ((4-{[(bis-(phosphonomethyl))-carbamoyl]methyl}-7,10-bis(carboxymethyl)-1,4,7,10-tetraazacyclododec-1-yl) acetic acid (BPAMD)[61] radiolabeled with ^{177}Lu for treatment of skeletal metastases and monitored follow-up care of the patients using ^{68}Ga-BPAMD for PET/CT imaging.[60b]

2.3.3   *Bifunctional chelating agents*

Appropriate bifunctional chelating agents (BFCAs) depend on the metallic radionuclide and its oxidation state. The BFCA should provide both functionalities for convenient coupling with the regulatory targeting peptide and ensure stable complexation of the radiometal (high thermodynamic stability and kinetic inertness). Different radiometals require different coordination chemistries, thus various BFCAs exist with varying donor atoms and ligand frameworks.[1-2,8,11,15a,c,26,41,62] Kinetic inertness of the radiometal-chelate complex *in vivo* is an important factor, since there are many endogenous metal binding proteins in the plasma that may compete with the chelating system for radiometal binding.[1-2,8,11,15a,c,62a] Sufficiently tight binding is crucial to inhibit transchelation of the radiometal to proteins *in vivo*. The release of the radiometal *in vivo* can lead to radiation damage to normal tissue and bone marrow toxicity. Especially ^{89}Zr, ^{90}Y, and ^{177}Lu are recognized "bone seekers".[2,8,15c] Examples of metal-binding serum proteins are superoxide dismutase and transferrin that reveal high affinity for copper and for gallium(III), indium(III), and other metals, respectively.[1-2,8,11,15a,c,62a,63] Kinetic inertness of the radiometal-chelate complex can be estimated *in vitro* by challenging or competition assays against proteins or blood serum during radiopharmaceutical development. However, *in vitro* stability data cannot always predict *in vivo* stability of the radiometal conjugate.[8] Equally important as thermodynamic stability and kinetic inertness of the radiometal-chelate complex are appropriate complexation kinetics under radiochemical labeling conditions, such as low concentrations, limited time, and, in the case of temperature-sensitive biomolecule, labeling at mild temperature.[8,62a] With the exception of brain tracers, the BFCA should also have a high hydrophilicity to enhance the blood-clearance and renal elimination of the radioconjugate.[1-2,8,11,15a,c,26,41,62a]

Each radiometal is unique and characterized by its coordination number, oxidation state, redox stability, hard-soft Lewis acid characteristics, and kinetic inertness. D-block transition metals (e.g., ^{99m}Tc and $^{186/188}$Re) form mainly octahedral complexes and therefore tetradentate to hexadentate chelating systems are often used for complexation of these radiometals.[1-2,8,11,15a,c,62] Lanthanides have a tendency to form eight or nine coordination sites in complexes with ionic character.[1-2,8,15a,62b] Octadentate carboxylate-containing chelates are often used for the hard metal center lanthanides (e.g., ^{177}Lu) to build kinetically inert complexes.[1-2,15a,c,62a] BFCAs for the different ^{99m}Tc cores have already been discussed in section 1.2.3. The most extensively evaluated BFCAs for stable complexation of other radiometals are acyclic or cyclic polyaminopolycarboxylic acid ligands.[1-2,8,11,15a,62,64]

2.3.3.1 Acyclic chelating systems

Radiometal complexation reactions with open-chain polyaminopolycarboxylates can usually be achieved under mild conditions and show fast metal-binding kinetics, which are advantageous when using temperature-sensitive biomolecules and short-lived radiometals, respectively. However, compared to macrocyclic chelators, acyclic chelating systems are usually less kinetically inert.[1-2,8,11,15a,c,62] The most common examples of acyclic chelators in radiopharmaceutical chemistry are ethylene diamine tetraacetic acid (EDTA) and diethylene triamine pentaacetic acid (DTPA) (Figure 18). The hard oxygen donor set and large binding spheres of DTPA are appropriate for stable complexation of large, hard-acid radiometals. DTPA has been widely used for complexation of the radiometals Cu^{2+}, In^{3+}, Y^{3+}, and Ga^{3+}.[1-2,8,15a,c,26,58d,62,64] Three radiopharmaceuticals that are approved by the Food-and-Drug-Administration (FDA) are chelated by DTPA or DTPA analogs, including ^{111}In-DTPA-octreotide (OctreoScan®; for imaging of neuroendocrine tumor), ^{111}In-capromab pendetide (ProstaScint®; for imaging of prostate cancer), and ^{90}Y-ibritumomab tiuxetan (Zevalin®, for treatment of non-Hodgkin's lymphoma).[2,8] To improve kinetic inertness of acyclic BFCA, pre-organized, backbone-rigidified DTPA analogs, such as the MX-DTPA analog tiuxetan or CHX-A"-DTPA (Figure 18) are also described.[1-2,8,15a,c,62] Desferrioxamine B (DFO, Figure 18) is an acyclic chelator widely used for iron chelation therapy.[8] DFO is a useful BFCA as it has three hydroxamate groups for radiometal complexation and a terminal primary amine for bioconjugation. DFO coordinates Ga^{3+} to form radiometal-complexes with high thermodynamic stability that can be conjugated to peptides and small molecules.[8,64] DFO complexes with Zr^{4+} have also been evaluated.[8,64-65] Bifunctional versions of acyclic chelators with isothiocyanate, maleimide derivatives, or activated tetrafluorophenolic ester are commercially available for bioconjugation (Figure 18).[64-65]
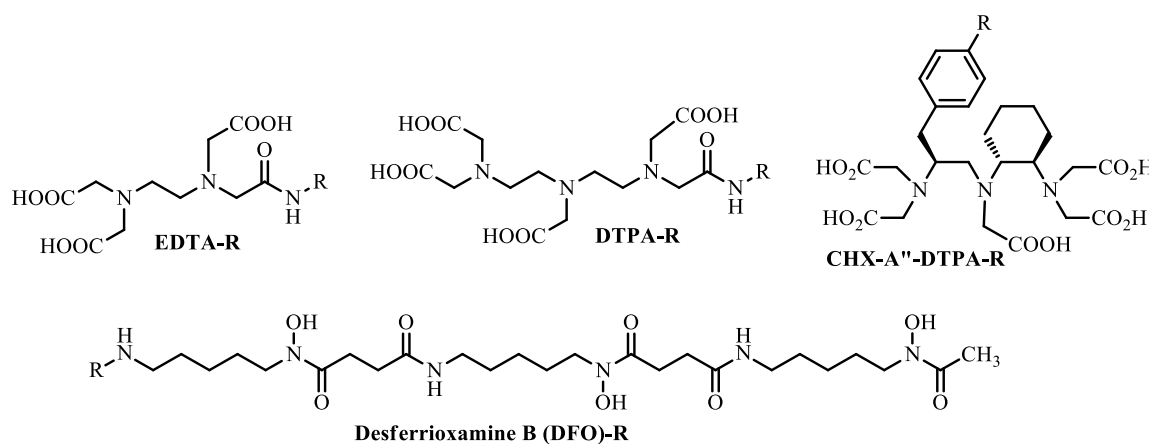
Figure 18. Selected acyclic, bifunctional chelators for radiometal labeling (e.g., ^{68}Ga, ^{89}Zr, ^{90}Y, ^{111}In); R represents a conjugated biomolecule (e.g., peptide).[8,15c,62b,64]

2.3.3.2 Macrocyclic chelating systems

In general, macrocyclic chelators provide thermodynamically more stable and kinetically more inert metal complexes than acyclic chelating agents but often require harsher radiolabeling conditions.[1-2,8,11,15a,c,62] Examples of macrocyclic chelating agents are either cyclen-type or cyclam-type tetraaza or triaza chelators. A ubiquitous chelator for +3-charged radiometals is the cyclen-type 1,4,7,10,-tetraazacyclododecane-1,4,7,10-tetraacetic acid (DOTA, Figure 19). Several M^{3+} radiometals, such as ^{68}Ga, ^{90}Y, ^{111}In, and ^{177}Lu form stable complexes with DOTA derivatives.[1-2,8,15a,c,26,62,64] An example of a cyclam-based macrocyclic chelator is 1,4,8,11-tetraazacyclotetradecane-1,4,8,11-tetraacetic acid

(TETA, Figure 19). TETA has been widely used for complexation of Cu^{2+} in radiopharmaceuticals. $[Cu(TETA)]^{2-}$ complexes are more kinetically inert than $[Cu(DOTA)]^{2-}$ complexes, but still reveal demetallation *in vivo*.[1-2,8,15a,c,58d,62b,64] The cross-bridged TETA analog 1,4,8,11-tetraazabicyclo[6.6.2]-hexadecane-4,11-diyldiacetic acid (CB-TE2A) forms Cu^{2+} radiometal complexes with superior *in vivo* characteristics, but harsh reaction conditions (>90 °C, ~1 h) are needed for radiolabeling.[1-2,8,15a,c,58d,62b,64] The comparably slow formation kinetics of macrocyclic chelators can be overcome by heating or microwave technology.[15c] However, the triaza macrocyclic chelator 1,4,7-triazacyclononane-1,4,7-triacetic acid (NOTA, Figure 19) rapidly forms very stable radiometal-complexes even under mild conditions and is commonly used to form hexadentate complexes with Ga^{3+} and Cu^{2+} radioisotopes.[1-2,8,15a,c,26,58d,62b,64] In DOTA and NOTA, if one of the pendant carboxylic acid arms is used for covalent bioconjugation to a targeting vector, the donor-ability and native binding sphere of the chelator is altered. To overcome this alteration, an extra carboxylic pendant arm is attached, forming 1,4,7,10-tetraazacyclododecane-4,7,10-triacetic acid-1-[2-glutaric acid] (DOTAGA) and NODAGA, respectively (Figure 19).[2,8,15a,c,62b,64] NOTA derived chelator 1,4,7-triazacyclononane-1,4,7-tris[methyl(2-carboxyethyl)phosphinic acid)] (TRAP, Figure 19) also rapidly forms very highly thermodynamically stable complexes with ^{68}Ga in high radiochemical yield.[8]
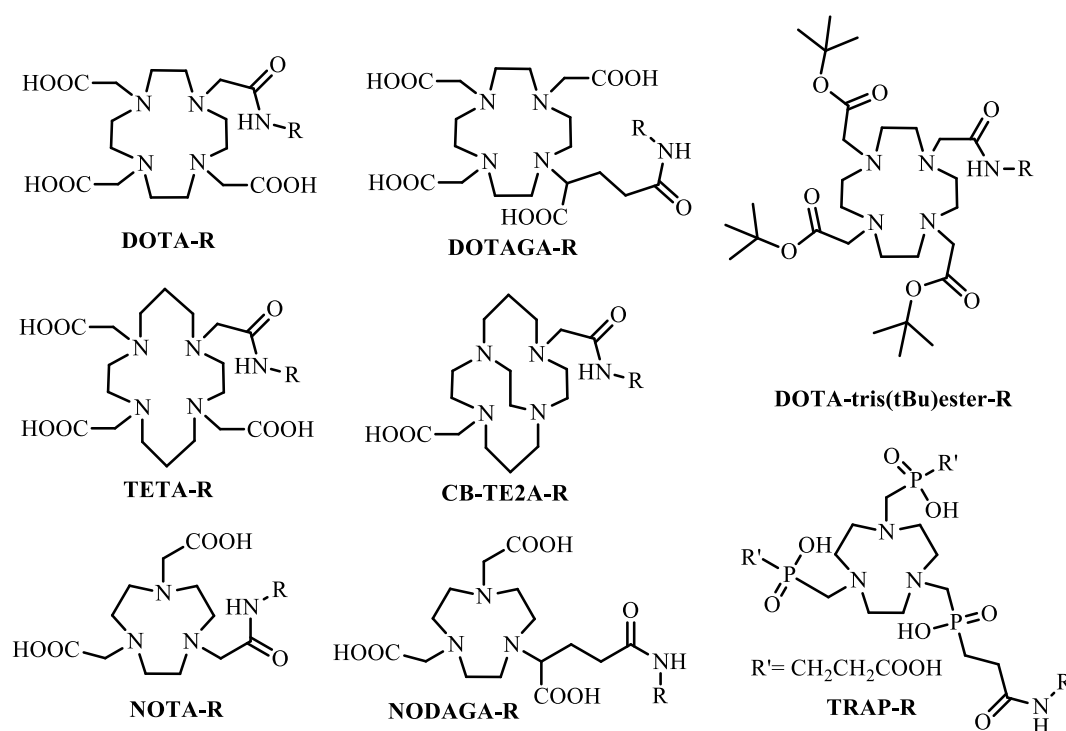
Figure 19. Selected commonly used macrocyclic bifunctional chelators to label peptides (R) with $M^{2+/3+}$ radiometals (e.g., ^{64}Cu, ^{68}Ga, ^{90}Y, ^{111}In, ^{177}Lu, and ^{213}Bi).[1-2,8,15a,c,58d,62b]

The triazole substituted bombesin analogs and the stabilized substance P derivative that are described in chapter V and VI of this thesis, respectively were prepared using the commercial 2-(4,7,10-tris(2-tert-butoxy)-2-oxoethyl)-DOTA (DOTA-tris(tBu) ester, Figure 19) *via* amide bond formation.[66]

2.3.3.3   Bioconjugation

BFCAs contain a conjugation group for covalent attachment of the targeting biomolecule. The BFCA can be conjugated to peptide sequences *via* the primary N-terminal amine or *via* functionalities in the side chain of the amino acids. Examples include ε-amine side chain functionality in lysine, phenol moiety in tyrosine, carboxylate group in glutamic or aspartic acid, and thiol group in cysteine.[8,16] Alternatively, reactive groups can be incorporated into the peptide sequence by chemical modification. Covalent conjugation of BFCAs occurs most often using one of four common conjugation strategies, which make use of N-hydroxysuccinimide (NHS) esters, maleimides, isothiocyanates, or azides/alkynes for click chemistry.[2,8,15a,c,16,62,64,67]

Activated NHS esters form an amide bond with a primary amine of, for example, lysine or the amine group at the N-terminus of the peptide sequence (Figure 20 A). NHS esters show intermediate reactivity but high selectivity for aliphatic amines. A basic pH (pH 8-9) is required for amide bond formation in aqueous media. Advantages of this approach are the stability of the amide bond formed and the versatility of this method, since nearly any molecule containing a carboxylic acid group can be activated to its NHS ester. Activated NHS esters are the most commonly used conjugation group for small biomolecules and proteins.[2,8,15c,16,62,64]

Maleimide as a strong electrophile reacts selectively with thiol-groups from cysteine side chains of biomolecules (peptide, or antibody) by forming a thioether bond (Figure 20 B). Under basic conditions (pH >8) maleimides may hydrolyze to non-reactive maleamic acids. The optimum pH for this conjugation reaction is neutral (pH 7).[2,8,15c,16,62,64]

Isothiocyanates react with primary amines of peptides or proteins to form thiourea bonds (Figure 20 C). To deprotonate the primary amine, more basic reaction conditions (pH 8-9.5) are needed therefore this strategy may not be suitable for conjugation of biomolecules that are alkaline-sensitive. Aromatic isothiocyanates are commonly applied in bioconjugation with DOTA and DTPA analogs.[2,8,15c,16,62,64]

The Cu(I)-catalyzed 1,3-dipolar Huisgen cycloaddition reaction of terminal azides and alkynes, leading to 1,2,3-triazoles ("click reaction")[30] is another commonly used bioconjugation method (Figure 20 D).[8,62b,64,67] This reaction will be discussed in more detail in the context of the "Click-to-Chelate" approach in chapter II, since the dual-targeting radioconjugates described in this thesis (chapter III and IV) are based on this bioconjugation strategy. Application of bioorthogonal copper-free click cycloaddition reactions[68] has also become increasingly popular for the development of radiotracers.[67]
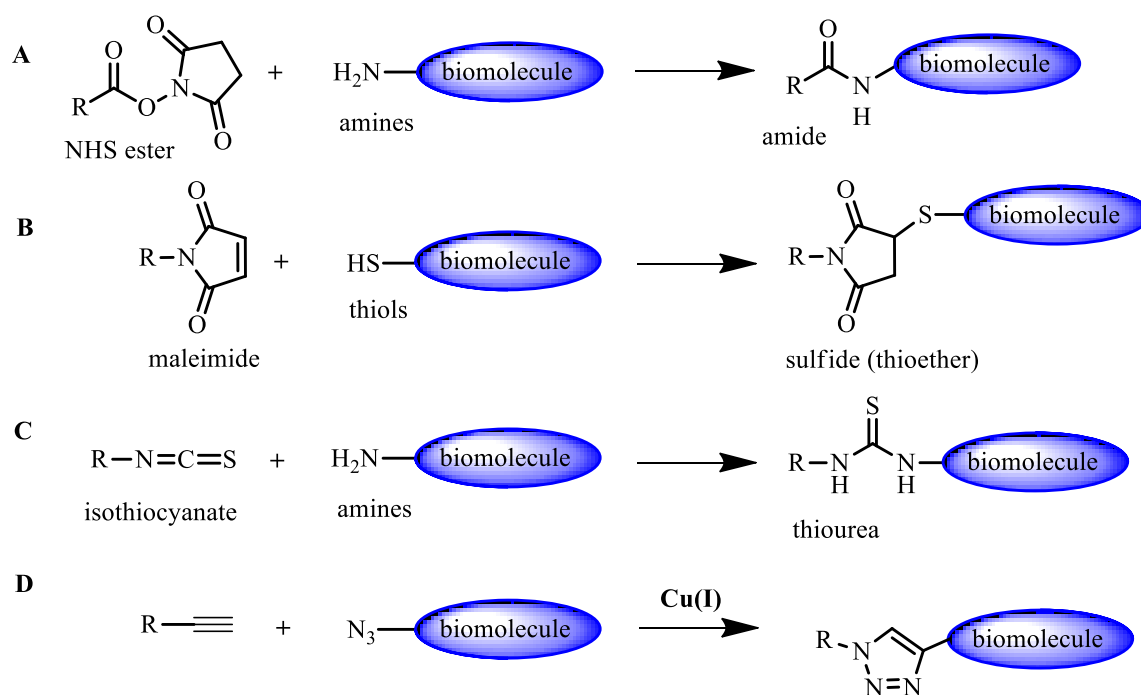
Figure 20. Common conjugation reactions for covalent attachment of a BFCA to a targeting biomolecule; (A) amide, (B) thioether, (C) thiourea, (D) triazole bond.[2,8,15c,16,62,64]

Other examples of conjugation strategies for covalent attachment of BFCAs to the targeting peptides are acid halogenides reacting with primary amines to form amides, haloacetyl groups with thiols to form sulfides (thiother), and thiol groups that couple to thiol functionalities in the peptide under oxidizing conditions by forming disulfide bonds.[2,16] Enzymes, such as e.g., transglutaminases have also been described for site-specific conjugation of chelators to proteins.[69]

Targeting radiopeptides are usually radiolabeled in a "post-labeling" approach; the BFCA is conjugated to the targeting peptide (e.g., by SPPS) before radiolabeling is performed. This sequence is compatible with ready-to-use kit formulations for routine applications in the clinic.[2,15c,16,26]

2.3.4 _Linkers_

A linker provides two orthogonal conjugation sites to connect both the radiometal-chelate complex and the targeting peptide. The linker can serve as a spacer between the targeting peptide and the radiometal to minimize possible binding interference caused by the radiometal-chelator complex and to maintain high binding affinity of the peptide towards the targeted receptor. In order to modify the pharmacokinetics of the conjugate, the linker can be lipophilic, hydrophilic, or carry charges.[70] Examples include hydrocarbon chains of different lengths, hydrophilic amino acid sequences to increase renal clearance (e.g., polyglycine, or polyaspartic acid),[70-71] or polyethylene glycol (PEG) entities to reduce hepatobiliary excretion[72] and potentially improve tumor uptake and tumor-to-background ratios (also section 2.6.1.1).[2,8,15a,c,16,58d] A linker may also be introduced to provide an additional functionality leading to bifunctional radioconjugates. Employing this approach, additional intracellular targeting entities can be introduced into the radioconjugate.[51b,73] Hydrophilic carbohydrates can also be covalently attached through an appropriate linker to increase the tumor-to-liver ratio.[74] Branched linkers with various functional groups can be used for the conjugation of multiple chelating agents[75] leading to higher specific activity.[2,8,15a,c,16,58d]

Bombesin analogs described in chapter III and IV of this thesis are N-terminally conjugated with a linker composed of three β-Ala[71] entities for pharmacokinetic improvements (also section 2.6.1.1). Following the β-Ala-spacer, a lysine precursor was N-terminally conjugated that serves both for conjugation of an entity for intracellular targeting and for chelation of ^{99m}Tc-tricarbonyl using the extended Click-to-Chelate strategy[31c] (chapter II). Bombesin triazole analogs (chapter V) were N-terminally conjugated to a PEG$_4$ linker that has proven useful in increasing tumor uptake.[76]

2.4   Administration of tumor targeting, radiolabeled peptides in nuclear medicine

The established treatment of primary tumors in oncology is surgery, adjuvant chemotherapy, and external radiation therapy.[10,77] Disseminated tumors and metastases are usually treated with chemotherapy, which has particularly high success rates in lymphoma.[10,77] However, chemotherapy is not always curative, but at most palliative and non-targeted chemotherapeutic drugs can cause severe side effects.[10] On the account of this, peptide-based, targeting radiopharmaceuticals are accordingly interesting for providing alternative complementary diagnosis and potential treatments of cancer.[10,77-78] In principle, tumor targeting, peptide-based radiopharmaceuticals are systemically administered into the blood circulation of patients suffering from a GPCR-positive tumor (Figure 21 A). After distribution (Figure 21 B) of the targeting radiotracer in the body, it will selectively bind to the particular GPCR. After binding of the agonistic peptide, the receptor-ligand complex is subsequently internalized through endocytosis (section 2.2.2). Binding or internalization of the radiopeptide leads to selective accumulation of radioactivity in the tumor whereas excess radiotracer and/or its metabolites are rapidly cleared from the blood pool and non-targeted tissue (Figure 21 C). Because of predominant renal excretion, the kidney and bladder show also significant but not persistent uptake of radioactivity.[5,15b,c,41,52-53,79]
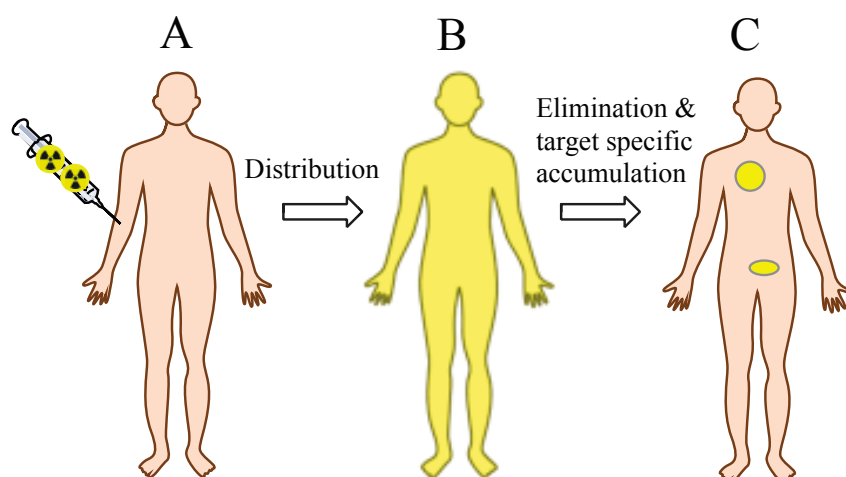
Figure 21. Principle of specific tumor targeting with systematically administered radiopeptides.[15b]

This principle can be diagnostically exploited for detection of tumors and their metastases, treatment planning, and dosimetric calculations of cancer patients, using SPECT or PET. Peptidic radiopharmaceuticals labeled with high energy, low range particle emitters (α, ß⁻), or Auger electron emitting radionuclides can be administered for targeted PRRT.[52-53] The challenge for internal radiation therapy is to balance the delivery of the MTD to the tumor while protecting normal healthy tissue from radiation damage. The mean absorbed doses to tumors and normal organs has to be accurately estimated and individual variation in dose delivery, different metabolism, or diverse receptor density in organs and tissue have to be carefully considered. Individual patient dosimetry is essential for PRRT.[5,15b,c,41,52-53,60a,79]

2.4.1   General considerations for peptide-receptor radionuclide therapy

Cancer patients with multiple inoperable metastases may benefit from PRRT. These patients are usually pretreated with chemotherapy or external radiotherapy.[53] Cancer patients who may benefit from PRRT are selected based on several criteria that have to be fulfilled.[5,53,80] As a basic prerequisite, overexpression of the targeted receptor in the cancerous tissue has to be proven. Ideally, the receptor should be homogeneously distributed at a high density and the occurring receptor subtypes have to be targeted with the administered radioligand.[53] It is important to deliver sufficient radiation dose to the tumor to cause cell death.[6,13] The minimal dose rate for sterilization of the tumor tissue (>0.4 Gy/h; accumulated tumor dose >50 Gy)[6] should be achieved and the tumor cells should be irradiated during the most radiation-sensitive cell cycle phases (section 1.2.2.1).[6] The choice of the radionuclide is based on the size and location of the tumor, type of emitted radiation, emission energies, range of radiation, and physical half-life (section 2.3.2).[5,10,41] Combinations of radionuclides with different energies and particle ranges may result in higher success rates.[41] Tumor response to radiotherapy depends on several factors, such as total absorbed radiation dose, dose rate, tumor radiosensitivity, and intracellular localization of short-range emitting radionuclides.[6,13,14b,53] Targeted radionuclide therapy towards multiple receptors can also be advantageous. The application of, for example, two or more radiotracers at the same time, or multivalent/-specific radiopeptides, can increase the therapeutic dose delivered to the tumor and can also overcome limitations, such as receptor heterogeneity.[5,10,41,53] For brain cancers, a loco-regional application or brachytherapy can be administered to overcome the blood-brain barrier.[53] This method will be introduced later using substance P as a targeting peptide for glioma treatment (section 2.6.2.2).

However, there are also limitations to targeted PRRT. Most importantly, radiation-induced destruction of the surrounding healthy tissue or distant receptor-positive healthy tissues has to be minimal. Radiosensitive tissues, such as bone marrow are limiting the MTD.[6,41,60a] Acute hematological toxicity can occur, especially after high energy ^{90}Y-labeled PRTT.[60a] High bone marrow doses, especially in patients that were pretreated with alkylating chemotoxic agents, may lead to severe side effects, such as myelodysplastic syndrome or leukemia after PRRT.[60a,81] The kidneys are also a dose-limiting organ, due to the excretion of radiopeptides and potential physiological receptor expression. Small-sized radiolabeled peptides are filtered through the glomerular capillaries, become subsequently reabsorbed, and are retained in the proximal tubular cells, leading to high uptake of radioactivity in the kidneys.[37,41,60a,81-82] Thus, the scintigraphic sensitivity for small tumors in the perirenal region is decreased. To reduce the kidney uptake and the risk of potential nephrotoxicity, infusions of positive charged amino acids (L-lysine and L-arginine) are continuously administered before, during, and after radionuclide therapy to block transporter sites in the kidneys.[37,60a,82] It has been shown that cytoprotective drugs, such as amifostine, and low doses of succinylated gelatin or gelatin-based gelofusine as a plasma expander can also decrease the renal uptake of radiopeptides.[37,41,60a,82]

2.5 Development of peptide-based radiopharmaceuticals – from bench to bedside and back to bench

2.5.1   *General aspects to be considered*

First, molecular targets (e.g., GPCRs) with relevance in human diseases, overexpressed at high density and homogeneity at the target site have to be identified. Identification of their peptide ligands and subsequent development of analogs thereof can lead to new radiopharmaceuticals. The required peptide sequence can be synthesized by versatile SPPS. A chelating system or prosthetic group is covalently bound to the peptide sequence for radiolabeling. Radiolabeling has to be conducted with a specific activity and radiochemical yield and purity as high as possible. Biological evaluation of the radiolabeled peptide is followed *in vitro* using appropriate tumor cell lines that overexpress the targeted receptor. *In vitro* evaluation usually includes receptor binding affinity (competition or saturation binding assays), tumor cell uptake (internalization), and efflux (externalization) assays. In case of successful *in vitro* results, the biological behavior of the radiolabeled peptide conjugate is studied *in vivo* for its pharmacokinetics and tumor-targeting efficacy in animal models, mainly xenograft models in mice or rats. *In vivo* evaluation includes biodistribution experiments, molecular imaging, or therapy studies. Important factors for a successful approach are metabolic stability of the radiotracer, sufficient extent of accumulation in the targeted tissue *versus* non-specific uptake in non-targeted, healthy tissue, radiation doses rates deposited, and excretion of radioactivity from the body. After successful preclinical assessment of the targeting radiopeptide, toxicological studies are conducted and an appropriate formulation protocol for clinic production under good manufacturing practice (GMP) conditions has to be established to enable first clinical studies in humans. Clinical trials with volunteers and patients are carried out (phase I-III) to evaluate safety, side effects, and optimal dosage of the targeting radiopeptide. After regulatory approval, the novel radiopharmaceutical is launched on the market and studies follow to assess long-term adverse side effects. As depicted in Figure 22, all these processes are iterative and failure of the radiopeptide in any of the developmental stages leads back to radiopharmaceutical chemistry research to identify and synthesize targeting radiopeptides with improved pharmacodynamics or pharmacokinetics.[5,9-10,15c,19a,41,52-53]
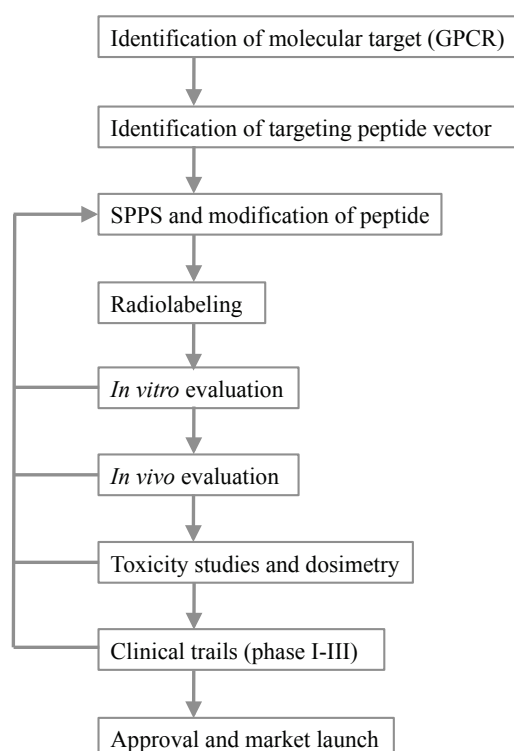

Figure 22. Steps in development of a targeting radiopharmaceutical – from bench to bedside and back to bench.[9-10,41]

This very short summary shows that there is a long way from the design of a targeting, peptidic radiopharmaceutical to its successful administration in the clinics and up to now only very few radiopeptides have succeeded.[8,10,15c,19a,37,41,83] Several radiolabeled peptide derivatives (e.g., somatostatin, bombesin, neurotensin, exendin, gastrin, α-MSH, vasoactive intestinal, and RGD peptides, Table 4) are currently under clinical evaluation for molecular imaging and therapy of different cancers.[5,10,15a,c,18a,19a,26,37,41,43b,52-53,57,58d,83] However, only a somatostatin analog (^{111}In-DTPA-octreotide, OctreoScan®) has so far been approved by the FDA for scintigraphy of neuroendocrine tumors (NET).[8,10,37,41,83] Thanks mainly to the pioneering collaboration of the groups of Reubi, Krenning, Lamberts, Mäcke, and Müller-Brand, who developed and evaluated this and other compounds, radiolabeled somatostatin derivatives are now routinely used for molecular imaging and therapy of NET.[5,15c,43,52-53]

2.5.2   *Somatostatin*

The first and currently most extensively studied examples of radiopharmaceuticals based on regulatory peptides are somatostatin (SST) analogs that are used for targeted imaging and therapy of neuroendocrine tumors.[5,15c,19a,26,37,41,43,52,58d,82-83] The derivatives SST-14 (Table 3) and SST-28 are naturally occurring cyclopeptides, which inhibit the secretion of growth and other hormones and are endogenous ligands of the five SST receptors (SST_1-SST_5).[84] The SST receptor family (predominantly SST_2 receptor subtype) is overexpressed on several tumors, such as NET (pituitary adenomas, islet cell carcinomas, paragangliomas, pheochromocytomas, medullary thyroid carcinomas (MTC), gastrinomas), tumors of the nervous system (astrocytomas, neuroblastomas, meningiomas), lymphomas, breast, and small-cell lung cancer (SCLC), which makes the SST receptors very interesting targets for cancer treatments.[5,52-53,85] However, the endogenous SST derivatives are metabolically unstable (biological half-life <3 minutes) and therefore, their medical use is limited.[15c] To overcome this limitation, several SST analogs with improved metabolic stability and maintained biological activity were developed over the last decades.[15c,42,44,54-55] Shortening of the bioactive peptide sequence and introduction of D-amino acids led to eight AA-containing analog octreotide (OC, Table 3). OC served as a lead compound for the development of several other SST analogs, such as DTPA-octreotide, DOTA-[Tyr^3]-octreotide (DOTA-TOC), DOTA-[Tyr^3, Thr^8]-octreotide (DOTA-TATE) with improved SST_2 receptor affinity, and DOTA-[NaI^3]-octreotide (DOTA-NOC).[15c] These SST analogs can be labeled with either ^{68}Ga, ^{64}Cu, ^{111}In for imaging or for therapy of NET, when labeled with ^{90}Y, or [177]Lu.[15c,41,43,52-53] These and many other different SST analogs (e.g., [99m]Tc- and ^{18}F-labeled SST-analogs, pan-somatostatin derivatives, and SST_2-receptor antagonists) currently under (pre)clinical evaluation are nicely summarized in several reviews.[5,15c,19a,26,37,41,43,52,58d,82-83] Also non-radioactive SST derivatives, such as octreotide, lanreotide, and vapreotide are administrated for long-term treatments of symptoms caused by NET to improve the quality of life of the patients.[5,43b]

Table 3. Selected somatostatin analogs.[15c] Peptide structures of SST analogs, substitutions of the original OC peptide sequence are in bold; 1-NaI: 1-Naphthyl-alanin.

Analogs	Chemical structure
SST-14	Ala-Gly-cyclo(Cys-Lys-Asn-Phe-Phe-Trp-Lys-Thr-Phe-Thr-Ser-Cys)
OC	D-Phe^1-cyclo(Cys^2-Phe^3-D-Trp^4-Lys^5-Thr^6-Cys^7)Thr(ol)^8
TOC	D-Phe^1-cyclo(Cys^2-**Tyr^3**-D-Trp^4-Lys^5-Thr^6-Cys^7)Thr(ol)^8
TATE	D-Phe^1-cyclo(Cys^2-**Tyr^3**-D-Trp^4-Lys^5-Thr^6-Cys^7)**Thr^8**
NOC	D-Phe^1-cyclo(Cys^2-**1-NaI^3**-D-Trp^4-Lys^5-Thr^6-Cys^7)Thr(ol)^8

2.6 Targeting peptides and their receptors for molecular imaging and therapy of different cancers

The successful implementation of radiolabeled SST derivatives into the clinics for visualization and treatment of NET increased interest in the development of other radiolabeled regulatory peptides. In the last two decades, it has been shown that several other commonly occurring cancers overexpress receptors of peptidic hormones.[5,52-53] Other extensively evaluated pairs of regulatory peptides and their receptors suitable for tumor targeting are summarized in Table 4. Further regulatory peptides as potential tumor targeting vectors for future developments are for example, atrial natural peptide, bradykinin, calcitonin, endothelin, luteinizing hormone-releasing hormone, opioid peptides, and oxytocin.[10,15c,41]

Table 4. Peptides, their receptors, and expression pattern for tumor targeting; main receptor subtypes that are overexpressed in human tumors are depicted in bold.[5,10,15a,c,19a,26,37,41,52-53,58d,83]

Targeting peptide	Receptor subtypes	Tumor expression
Somatostatin (SST)	SST_1, **SST_2**, SST_3, SST_4, SST_5	Neuroendocrine tumors, gastroenteropancreatic tumors, non-Hodgkin's lymphoma, paragangliomas, melanoma, breast, brain, renal, SCLC, and MTC
Bombesin (BBS, BBN) Gastrin-releasing peptide (GRP)	BB_1 (NMB-R), **BB_2 (GRP-r)**, BB_3, BB_4	Prostate, breast, gastric, colorectal, pancreas, and SCLC
Substance P (SP)	**NK_1**, NK_2, NK_3	Glial tumors, MTC, pancreas, breast, SCLC, and intra- and peritumoral blood vessels
Neurotensin (NT)	**NTR_1**, NTR_2, NTR_3	Colon, exocrine ductal pancreatic, SCLC, Ewing's sarcoma, astrocytoma, meningioma, prostate, and breast cancer
Neuropeptide Y (NPY)	**Y_1, Y_2**, Y_3, Y_4, Y_5	Breast, ovarian, prostate cancer, neuroblastoma, and lymph node metastases
Glucagon-like peptide (GLP) Exendin	**GLP-1**-R	Insulinomas, gastrinomas, paragangliomas, MTC, and pheochromocytomas
Vasoactive intestinal peptide (VIP)	**$VPAC_1$**, $VPAC_2$	Prostate, breast, colon, stomach, lung, and liver adenocarcinomas
Cholecystokinin (CCK) Gastrin	CCK_1, **CCK_2**	MTC, gastrointestinal stromal cancer, astrocytomas, ovarian, and SCLC
α-melanocyte-stimulating hormone (α-MSH)	**$MC_{1-5}R$**	Melanomas
Arg-Gly-Asp (RGD)	**$α_v β_3$-integrin R**	Breast, lung, ovarian, prostate cancer, melanoma, and glioma

The radiopeptides described in this thesis are based on the regulatory peptides bombesin and substance P, which will be described in the following sections.

2.6.1   Bombesin

The amphibian, amidated tetradecapeptide bombesin (BBS, Table 5) was originally isolated from the skin of the European frog *bombina bombina* in the early 1970s (Figure 23).[86]
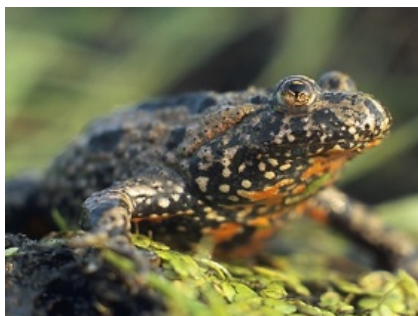

Figure 23. European fire-bellied toad, *bombina bombina*.[87]

Later, other related amphibian peptides were isolated and categorized, for example, ranatesin, and peptides of the phyllolitorin group. Three mammalian BBS-like endogenous peptides, gastrin-releasing peptide (GRP)[88], neuromedin B (NMB), and neuromedin C (GRP-10) were isolated from porcine organs. GRP is a 27 amino acid peptide, which shares the final seven C-terminal residues with bombesin (Table 5).[5,18a,78,89] BBS(7-14) has been shown to be the minimum binding sequence required for receptor recognition, signal transduction, and biological activity.[5,18a,78,89] GRP and NMB are widely expressed in the mammalian nervous and peripheral system. They are especially found in the gastrointestinal (GI) tract and mediate a broad variety of pharmacological and biological responses, such as stimulation of smooth muscle contraction (GI and urogenital tract), GI motility, and the release of several gastrointestinal hormones and neurotransmitters.[5,18a,78,89] The secretion of GRP and NMB induces growth processes in normal human tissues and tumors. These hormones also control several processes of the CNS, such as regulation of circadian rhythm, thermoregulation, anxiety, and behavioral effects.[5,18a,78,89] Binding studies identified four different bombesin receptor subtypes, namely NMB-receptor (BB$_1$)[90], GRP-receptor (GRP-r; BB$_2$)[91], BB$_3$[92] (orphan receptor), and BB$_4$[93] (amphibian only).[89] More detailed information on all bombesin receptor subtypes, their receptor expression, pharmacology, structural basis for receptor binding activation, receptor function, and their broad therapeutic implications is comprehensively described by Jensen *et al.* and others.[5,18a,78,89] Both GRP and BBS have high affinities in the low nanomolar range and show specificity for the GRP-r.[18a,89] The GRP-r consists of 384 AA and belongs to the family of GPCRs (Gα_q).[89] GRP-r expression was studied in humans and mice. The receptor was found in the GI-tract, pancreas, stomach, brain, and adrenal gland in humans, as well as in the brain, pancreas, and the colon, but not in the stomach or small intestine of mice.[89] In addition, the GRP-r is overexpressed in a number of most frequently occurring human tumors, such as prostate, small cell lung, and breast cancer. GRP-receptors are also overexpressed in a variety of other cancers, including head and neck squamous cell, colon, uterine, various CNS, ovarian, gastrointestinal, and renal cancers.[5,18a,52-53,78,89,94] Also BB$_1$ and BB$_3$ receptor subtypes were identified to be overexpressed in different cancer tissues, including intestinal, bronchial, thymic, renal carcinoids, and SCLC (Table 4).[94] Thus, bombesin receptors (especially the GRP-r) are very interesting targets for the management of different cancers.[5,18a,26,52-53,57,78,89] Additionally, several of these cancers have poor prognosis in advanced states of the diseases and current treatments could be improved.[78] The development of bombesin derivatives is a promising approach for imaging of tumors and for targeted delivery of cytotoxic agents for the treatment of cancers mentioned above.[18a,78] This thesis is focused on the specific delivery of radioactivity, but also several non-radioactive approaches have been reported for the targeted delivery of cytotoxic agents using BBS analogs that are coupled to e.g., chemotherapeutic agents (camptothecin, paclitaxel, and doxorubicin), various cytotoxins, immune activating agents, mitochondria-disrupting peptides, photosensitizer for photodynamic therapy, mRNA

interfering agents, or gene-delivery enhancing agents.[15c,18a,77-78,89] However, there are only very limited *in vivo* studies and the effectiveness of these cytotoxic bombesin analogs for the treatment of cancer is under evaluation.[15c,18a,77-78,89]

2.6.1.1   Radiolabeled bombesin derivatives for targeted imaging or therapy of different cancers

Utilizing the unique feature of GRP-r overexpression on the membranes of cancer cells, a large number of radiolabeled bombesin derivatives has been designed and preclinically evaluated. The most common cell line for *in vitro* assays has been the human prostate adenocarcinoma cell line PC-3, overexpressing GRP-r.[95] Typically, PC-3 cells were subcutaneously injected into animals for the induction of xenografts of solid tumors for *in vivo* biodistribution, molecular imaging, and therapy studies.[18a,78] Substantial efforts have been made in the last decades to develop compounds that would achieve high metabolic stability, high GRP-r affinity, high tumor uptake, and long tumor retention in order to enhance molecular imaging quality and therapy efficacy. Different approaches were applied, for example, alterations in the amino acid sequence, comparison of various linker moieties, different chelating/-radiometals systems, or organic radionuclides for utilization of either SPECT (e.g., ^{67}Ga, ^{99m}Tc, ^{111}In) or PET-imaging (e.g., ^{18}F, ^{64}Cu, ^{68}Ga) modalities, or PRRT (^{90}Y, ^{177}Lu, $^{186/188}$Re, ^{213}Bi).[5,15a,c,18a,26,37,41,53,57,58d,89] There has been much progress in this field and it is far beyond the scope of this thesis to comprehensively cover all of the radiolabeled bombesin-based conjugates described in the literature. Some excellent reviews cover the huge variety of radiolabeled bombesin derivatives evaluated.[5,15a,c,18a,26,37,41,53,57,58d,83,89] In the following section, only some selected highlights and examples relating to the bombesin derivatives described in this thesis will be emphasized.

Radiolabeled BBS analogs are based either on the full-length BBS(1-14) sequence or the minimum binding sequence of the C-terminus (BBS(7-14) or BBS(6-14), Table 5).[18a] Van de Wiele *et al.* reported first proof of the GRP-r targeting concept *in vivo* in a clinical study by administration of ^{99m}Tc-RP527 (Table 5) to ten patients suffering from metastatic prostate or breast cancer.[96] Specific uptake was reported in breast (67%) and prostate (25%) carcinomas by SPECT and no short-term side effects were described.[96]

Influences of different spacer moieties were evaluated in several ^{99m}TcO-N$_3$S-X-BBS(7-14) analogs (N$_3$S: dimethylglycyl-L-seryl-L-cysteinglycinamide) with varying length of hydrocarbon linkers (X: no spacer, β-Ala, 5-aminovaleric acid, 8-aminoocatanoic acid, or 11-aminoundecanoic acid).[97] Spacers with between three and eight carbon atoms do not adversely affect agonistic binding to GRP-receptors. β-Ala linker revealed highest uptake in the pancreas (GRP-r-positive organ in mice). Increasing the size of the linker resulted in decreased pancreas uptake.[97] Natural BBS has a biological half-life of about 2-3 min *in vivo*.[15c] Therefore, more metabolic stable analogs have to be developed for potential clinic administration to cancer patients.[15c] In order to increase the metabolic stability *in vivo* and to reduce the formation of unwanted side products, e.g., oxidation of the oxidation-sensitive C-terminal methionine (Met) to sulfoxide during radiolabeling, García-Garayoa *et al.* reported the replacement of Leu[13] by cyclohexylalanine (Cha) and Met[14] by norleucine (Nle), respectively.[71] They also introduced a linker of two ß-Ala moieties, conjugated to the (N$^\alpha$His)Ac chelator for stable complexation of $[^{99m}Tc(CO)_3(H_2O)]^+$ (BBS-38, Table 5).[71] The substitution of Leu[13] by Cha increased the metabolic stability and improved tumor uptake, while maintaining high receptor affinity to the GRP-r. Introduction of the polar (ß-Ala)$_2$-linker led to improved pharmacokinetics (increased tumor-to-blood/kidney/liver ratios) by compensating for the high lipophilicity of the ^{99m}Tc-tricarbonly-His complex.[71] To decrease further the lipophilicity of the tricarbonyl core, Schweinsberg *et al.* introduced

hydrophilic carbohydrate moieties (shikimic acid, glucose derivatives) to lysine or the propargylglycine linker.[74a] Glycation of radiolabeled [Cha^{13},Nle^{14}]BBS(7-14) analogs resulted in reduced abdominal accumulation, increased tumor uptake, and improved tumor-to-background ratios *in vivo*.[74a] García-Garayoa *et al.* also evaluated the influence of molecular charge on the biodistribution of ^{99m}Tc-tricarbonyl labeled [^{13}Cha,^{14}Nle]BBS(7-14) analogs.[70] They introduced different polar spacers containing β-amino acids with either positively charged $β^3$-homolysine ($β^3$hLys), neutral $β^3$-homoserine ($β^3$hSer), or negatively charged $β^3$-homoglutamic acid ($β^3$hGlu) between the BBS-analogs and the ($N^α$His)Ac chelator.[70] They concluded that both the polarity and charge influence the biodistribution profile. Positive charge ($β^3$hLys) resulted in increased kidney uptake and unfavorable biodistribution, whereas uncharged $β^3$hSer-analogs revealed significantly improved tumor-to-tissue ratio. One negative charge of the $β^3$hGlu-BBS analog significantly increased both the tumor uptake and the tumor-to-tissue ratios.[70] Mindt *et al.* reported the use of CuAAC for the assembly of bombesin conjugates and simultaneous synthesis of a tridentate chelating system for stable complexation of the ^{99m}Tc-tricarbonyl core.[29,31c,98] This elegant and versatile "Click-to-Chelate"[29] methodology will be described in more detail in chapter II.

BBS-analogs with macrocyclic chelating systems have also been evaluated. The first radiolabeled BBS analog for therapeutic cancer treatment was ^{177}Lu-AMBA, based on BBS(7-14) conjugated to DOTA by a glycine-4-aminobenzoyl spacer (Table 5) that showed high affinity to both GRP- and BB$_1$ receptor.[44a] Because of its favorable affinity, internalization, and retention profile *in vivo*, a small phase I clinical study was conducted in seven patients for treatment of prostate cancer.[44b] However, uptake was not detected in all lesions of the patients and adverse side effects (diarrhea, nausea, abdominal convulsions) was observed.[44b] Zhang *et al.* incorporated a PEG$_4$ spacer between BBS(7-14) and DOTA (DOTA-PESIN, Table 5).[76] ^{67}Ga/^{177}Lu-DOTA-PESIN showed a favorable biodistribution profile in tumor-bearing mice.[76] Wild *et al.* compared α-emitting ^{213}Bi-DOTA-PESIN with ^{213}Bi-AMBA and ^{177}Lu-DOTA-PESIN in PC-3 tumor-bearing mice.[99] At the MTD, both ^{213}Bi-radiolabeled BBS-analogs were superior to ^{177}Lu-DOTA-PESIN for prostate cancer treatment, and ^{213}Bi-DOTA-PESIN showed a better safety profile in terms of kidney toxicity than ^{213}Bi-AMBA.[99] The authors conclude that administration of ^{213}Bi-DOTA-PESIN could be an important strategy for PRRT of recurring prostate cancer.[99] Recently, multimers of PESIN, radiolabeled with ^{68}Ga-NODAGA were reported with substantially improved binding avidities to the GRP-r *in vitro* and increased tumor uptake and higher tumor-to-background ratios than monomeric DOTA-PESIN radioconjugate in PC-3 tumor-bearing mice.[100]

Since BB$_1$ and BB$_3$ receptor subtypes are also overexpressed in several cancers,[94] Zhang *et al.* reported ^{111}In, ^{90}Y, and ^{177}Lu radiolabeled pan-bombesin conjugates[101] derivatives, which bind to all three mammalian bombesin receptor subtypes.[102] Analogs BZH1 and BZH2 (Table 5) revealed high binding affinity to all bombesin receptor subtypes in the low nanomolar range and specific and high uptake in AR4-2J tumor-bearing rats.[102] Schuhmacher *et al.* incorporated a PEG$_2$ linker into BZH3, radiolabeled with ^{68}Ga (Table 5).[103] High uptake and improved tumor-to-tissue ratio were reported in biodistribution and PET imaging experiments with AR42J tumor-bearing mice.[103] ^{68}Ga-BZH3 was compared to 2'-[^{18}F]fluoro-2'-deoxyglucose (^{18}F-FDG) for PET imaging of patients with gastrointestinal stromal tumors (GIST).[104] Since one recurrent tumor of the stomach could only be detected with ^{68}Ga-BZH3, the authors conclude that ^{68}Ga-BZH3 may be helpful for tumor diagnosis in a subgroup of GIST patients where PET imaging with ^{18}F-FDG gives false negative results.[104]

In addition, radiolabeled bombesin antagonists were developed and preclinically evaluated. In 2003 Nock *et al.* reported [^{99m}TcO$_2$]$^+$-demobesin 1 (Table 5), a very potent BBS-antagonist that showed high affinity to the GRP-r and high binding to PC-3 cells *in vitro*.[56a] Compared to agonists, such as ^{99m}Tc-demobesin 4, ^{111}In-DOTA-PESIN, and ^{111}In-AMBA, ^{99m}Tc-demobesin 1 displayed substantially

improved and prolonged uptake in PC-3 tumor-bearing mice, which lead to a change of paradigm in terms of necessity for tumor cell internalization of radioconjugates.[105] Meanwhile, there is rapid progress in the field and several other BBS-antagonists were preclinically evaluated.[15c] Abiraj *et al*. reported another potent bombesin antagonist, AR (Table 5) conjugated to DOTA, 6-carboxy-1,4,7,11-tetraazaundecane (N4), NODAGA, and CB-TE2A for radiolabeling of ^{111}In, ^{99m}Tc, ^{68}Ga, and ^{64}Cu, respectively.[106] The antagonists were evaluated in biodistribution experiments in PC-3 tumor-bearing mice and imaging with SPECT and PET were performed.[106] The different chelators employed influenced receptor affinity towards GRP-r, uptake to the tumor, and pharmacokinetics of the conjugates. All four radiolabeled bombesin analogs showed promising *in vitro* and *in vivo* results.[106] ^{64}Cu-CB-TE2A-AR06 was most promising and evaluated further in a clinical study for PET-imaging of four patients suffering from prostate cancer.[107] Also ^{18}F-labeled analogs of BBS-antagonist were reported,[15c] of which ^{18}F-BAY86-4367 (Table 5) showed most favorable preclinical results and first clinical studies are underway.[108] Recently, a first clinical study was reported using the analog ^{68}Ga-BAY86-7548 (Table 5).[109] PET-imaging of prostate cancer with ^{68}Ga-BAY86-7548 was very promising, resulting in high specificity, sensitivity, and accuracy for the detection of primary prostate cancers and metastatic lymph nodes.[109] Combining bombesin agonists and antagonists, structurally defined radiolabeled hybrid conjugates based on oligoproline scaffolds were recently designed.[110] Amongst those, a hybrid-analog revealed the highest reported total cellular uptake for BBS derivatives in PC-3 cells.[110] The hybrid constructs combined the advantageously high internalization of agonists with the high tumor binding of antagonists, leading to superior tumor uptake and long retention *in vivo*.[110]

Table 5. Selected bombesin analogs; peptide structures based on the BBS(7-14) binding sequence, substitutions in the bombesin analogs are in bold.[15c,18a,41,83]

Analogs	Chemical structure
GRP[88]	Ala^1-Pro-Val-Ser-Val-Gly-Gly-Gly-Thr-Val-Leu-Ala-Lys-Met-Try-Pro-Arg-Gly-Asn-His-Trp^{21}-Ala-Val-Gly-His-Leu-Met^{27}-NH_2
BBS, BN	$pGlu^1$-Gln^2-Arg^3-Leu^4-Gly^5-Asn^6-Gln^7-Trp^8-Ala^9-Val^{10}-Gly^{11}-His^{12}-Leu^{13}-Met^{14}-NH_2
BBS(7-14)	Gln^7-Trp^8-Ala^9-Val^{10}-Gly^{11}-His^{12}-Leu^{13}-Met^{14}-NH_2
RP527	N_3S-Gly-5-Ava-[Gln^7-Trp^8-Ala^9-Val^{10}-Gly^{11}-His^{12}-Leu^{13}-Met^{14}-NH_2]
BBS-38	$(N_\alpha His)$Ac-β-Ala-β-Ala-[Gln^7-Trp^8-Ala^9-Val^{10}-Gly^{11}-His^{12}-**Cha^{13}**-**Nle^{14}**-NH_2]
AMBA	DOTA-Gly-4-aminobenzoyl-[Gln^7-Trp^8-Ala^9-Val^{10}-Gly^{11}-His^{12}-Leu^{13}-Met^{14}-NH_2]
DOTA-PESIN	DOTA-PEG_4-[Gln^7-Trp^8-Ala^9-Val^{10}-Gly^{11}-His^{12}-Leu^{13}-Met^{14}-NH_2]
BZH1/BZH2	DTPA/DOTA-GABA-[**D-Tyr^6**-Gln^7-Trp^8-Ala^9-Val^{10}-**$β$-Ala^{11}**-His^{12}-**Thi^{13}**-**Nle^{14}**-NH_2]
BZH3	DOTA-PEG_2-[**D-Tyr^6**-Gln^7-Trp^8-Ala^9-Val^{10}-**$β$-Ala^{11}**-His^{12}-**Thi^{13}**-**Nle^{14}**-NH_2]
Demobesin 1	N_4^{0-1}-bzlg^0-[**D-Phe^6**-Gln^7-Trp^8-Ala^9-Val^{10}-Gly^{11}-His^{12}-**Leu-$NHEt^{13}$**]
Demobesin 4	N_4-[**Pro^1**-Gln^2-Arg^3-**Tyr^4**-Gly^5-Asn^6-Gln^7-Trp^8-Ala^9-Val^{10}-Gly^{11}-His^{12}-Leu^{13}-**Nle^{14}**-NH_2]
AR	PEG_4-[**D-Phe^6**-Gln^7-Trp^8-Ala^9-Val^{10}-Gly^{11}-His^{12}-**Sta^{13}**-**Leu^{14}**-NH_2]
BAY86-4367	3-cyano-4-^{18}F-fluorobenzoyl-Ala(SO$_3$H)-Ala(SO$_3$H)-Ava-[Gln^7-Trp^8-Ala^9-Val^{10}-**$NMeGly^{11}$**-His^{12}-**Sta^{13}**-**Leu^{14}**-NH_2]
BAY86-7548	DOTA-4-amino-1-carboxymethyl-piperidine-[**D-Phe^6**-Gln^7-Trp^8-Ala^9-Val^{10}-Gly^{11}-His^{12}-**Sta^{13}**-**Leu^{14}**-NH_2]

N_3S: *N,N*-dimethyl-Gly-L-Ser-L-Cys(acm), Ava: 5-aminovaleric acid, PEG_4: 15-amino-4,7,10,13-tetraoxapentadecanoic acid, GABA: γ-aminobutyric acid, N_4: 6-carboxy-1,4,8,11-tetraazaundecanetetramine, bzlg: benzylaminodiglycolic acid, Sta: statin ((3*S*,4*S*)-4-amino-3-hydroxy-6-methylheptanoic acid), Ala(SO$_3$H): L-cysteic acid.

Despite the enormous quantity of reported radiolabeled bombesin derivatives that were preclinically evaluated, only a very limited number of clinical trials has been reported. Most of them included imaging studies (12 studies; 83% based on ^{99m}Tc and 17% based on ^{68}Ga analogs)[18a] and so far, only one bombesin derivative, ^{177}Lu-AMBA, was evaluated in a phase I study with a small number of prostate cancer patients for targeted therapy.[44b]

Due to the discussed findings, bombesin derivatives described in this thesis are based on the oxidation-insensitive [Nle[14]]BBS(7-14) sequence. Compounds reported in chapter III and IV (dual-targeting analogs) are N-terminally conjugated with a polar linker of three ß-Ala units and assembled by "Click-to-Chelate"[29] strategy for radiolabeling with ^{99m}Tc-tricarbonyl. Triazole-BBS derivatives, described in chapter V (triazole-scan) are modified with a polar PEG$_4$-spacer and conjugated to macrocyclic DOTA for the stable complexation of [177]Lu.

2.6.2   *Substance P*

The neuropeptide substance P (SP; Arg-Pro-Lys-Pro-Gln-Gln-Phe-Phe-Gly-Leu-Met-NH$_2$) is a member of the tachykinin (TK) peptide family sharing the C-terminal sequence Phe-X-Gly-Leu-Met-NH$_2$.[111] Substance P was already discovered in the early 1930s, followed by the exploration of the mammalian tachykinins neurokinin A (NKA) and neurokinin B (NKB) in the mid-1980s.[111] Tachykinins are found in neuronal and glial cells of the human central and peripheral nervous system.[111] SP, NKA, and NKB are all ligands of the tachykinin receptor family, consisting of three mammalian GPCRs, named NK$_1$, NK$_2$, and NK$_3$.[111] Their receptor affinities are varying, as the NK$_1$ receptor (NK$_1$R) has the highest affinity and preference for substance P, NK$_2$R for neurokinin A, and NK$_3$R for neurokinin B.[111] The NK receptors are involved in multiple intracellular signaling pathways, such as IP3 and cAMP-signaling mechanism (section 2.2.1). Several (patho)physiological effects are mediated through TKs, including regulation of synaptic transmission, nociception, and neuroimmunomodulation. TKs effect as well smooth muscle contraction, cardiovascular function, respiration control, and emesis.[111] The NK$_1$ receptors are broadly distributed in the central and peripheral nervous system in human and in several other species. It has been shown that two different isoform of the NK$_1$R exist that are varying in the length of their C-terminus. A full-length form, containing 407 amino acids and a truncated isoform, containing only 311 AA have been isolated that reveal differences in biological function.[111-112] Compared to the full-length isoform, SP shows less binding affinity to the truncated NK$_1$R isoform, which is less effective in stimulation of an electrophysiological response.[111-112] SP acts as a immune cells activator, neurotransmitter, neuromodulator, and is especially involved in the transmission of peripheral pain stimuli.[111b] SP reveals intrinsic neuroprotective and neurodegenerative characteristics and thus, acts as non-specific growth factor for tissues of the peripheral and central nervous system. SP derivatives play an important role for neurodegenerative disorders, such as Alzheimer's disease, Parkinson, and Amyotrophic Lateral Sclerosis.[111b] Substance P is also associated in control of emesis, inflammatory conditions, regulation of mood, affective behavior, anxiety, and depression.[111b,113] Thus, SP-antagonists might be potential antiemetic, antiinflammative, analgetic, anxiolytic, and antidepressive agents.[111b,113] NK$_1$R-antagonist aprepitant is FDA approved and clinically administered for cytostatic induced nausea.[111b] SP and its preferred NK$_1$-receptor are also involved in development and progression of cancer cells.[111b,114] It has been shown that NK$_1$R is overexpressed in malignant gliomas, but not in healthy neighboring brain tissue or benign neoplasms.[53,115] Hennig *et al.* proved NK$_1$R expression in glioblastoma multiforme, astrocytoma, medullary thyroid carcinoma, ganglioneuroblastoma, and breast carcinoma.[115] Thus, targeting of NK$_1$R with radiolabeled SP derivatives is interesting for diagnosis and therapy of cancers, especially of gliomas.[53,83,115] In 1996,

van Hagen *et al.* reported radiolabeled SP analog ^{111}In-DTPA-[Arg^1]-SP for visualization of the thymus in 12 patients suffering from immune-mediated diseases.[116] The radiolabeled SP analog revealed rapid washout, a short biological half-life, and uptake of radioactivity was found in all patients in the *mammae*, spleen, in the excretory organs.[116] A high uptake in the thymus was reported and the authors concluded ^{111}In-DTPA-[Arg^1]-SP as useful for imaging of the thymus in immune-mediated diseases.[116] Uptake in non-targeted tissue, a short biological half-life, and rapid clearance may be acceptable for molecular imaging.[117] However, these characteristics may impede systemic treatments of cancer with radiolabeled SP-derivatives where efficient radiation dose in the targeted tissue has to be achieved, while protecting non-targeted healthy tissues.[66] Circumventing these obstacles, loco-regional administration of radiolabeled SP analogs was clinically evaluated for glioma therapy,[83,118] which will be discussed in the following sections.

2.6.2.1   *Gliomas*

High grade gliomas (glioblastoma multiforme, GBM, WHO IV °)[119] are the most common, aggressive, proliferative, and rapidly growing type of intrinsic brain tumors, leading to poor prognosis for the patient. There is currently no cure and only little progress has been achieved in the control of the disease.[114a,119-120] GBM shows very high cell density and sometimes widespread infiltration of surrounding tissues.[119,120b,c] The current therapeutic standard for GBM is surgical resection and combined radio- and chemotherapy. [119,120b,c] A high extent of surgical resection is positively correlated with prolonged periods until tumor recurrence.[118a,b,119,120b] However, certain obstacles have to be overcome for the successful treatment of gliomas, for example, incapability of complete tumor resection in order to preserve functionally important brain areas.[118a,b] Another hindrance is poor penetration of the blood-brain barrier of most cytostatic drugs and accordingly only insufficient concentration of the drug in the desired tumor location can be achieved.[114a,120b] Therefore, new delivery techniques have to be established that allow glioma therapy beyond the blood-brain barrier and target glioma cells without affecting normal healthy surrounding tissue.[114a,120a,b]

2.6.2.2   *Loco-regional tumor targeting of gliomas using radiolabeled peptides*

Most glioblastomas occur as unifocal lesions (90%) that recur at the primary site and therefore, therapy of the surrounding infiltration zone is equally important.[83,118c,121] To overcome insufficient local distribution through the blood-brain barrier, loco-regional drug administration of therapeutic, targeting radiopeptides has been evaluated.[53,83,118d,e] Low-grade gliomas are known to express the SST_2 receptor (Table 4). Therefore, ^{90}Y-DOTA-TOC was locally administered as novel therapeutic application of diffusible brachytherapy through an implanted catheter system (port-a-cath device, Figure 24) into the tumor or resection cavity of glioma patients in a clinical pilot study.[118d,e]
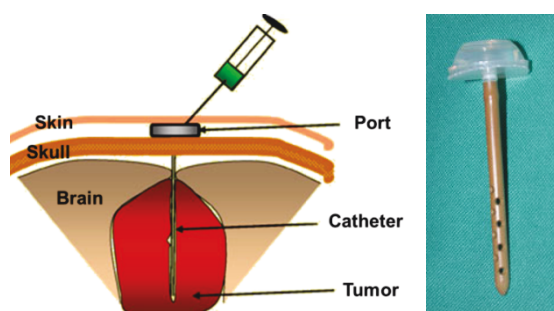

Figure 24. Intratumoral catheter system (port capsule and connected intraventricular catheter).[118b]

Compared to systemic application, this technique resulted in enormous improved tumor uptake and rapid intratumoral distribution.[118d,e] ^{90}Y-DOTA-TOC was well tolerated and no severe adverse side effects occurred.[118d,e] However, glioblastomas cannot be efficiently targeted with radiolabeled DOTA-TOC, since the levels of SST_2 receptor expression is gradually lost with malignancy progression.[85,118d,e] Primary malignant gliomas and glioblastomas overexpress NK_1 receptors and thus, can be targeted with radiolabeled SP derivatives.[5,53,83,115] Kneifel and Cordier *et al.* reported the use of radiolabeled DOTA- and DOTAGA-SP derivatives that showed high affinity in the low nanomolar range to the NK_1R.[118c] The radioconjugates were rapidly internalized into tumor cells and showed good metabolic stability.[118c] ^{90}Y, ^{177}Lu, or ^{213}Bi labeled DOTAGA-SP radioconjugates were locally applied into the tumor or resection cavity of 20 patients (glioma WHO°II-IV) in a clinical pilot study.[118c] Extensive radiation necrosis of the tumor tissue could be observed, which enabled and considerably facilitated subsequent surgical resection due to improved demarcation of tumor margins and reduced intraoperative bleeding, caused by radiation effects on tumor vasculature.[118c] Local radionuclide therapy of NK_1 receptors with SP derivatives was superior than targeting of SST receptors with ^{90}Y-DOTA-TOC.[118c] To improve the metabolic stability of radiolabeled SP derivatives, while maintaining high affinity to the NK_1R, several radiolabeled SP derivatives have been developed and preclinically evaluated.[66] Compared to ^{111}In-DOTA-SP, ^{111}In-DOTA-[Thi^8,Met(O$_2$)^{11}]-SP and ^{111}In-DOTAGA-[Thi^8,Met(O$_2$)^{11}]-SP displayed increased metabolic stability and binding affinity to the NK_1 receptor.[66] To spare surrounding healthy brain tissue, short range ^{213}Bi-DOTA-[Thi^8,Met(O$_2$)^{11}]-SP was locally administrated to five glioma patients (WHO II°-IV°).[118a] The groups of Merlo, Müller-Brand, and Mäcke also evaluated ^{90}Y-DOTAGA-SP as neoadjuvant treatment to assess feasibility, extent of possible tumor resection, functional clinical outcome, and toxicity.[118b] It was possible to achieve a high extent of tumor resection (in average 96%) and the authors conclude this therapeutic approach as potentially beneficial to prolong recurrence time, improve overall time of survival, and quality of life of glioma patients.[118b]

2.7 Ideal peptide-based radiopharmaceuticals for targeted imaging and therapy of cancer

Radiopeptides are very promising for targeted diagnosis and therapy of various cancers, overexpressing their corresponding GPCRs.[5,8,10,15a,c,19a,26,37,41,52-53,58d,83] Despite the enormous effort that has been made in radiopharmaceutical chemistry for the development of targeting radiopeptides in the last decades, only somatostatin derivatives are now routinely administered for diagnosis and therapy of NET and only one SST analog got approved by the FDA so far.[8,10,37,41,83] There is still a need for the improvement of targeting radiopeptides for successful routine treatments of cancers in nuclear medicine.[8,10,19a,37,41,83] Several crucial requirements needed to obtain ideal targeting radiopeptides to enhance the quality of molecular imaging and the efficacy of radionuclide therapy of cancers are summarized in Table 6.

In regard to pharmacodynamics, the radiopeptide should display specific and very high affinity in the low nanomolar range towards its targeted GPCR. High affinity to the receptor decreases background and non-specific binding and allows administration of the radiopharmaceutical in very low concentrations. Since some regulatory peptides are pharmacologically very potent (e.g., VIP, exendin),[41] the applied dose of the radiopharmaceuticals should be in the subpharmacological level to reduce any risk of pharmacological side effects. High specific activity and high radiochemical purity of the radiopeptide are essential to deliver sufficient amounts of radioactivity in subpharmacological peptide concentrations. Ideal pharmacokinetic and biodistribution profiles include rapid clearance

from the blood and non-targeted tissue, fast distribution, efficient penetration of the tumor, high accumulation and retention in the tumor, and fast renal clearance of excess of the radiopharmaceutical or metabolites thereof. Therefore, sufficient metabolic stability of the radiopeptides *in vivo* and suitable radio-physical properties of the radionuclides are crucial. Ensuring these requirements, high tumor-to-background ratios can be obtained, leading to improved quality of molecular imaging and enhanced radionuclide therapy, while reducing the radiation burden on surrounding healthy tissues.[1,5,8,10,15a,19a,26,37,41,52-53,57,58d,82-83]

Table 6. General requirements for radiolabeled peptides as targeting vectors.[1,5,8,10,15a,19a,26,37,41,52-53,57,58d,82-83]

Specific targeting of a relevant biological structure (e.g., GPCRs)
Homogenous overexpression of the biological target in diseased but not in normal tissues
Small in size (leading to rapid blood clearance, good tissue penetration, and renal elimination)
Easy synthesis by SPPS and amenable to chemical modifications (e.g., for pharmacokinetic modifications and conjugation of the BFCA)
Convenient radiolabeling with high specific activity, RCY, and RCP (favored in a kit formulation in aqueous solutions)
Thermodynamically stable and kinetically inert complexation of the radiometal by an appropriate BFCA
Favorable pharmacokinetics (rapid clearance from the blood and non-targeted tissues, fast, high, and prolonged tumor uptake, low non-specific accumulation in the background, and fast renal clearance)
High metabolic stability to allow distribution and sufficient tumor accumulation
Specificity and high binding affinity to the targeted GPCR (nM)
Minimum adverse side effects (e.g., no pharmacologic effects, no immunogenicity, reduced nephrotoxicity, and minimum radiation burden on healthy tissues)

3.   Rationales, hypotheses, and goals of the projects

Targeting radiopeptides have high potential for employment in molecular imaging and treatment of cancers in nuclear oncology. However, only a limited number of radiopeptides has been successfully introduced to the clinic so far.[8,10,37,41,57,83] There are still several challenges to be met in order to develop radiopeptides, which provide enhanced imaging quality and therapeutic efficacy.[8,10,19a,37,41,83] Current obstacles of targeting radiopeptides will be described and different approaches introduced and discussed in this Ph.D. thesis to optimize radiolabeled, targeting peptides for molecular imaging and therapy of different cancers.

3.1   Dual-targeting conjugates designed to improve the efficacy of radiolabeled peptides

Radiolabeled agonists of regulatory peptides can be used for the specific delivery of radionuclides into cancer cells *via* receptor-mediated internalization for molecular imaging or targeted therapy of different cancers. However, after uptake of many radiopeptides into tumors, a rapid efflux of a significant fraction of the internalized radiotracers is often observed *in vitro* and *in vivo*.[51b,70,122] This phenomenon impedes the initial efforts of targeted delivery of radioactivity to cancers. It also impairs imaging quality and efficacy of PRRT, since it is generally assumed that these features correlate with a high rate of internalization into tumor cells and a low rate of externalization from tumor tissues.[5,10,19a,37,41,52] In some cases, the externalization of radioactivity occurs at rates comparable to the internalization (Figure 25).[51b,122a-c]
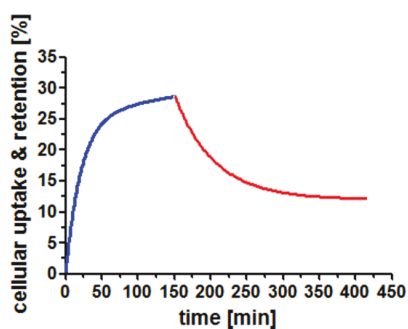

Figure 25. Example of *in vitro* internalization (blue) and subsequent externalization (red) profiles of a radiolabeled, agonistic bombesin analog in PC-3 cells (chapter III/IV).

To overcome the rapid washout of radioactivity from cancer cells, new strategies are needed to enhance the retention of radioactivity inside tumor cells. A possible approach to increase cellular retention of radioactivity is the application of dual-targeting radioconjugates that bind not only to the respective extracellular GPCR, but also to intracellular targets. We envisioned that after endocytotic cellular uptake, additional intracellular targeting with bifunctional radioconjugates (Figure 26) could improve the cellular retention of radioactivity.

Additional functionality for intracellular targeting

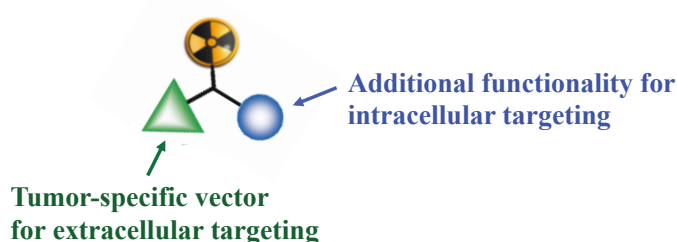**Tumor-specific vector for extracellular targeting**

Figure 26. Schematic composition of bifunctional radioconjugate for dual-targeting purposes.

A bifunctional radioconjugate is first recognized by an extracellular target (e.g., a GPCR), triggering cell internalization by endocytosis. Once inside the cell, the additional second functionality of the radioconjugate interacts with its intracellular target (e.g., a cell organelle or cytosolic protein), which could lead to entrapment of the radioactive cargo inside the cell (Figure 27). An increased retention time of the radioactivity within the tumor holds the promise to improve the signal-to-background ratio, which is important for molecular imaging. Furthermore, it may enhance the efficacy of therapeutic radionuclides because of increased radiation energy deposited in cancerous tissues over time. The dual-targeting approach bears a particularly high potential for targeted PRRT in nuclear medicine. While increasing the efficacy of targeting peptides for PRRT, the radioactive dose administered to the patient to cause sterilization of the tumor could be decreased and, consequently, the overall radiation burden of the patient could be reduced.

Only a few bifunctional radioconjugates, each specific for an extra- and intracellular target, respectively, have been reported. Ginj *et al.* reported the combination of radiolabeled somatostatin derivatives with a nuclear localization signal (NLS) sequence to transport the Auger electron emitter ^{111}In to the cell nucleus for PRRT.[51b] The reported conjugates targeted specifically the cell nucleus and displayed a decreased externalization rate *in vitro*; however, no according *in vivo* data is reported.[51b] With the same goal of targeting the cell nucleus, the groups of Alberto and Santos combined a ^{99m}Tc-labeled BBS derivative with the DNA intercalator acridine orange, which also serves as a fluorescent probe for optical imaging.[73] The *in vitro* results reported on the ability of the conjugates to target the cell nucleus are inconsistent and no data on the externalization of radioactivity from cells is given.[73] The group of Garrison investigated the combination of a radiolabeled BBS derivative with 2-nitroimidazoles, a hypoxia-specific prodrug, which is covalently conjugated to intracellular proteins upon enzymatic reduction.[123] While an enhancement of the retention of radioactivity in PC-3 cells, as a result of 2-nitroimidazole moieties, was demonstrated for the conjugates under hypoxic conditions *in vitro*, the effect was less pronounced in an *in vivo* mouse model.[123]

To achieve the goal of intracellular trapping of radioactivity, we envisioned the application of bifunctional radiopeptides, bearing a tumor-targeting vector for extracellular targeting of GPCRs and an additional entity for intracellular targeting towards a cell organelle or a cytosolic protein (Figure 27).
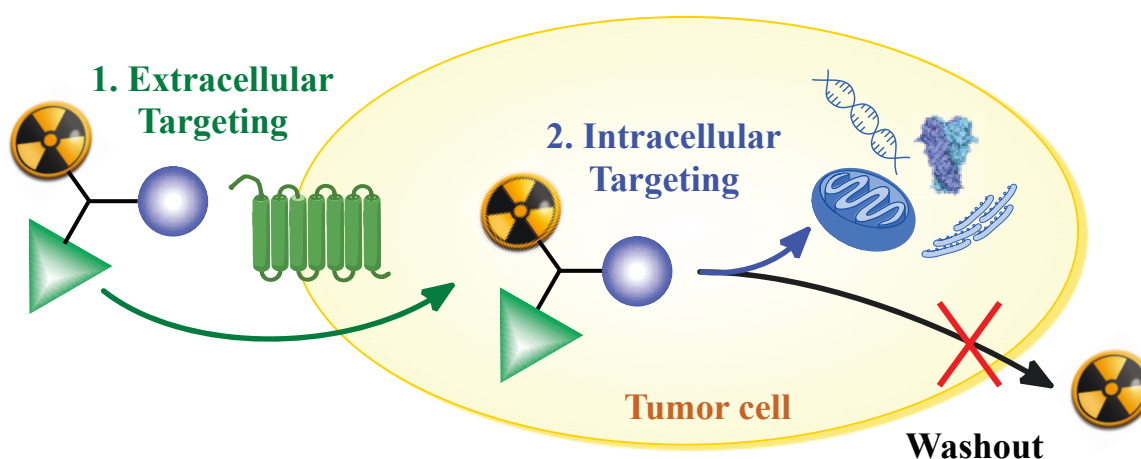

Figure 27. Concept of dual-targeting radioconjugates to reduce cellular washout of radioactivity from cancer cells.[124]

The application of bifunctional radioconjugates to exploit the individual properties of the single components is intriguing. However, the synthesis of bifunctional radioconjugates can be challenging. We chose the modular synthetic "extended Click-to-Chelate" approach[31c] (chapter II) for the efficient

preparation of the dual-targeting conjugates. In this approach, $N(\alpha)$-propargyl lysine represents the key point of the final radioconjugate by providing the possibility for the orthogonal conjugation of two different functionalities (regulatory peptide analog for extracellular targeting and an entity for intracellular targeting) by selective amide bond formation (primary amine in ε-position) and by Copper(I)-catalyzed azide-alkyne cycloaddition (CuAAC). In the course of the CuAAC, a 1,2,3-triazole is formed and the prochelator $N(\alpha)$-propargyl lysine transforms into a tridentate ligand system for the stable complexation of the *fac*-$[M(CO)_3(H_2O)_3]^+$ (M= ^{99m}Tc, $^{186/188}$Re) tricarbonyl core (Figure 28 and section 1.2.3.4).[31c]
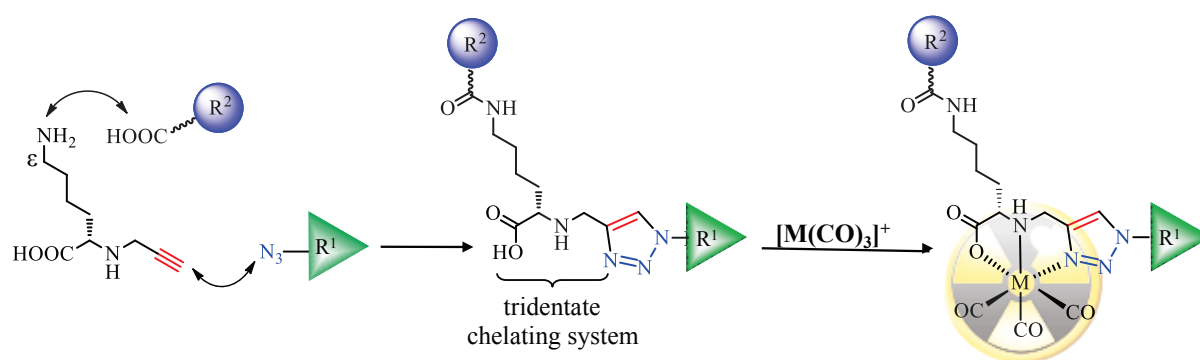

Figure 28. Assembly of bifunctional radioconjugates by selective amide bond formation, CuAAC, and radiometal complexation;[31c] residues R^1 and R^2 represent any ligand for extra- and intracellular targeting, respectively.

The first generation of dual-targeting, ^{99m}Tc-tricarbonyl-labeled conjugates is based on the stabilized minimum binding sequence of bombesin, [Nle^{14}]BBS(7-14)[71] for extracellular targeting of the GRP-r (section 2.6.1). The peptide is linked *via* a (β-Ala)$_3$ spacer to the tridentate chelating system, which is equipped with a triphenylphosphonium (TPP) moiety[125] for intracellular targeting of the organelle mitochondria to form the active conjugate [^{99m}Tc(CO)$_3$(BBS-TPP)]$^+$ (Figure 29 and chapter III). It has been shown that lipophilic, cationic TPP derivatives are driven through negatively charged transmembranes in an electrophoretic manner, resulting in an intracellular accumulation of the compounds in energized mitochondria.[126] TPP derivatives have been used as drug delivery systems for the transport of therapeutic agents into mitochondria.[126] Radiolabeled TPP derivatives have also been reported for imaging of tumors[125,127] and myocardial perfusion.[128] The utilization of TPP entities, combined with a receptor-specific peptide to enhance intracellular retention of radioactivity represents a novel and promising approach.
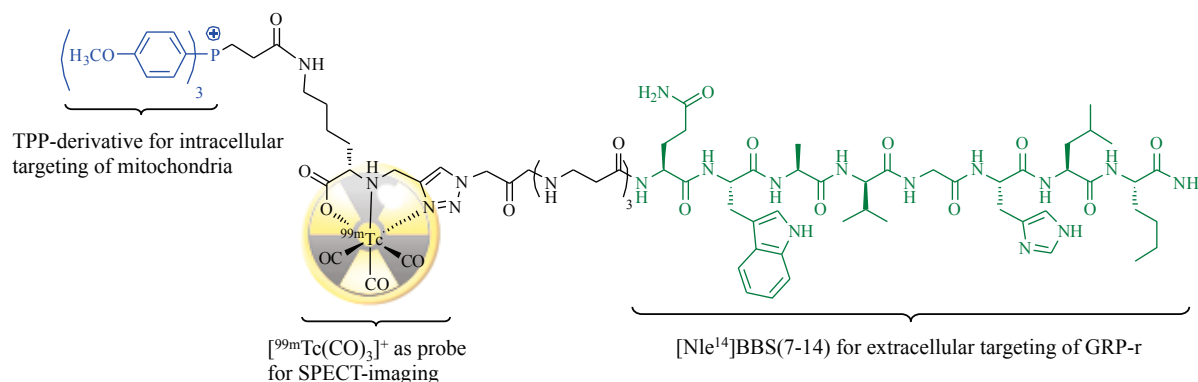

Figure 29. Bifunctional [^{99m}Tc(CO)$_3$(BBS-TPP)]$^+$ conjugate for targeting both extracellular GRP-r and intracellular mitochondria, based on [Nle^{14}]BBS(7-14), 3-tris(p-methoxyphenyl)-phosphonium moiety,[125] and ^{99m}Tc-tricarbonyl core.

The second generation of ^{99m}Tc-tricarbonyl-labeled, dual-targeting conjugates (Figure 30) is designed for intracellular targeting of the molecular, cytosolic chaperone heat-shock protein 90 (Hsp90). Hsp90 represents an ubiquitous protein, which is essential for several biochemical processes, such as cell proliferation and survival.[129] As such, it is found at high concentrations in normal cells and overexpressed by nearly all cancer cells.[129-130] Hsp90 assists and controls the non-covalent folding/unfolding of many client proteins, for example, survivin.[129b,131] The group of Altieri identified the peptide sequence of survivin (K79-L87), termed "shepherdin" as an inhibitor of both the survivin-Hsp90 interaction and Hsp90 ATPase activity.[132] The anticancer activity of conjugates consisting of cell penetrating peptides combined with shepherdin[79-87] (KHSSGCAFL) and its truncated form shepherdin[79-83] (KHSSG), respectively, have been demonstrated.[132-133] Applications of radiolabeled derivatives of shepherdin or its combination with tumor targeting peptides for receptor-specific delivery have not been described yet.

Figure 30. Bifunctional [[99m]Tc(CO)₃(BBS-shepherdin[79-87])] and [[99m]Tc(CO)₃(BBS-shepherdin[79-83])] radioconjugates for extracellular targeting of GRP-r and intracellular targeting of Hsp90.

The novel, dual-targeting radioconjugates were evaluated for their hydrophilicity (logD), their cellular binding and uptake (internalization), their binding affinity towards the GRP-r (receptor saturation binding assays), and the cellular washout of radioactivity (externalization) *in vitro*, using PC-3 cells (chapter III and IV).

3.2   1,2,3-Triazoles as amide bond mimics to yield protease-resistant peptidomimetics for tumor targeting

Due to rapid degradation by various endogenous peptidases and proteases,[55,134] a major obstacle for successful clinical use of radiolabeled derivatives of linear regulatory peptides is their very short biological half-life.[10,15a,19a,26,37,41] Because of their poor metabolic stability, they may be degraded before reaching their target structures, which significantly restricts their use as targeting vectors.[15c,19a,26,41] There are several synthetic strategies for the stabilization of peptides. Examples include the insertion of non-natural amino acids (e.g., D-amino acids or amino acids with modified side-chains), peptide backbone modifications (e.g., N-methylation, carbonyl reduction, or the use of amide bonds isosteres), and pegylation.[10,19a,26,37,41,55] Considerable efforts have been made to develop stabilized targeting peptides, while maintaining favorable biological properties, for example, good tissue penetration and high affinity towards the corresponding GPCRs, however, with varying degree of success.[10,19a,26,37,41,55] The replacement of α-AA residues by β-amino acids and their derivatives is known to result in significantly improved stability.[10,135] For example, ^{14}C-radiolabeled β-nonapeptide H(β-HAla-β-HLys-β-HPhe)₃-OH revealed outstanding metabolic stability in animal models.[136] However, such prolonged residence time in the body may bear the risk of increased radiation dose at

non-targeted tissues and unwanted side effects of radiation.[10] Thus, a fine-tuned balance between stability and biological half-life of radiopeptides is required. A very promising approach is the substitution of peptidase-sensitive amide bonds by enzyme-resistant entities.[10,15a,41,137] For example, it is known that 1,4-disubstituted 1,2,3-triazoles can effectively mimic *trans*-amide bonds because of their similar size, planarity, H-bonding capabilities, and dipole moment (Figure 31).[30c,137-138]
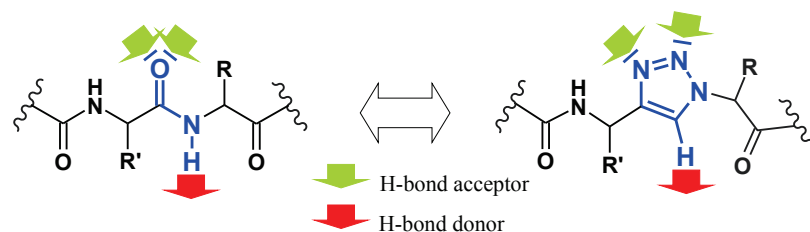
Figure 31. 1,4-disubstituted 1,2,3-triazoles as amide bond mimics.

It has also been suggested that the replacement of an amide bond by a 1,2,3-triazole isostere could afford protease-resistant peptidomimetics.[30c,137-138] However, the influence of such backbone modifications on the stability of radiopeptides has not been reported yet. We replaced systematically amide bonds of linear peptides with 1,4-disubstituted 1,2,3-triazoles by CuAAC, with the goal to develop tumor targeting vectors with increased metabolic stability and maintained high affinity towards the receptor. To prove the concept of this new approach (termed "triazole scan"), we chose the bombesin analog ([Nle^{14}]BBS(7-14),[71] which was N-terminally conjugated to a short PEG$_4$ spacer and the macrocyclic chelator DOTA for stable complexation of ^{177}Lu (Figure 32).
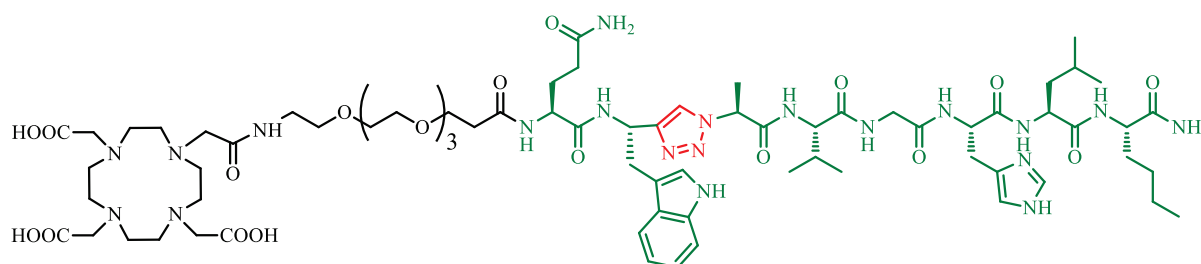
Figure 32. Example of novel triazole-peptidomimetic of DOTA-PEG$_4$-[Nle^{14}]BBS(7-14).

Radiolabeled triazole-peptidomimetics of bombesin were evaluated for metabolic stability, hydrophilicity, internalization, and affinity towards the GRP-r, using PC-3 cells. The best candidate was evaluated *in vivo* by biodistribution experiments using tumor-bearing mice (chapter V).

3.3 Expression of different neurokinin-1 receptor (NK$_1$R) isoforms in glioblastoma multiforme: potential implications for targeted therapy

Radiolabeled ^{90}Y and ^{213}Bi-substance P derivatives have previously been evaluated in clinical trials for the treatment of gliomas (subchapter 2.6.2.2).[83] Before treatment, the overexpression of NK$_1$ receptors was confirmed in every patient by local injection of ^{111}In-labeled SP derivatives.[118a-c] The majority of patients within the study showed clinical response to locally administered SP radionuclide therapy.[118a-c] However, despite proven NK$_1$R overexpression, the response of several patients was not as pronounced as expected.[118a,c] Since sufficient intratumoral distribution was proven by pre-therapeutic test injections, there might be specific features leading to variable responses of patients to NK$_1$R-targeted therapy with radiolabeled SP derivatives.

Two isoforms of the NK_1R exist, a full-length (NK_1R-*Fl*) and a truncated isoform (NK_1R-*Tr*; subchapter 2.6.2).[111-112] They consist of identical domains for ligand binding, but show differences in the C-terminal region, which is important for phosphorylation by kinases of GPCRs. The C-terminus of NK_1R-*Tr* lacks 96 amino acids (Figure 33) and thus, shows reduced capacity to undergo SP-induced internalization and desensitization.[111-112]
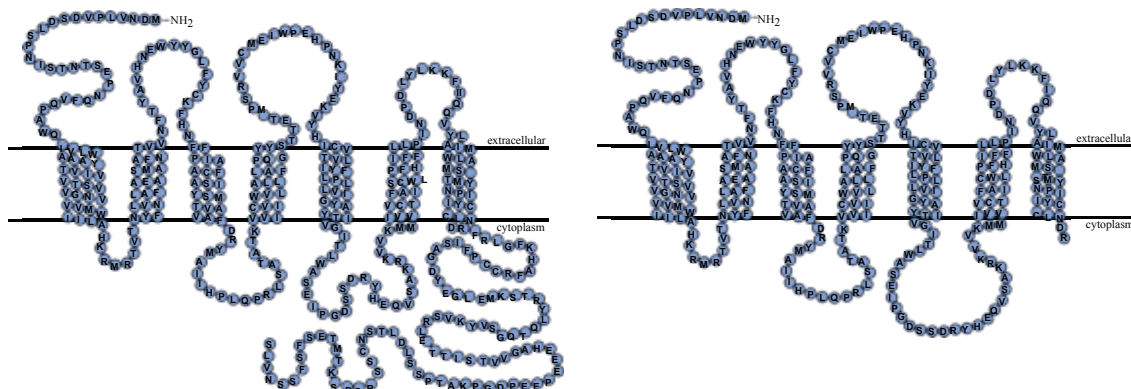

Figure 33. Schematic illustration of full-length and truncated isoforms of human NK_1Rs.[111b]

Towards the goal of identifying factors that may be responsible for the varying therapeutic response of patients suffering from glioma, four different, commonly used glioma cell lines (LN71, LN229, LN319, and LN405) were analyzed for their RNA levels of NK_1R-*Fl* and NK_1R-*Tr* isoforms. Using these cell lines, NK_1R-mediated binding and internalization of three different analogs of SP (Table 7) were evaluated. Potential therapeutic effect of saporin-SP analog for toxin-based, targeted therapy of gliomas was analyzed as well (chapter VI).

Table 7. Structures of analyzed SP analogs.

SP	Arg^1-Pro^2-Lys^3-Pro^4-Gln^5-Gln^6-Phe^7-Phe^8-Gly^9-Leu^{10}-Met^{11}-NH_2
radiolabeled	^{177}Lu-DOTA-[Thi^8,$Met(O)_2^{11}$]-SP^{66} (Thi: thienylalanine)
fluorescently-labeled	FAM-SP (FAM: carboxyfluorescein), commercial
toxin-based	SP-SAP: [Sar^9,$Met(O)_2^{11}$]-SP-saporin (Sar: sarcosine), commercial

II. Click-to-Chelate: Development of Technetium and Rhenium-Tricarbonyl Labeled Radiopharmaceuticals

Christiane A. Kluba and Thomas L. Mindt[*]

Division of Radiopharmaceutical Chemistry, Clinic of Radiology and Nuclear Medicine, University of Basel Hospital, Petersgraben 4, 4031 Basel; Switzerland
([*]corresponding author)

Kluba, C.A.; Mindt, T.L. Click-to-Chelate: Development of Technetium and Rhenium-Tricarbonyl Labeled Radiopharmaceuticals. *Molecules* **2013**, 18, 3206-3226.

http://www.mdpi.com/1420-3049/18/3/3206

(This article belongs to the Special Issue "Advances in Click Chemistry";
Guest Editor: Dr. Arnaud Gautier)

Abstract: The Click-to-Chelate approach is a highly efficient strategy for the radiolabeling of molecules of medicinal interest with technetium and rhenium-tricarbonyl cores. Reaction of azide-functionalized molecules with alkyne prochelators by the Cu(I)-catalyzed azide-alkyne cycloaddition (CuAAC; click reaction) enables the simultaneous synthesis and conjugation of tridentate chelating systems for the stable complexation of the radiometals. In many cases, the functionalization of (bio)molecules with the ligand system and radiolabeling can be achieved by convenient one-pot procedures. Since its first report in 2006, Click-to-Chelate has been applied to the development of numerous novel radiotracers with promising potential for translation into the clinic. This review summarizes the use of the Click-to-Chelate approach in radiopharmaceutical sciences and provides a perspective for future applications.

Contributions:
The review was written by Thomas L. Mindt and Christiane A. Fischer.

Review

Click-to-Chelate: Development of Technetium and Rhenium-Tricarbonyl Labeled Radiopharmaceuticals

Christiane A. Kluba and Thomas L. Mindt [*]

Division of Radiopharmaceutical Chemistry, Department of Radiology and Nuclear Medicine, University of Basel Hospital, Petersgraben 4, 4031 Basel; Switzerland; E-Mail: Christiane.Kluba@usb.ch

[*]   Author to whom correspondence should be addressed; E-Mail: Thomas.Mindt@usb.ch; Tel.: +41-(0)-61-556-5380; Fax: +41-(0)-61-265-5559.

Abstract: The Click-to-Chelate approach is a highly efficient strategy for the radiolabeling of molecules of medicinal interest with technetium and rhenium-tricarbonyl cores. Reaction of azide-functionalized molecules with alkyne prochelators by the Cu(I)-catalyzed azide-alkyne cycloaddition (CuAAC; click reaction) enables the simultaneous synthesis and conjugation of tridentate chelating systems for the stable complexation of the radiometals. In many cases, the functionalization of (bio)molecules with the ligand system and radiolabeling can be achieved by convenient one-pot procedures. Since its first report in 2006, Click-to-Chelate has been applied to the development of numerous novel radiotracers with promising potential for translation into the clinic. This review summarizes the use of the Click-to-Chelate approach in radiopharmaceutical sciences and provides a perspective for future applications.

Keywords: CuAAC; Click-to-Chelate; radiolabeling; radiopharmaceuticals; ^{99m}Tc-tricarbonyl; $^{186/188}$Re-tricarbonyl

1. Introduction

Even though new generator-based radionuclides (e.g., ^{68}Ga) are emerging [1], technetium 99m remains the workhorse of nuclear medicine due to its convenient availability via ^{99m}Mo/^{99m}Tc

generators, reasonable cost, and ideal decay characteristics ($t_{1/2}$ = 6.02 h, 140 keV, 89% abundance) for Single Photon Emission Computed Tomography (SPECT). Approximately 80% of all routine nuclear imaging applications are based on ^{99m}Tc, which translates into estimated 50 million doses of diagnostic radiopharmaceuticals annually worldwide, or more than 50,000 applications per day in the US alone [2,3]. In addition, the availability of β-particle-emitting rhenium 186/188 as group 7 transition metal congeners of ^{99m}Tc with similar chemical properties provides a "matched pair" constellation of radionuclides for both diagnostic and therapeutic applications. The possibility to radiolabel molecules of medicinal interest with diagnostic or therapeutic radionuclides by the same chemistry approach has recently received considerable interest in the field of nuclear medicine for the development of theranostic agents [4].

Because of the diverse redox chemistry of technetium and rhenium, a wealth of complexes differing in coordination numbers and geometries has been reported. Here, we focus on the technetium and rhenium-tricarbonyl cores ($[M(H_2O)_3(CO)_3]^+$, or short $[M(CO)_3]^+$; M = ^{99m}Tc(I), $^{186/188/nat}$Re(I)). ^{99m}Tc- and $^{186/188}$Re-tricarbonyl can be prepared by reduction of the corresponding permetallates ($[M(VII)O_4]^-$) using $K_2[H_3BCO_2]$ (e.g., by the commercial IsoLink^{TM} kit; Scheme 1). $[M(CO)_3]^+$ contains three tightly coordinated CO ligands and three water molecules, the latter of which can be readily replaced by mono-, bi-, and tridentate ligand systems, or a combination thereof. Complexes of $[M(CO)_3]^+$ exhibit a low spin d^6 configuration, which renders the metal inert and hence, provides complexes with high *in vivo* stability essential for medical applications [5]. In addition, octahedral complexes of $[M(CO)_3]^+$ are generally smaller than octahedral or square-pyramidal complexes of the corresponding metals in higher oxidation states (e.g., M(V)-oxo cores) and are therefore considered less likely to impact important characteristics of (bio)molecules to which they are conjugated to.

Scheme 1. Synthesis of $[M(CO)_3]^+$ from permetallates and subsequent complexation with ligands (L). (a) For M = ^{99m}Tc: (i) IsoLink^{TM} kit (containing $K_2[H_3BCO_2]$), saline, 100 °C, 20 min; for M = ^{188}Re: (i) SnCl$_2$, gluconate, H$_3$PO$_4$; (ii) $K_2[H_3BCO_2]$.
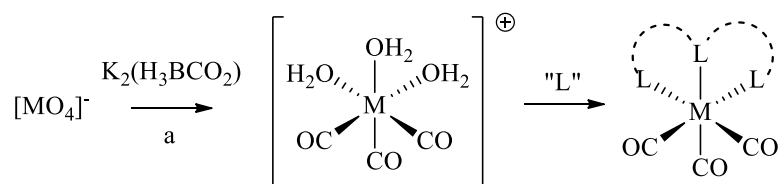
Since the first report of the ^{99m}Tc-tricarbonyl core $[^{99m}$Tc(H$_2$O)$_3$(CO)$_3]^+$ in 1998 by Alberto and Schibli *et al.* [6] numerous ligand systems and their coordination with $[M(CO)_3]^+$ have been investigated. In particular, tridentate chelators containing *N*-, *S*-, or *O*-donors have been shown to provide well-defined and stable organometallic complexes, which are suitable for application *in vivo* (Figure 1) [7,8] Also, functionalized η^5-ligand cyclopentadienide as well as carboranes [9] have been used for the stable complexation of the tricarbonyl core. A thorough discussion of the literature on ligand systems reported for the complexation of $[M(CO)_3]^+$ is beyond the scope of this article and instead, it is referred to some excellent reviews on the general topic of ^{99m}Tc chelation chemistry (see e.g., [10]).

Figure 1. Representative examples of bifunctional chelating agents (BFCAs) for the complexation of the $[^{99m}Tc(CO)_3]^+$ core and conjugation to (bio)molecules.
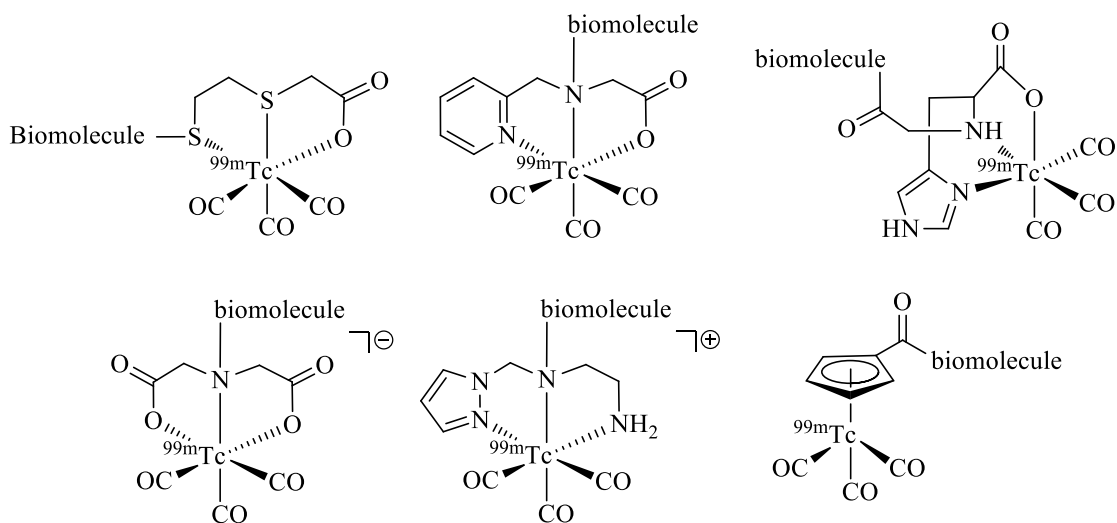
Radiolabeling of molecules of medicinal interest with $[M(CO)_3]^+$ is usually achieved by a post-labeling approach using bifunctional chelating agents (BFCAs). As the name implies, BFCAs enable both the covalent linkage to a (bio)molecule and the coordination of the radiometal. For many of the ligand systems reported for $[M(CO)_3]^+$, appropriately functionalized derivatives for conjugation to (bio)molecules *via* different functional groups (e.g., amines, carboxylates, thiols) have been reported [10]. However, the multifunctional character of both the ligand system and (in most cases) the (bio)molecule of interest can make a selective conjugation in solution a difficult endeavor. To overcome these problems, protective group strategies are often employed; though, such approaches usually result in multi-step reaction sequences, which can significantly lower the overall efficiency of the labeling procedure.

Despite the success of the metal tricarbonyl cores in the field of radiopharmaceutical sciences, there is still a need for novel and innovative strategies for (bio)conjugation techniques and radiolabeling procedures in order to expedite the development of radiotracers based on $[M(CO)_3]^+$. In the following, this review will focus on such a recently developed approach that utilizes click chemistry in this context.

2. Click Chemistry in Radiopharmaceutical Sciences

Click chemistry, a term minted by Sharpless [11] *et al.* in 2001, is an attempt to define the characteristics of a perfect (or nearly perfect) chemical reaction that generates structurally diverse new substances by joining small building blocks in a quick, selective, efficient, and reliable manner. The prime example of a click reaction within the click chemistry concept is the copper (Cu(I))-catalyzed azide-alkyne cycloaddition (CuAAC), reported at the same time by the groups of Sharpless and Meldal in 2002 [12,13]. The CuAAC proceeds efficiently and selectively under mild reaction conditions (e.g., in water at room temperature) in the presence of other functional groups, and provides a stable 1,4-disubstituted 1,2,3-triazole heterocyclic linkage between the reaction partners. Not surprisingly, the attractive features of this click reaction have inspired numerous applications across different scientific disciplines [14–16], including examples of the development of radiotracers.

The first examples on the use of the CuAAC in radiopharmaceutical sciences were published in 2006. Kolb *et al.* [17] and Marik *et al.* [18] described the click reaction of $[^{18}F]$fluorinated alkyne derivatives with azide acceptors, such as azido thymidine (AZT) and azide-functionalized peptides. These applications employ a two-step prosthetic group approach, which enables the efficient and selective ^{18}F radiolabeling of molecules in aqueous media. For an overview on the CuAAC-mediated

radiolabeling of molecules with ^{18}F- (and ^{11}C-) radionuclides, it is herein referred to some of the several recent review articles on the topic [19,20].

Also in 2006, Mindt and Schibli *et al.* reported the first example of an application of the CuAAC to metallic radionuclides [21]. In their approach, the click reaction is employed to the synthesis of tridentate ligand systems for the stable complexation of [^{99m}Tc(CO)$_3$]$^+$ while conjugating them simultaneously to (bio)molecules. Unlike subsequently published applications of the CuAAC for the labeling of molecules with radiometals, their approach utilizes the 1,2,3-triazole not only as a mere linker to connect a molecule with a radiometal chelate (conjugate design), but makes use of the excellent coordination properties of the heterocycle as part of a functional ligand system in an integrated approach [22]. The broad applicability and efficiency of this ^{99m}Tc-radiolabeling strategy, in particular those provided by convenient one-pot procedures developed in the course of the work, prompted the authors to term their approach "Click-to-Chelate" [21]. This review summarizes original articles on the Click-to-Chelate concept published since 2006. Examples of applications of the CuAAC in which the 1,2,3-triazole is not part of a chelating system but just tethers a radiometal complex to various molecules are not included. Particular attention has been paid to examples of "clicked" ^{99m}Tc-radiotracers, which describe biological evaluations *in vitro* and *in vivo*, as this is an important aspect for potential translation of the compounds into the clinic.

3. Click-to-Chelate

As discussed in the introduction, the preparation of tridentate chelating systems (and BFCAs thereof) for the complexation of [M(CO)$_3$]$^+$ generally requires multi-step synthesis and their incorporation into (bio)molecules often lacks efficiency and selectivity due to cross-reactivity with other functional groups present. The chemical orthogonality of the CuAAC together with the ease of the introduction of alkyne and azide moieties into molecules by synthetic or biochemical methods [23–27] provides a solution to these shortcomings. Thus, the reaction of azide-functionalized compounds with alkyne prochelators provides 1,4-disubstituted 1,2,3-triazole-containing tridentate ligand systems (termed "regular click ligands"; Scheme 2A) [21]. Similarly, cycloaddition of alkyne derivatives with azide prochelators yields isomeric triazolyl products (referred to as "inverse click ligands"; Scheme 2B), which are set up to coordinate to [M(CO)$_3$]$^+$ *via* the nitrogen in position 2 of the triazole heterocycle, rather than the nitrogen in position 3 of "regular click ligands" (see below). Noteworthy, all ligand systems can be prepared without the use of protective groups in a single step, high yields, and under mild reaction conditions suitable for the functionalization of delicate biomolecules. Reaction of the tridentate chelators with [M(CO)$_3$]$^+$ gives structurally diverse organometallic complexes that differ in size, lipophilicity, and overall charge (Table 1). All these characteristics are important for fine-tuning the physicochemical properties of a radiotracer for its application *in vivo*.

Scheme 2. Schematic representation of the synthesis of regular (A) and inverse (B) 1,2,3-triazolyl ligand systems for the complexation of the $[M(CO)_3]^+$ core. A and B represents various functional groups for coordination of the tricarbonyl core.

$$M = {}^{99m}Tc, Re$$
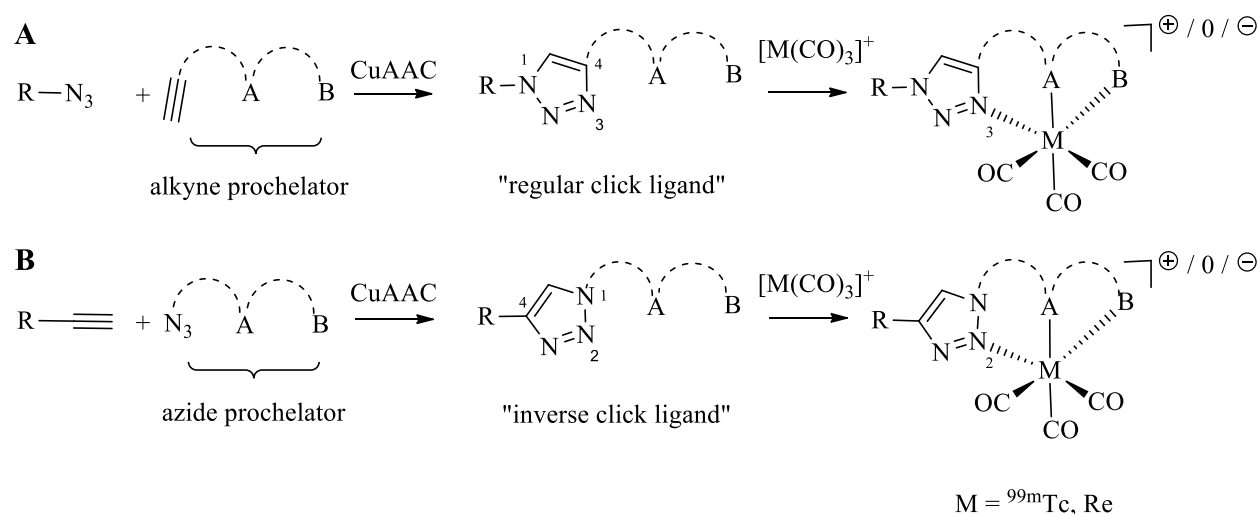
The radiolabeling of regular click ligands (**L**; Table 1, entries 1–5) with $[{}^{99m}Tc(CO)_3]^+$ proceeds smoothly under standard reactions conditions (PBS, pH 7.4, 100 °C, 20–30 min) [21]. Quantitative formation of $[{}^{99m}Tc(CO)_3(L)]$ can be achieved at a ligand concentration in the micromolar range (10^{-5}–10^{-6} M), which is comparable to that of histidine (or Nτ-substituted histidines), one of the most efficient chelators for complexation of the ${}^{99m}Tc$ tricarbonyl core [28]. Particularly for receptor targeting radiopharmaceuticals, it is important that high specific activities can be achieved (e.g., by employing low ligand concentrations) in order to avoid interfering receptor saturation. On the other hand, quantitative radiolabeling of the ${}^{99m}Tc$-tricarbonyl core with inverse click ligands (e.g., Table 1, entry 6; for additional examples see ref. [21]) requires a ligand concentration orders of magnitudes higher (10^{-3}–10^{-2} M) than that of regular click ligands. This indicates a decreased efficiency of the inverse click ligand systems likely due to the lower electron density at N2 compared to that of N3 of the triazole heterocycle as shown by density functional theory (DFT) calculations [21].

Brans *et al*. have conjugated both variations of click ligands to the N-terminus of a tumor targeting bombesin (BBS) derivative (Scheme 3; see below for the relevance of BBS in nuclear oncology) [29]. Radiolabeling of the two peptides with $[{}^{99m}Tc(CO)_3]^+$ under standard conditions revealed a significantly lower radiolabeling yield for the peptide with the inverse click ligand (<60%) in comparison to the compound with the regular click ligand (>95%). Moreover, the ${}^{99m}Tc$ adduct of the inverse ligand system was found to be unstable and thus, not suitable for *in vivo* evaluation. Anderson *et al*. have reported a similar instability of a ${}^{nat}Re$-tricarbonyl based luminescent probe in which the metal is coordinated by the N2 nitrogen of triazole ligands [30]. Even though different metal complexes of 1,4-disubstituted 1,2,3-triazoles with coordination can be synthesized via the N2 [31], the low chelation efficiency combined with the modest stability of the complexes in biological media makes them unlikely to find biological or medical applications. It is therefore important that 1,2,3-triazole-based metallic bioprobes are designed in a way that ensures coordination *via* the N3 of the heterocycle.

Table 1. Examples of prochelators, formation of tridentate triazolyl ligands by CuAAC with benzyl azide (entry 1–5) or 3-phenyl-1-propyne (entry 6), and complexes with $[M(CO)_3]^+$ thereof.

| Entry	Prochelator	Tridentate ligand (L) [1]	Metal complex [2]
1 [3]			
2 [4]			
3			
4			
5			
6 [3,5]			

[1] Coordinating nitrogen of the 1,2,3-triazole heterocycle is indicated; [2] M = ^{99m}Tc, ^{nat}Re; [3] commercial compounds; [4] prochelators derived from amino acids (R = amino acid specific side chain); [5] example of an inverse click ligand.

Scheme 3. Regular and inverse click ligands conjugated to the N-terminus of a bombesin derivative. Peptide = (ßAla)$_{1–2}$[Cha^{13}, Nle^{14}]BBS(7–14); the N-terminal ßAla units serve as a spacer between the peptide and the metal chelate.
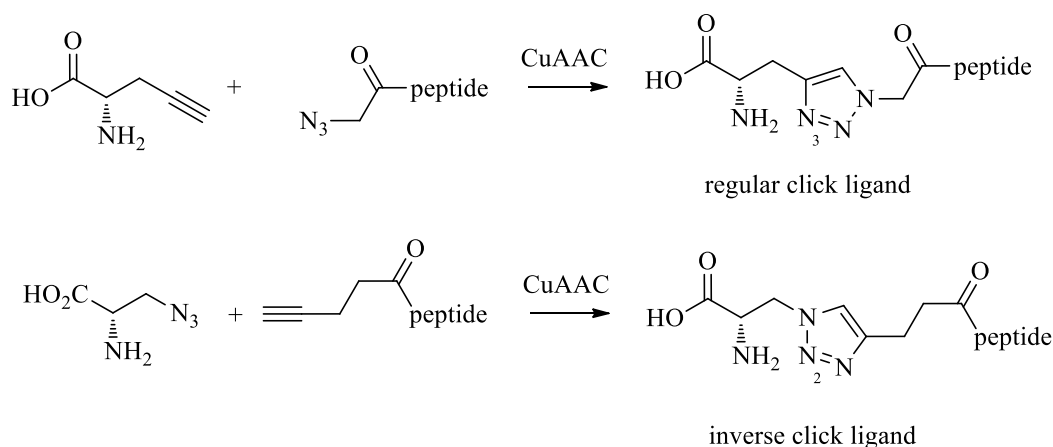
It is common practice to identify ^{99m}Tc-complexes prepared on a no carrier added (n.c.a.) level by comparison with the corresponding non-radioactive ^{nat}Re analogues by HPLC (γ-trace *versus* UV-trace; Scheme 4). In addition, the corresponding ^{nat}Re-tricarbonyl complexes allow structural analysis by spectrometric and spectroscopic methods including IR, MS, and NMR. ^{nat}Re analogues of ^{99m}Tc-tricarbonyl complexes can be synthesized conveniently on a macroscopic scale by the reaction of the ligand system of interests with [Et$_4$N]$_2$[Re(CO)$_3$(Br)$_3$] [32] in alcohol or water according to published procedures. In all cases discussed above (and more examples have been reported in the meantime), the corresponding ^{nat}Re-tricarbonyl complexes were prepared and fully characterized. In addition, more than half a dozen reported X-ray structures confirm the formation of *fac*-M(CO)$_3$ complexes by tridentate coordination of the triazolyl ligands as depicted in, e.g., Figure 1, Table 1, or Scheme 5B [33–36].

Scheme 4. Labeling of a representative example of a regular click ligand with ^{99m}Tc- and ^{nat}Re-tricarbonyl for identification and characterization of the organometallic products.
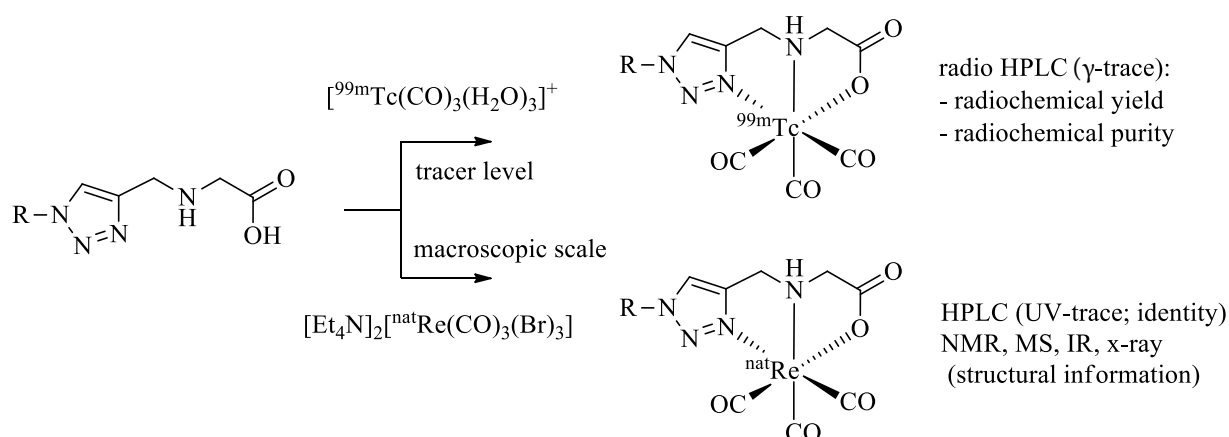
Scheme 5. Extension of the Click-to-Chelate approach provides efficiently trifunctional (**A**), or tetrafunctional (**B**) conjugates. TMS = trimethylsilyl group.
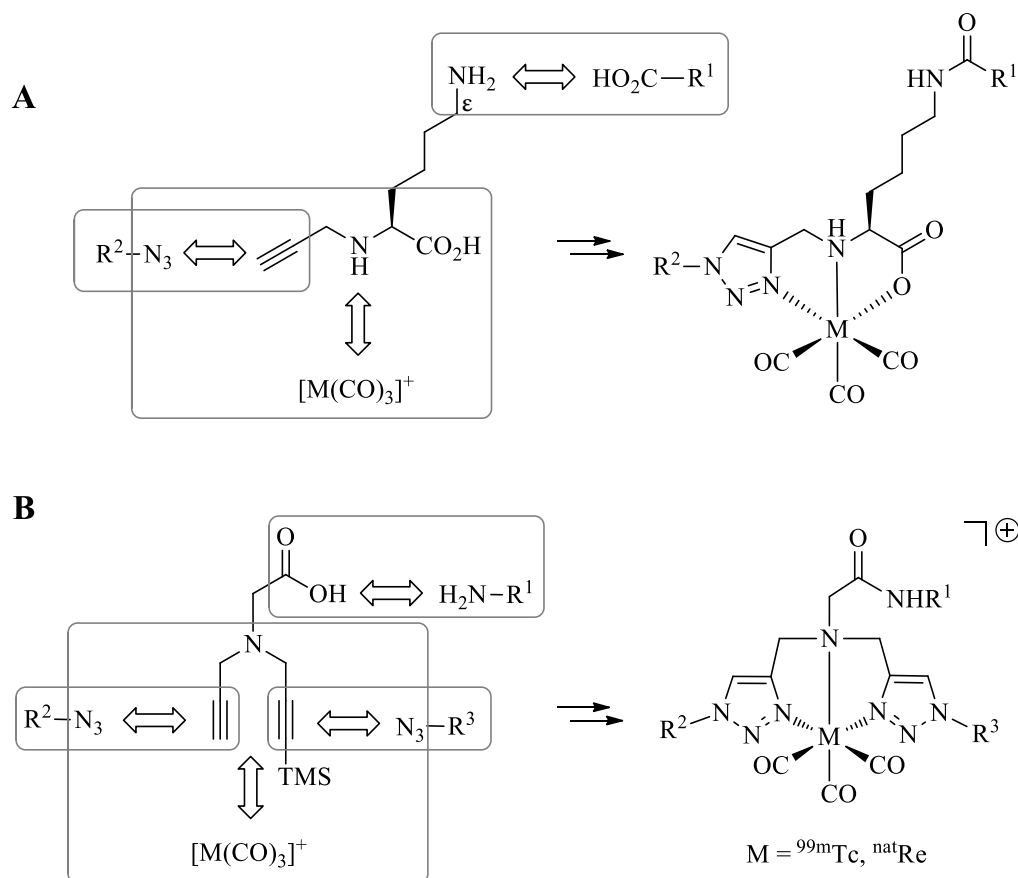
As pointed out above, a large number of non-radioactive ^{nat}Re-tricarbonyl complexes have been reported for structural elucidation and identification of the analogous ^{99m}Tc complexes. Only recently have Wang *et al*. reported the first example of a chelate in which the ^{188}Re-tricarbonyl core is coordinated by a click ligand (Figure 2) [37]. In their work, the efficiency of the complexation of $[^{188}Re(CO)_3(H_2O)_3]Br$ with bis(pyridine-2-ylmethyl)amine (dpa) was compared with that of a regular click ligand. Even though dpa was shown to be the more efficient chelator, respectable radiolabeling yields (>80%) were achieved with the regular click ligand system.

Figure 2. *Fac*-^{188}Re-tricarbonyl complexes of dpa and a regular click ligand.

$[^{188}Re(CO)_3(dpa)]$ clicked dpa analog
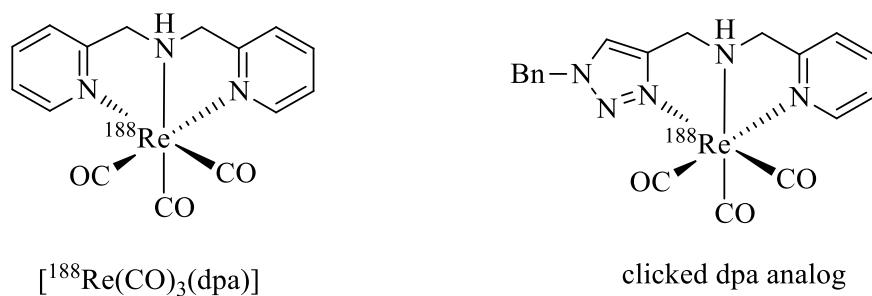
4. One-Pot Click-to-Chelate Procedures

While the ligands described above, in particularly the regular click ligands, represent a class of excellent chelators for the complexation of $[M(CO)_3]^+$, the individual azide and alkyne substrates as well as the various additives required for CuAAC are poor ligands and do not form stable or defined complexes with the organometallic tricarbonyl core [21]. Exploitation of this observation led to the development of efficient procedures by which the synthesis of the ligand system, its conjugation to a molecule of interest, and the radiolabeling with $[M(CO)_3]^+$ can be achieved in a single pot without isolation and purification of intermediates. Thus, heating of an aqueous solution of azide substrates and alkyne prochelators in the presence of catalytic amounts of Cu(I) for 20–30 min at 100 °C followed by addition of $[^{99m}Tc(CO)_3]^+$ and a second heating step (Scheme 6A) provided cleanly the same ^{99m}Tc tricarbonyl labeled compounds in identical radiochemical yields and purity as obtained by the reaction of pre-synthesized and isolated triazolyl ligands with $[^{99m}Tc(CO)_3]^+$ (Scheme 6C). Remarkably, the same ^{99m}Tc-tricarbonyl complexes can be obtained in some instances by simply mixing all substrates with the generator eluent containing pertechnetate ($[^{99m}TcO_4]^-$) in the presence of the IsoLink™ kit (Scheme 6B). In the meantime, a number of examples of successful one-pot, two-step- or single-step procedures have been reported for different click-ligand systems (see below). In some cases, the reaction time of individual steps can be accelerated by microwave heating (unpublished results). Simplification of radiolabeling procedures as illustrated by the one-pot examples shown are of fundamental importance for facilitating the translation of novel labeling strategies into routine practice for clinical applications in nuclear medicine.

Scheme 6. Example of one-pot, two-step (**A**) and one-pot, single-step (**B**) Click-to-Chelate procedures yielding the same radiolabeled compounds as obtained by multi-step synthesis with pre-synthesized and isolated triazolyl ligand systems (**C**).
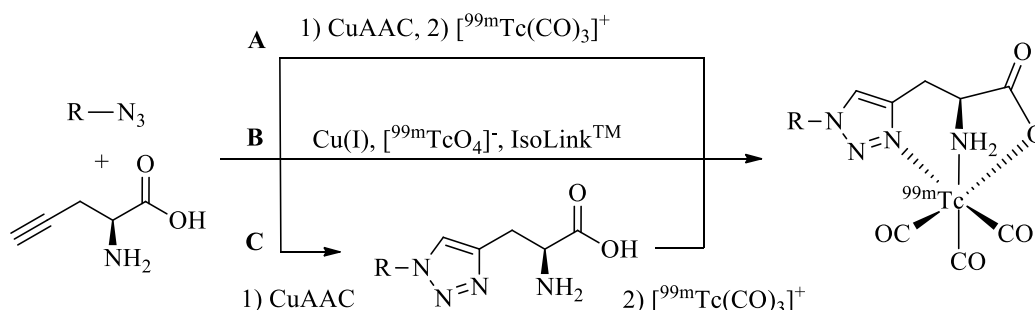
5. Comparison of Click Ligands with Established Chelators for $[M(CO)_3]^+$

As true for any new ligand system designed for the formation of radiometal complexes for use in nuclear medicine, its performance should be scrutinized and compared with established systems in order to evaluate its general utility. For regular click ligands, this was accomplished by a direct side-by-side comparison *in vitro* and *in vivo* with two gold standard chelators for $[^{99m}Tc(CO)_3]^+$, namely Nτ-derivatised histidine (His) and Nα-acetylated His (Figure 3). Towards this goal, Mindt *et al.* [38] Brans *et al.* [29], and Zhang *et al.* [39] have applied the click-to-chelate approach to tumor targeting vectors of relevance in nuclear oncology and studied the biological characteristics of the ^{99m}Tc-labeled conjugates.

Radiolabeled folic acid derivatives functionalized at the γ-position with a radiometal chelate have been shown to be promising candidates for the development of radiotracers specific for folate receptors (FR), which are overexpressed by tumors of the ovary, cervix, endometrium, lung, kidney, breast, colon, and brain [40]. Bombesin (BBS) is a peptide, which targets the gastrin-releasing peptide

receptor (GRP-r). BBS and derivatives thereof are interesting vectors for the development of tumor targeting agents because of the overexpression of the GRP-r by different tumor cells including prostate, breast, colon, and small-cell lung carcinomas [41]. Finally, the peptide KCCYSL, identified by phage display, is a small peptide specific for the ErbB-2 receptor, a member of the epidermal growth factor receptor family, which is overexpressed by breast and prostate carcinoma cells [39].

The comparative studies of the ^{99m}Tc-tricarbonyl labeled folate (Figure 3A), BBS, and ErbB-2-targeting peptide derivatives (Figure 3B) clearly demonstrated the equivalence of the clicked ligand system *versus* the established Nτ-derivatized His and Nα-acetylated His chelators. Radiolabeling yields and purities achieved with the conjugates bearing a regular click ligand were equal to that of the conjugates equipped with the reference chelators, as were their blood serum stabilities, cell internalization properties, receptor affinities, and receptor specificities. Most importantly, the nature of the ligand system did not influence the biodistribution of the radioconjugates as determined by experiments *in vivo* with the corresponding mouse models.

Also, Ferro-Flores *et al*. have compared a bombesin derivative, [Lys^3]BBS(1–14), radiolabeled with $[^{99m}$Tc(CO)$_3]^+$ via a regular click ligand with an analogous compound radiolabeled with technetium(III) using the EDDA/HYNIC (ethylenediamine N,N'-diacetic acid/hydrazinonicotinamide) chelating system [42]. As expected, the ^{99m}Tc-tricarbonyl radiopeptide exhibited an increased lipophilicity and thus, higher hepatobiliary excretion than the EDDA/HYNIC derivative. The authors conclude that the BBS conjugate radiolabeled with the ^{99m}Tc-tricarbonyl core *via* a regular click ligand is nevertheless the more promising candidate for clinical development because, unlike in the case of HYNIC chelates [43], it consists of a structurally defined metal complex on a tracer level, an important prerequisite for the approval of new radiopharmaceuticals by regulatory authorities.

It is important to note that Click-to-Chelate not only offers an efficient and convenient way for the introduction of a ligand system into (bio)molecules of interest and their radiolabeling with $[^{99m}$Tc(CO)$_3]^+$ but also reduces significantly the synthetic effort to obtain the corresponding precursors, e.g., alkyne prochelators (or BFCAs with respect to other ligand systems). This benefit of Click-to-Chelate may not be obvious in the case of the modification of peptides to which different entities, including various ligand systems, can conveniently conjugated to on solid support. However, the advantages of Click-to-Chelate become more apparent when applied to the synthetically more challenging situation of the selective modification of polyfunctional molecules in solution. For example, the synthesis of 1,2,3-triazole-modified folic acid (Figure 3A) was achieved by Click-to-Chelate in eight synthetic steps with an overall yield of approx. 80% [38]. In comparison, the analogous ^{99m}Tc-tricarbonyl labeled folic acid derivative equipped with an Nτ-derivatized His chelator required ten synthetic steps and provided the final radiotracer in < 1% yield [44]. This example, as well as others discussed below, demonstrates the synthetic efficiency of the Click-to-Chelate strategy for the assembly of ^{99m}Tc tricarbonyl radiotracers.

Figure 3. Comparison of regular click ligands with established chelators for the labeling of tumor-seeking vectors with the ^{99m}Tc tricarbonyl core. (**A**) Folic acid conjugated to a Nτ-derivatized His chelator or a regular click ligand. (**B**) Two peptides functionalized with a NαAc His chelator or a regular click ligand. The ßAla and the GSG motifs are spacer units that separate the receptor targeting peptide from the chelate.
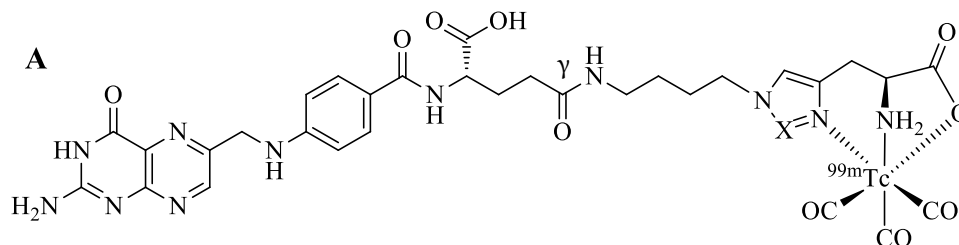
X = CH = N(τ)-functionalized His *versus* X = N = regular click ligand

regular click ligand   N(α)-acetylated His
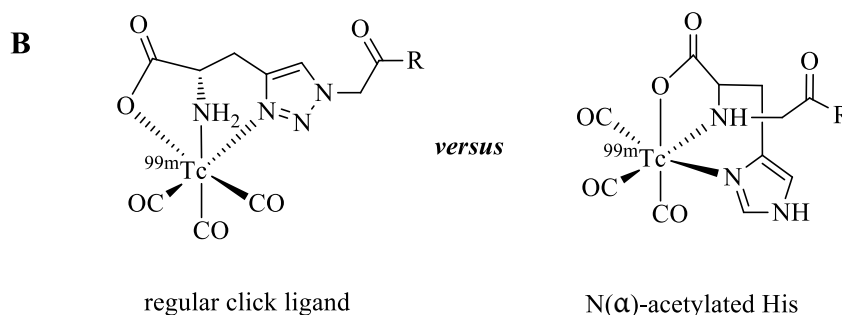
R = peptide: 1) bombesin: βAla-[Cha^{13}, Nle^{14}]BBS(7-14)
2) ErbB-2 targeting peptide: GSG-KCCYSL

6. Multifunctional Radioconjugates by Extended Click-to-Chelate

So far, the synthesis of tridentate 1,4-disubstituted 1,2,3 triazole-containing ligand systems and their simultaneous conjugation to molecules of interest by means of the CuAAC have been discussed. The Click-to-Chelate approach can be readily extended to the preparation of multifunctional ^{99m}Tc-tricarbonyl radioconjugates by structural modifications of the prochelators employed. Mindt *et al.* have demonstrated the feasibility of such applications by two different approaches [34,36]. In a first strategy, a lysine-derived prochelator is employed to which various molecules of interest (R^1) can be selectively conjugated to *via* the Nε-amine functionality by amide bond formation (Scheme 5A). CuAAC with a second, azide-functionalized molecule (R^2) covalently links the two molecules *via* the formed regular click ligand. Thus, the final product combines a nuclear reporter probe (^{99m}Tc) with two different chemical (or biological) entities in a trifunctional conjugate. The strategy was successfully applied to the preparation of a ^{99m}Tc-labeled conjugate comprising a tumor targeting peptide sequence ([Cha^{13}, Nle^{14}]bombesin(7–14)) and a low molecular weight albumin binder, a pharmacological modifier to elongate the blood circulation time of the conjugate. Evaluation of the trifunctional conjugate *in vitro* and *in vivo* provided promising results for its use as a SPECT imaging agent for the visualization of GRP-r-positive tumors [34]. Recently, Kluba *et al.* have reported yet another application of this strategy by combining the ^{99m}Tc-tricarbonyl core with two moieties, each specific for an extra- and intracellular target, respectively [45]. The trifunctional conjugate was designed to target cancer cells by interaction of a BBS fragment (R^2) with GRP-r and, after

internalization, with mitochondria *via* an organelle-specific triphenylphosphonium moiety (R^1). Adding a moiety specific for an intracellular target to a tumor targeting peptide conjugate could improve the cellular retention of radioactivity after its successful delivery to tumors and metastases and thus, improve the efficacy of radiopeptide conjugates.

The second approach to multifunctional conjugates involves chelators containing two 1,4-disubtituted 1,2,3-triazoles derived from the CuAAC of azides with a bis-alkyne precursor (Scheme 5B) [36]. The latter can be readily obtained by the stepwise Nα-alkylation of, e.g., glycine with propargyl bromide or silyl protected derivatives thereof. One molecule (R^1) can be selectively linked to the glycine precursor by amide bond formation. The other two molecules (R^2 and R^3) are conjugated by sequential CuAAC, first with the terminal alkyne and, after removal of the silyl protective group, with the second alkyne functionality. Thus, this strategy provides access to overall tetrafunctional conjugates by joining three different chemical or biochemical moieties with the ^{99m}Tc-tricarbonyl core. The utility of the approach was demonstrated by the conjugation of a GRP-r targeting bombesin derivative with a related bis-triazole ligand system to which two carboxylates were linked to by the CuAAC [36]. The observed low renal uptake and retention of the conjugate *in vivo* suggests that the two appending carboxylates act as pharmacological modulators, which successfully masked the otherwise unfavorable positive charge of the conjugate as the result of the cationic metal chelate.

An almost infinite number of possible combinations of different chemical or biological moieties with the ^{99m}Tc-tricarbonyl core can be envisioned by the extended Click-to-Chelate approach and potential applications to radiopharmaceutical development are galore. For example, the combination of tumor avid vectors with pharmacological modifiers could lead to the development of radiotracers with improved pharmacological profiles, whereas the use of additional imaging probes or therapeutic agents may lead to the design of multimodal conjugates or theranostics. The exploitation of the strategies described has just begun and it is possible that ongoing research efforts directed towards the combination of different entities with the ^{99m}Tc-tricarbonyl core will lead to the development of novel radiopharmaceuticals with improved properties for application in molecular imaging and/or receptor-mediated radionuclide therapy.

7. Applications of Click-to-Chelate to Radiotracer Development

In the following section, various reported applications of Click-to-Chelate to the development of radiotracers will be summarized, some examples of which have been mentioned already in the text above (including an example of a vitamin, namely folic acid, vitamin B9) [38]. Compounds reported without preclinical *in vitro* and/or *in vivo* data were not included (e.g., "clicked" phospholipids) [21].

Click-to-Chelate has been successfully applied to the ^{99m}Tc-tricarbonyl labeling of different tumor avid peptides including derivatives of bombesin and the ErbB-2-targeting peptides (see above). In these studies, the general utility of "clicked" triazolyl ligand systems for applications to ^{99m}Tc-tricarbonyl labeled peptides and multifunctional radioconjugates was demonstrated. A further example has been reported by Kim *et al*. (Figure 4) who have labeled an epitope-mimicking peptide of the hepatocyte growth factor (HGF)-mesenchymal-epithelial transition factor (Met) molecular pathway, which affects cancer development at different stages [46]. In their work, the length of a spacer unit that separates the c-met binding peptide from the ^{99m}Tc-tricarbonyl chelate was investigated. They have shown that the modification of the peptide was readily accomplished by Click-to-Chelate providing radiopeptides of good stability and excellent binding affinity to the c-met receptor. Based on the *in vitro* evaluation of the radiopeptides investigated, a spacer unit consisting of three glycine units (n = 3) provided the most promising results.

Figure 4. Investigations of the effect of the length of the spacer between a clicked-^{99m}Tc-tricarbonyl chelate and the tumor targeting c-met binding peptide.
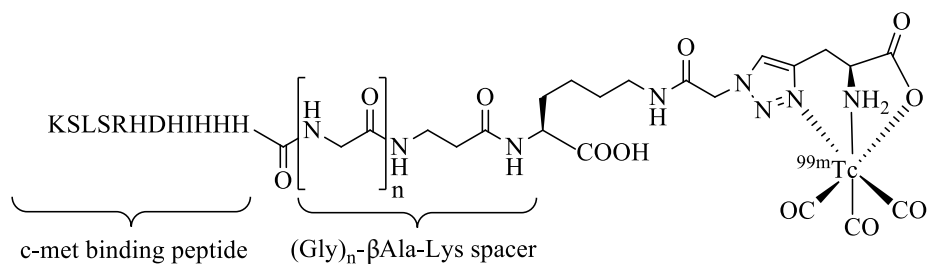

Glucose is considered as a key molecule in metabolic evaluation of tumors due to the up-regulation of glycolysis, which results in an increased consumption of the carbohydrate in tumor tissue [47]. In the past, different strategies have been reported for the identification of a ^{99m}Tc labeled glucose derivative as a more readily available SPECT surrogate of the established PET tracer [^{18}F]-2-fluoro-2-deoxy-D-glucose (FDG) [48]. Fernández *et al.* have prepared a glucose derivative functionalized at the C2 position by the one-pot, 2-step Click-to-Chelate protocol (Figure 5) and studied its biodistribution in comparison to FDG in a lung carcinoma mouse model [49]. Reported tumor uptake *in vivo* of the radiotracer was moderate in comparison to FDG and likely due to passive diffusion of the hydrophilic compound. As in the case of other reported ^{99m}Tc/^{nat}Re-labeled glucose derivatives, specific uptake via the GLUT-1 receptor pathway could not be confirmed.

Figure 5. A glucose derivative functionalized at the C2 position with a regular click ligand by the one-pot, 2-step Click-to-Chelate procedure.
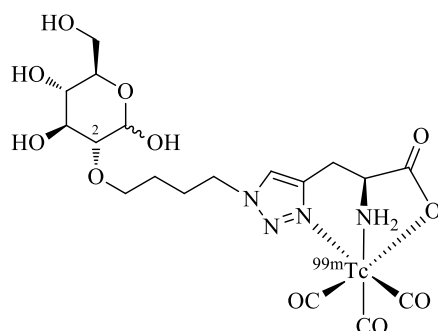

Click-to-Chelate has also been employed to the development of hypoxia imaging agents, which are important radiotracers for the assessment of the oxygenation status of tumors critical for determining the effectiveness of radiation therapy [50]. Fernández *et al.* have investigated the utility of bi- and tridentate click chelators for the ^{99m}Tc-tricarbonyl labeling of 5-nitro-imidazole derivatives prepared by one-pot Click-to-Chelate protocols (Figure 6) [51]. Evaluation of the compounds *in vitro* and *in vivo* revealed that the compound equipped with a tridentate chelator was superior in terms of blood serum stability, plasma protein binding, and tumor uptake. In addition, the "clicked" 5-nitro-imidazole outperformed other ^{99m}Tc-labeled hypoxia imaging agents previously investigated by the same group (e.g., 5-nitroimidazol labeled with ^{99m}Tc(V) nitrido- or ^{99m}Tc(III) [4+1] chelates). The authors conclude that the compound with a tridentate regular click ligand is so far their most promising candidate for the development of a ^{99m}Tc radiopharmaceutical for hypoxia tumor diagnosis.

Figure 6. Comparison of tri- and bidentate click chelators applied to the development of novel hypoxia radiotracers based on 5-nitro-imidazoles.
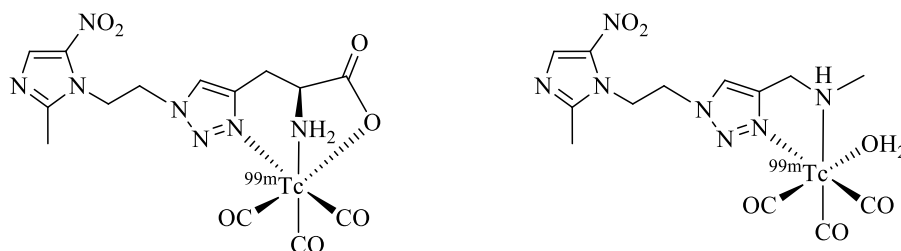
Analogs of the nucleoside thymidine have the potential to be recognized as substrates by the human cytosolic thymidine kinase (hTK1). Since hTK1 is overexpressed in a wide variety of cancer cells, radiolabeled thymidine derivatives represent potential markers for cancer cell proliferation. Struthers *et al.* have reported the synthesis and *in vitro* evaluation of ^{99m}Tc-tricarbonyl labeled thymidine analogs in an effort to develop a radiotracer for SPECT more readily available compared to the currently used PET tracer 3-deoxy-3'-[^{18}F]fluorothymidine (FLT) [35,52]. They prepared a set of ^{99m}Tc-tricarbonyl labeled thymidine derivatives in a combinatorial fashion by parallel one-pot Click-to-Chelate synthesis (Scheme 7; see Table 1, entry 1–5 for examples of alkyne precursors employed). The products obtained differ not only in the position of functionalization (C3' *versus* N3) but also with regards to the size and overall charge of the radiometal chelate. Substrate activity studies carried out by phosphorylation assays showed that substrate recognition by hTK1 is dependent on both, the site of functionalization of thymidine as well as the charge of the ^{99m}Tccomplex. In general, C3'-functionalized compounds were the better substrates for hTK1 and a preference for neutral or anionic complexes was demonstrated. This elegant work has led to the identification of the first metal containing hTK1substrates.

Scheme 7. Synthesis of thymidine analogs functionalized with regular click ligands at the C3' or N3 position developed as substrates for hTK1. dT = deoxythymidine; A and B represent functional groups for coordination of the ^{99m}Tc-ricarbonyl core.
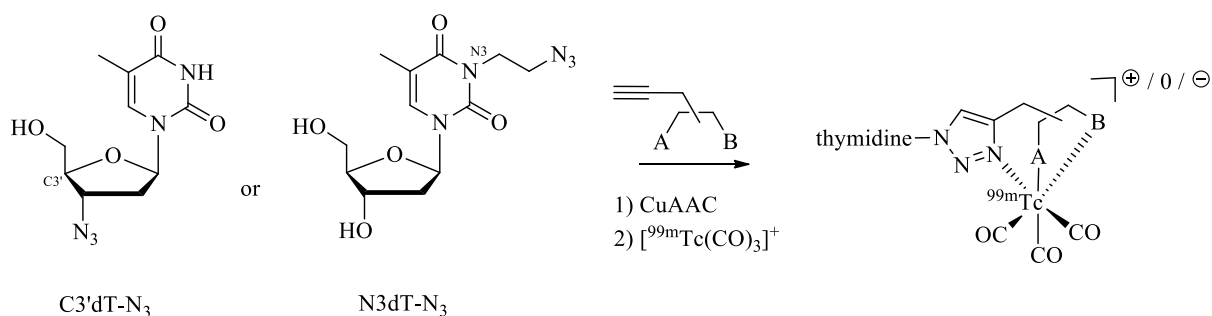
Seridi *et al.* [53] and Hassanzadeh *et al.* [54,55] have used CuAAC in the development of brain radiotracers. They describe the conjugation of bi- and tridentate regular click ligands to 1-(2-methoxyphenyl)piperazine (MPP), a pharmacophore frequently found in imaging agents selective for 5-HT$_{1A}$, a receptor subtype for the neurotransmitter serotonin (5-hydroxytryptamine, 5-HT; Figure 7). The radiotracers exhibited favorable low protein binding, good blood serum stability, and a lipophilicity suitable to cross the blood-brain barrier (BBB). The compound functionalized with a tridentate click ligand was labeled with [^{99m}Tc(CO)$_3$]$^+$ and evaluated *in vitro* and *in vivo*. Receptor saturation experiments performed with homogenated hippocampus membranes of rats revealed a high receptor affinity (K$_D$) of the compound in the single-digit nanomolar range. *In vivo* experiments with rats indicated a specific uptake of the radiotracer in the brain, being highest in the hippocampus. Both

groups conclude that the ^{99m}Tc-labeled MPP derivatives have suitable characteristics for use as central nervous system (CNS) receptor specific imaging agents.
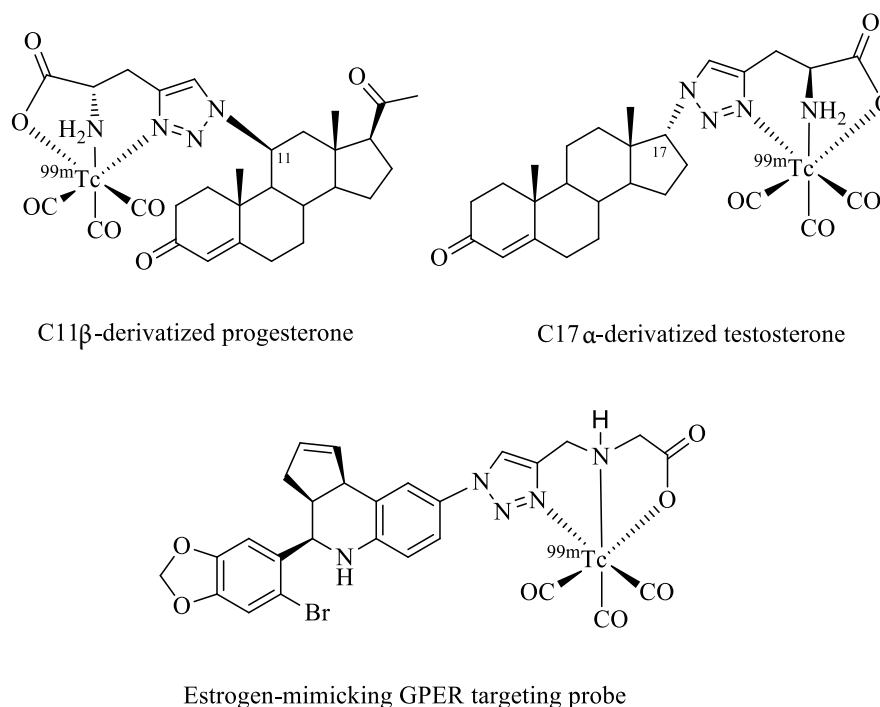
Figure 7. Bi- and tridentate clicked ligands conjugated to MPP for the development of CNS imaging agents.
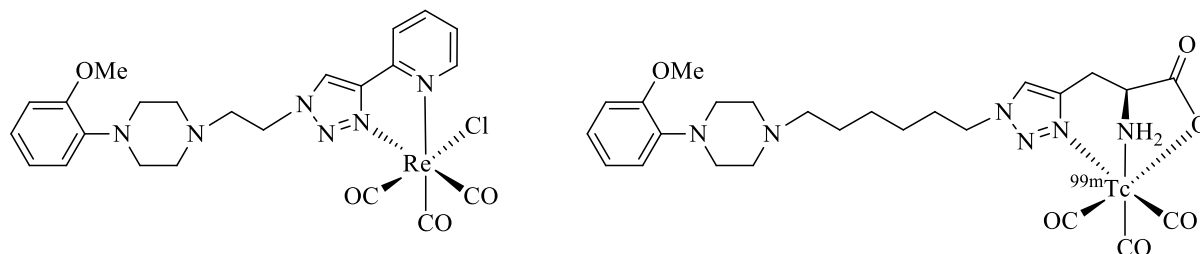
Finally, implementation of Click-to-Chelate to steroid-based radiotracers is discussed (Figure 8). Dhyani *et al*. have investigated ^{99m}Tc-tricarbonyl-labeled derivatives of 11ß-progesterone and 17α-testosterone for targeting progesterone (PR) and androgen receptors (AR), which are overexpressed in breast and prostate cancer, respectively [56,57]. The compatibility of the site of functionalization of the steroids with regards to biological function as well as stereochemical considerations were taken into account for the design of the radiotracers. While the synthesis of the compounds was straightforward and the stability of the radiometal complexes in biological media was excellent, experiments *in vivo* using Swiss mice or Wistar rats did not reveal specificities towards the corresponding receptors. These findings may be the result of the bulkiness of the ^{99m}Tc chelate in comparison to the steroid vector, which could interfere with the interaction of the compound with its binding site.

Burai *et al*. have reported the ^{99m}Tc-tricarbonyl labeling of tetrahydro-*3H*-cyclopenta[c]quinoline, the structural design of which was inspired by estrogen steroids (Figure 8) [58]. Derivatives of the parent compound are specific agonists/antagonists of the recently identified G protein-coupled estrogen receptor (GPER), but not the estrogen ERα/ß receptors. GPERs are involved in tumor signaling pathways and have shown promising properties as putatively important biomarkers or therapeutic targets in oncology. Again, receptor specificity of the vector was lost upon functionalization with the radiometal chelate as shown by *in vitro* assays measuring intracellular calcium immobilization or PI3K activation. In the same work, a series of other ^{99m}Tc-labeled derivatives of the parent compound was investigated of which some, particularly those with a spacer moiety between the radiometal chelate and the vector, showed retained activities as GPER agonists/antagonists. Surprisingly, in none of the "clicked" steroid examples discussed above, the effect of a spacer unit between the receptor specific vector and the radiometal chelate has been investigated.

Figure 8. Examples of steroids or analogs thereof radiolabeled with the ^{99m}Tc-tricarbonyl core by Click-to-Chelate.

C11β-derivatized progesterone   C17α-derivatized testosterone

Estrogen-mimicking GPER targeting probe

8. Summary and Perspectives

Since first reported in 2006, the Click-to-Chelate approach has found numerous applications for the development of radiopharmaceuticals based on the ^{99m}Tc-tricarbonyl core. Examples include organometallic radiotracers with potential for applications in nuclear medicine ranging from peptides, vitamins, carbohydrates, steroids to hypoxia imaging agents, substrates for tumor-associated enzymes (e.g., hTK1), and CNS imaging probes. Thus, Click-to-Chelate has had a demonstrated impact on the community involved in radiopharmaceutical sciences.

The majority of applications discussed in this review employ propargyl glycine (Table 1, entry 1) as an alkyne prochelator. This is likely due to its commercial availability and demonstrated equivalency of the resulting tridentate triazolyl ligand system to Nτ-functionalized His. However, other alkyne derivatives (e.g., readily accessible Nα-propargylated amino acid derivatives; Table 1, entry 2) also hold great promise for future applications, especially in terms of the development of multifunctional radioconjugates.

Meanwhile, new and innovative approaches have been described, which expand the portfolio of click chemistry applications in radiopharmaceutical sciences and eventually in nuclear medicine. With respect to radionuclides of technetium and rhenium, the CuAAC has been employed to BFCAs suitable for the complexation of oxo-technetium species [59], the development of a "click-to-cyclize and chelate" strategy for the cyclization of peptides and their radiolabeling [60], and pre-labeling strategies [61] for the labeling of molecules with pre-formed radiometal complexes. The CuAAC technique has also been applied to the preparation of multiple imaging probes derived from the same precursor for a direct comparison of different imaging probes as well imaging modalities [62]. In addition, copper-free click reactions [63] have become increasingly popular for the development of radiotracers [64–69] including examples of pre-targeting approaches [70].

Click chemistry, in particular the CuAAC reaction, has demonstrated its high potential for the development of radiotracers. However, there are ample opportunities left for new innovations to be reported in the future and first clinical applications of "clicked" probes are being awaited. Among the

many potential applications of click reactions in radiopharmaceutical sciences, Click-to-Chelate will continue to play an important role for the radiolabeling of molecules with the technetium- and rhenium-tricarbonyl cores.

Conflict of Interests

The authors declare no conflicts of interest.

References

1. Fani, M.; André, J.P.; Mäcke, H.R. ^{68}Ga-PET: a powerful generator-based alternative to cyclotron-based PET radiopharmaceuticals. *Contrast Media Mol. Imaging* **2008**, *3*, 53–63.
2. Amato, I. Nuclear Medicine's Conundrum. *Chem. Eng. News Arch.* **2009**, *87*, 58–64.
3. National Research Council/National Academy of Science (USA). *Medical Isotope Production without Highly Enriched Uranium*; National Academies Press: Washington, DC, USA, 2009.
4. Rösch, F.; Baum, R.P. Generator-based PET radiopharmaceuticals for molecular imaging of tumours: on the way to THERANOSTICS. *Dalton Trans.* **2011**, *40*, 6104–6111.
5. Mindt, T.; Struthers, H.; García-Garayoa, E.; Desbouis, D.; Schibli, R. Strategies for the Development of Novel Tumor Targeting Technetium and Rhenium Radiopharmaceuticals. *Chimia* **2007**, *61*, 725–731.
6. Alberto, R.; Schibli, R.; Egli, A.; Schubiger, A.P.; Abram, U.; Kaden, T.A. A Novel Organometallic Aqua Complex of Technetium for the Labeling of Biomolecules: Synthesis of $[^{99m}Tc(OH_2)_3(CO)_3]^+$ from $[^{99m}TcO_4]^-$ in Aqueous Solution and Its Reaction with a Bifunctional Ligand. *J. Am. Chem. Soc.* **1998**, *120*, 7987–7988.
7. Schibli, R.; la Bella, R.; Alberto, R.; García-Garayoa, E.; Ortner, K.; Abram, U.; Schubiger, P.A. Influence of the Denticity of Ligand Systems on the *in Vitro* and *in Vivo* Behavior of $^{99m}Tc(I)$-Ttricarbonyl Complexes: A Hint for the Future Functionalization of Biomolecules. *Bioconjug. Chem.* **2000**, *11*, 345–351.
8. Alberto, R.; Pak, J.K.; van Staveren, D.; Mundwiler, S.; Benny, P. Mono-, Bi-, or Tridentate Ligands? The Labeling of Peptides with ^{99m}Tc-Carbonyls. *Biopolymers* **2004**, *76*, 324–333.
9. Valliant, J.F.; Morel, P.; Schaffer, P.; Kaldis, J.H. Carboranes as Ligands for the Preparation of Organometallic Tc and Re Radiopharmaceuticals. Synthesis of $[M(CO)_3(\eta^5\text{-}2,3\text{-}C_2B_9H_{11})]^-$ and $rac\text{-}[M(CO)_3(\eta^5\text{-}2\text{-}R\text{-}2,3\text{-}C_2B_9H_{11})]^-$ (M = Re, ^{99}Tc; R = $CH_2CH_2CO_2H$) from $[M(CO)_3Br_3]^{2-}$. *Inorg. Chem.* **2002**, *41*, 628–630.
10. Liu, S. The role of coordination chemistry in the development of target-specific radiopharmaceuticals. *Chem. Soc. Rev.* **2004**, *33*, 445–461.
11. Kolb, H.C.; Finn, M.G.; Sharpless, K.B. Click Chemistry: Diverse Chemical Function from a Few Good Reactions. *Angew. Chem. Int. Ed.* **2001**, *40*, 2004–2021.
12. Rostovtsev, V.V.; Green, L.G.; Fokin, V.V.; Sharpless, K.B. A Stepwise Huisgen Cycloaddition Process: Copper(I)-Catalyzed Regioselective "Ligation" of Azides and Terminal Alkynes. *Angew. Chem. Int. Ed. Engl.* **2002**, *41*, 2596–2599.
13. Tornøe, C.W.; Christensen, C.; Meldal, M. Peptidotriazoles on Solid Phase: [1,2,3]-Triazoles by Regiospecific Copper(I)-Catalyzed 1,3-Dipolar Cycloadditions of Terminal Alkynes to Azides. *J. Org. Chem.* **2002**, *67*, 3057–3064.
14. Meldal, M.; Tornøe, C.W., Cu-Catalyzed Azide-Alkyne Cycloaddition. *Chem. Rev.* **2008**, *108*, 2952–3015.
15. Finn, M.G.; Fokin, V.V. Click chemistry: Function follows form (Special Issue). *Chem. Soc. Rev.* **2010**, *39*, 1221–1408.
16. Hein, C.D.; Liu, X.-M.; Wang, D. Click chemistry, a powerful tool for pharmaceutical sciences. *Pharm. Res.* **2008**, *25*, 2216–2230.
17. Kolb, H.C.; Walsh, J.C.; Chen, K. Click chemistry method for synthesizing molecular imaging probes. WO2006116629(A2), 2 November 2006.
18. Marik, J.; Sutcliffe, J.L. Click for PET: rapid preparation of [^{18}F]fluoropeptides using Cu^I catalyzed 1,3-dipolar cycloaddition. *Tetrahedron Lett.* **2006**, *47*, 6681–6684.

19. Mamat, C.; Ramenda, T.; Wuest, F.R. Recent Applications of Click Chemistry for the Synthesis of Radiotracers for Molecular Imaging. *Mini Rev. Org. Chem.* **2009**, *6*, 21–34.

20. Wängler, C.; Schirrmacher, R.; Bartenstein, P.; Wängler, B. Click-Chemistry Reactions in Radiopharmaceutical Chemistry: Fast & Easy Introduction of Radiolabels into Biomolecules for *In Vivo* Imaging. *Curr. Med. Chem.* **2010**, *17*, 1092–1116.

21. Mindt, T.L.; Struthers, H.; Brans, L.; Anguelov, T.; Schweinsberg, C.; Maes, V.; Tourwé, D.; Schibli, R. "Click to Chelate": Synthesis and Installation of Metal Chelates into Biomolecules in a Single Step. *J. Am. Chem. Soc.* **2006**, *128*, 15096–15097.

22. Struthers, H.; Mindt, T.L.; Schibli, R. Metal chelating systems synthesized using the copper(I) catalyzed azide-alkyne cycloaddition. *Dalton Trans.* **2010**, *39*, 675–696.

23. Van Kasteren, S.I.; Kramer, H.B.; Jensen, H.H.; Campbell, S.J.; Kirkpatrick, J.; Oldham, N.J.; Anthony, D.C.; Davis, B.G. Expanding the diversity of chemical protein modification allows post-translational mimicry. *Nature* **2007**, *446*, 1105–1109.

24. Beatty, K.E.; Liu, J.C.; Xie, F.; Dieterich, D.C.; Schuman, E.M.; Wang, Q.; Tirrell, D.A. Fluorescence Visualization of Newly Synthesized Proteins in Mammalian Cells. *Angew. Chem. Int. Ed. Engl.* **2006**, *45*, 7364–7367.

25. Ohta, A.; Yamagishi, Y.; Suga, H. Synthesis of biopolymers using genetic code reprogramming. *Curr. Opin. Chem. Biol.* **2008**, *12*, 159–167.

26. Wang, L.; Schultz, P.G. Expanding the Genetic Code. *Angew. Chem. Int. Ed.* **2005**, *44*, 34–66.

27. Baskin, J.M.; Bertozzi, C.R. Bioorthogonal Click Chemistry: Covalent Labeling in Living Systems. *QSAR Comb. Sci.* **2007**, *26*, 1211–1219.

28. Pak, J.K.; Benny, P.; Spingler, B.; Ortner, K.; Alberto, R. N^ε Functionalization of Metal and Organic Protected L-Histidine for a Highly Efficient, Direct Labeling of Biomolecules with $[Tc(OH_2)_3(CO)_3]^+$. *Chem. Eur. J.* **2003**, *9*, 2053–2061.

29. Brans, L.; García-Garayoa, E.; Schweinsberg, C.; Maes, V.; Struthers, H.; Schibli, R.; Tourwé, D. Synthesis and Evaluation of Bombesin Analogues Conjugated to Two Different Triazolyl-Derived Chelators for ^{99m}Tc Labeling. *ChemMedChem* **2010**, *5*, 1717–1725.

30. Anderson, C.B.; Elliott, A.B.S.; Lewis, J.E.M.; McAdam, C.J.; Gordon, K.C.; Crowley, J.D. *fac*-Re(CO)$_3$ complexes of 2,6-bis(4-substituted-1,2,3-triazol-1-ylmethyl)pyridine"click" ligands: synthesis, characterisation and photophysical properties. *Dalton Trans.* **2012**, *41*, 14625–14632.

31. Urankar, D.; Pinter, B.; Pevec, A.; de Proft, F.; Turel, I.; Košmrlj, J. Click-Triazole N2 Coordination to Transition-Metal Ions Is Assisted by a Pendant Pyridine Substituent. *Inorg. Chem.* **2010**, *49*, 4820–4829.

32. Alberto, R.; Egli, A.; Abram, U.; Hegetschweiler, K.; Gramlich, V.; Schubiger, P.A. Synthesis and Reactivity of [NEt$_4$]$_2$[ReBr$_3$(CO)$_3$]. Formation and Structural Characterization of the Clusters [NEt$_4$][Re$_3$(μ_3-OH)(μ-OH)$_3$(CO)$_9$] and [NEt$_4$][Re$_2$(μ-OH)$_3$(CO)$_6$] by Alkaline Titration. *J. Chem. Soc. Dalton Trans.* **1994**, *1*, 2815–2820.

33. Struthers, H.; Hagenbach, A.; Abram, U.; Schibli, R. Organometallic [Re(CO)$_3$]$^+$ and [Re(CO)$_2$(NO)]$^{2+}$ Labeled Substrates for Human Thymidine Kinase 1. *Inorg. Chem.* **2009**, *48*, 5154–5163.

34. Mindt, T.L.; Struthers, H.; Spingler, B.; Brans, L.; Tourwé, D.; García-Garayoa, E.; Schibli, R. Molecular Assembly of Multifunctional ^{99m}Tc Radiopharmaceuticals Using "Clickable"Amino Acid Derivatives. *ChemMedChem.* **2010**, *5*, 2026–2038.

35. Struthers, H.; Spingler, B.; Mindt, T.L.; Schibli, R. "Click-to-Chelate": Design and Incorporation of Triazole-Containing Metal-Chelating Systems into Biomolecules of Diagnostic and Therapeutic Interest. *Chem. Eur. J.* **2008**, *14*, 6173–6183.

36. Mindt, T.L.; Schweinsberg, C.; Brans, L.; Hagenbach, A.; Abram, U.; Tourwé, D.; García-Garayoa, E.; Schibli, R. A Click Approach to Structurally Diverse Conjugates Containing a Central Di-1,2,3-triazole Metal Chelate. *ChemMedChem* **2009**, *4*, 529–539.

37. Wang, C.; Zhou, W.; Yu, J.; Zhang, L.; Wang, N. A study of the radiosynthesis of *fac*-[^{188}Re(CO)$_3$(H$_2$O)$_3$]$^+$ and its application in labeling 1,2,3-triazole analogs obtained by click chemistry. *Nucl. Med. Commun.* **2012**, *33*, 84–89 .

38. Mindt, T.L.; Müller, C.; Melis, M.; de Jong, M.; Schibli, R. "Click-to-Chelate": In Vitro and In Vivo Comparison of a ^{99m}Tc(CO)$_3$-Labeled N(τ)-Histidine Folate Derivative with Its Isostructural, Clicked 1,2,3-Triazole Analogue. *Bioconjug. Chem.* **2008**, *19*, 1689–1695.

39.   Zhang, X.; Cabral, P.; Bates, M.; Gambini, J.P.; Fernandez, M.; Calzada, V.; Gallazzi, F.; Larimer, B.; Figueroa, S.D.; Alonso, O.; *et al. In Vitro* and *In Vivo* Evaluation of [^{99m}Tc(CO)$_3$]-Radiolabeled ErbB-2-Targeting Peptides for Breast Carcinoma Imaging. *Curr. Radiopharm.* **2010**, *3*, 308–321.

40.   Müller, C.; Schibli, R. Folic Acid Conjugates for Nuclear Imaging of Folate Receptor-Positive Cancer. *J. Nucl. Med.* **2011**, *52*, 1–4.

41.   Sancho, V.; di Florio, A.; Moody, T.W.; Jensen, R.T. Bombesin receptor-mediated imaging and cytotoxicity: review and current status. *Curr. Drug. Deliv.* **2011**, *8*, 79–134.

42.   Ferro-Flores, G.; Rivero, I.A.; Santos-Cuevas, C.L.; Sarmiento, J.I.; Arteaga de Murphy, C.; Ocampo-García, B.E.; García-Becerra, R.; Ordaz-Rosado, D. Click chemistry for [^{99m}Tc (CO)$_3$] labeling of Lys^3-bombesin. *Appl. Radiat. Isotopes* **2010**, *68*, 2274–2278.

43.   Liu, S. 6-Hydrazinonicotinamide Derivatives as Bifunctional Coupling Agents for ^{99m}Tc-Labeling of Small Biomolecules. *Top. Curr. Chem.* **2005**, *252*, 117–153.

44.   Sparr, C.; Michel, U.; Marti, R.E.; Müller, C.; Schibli, R.; Moser, R.; Groehn, V. Synthesis of a Novel γ-Folic Acid-N^τ-Histidine Conjugate Suitable for Labeling with ^{99m}Tc and ^{188}Re. *Synthesis* **2009**, *5*, 787–792.

45.   Kluba, C.A.; Bauman, A.; Valverde, I.E.; Vomstein, S.; Mindt, T.L. Dual-targeting conjugates designed to improve the efficacy of radiolabeled peptides. *Org. Biomol. Chem.* **2012**, *10*, 7594–7602.

46.   Kim, E.-M.; Joung, M.-H.; Lee, C.-M.; Jeong, H.-J.; Lim, S.T.; Sohn, M.-H.; Kim, D.W. Synthesis of Tc-99m labeled 1,2,3-triazole-4-yl c-met binding peptide as a potential c-met receptor kinase positive tumor imaging agent. *Bioorg. Med. Chem. Lett.* **2010**, *20*, 4240–4243.

47.   Pauwels, E.K.J.; Sturm, E.J.C.; Bombardieri, E.; Cleton, F.J.; Stokkel, M.P.M. Positron-emission tomography with [^{18}F]fluorodeoxyglucose. Part I. Biochemical uptake mechanism and its implication for clinical studies. *J. Cancer Res. Clin. Oncol.* **2000**, *126*, 549–559.

48.   Dumas, C.; Petrig, J.; Frei, L.; Spingler, B.; Schibli, R. Functionalization of Glucose at Position C-3 for Transition Metal Coordination: Organo-Rhenium Complexes with Carbohydrate Skeletons. *Bioconjug. Chem.* **2005**, *16*, 421–428.

49.   Fernández, S.; Crócamo, N.; Incerti, M.; Giglio, J.; Scarone, L.; Rey, A. Preparation and preliminary bioevaluation of a ^{99m}Tc(CO)$_3$-glucose derivative prepared by a click chemistry route. *J. Label. Compd. Radiopharm.* **2012**, *55*, 274–280.

50.   Kizaka-Kondoh, S.; Konse-Nagasawa, H. Significance of nitroimidazole compounds and hypoxia-inducible factor-1 for imaging tumor hypoxia. *Cancer Sci.* **2009**, *100*, 1366–1373.

51.   Fernández, S.; Giglio, J.; Rey, A.M.; Cerecetto, H. Influence of ligand denticity on the properties of novel ^{99m}Tc-(I)-carbonyl complexes. Application to the development of radiopharmaceuticals for imaging hypoxic tissue. *Bioorg. Med. Chem.* **2012**, *20*, 4040–4048.

52.   Struthers, H.; Viertl, D.; Kosinski, M.; Spingler, B.; Buchegger, F.; Schibli, R. Charge Dependent Substrate Activity of C3′ and N3 Functionalized, Organometallic Technetium and Rhenium-Labeled Thymidine Derivatives toward Human Thymidine Kinase 1. *Bioconjug. Chem.* **2010**, *21*, 622–634.

53.   Seridi, A.; Wolff, M.; Boulay, A.; Saffon, N.; Coulais, Y.; Picard, C.; Machura, B.; Benoist, E. Rhenium(I) and technetium(I) complexes of a novel pyridyltriazole-based ligand containing an arylpiperazine pharmacophore: Synthesis, crystal structures, computational studies and radiochemistry. *Inorg. Chem. Commun.* **2011**, *14*, 238–242.

54.   Hassanzadeh, L.; Erfani, M.; Ebrahimi, S.E.S., 2-Amino-3-(1-(4-(4-(2-methoxyphenyl) piperazine-1-yl)butyl)-1*H*-1,2,3-triazol-4-yl) propanoic acid: synthesized, ^{99m}Tc-tricarbonyl labeled, and bioevaluated as a potential 5HT$_{1A}$ receptor ligand. *J. Label. Compd. Radiopharm.* **2012**, *55*, 371–376.

55.   Hassanzadeh, L.; Erfani, M.; Najafi, R.; Shafiei, M.; Amini, M.; Shafiee, A.; Ebrahimi, S.E.S. Synthesis, radiolabeling and bioevaluation of a novel arylpiperazine derivative containing triazole as a 5-HT$_{1A}$ receptor imaging agents. *Nucl. Med. Biol.* **2013**, *40*, 227–232.

56.   Dhyani, M.V.; Satpati, D.; Korde, A.; Sarma, H.D.; Kumar, C.; Banerjee, S. Preparation and preliminary bioevaluation of ^{99m}Tc(CO)$_3$-11ß-progesterone derivative prepared via click chemistry route. *Nucl. Med. Biol.* **2010**, *37*, 997–1004.

57.   Dhyani, M.V.; Satpati, D.; Korde, A.; Banerjee, S. Synthesis and Preliminary Bioevaluation of ^{99m}Tc(CO)$_3$-17α-Triazolylandrost-4-Ene-3-One Derivative Prepared via Click Chemistry Route. *Cancer Biother. Radio.* **2011**, *26*, 5, 539–545.

58. Burai, R.; Ramesh, C.; Nayak, T.K.; Dennis, M.K.; Bryant, B.K.; Prossnitz, E.R.; Arterburn, J.B. Synthesis and Characterization of Tricarbonyl-Re/Tc(I) Chelate Probes Targeting the G Protein-Coupled Estrogen Receptor GPER/GPR30. *PLOS One* **2012**, *7*, e46861.

59. Martinage, O.; Le Clainche, L.; Czarny, B.; Dugave, C. Synthesis and biological evaluation of a new triazole-oxotechnetium complex. *Org. Biomol. Chem.* **2012**, *10*, 6484–6490.

60. Simpson, E.J.; Hickey, J.L.; Luyt, L.G. Click to Cyclize and Chelate. *J. Label. Compd. Radiopharm* **2011**, *54*, S350–S350.

61. Moore, A.L.; Bučar, D.-K.; MacGillivray, L.R.; Benny, P.D. "Click" labeling strategy for M(CO)$_3$ (M = Re, ^{99m}Tc) prostate cancer targeted Flutamide agents. *Dalton Trans.* **2010**, *39*, 1926–1928.

62. Mindt, T.L.; Müller, C.; Stuker, F.; Salazar, J.-F.; Hohn, A.; Mueggler, T.; Rudin, M.; Schibli, R. A "Click Chemistry" Approach to the Efficient Synthesis of Multiple Imaging Probes Derived from a Single Precursor. *Bioconjug. Chem.* **2009**, *20*, 1940–1949.

63. Jewett, J.C.; Bertozzi, C.R. Cu-free click cycloaddition reactions in chemical biology. *Chem. Soc. Rev.* **2010**, *39*, 1272–1279.

64. Van Berkel, S.S.; Dirks, A.J.; Meeuwissen, S.A.; Pingen, D.L.L.; Boerman, O.C.; Laverman, P.; van Delft, F.L.; Cornelissen, J.J.L.M.; Rutjes, F.P.J.T. Application of Metal-Free Triazole Formation in the Synthesis of Cyclic RGD-DTPA Conjugates. *ChemBioChem* **2008**, *9*, 1805–1815.

65. Campbell-Verduyn, L.S.; Mirfeizi, L.; Schoonen, A.K.; Dierckx, R.A.; Elsinga, P.H.; Feringa, B.L. Strain-Promoted Copper-Free "Click" Chemistry for ^{18}F Radiolabeling of Bombesin. *Angew. Chem. Int. Ed. Engl.* **2011**, *50*, 11117–11120.

66. Bouvet, V.; Wuest, M.; Wuest, F. Copper-free click chemistry with the short-lived positron emitter fluorine-18. *Org. Biomol. Chem.* **2011**, *9*, 7393–7399.

67. Zeglis, B.M.; Mohindra, P.; Weissmann, G.I.; Divilov, V.; Hilderbrand, S.A.; Weissleder, R.; Lewis, J.S. Modular Strategy for the Construction of Radiometalated Antibodies for Positron Emission Tomography Based on Inverse Electron Demand Diels-Alder Click Chemistry. *Bioconjug. Chem.* **2011**, *22*, 2048–2059.

68. Chen, K.; Wang, X.; Lin, W.-Y.; Shen, C.K.F.; Yap, L.-P.; Hughes, L.D.; Conti, P.S. Strain-Promoted Catalyst-Free Click Chemistry for Rapid Construction of ^{64}Cu-Labeled PET Imaging Probes. *ACS Med. Chem. Lett.* **2012**, *3*, 1019–1023.

69. Devaraj, N.K.; Weissleder, R. Biomedical Applications of Tetrazine Cycloadditions. *Accounts Chem. Res.* **2011**, *44*, 816–827.

70. Rossin, R.; Verkerk, P.R.; van den Bosch, S.M.; Vulders, R.C.M.; Verel, I.; Lub, J.; Robillard, M.S. *In Vivo* Chemistry for Pretargeted Tumor Imaging in Live Mice. *Angew. Chem. Int. Ed.* **2010**, *49*, 3375–3378.

III.   Dual-Targeting Conjugates Designed to Improve the Efficacy of Radiolabeled Peptides

Christiane A. Kluba, Andreas Bauman, Ibai E. Valverde, Sandra Vomstein, and Thomas L. Mindt[*]

Division of Radiopharmaceutical Chemistry, Clinic of Radiology and Nuclear Medicine, University of Basel Hospital, Petersgraben 4, 4031 Basel; Switzerland
([*]corresponding author)

Abstract: Radiolabeled regulatory peptides are useful tools in nuclear medicine for the diagnosis (imaging) and therapy of cancer. The specificity of the peptides towards GPC receptors, which are overexpressed by cancer cells, and their favorable pharmacokinetic profile make them ideal vectors to transport conjugated radionuclides to tumors and metastases. However, after internalization of the radiopeptide into cancer cells and tumors, a rapid washout of a substantial fraction of the delivered radioactivity is often observed. This phenomenon may represent a limitation of radiopeptides for clinical applications. Here, we report the synthesis, radiolabeling, stability, and *in vitro* evaluation of a novel, dual-targeting peptide radioconjugate designed to enhance the cellular retention of radioactivity. The described bifunctional radioconjugate is comprised of a Tc-99m SPECT reporter probe, a cell membrane receptor-specific peptide, and a second targeting entity directed towards mitochondria. While the specificity of the first generation of dual-targeting conjugates towards its extracellular target was demonstrated, intracellular targeting could not be confirmed probably due to non-specific binding or hindered passage through the membrane of the organelle. The work presented describes a novel approach with potential to improve the efficacy of radiopharmaceuticals by enhancing the intracellular retention of radioactivity.

Contributions:

Christiane A. Fischer carried out the syntheses, characterization, radiolabeling, organization and conduction of *in vitro* evaluation, and wrote the paper with Thomas L. Mindt.

PAPER

Dual-targeting conjugates designed to improve the efficacy of radiolabeled peptides†

Christiane A. Kluba, Andreas Bauman, Ibai E. Valverde, Sandra Vomstein and Thomas L. Mindt*

Radiolabeled regulatory peptides are useful tools in nuclear medicine for the diagnosis (imaging) and therapy of cancer. The specificity of the peptides towards GPC receptors, which are overexpressed by cancer cells, and their favorable pharmacokinetic profile make them ideal vectors to transport conjugated radionuclides to tumors and metastases. However, after internalization of the radiopeptide into cancer cells and tumors, a rapid washout of a substantial fraction of the delivered radioactivity is often observed. This phenomenon may represent a limitation of radiopeptides for clinical applications. Here, we report the synthesis, radiolabeling, stability, and *in vitro* evaluation of a novel, dual-targeting peptide radioconjugate designed to enhance the cellular retention of radioactivity. The described trifunctional conjugate is comprised of a Tc-99m SPECT reporter probe, a cell membrane receptor-specific peptide, and a second targeting entity directed towards mitochondria. While the specificity of the first generation of dual-targeting conjugates towards its extracellular target was demonstrated, intracellular targeting could not be confirmed probably due to non-specific binding or hindered passage through the membrane of the organelle. The work presented describes a novel approach with potential to improve the efficacy of radiopharmaceuticals by enhancing the intracellular retention of radioactivity.

Introduction

Conjugation of radionuclides to tumor-targeting peptides enables their application for the diagnosis (using gamma- or positron-emitting nuclides) and therapy (employing beta- or alpha-particle emitters) of cancer. In particular, radiometal-labeled regulatory peptides, which target G-protein-coupled receptors (GPCRs) overexpressed in different cancers, have been a focus of radiopharmaceutical and nuclear medicinal research over the past decade. As a result, some radiometal-labeled peptides have found routine application in the clinic (*e.g.*, somatostatin derivatives for the management of neuroendocrine tumors), while other promising candidates are currently the subject of preclinical evaluation or have recently advanced to clinical trials.[1–4]

Radiolabeled regulatory peptides internalize into tumor cells by GPCR-mediated endocytosis. A potential drawback of a number of reported radiopeptides is represented by a rapid washout of a substantial fraction of the intracellular radioactivity from cancer cells (*in vitro*) and tumors (*in vivo*). In some instances, the *in vitro* externalization of radioactivity from cancer cells occurs at a rate comparable to the internalization.[5–8] Also, a significant washout of radioactivity from tumors over time is often observed *in vivo*.[6,9–11] This phenomenon can render the initial efforts of delivering specifically radioactive nuclides to cancer cells and tumors in part futile. The mechanism by which the radioactivity is externalized from cancer cells and tumors is yet not fully understood and can vary depending on, *e.g.*, the peptide carrier or the composition of the radioconjugate employed. For example, cellular washout of radioactivity in the form of metabolic degradation products has been reported for radiometal-labeled derivatives of bombesin and minigastrins.[12,13] On the other hand, the externalization of intact radiometal conjugates has been observed for somatostatin and exendin-4 derivatives.[7,9,11] Regardless of the metabolic fate of the tumor-targeting peptide vector, it is generally accepted that the efficacy of radioconjugates correlates with a high rate of internalization into, and a low rate of externalization from targeted tissue.

We herein wish to report our efforts to combine tumor-targeting radiolabeled peptides with a second moiety which targets intracellular components. We hypothesized that such an additional moiety (*e.g.*, directed against intracellular proteins, enzymes, or cell compartments) of the resulting dual-targeting radioconjugates will decrease the externalization rate of radioactivity from cancer cells and tumors independent of the vector used. An increased retention time of the delivered radioactivity within tumors holds the promise to improve the signal-to-background ratio important for diagnostic (imaging) applications and

University of Basel Hospital, Department of Radiological Nuclear Medicine, Division of Radiological Chemistry, Petersgraben 4, 4031 Basel, Switzerland. E-mail: TMindt@uhbs.ch; Fax: +41 (0)61 265 55 99; Tel: +41 (0)61 556 53 80

to enhance the efficacy of therapeutic radionuclides as a result of the increased energy deposited in cancerous tissue.

In recent years, new approaches for the development of radiopharmaceuticals have emerged, which aim at the combination of the tumor-targeting properties of radiolabeled peptides with other entities of interest. Reported examples include the combination of radiopeptides with pharmacological modifiers to improve their pharmacokinetic and/or –dynamic characteristics[14–16] or therapeutic efficacy,[7,17–19] optical dyes for the design of dual-modal imaging probes for high sensitivity and high resolution imaging,[20,21] and therapeutic agents[22] for the development of theranostics.[23] The potential of multifunctional radioconjugates, which exploit the individual properties of components or synergistic effects thereof, respectively, for applications in nuclear medicine is intriguing, however, their synthesis can be challenging.

We have previously reported a modular synthetic approach which employs the Cu(I)-catalyzed alkyne–azide cycloaddition (CuAAC; click chemistry)[24,25] for the efficient preparation of multifunctional radioconjugates.[14,26] In this approach, an $N(\alpha)$-propargyl derivative of the amino acid lysine functions as the center piece of the final conjugate by providing the means for conjugation of two different chemical/biological moieties by selective amide bond formation and CuAAC (Fig. 1). In addition, the $N(\alpha)$-propargyl lysine derivative is a prochelator which forms, after formation of the 1,2,3-triazole by CuAAC, a tridentate ligand system for the stable complexation of the ^{99m}Tc-tricarbonyl core suitable for imaging by single photon emission computed tomography (SPECT).[27,28] The diagnostic isotope technetium-99m forms a "matched pair" with chemically related therapeutic β^--particle emitters rhenium-186/188 and, therefore, the chemistry developed has the potential to be used for the development of radioconjugates for both diagnostic and therapeutic applications in nuclear medicine.[29]

We set out to investigate the use of the "click chemistry" strategy for the assembly of trifunctional conjugates made up of a ^{99m}Tc-tricarbonyl reporter probe for SPECT, a tumor-targeting peptide, and an additional entity specific for an intracellular target, *e.g.*, a cellular compartment. For the first generation of the proposed dual-targeting radioconjugates, we selected a reported, stabilized variation of the minimal binding sequence of bombesin (BBS), [Nle^{14}]BBS(7–14),[12] as an extracellular tumor-targeting component. BBS is a regulatory peptide that targets the gastrin-releasing peptide (GRP) receptor, which is overexpressed

by various cancer cell types including prostate, breast, and small-cell lung cancer.[30] The potential of derivatives of [Nle^{14}]-BBS(7–14) radiolabeled with the ^{99m}Tc(CO)$_3$ core for cancer imaging has been demonstrated *in vitro* and *in vivo*.[12,15,28] Based on literature precedence, we introduced a spacer made of multiple β-alanine units to separate the tumor-targeting peptide from other parts of the conjugate in order to minimize potentially unfavorable interferences.[10,12] As an intracellular target, we chose the organelle mitochondria. It has been shown that lipophilic, cationic species such as triphenylphosphonium (TPP) moieties can be driven electrophoretically through negatively charged transmembranes, resulting in an accumulation of the compounds inside the energized mitochondria of cells. TPPs have been used as a drug delivery system for the transport of therapeutic agents to the mitochondria.[31] Also, radioactive labeled TPP derivatives have been studied for myocardial imaging and tumor imaging.[32]

The combination of receptor-targeting radiopeptides with moieties specific for the cell nucleus (*e.g.*, DNA intercalator or cell penetrating peptides) has been reported to exploit potentially the therapeutic effect of short-range Auger electron-emitting radionuclides, however with varying degrees of success.[7,19] The use of mitochondria-specific entities (*e.g.*, TPPs) for improving the intracellular retention of radioactivity after selective delivery by tumor-avid peptides has yet not been described in the context of dual-targeting radioconjugates.

Results and discussion

Scheme 1 outlines the synthesis of building blocks required for the assembly of trifunctional conjugates. The preparation of the
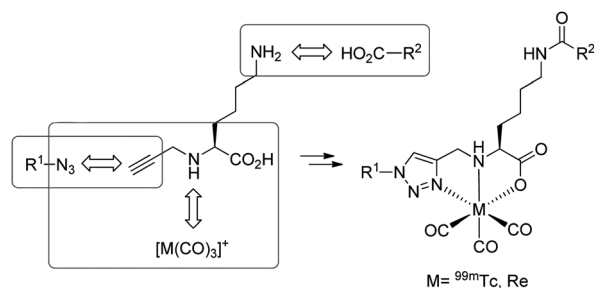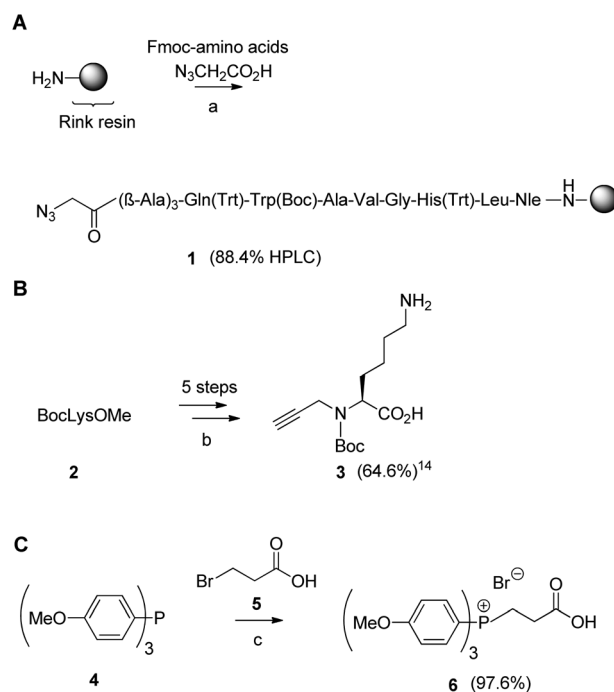

Fig. 1 Assembly of trifunctional conjugates by selective amide bond formation, CuAAC (click chemistry), and (radio)metal complexation; residues R^1 and R^2 represent two different moieties of biological function to be combined in the final (radio)metal conjugate.
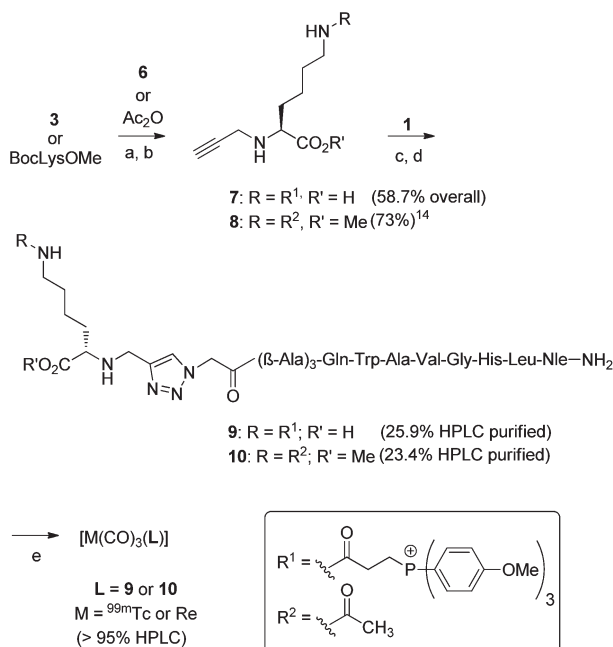

Scheme 1 Synthesis of building blocks. (a) SPPS: (i) piperidine (20%) in DMF; TBTU–HOBt (4 equiv.), (ii) Fmoc-amino acids or azidoacetic acid (3 equiv.), HATU (3 equiv.); (b) see ref. 14; (c) toluene, reflux, 5 h.

tumor targeting peptide [Nle[14]]BBS(7–14), its N-terminal elongation with three β-Ala units, and azidoacetic acid was accomplished by standard solid phase peptide synthesis (SPPS) yielding protected azide-functionalized peptide **1** on the resin (Scheme 1A; see the Experimental section for details). The central piece of the trifunctional conjugate, $N(\alpha)$Boc-$N(\alpha)$propargyl lysine **3**, was prepared from commercial BocLysOMe (**2**) in five steps as previously described (Scheme 1B).[14] An appropriately functionalized mitochondria-targeting entity, 3-tris(p-methoxyphenyl)-phosphonium propionic acid **6**, was synthesized by the reaction of tris(p-methoxyphenyl)phosphine (**4**) with 3-bromo-propionic acid (**5**; Scheme 1C).[33]

The assembly of the trifunctional conjugate started with the coupling of TPP derivative **6** to the $N(\varepsilon)$-amine of the side chain of Lys-derivative **3** followed by TFA-mediated removal of the $N(\alpha)$Boc protective group (Scheme 2). The resulting intermediate **7** was then reacted with protected, azide-functionalized peptide **1** by CuAAC on a solid support. After cleavage from the resin and deprotection, conjugate **9** was purified by preparative HPLC and its structure was confirmed by mass spectrometric analysis (Table 2). To study the effect of the mitochondria-targeting TPP moiety, we also synthesized reference compound **10** from intermediate **8**[14] by the same synthetic pathway (see the Experimental part for details). Compound **10** is identical to conjugate **9** in all respects but lacks the TPP moiety at the $N(\varepsilon)$-amine of the Lys residue (replaced by an acetate group).

Both peptide conjugates **9** and **10** were readily radiolabeled with [^{99m}Tc(CO)$_3$(H$_2$O)$_3$]$^+$ within 30 min at 100 °C, providing the desired radiopeptides [^{99m}Tc(CO)$_3$(L)] (L = **9**, **10**) in >95% radiochemical yield and purity. The radioconjugates were obtained with a specific activity of up to 17.4 GBq µmol^{-1} (not optimized). In the case of methyl ester **10**, ester hydrolysis and labeling with ^{99m}Tc-tricarbonyl occurred simultaneously under the reaction conditions applied.[14] For characterization purposes, the corresponding non-radioactive rhenium tricarbonyl complexes [Re(CO)$_3$(L)] (L = **9**, **10**) were prepared by the reaction of conjugates **9** and **10** with [Re(CO)$_3$Br$_3$][Et$_4$N]$_2$[34] for 60 min at 100 °C and analyzed by mass spectrometry. The identity of [^{99m}Tc(CO)$_3$(L)] (L = **9**, **10**) was confirmed in each case by comparison of the γ-HPLC trace with the UV trace of the corresponding rhenium complexes [Re(CO)$_3$(L)] (L = **9**, **10**), a procedure which is common practice with ^{99m}Tc complexes on an n.c.a. (no carrier added) level (Fig. 2).

The stability of the radiolabeled peptides was evaluated in different media at 37 °C. Both [^{99m}Tc(CO)$_3$(L)] (L = **9**, **10**) were stable (>95% as determined by HPLC) in PBS (pH 7.4), NaCl (0.9%), and in a cell culture medium (1% FBS) for >4 h, the period of time required for the *in vitro* experiments described below (see the Experimental part for details). We also verified the stability of the Tc-99m complexes in a ligand challenge experiment.[35] Thus, [^{99m}Tc(CO)$_3$(L)] (L = **9**, **10**) were incubated at 37 °C in PBS containing a 4500-fold excess of histidine, an excellent tridentate chelator for complexation of the Tc-99m tricarbonyl core. No transmetallation was observed over a period of 24 h, therefore demonstrating the suitability of the employed Lys-based chelator unit of the conjugates.
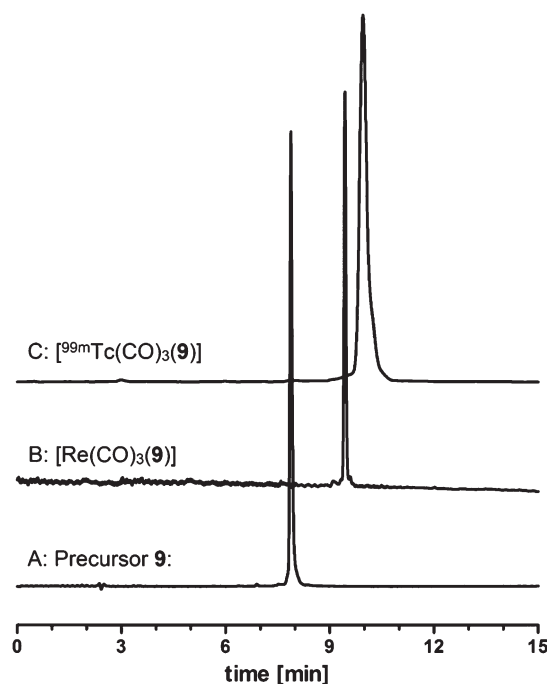

Scheme 2 Assembly of dual targeting radiopeptide conjugates. (a) For **7**: **6**, SOCl$_2$, CH$_2$Cl$_2$, rt overnight; then **3** and Et$_3$N, −78 °C, 4 h; for **8**: see ref. 14; (b) CH$_2$Cl$_2$–TFA (3 : 1), rt overnight; (c) DIPEA, [Cu(CH$_3$CN)$_4$]PF$_6$, TBTA, DMF, rt overnight; (d) trifluoroacetic acid, phenol, water, triisopropylsilane (87.5/5/5/2.5%), 2 h, rt; (e) for M = Tc-99m: 0.1 mM of **9** or **10** in water, [^{99m}Tc(CO)$_3$(H$_2$O)$_3$]$^+$ (100–250 MBq), 100 °C, 30 min; for Re complexes: 0.4 mM of **9** or **10** in water, [Re(CO)$_3$Br$_3$][Et$_4$N]$_2$ (1.5 equiv.), 100 °C, 60 min.

Fig. 2 HPLC chromatographs of peptide precursor **9** (UV-trace A), the corresponding metal conjugates [Re(CO)$_3$(**9**)] (UV-trace B), and [^{99m}Tc(CO)$_3$(**9**)] (γ-trace C). The small difference of retention times between [Re(CO)$_3$(**9**)] and [^{99m}Tc(CO)$_3$(**9**)] (traces B and C) is due to the serial arrangement of the UV- and γ-detectors.

We next investigated *in vitro* the receptor affinity as well as internalization and externalization characteristics of the conjugates $[^{99m}Tc(CO)_3(L)]$ (L = **9**, **10**) using PC-3 cells (n = 3–4 in triplicate). The binding affinity of the bombesin derivatives towards GRP-receptors was determined by receptor saturation binding experiments employing increasing amounts of the radio-conjugates (Fig. 3). Non-specific receptor binding was assessed by using an excess of natural bombesin BBS(1–14). Reference peptide $[^{99m}Tc(CO)_3(\mathbf{10})]$ displayed a dissociation constant (K_d) of 5.6 ± 0.8 nM. In comparison, dual-targeting $[^{99m}Tc(CO)_3(\mathbf{9})]$ exhibited a decreased receptor binding affinity with a K_d of 41.6 ± 5.8 nM. Values of dissociation constants in the single- to lower double-digit nanomolar range are usually reported for radiolabeled regulatory peptides.

Despite the differences in receptor binding affinities, we observed that both radioconjugates internalized into PC-3 cells to the same extent and at a comparable rate (approx. 25% of the applied radioactivity within 30–90 min; Fig. 4). These results are comparable with those reported for related BBS derivatives labeled with the ^{99m}Tc-tricarbonyl core.[15] In comparison to reference compound $[^{99m}Tc(CO)_3(\mathbf{10})]$, $[^{99m}Tc(CO)_3(\mathbf{9})]$ exhibited some degree of non-specific internalization as determined by blocking experiments using a 1000-fold excess of natural bombesin BBS(1–14). Albeit not ideal, low levels of non-specific binding and internalization have been described for a number of receptor-specific radiotracers, some of which have advanced to the stage of preclinical or clinical investigations nevertheless.[11,36] In the case reported herein, however, the lipophilicity introduced by the TPP moiety and/or the ^{99m}Tc-$(CO)_3$ core could also be in part responsible for the observed non-specific binding and internalization of the trifunctional conjugate.

Determination of the log D of peptide precursors **9** and **10**, and the corresponding metal conjugates by HPLC indeed revealed increased lipophilicities for TPP-containing peptide **9** and, more pronounced, its metal-labeled analogues $[M(CO)_3(L)]$ (M = ^{99m}Tc, Re; L = **9**) (Table 1, n = 3). While some non-specific binding and internalization of a peptidic radiotracer is not necessarily a criterion for exclusion from further developments, one has to critically acknowledge that an increased lipophilicity can result in an unfavorable biodistribution. On the other hand, it is known that the lipophilicity of a radiopeptide can be adjusted by the attachment of polar groups (*e.g.*, by pegylation or glycosylation), or the use of charged and/or polar linkers.[16,37]

Experiments performed with radiopeptides $[^{99m}Tc(CO)_3(L)]$ (L = **9**, **10**) showed, undesirably, a very similar externalization pattern for both conjugates, resulting in a washout of *ca.* 50% of intracellular radioactivity after 90 min, approximately the same time required for specific internalization of the radioconjugates into GRP-receptor expressing PC-3 cells (Fig. 5).

Fig. 4 Internalization of radiometal conjugates in GRP-receptor expressing PC-3 cells; normalized to 10^6 cells per well; total binding of $[^{99m}Tc(CO)_3(\mathbf{10})]$ (○, dotted line) and $[^{99m}Tc(CO)_3(\mathbf{9})]$ (△, continuous line); non-specific binding as determined by blocking experiments in the presence of excess natural BBS: $[^{99m}Tc(CO)_3(\mathbf{10})]$ (●, dotted line) and $[^{99m}Tc(CO)_3(\mathbf{9})]$ (▲, continuous line).
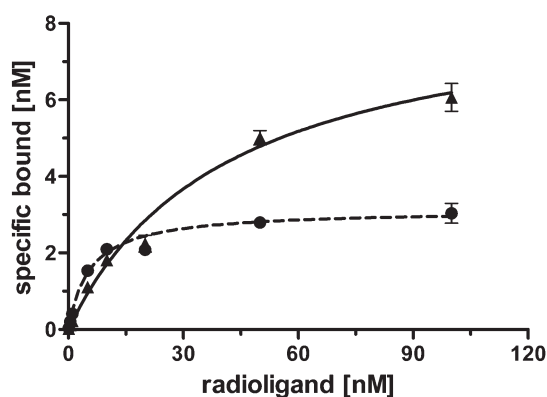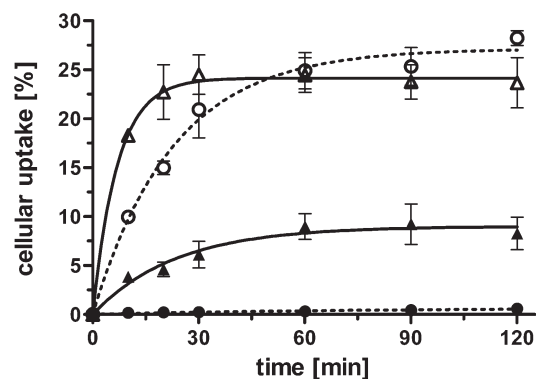

Fig. 3 Receptor saturation binding experiments of radiometal conjugates using GRP-receptor expressing PC-3 cells; normalized to 10^6 cells per well; specific binding of $[^{99m}Tc(CO)_3(\mathbf{10})]$ (●, dotted line) and $[^{99m}Tc(CO)_3(\mathbf{9})]$ (▲, continuous line); K_d values were determined by nonlinear regression.

Table 1 Log D of peptides and (radio)metal-labeled analogues determined by HPLC

Compound	Log D
9	1.23 (±0.04)
$[Re(CO)_3(\mathbf{9})]$	3.01 (±0.01)
$[^{99m}Tc(CO)_3(\mathbf{9})]$	3.11 (±0.02)
10	0.51 (±0.06)
$[Re(CO)_3(\mathbf{10})]$	0.80 (±0.07)
$[^{99m}Tc(CO)_3(\mathbf{10})]$	0.78 (±0.01)

Table 2 Yields and analytical data of synthesized peptides

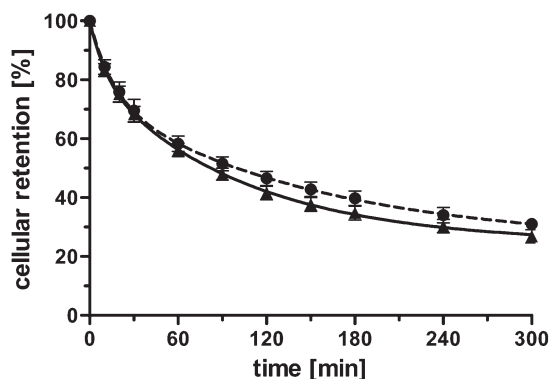| Compound	Molecular formula	Yield (isolated)	Calcd M_W (g mol^{-1})	MALDI-MS m/z	Purity (HPLC)
9	$C_{88}H_{123}N_{21}O_{19}P$	25.9%	1808.90	$[M]^+$: 1808.86	98.6%
10	$C_{67}H_{103}N_{21}O_{16}$	23.4%	1457.79	$[M + H]^+$: 1459.2, $[M + 2H]^{2+}$: 730.2	97.6%

Fig. 5 Externalization of radioactivity from GRP-receptor expressing PC-3 cells. Externalization of the total internalized fraction at $t = 0$ (100%) of radiotracers: $[^{99m}Tc(CO)_3(\mathbf{10})]$ (●, dotted line) and $[^{99m}Tc(CO)_3(\mathbf{9})]$ (▲, continuous line).
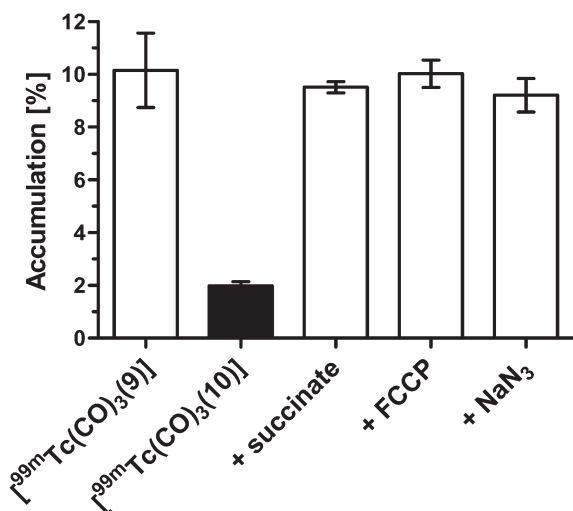

Fig. 6 Accumulation of radiometal conjugates in mitochondria. $[^{99m}Tc(CO)_3(\mathbf{9})]$ (white bars) and $[^{99m}Tc(CO)_3(\mathbf{10})]$ (black bar) without additives, and $[^{99m}Tc(CO)_3(\mathbf{9})]$ in the presence of succinate (10 mM), FCCP (0.5 μM), or sodium azide (20 mM).

Puzzled by the results obtained from these experiments we resorted to investigating in more detail the binding of the radioconjugates to mitochondria. Subcellular fractionation following internalization experiments did not reveal a statistically significant accumulation of the dual-targeting conjugate $[^{99m}Tc(CO)_3(\mathbf{9})]$ in the target organelle (data not shown). To simplify the experimental set-up, additional tests were conducted with mitochondria isolated from PC-3 cells (see the Experimental part). In brief, $[^{99m}Tc(CO)_3(L)]$ (L = $\mathbf{9}$, $\mathbf{10}$; 11.5 kBq and 15.3 kBq, respectively; 5 pmol of peptide) were incubated with mitochondria (1 μg protein per mL) for 30–120 min (Fig. 6; $n = 4$ for all experiments described henceforth). In these experiments, the multifunctional conjugate $[^{99m}Tc(CO)_3(\mathbf{9})]$ exhibited a steady and statistically significantly enhanced binding to mitochondria (10.15 ± 1.41%) in comparison to reference compound $[^{99m}Tc(CO)_3(\mathbf{10})]$ (1.98 ± 0.16%; unpaired t-test; $p < 0.0001$). To the best of our knowledge these data represent the first report

of quantification of the binding of a radiotracer to isolated mitochondria.

In a further effort to verify the specificity of $[^{99m}Tc(CO)_3(\mathbf{9})]$ towards mitochondria, we performed experiments following procedures described by Murphy *et al.* and others,[38–40] in which isolated mitochondria are pretreated with established reagents that either disrupt the transmembrane potential of the organelle (sodium azide (NaN_3) or carbonyl cyanide 4-(trifluoromethoxy) phenylhydrazone (FCCP)) or enhance it (succinate), respectively. In all cases, the binding of $[^{99m}Tc(CO)_3(\mathbf{9})]$ to mitochondria was not influenced by the presence of the additive (Fig. 6). It is therefore possible that the binding of $[^{99m}Tc(CO)_3(\mathbf{9})]$ to mitochondria described above is not driven by the transmembrane potential of the organelle but may be the result of non-specific binding. Alternatively, the ability of TPPs to shuttle conjugated cargo into mitochondria can vary depending on the composition of the conjugate. For instance, examples for successful and unsuccessful mitochondria-targeting of TPP moieties conjugated to (not receptor specific) peptides have both been reported.[38,41] Thus, it is also feasible that the passage of $[^{99m}Tc(CO)_3(\mathbf{9})]$ through the membrane of mitochondria is hindered and therefore interfered with the intracellular targeting. Distinction of the two possible processes, which could impede the specific accumulation of the dual-targeting radioconjugate in mitochondria, may be challenging and requires further investigations. In the meantime, we are examining a second generation of dual-targeting radioconjugates, which target cytosolic proteins instead of organelles and therefore do not require trafficking through intracellular membranes. By simplifying the intracellular targeting system we expect to gain more insights into the structural requirements of a dual-targeting radioconjugate leading to an improved retention of radioactivity in cancer cells and tumors.

Experimental

CAUTION: ^{99m}Tc is a γ-emitter (140 keV) with a half-life of 6.01 h. All reactions involving ^{99m}Tc were performed in a laboratory approved for the handling of radionuclides and appropriate safety procedures were followed at all times to prevent contamination.

General procedures

Fmoc-amino acids, Rink Amide MBHA LL resin (100–200 mesh), HOBt, HATU, and TBTU were purchased from Merck Biosciences (Nottingham, UK). Bombesin (1–14) trifluoroacetate and BocLysOMe were purchased from Bachem (Bubendorf, Switzerland). Solvents and all other chemicals were purchased from Acros Organics (Geel, Belgium), Merck (Darmstadt, Germany), or Sigma Aldrich (Buchs, Switzerland) and used as supplied unless stated otherwise. Polypropylene syringes for manual peptide couplings, fitted with polypropylene frits and a polypropylene plunger, were obtained from MultiSyntech (Witten, Germany) and Teflon taps from Biotage (Uppsala, Sweden). $Na[^{99m}TcO_4]$ was eluted from a Mallinckrodt $^{99}Mo/^{99m}Tc$ generator (Tyco Healthcare, Petten, The Netherlands) using 0.9% saline. The precursor $[^{99m}Tc(CO)_3(H_2O)_3]^+$ was prepared by using the IsoLink™ kit (Mallinckrodt-Tyco,

Petten, The Netherlands). Column chromatography was carried out using silica gel C60 (particle size 0.04–0.063 mm) (Sigma) and TLC was performed on precoated silica gel plates (0.25 mm, 60F^{254}, Merck). ^{1}H-, ^{13}C- and ^{31}P-NMR spectra were recorded on a Bruker DPX 400 instrument. Chemical shifts are reported in parts per million (ppm) relative to tetramethylsilane (0.00 ppm) and coupling constants (J) in hertz (Hz). Standard abbreviations indicating multiplicity are singlet (s), doublet (d), doublet of doublets (dd), triplet (t), and multiplet (m). Analytical and preparative HPLC were carried out with systems from Bischoff Chromatography, equipped with a λ-1010 UV/Vis and an LB509 radioflow detector (Berthold Technologies), using C18 reversed-phase columns (Macherey Nagel Nucleodur C18 ISIS, 5 μm, 250 × 4.6 mm (column A) or Phenomenex Jupiter 4u Proteo 90 Å, 4 μm, 250 × 4.6 mm (column B) for analysis and Macherey Nagel Nucleodur C18 ISIS, 5 μm, 250 × 16 mm (column C) or Nucleosil 100-5 C18, 5 μm, 250 × 21.0 mm (column D) for purifications). HPLC solvents were 0.1% TFA in H$_2$O (A) and MeCN (B). Quality control of (radio)metal labeled peptides was performed using column B and a linear gradient from 80% to 30% A in 15 min (flow: 1.5 mL min^{-1}); peptide purification was performed using column C and a linear gradient from 70% to 50% A in 15 min (flow: 8 mL min^{-1}); purification of compound **7** was done using column D and a linear gradient from 55% to 35% A in 20 min (flow: 10 mL min^{-1}). Log D measurements were performed using column A and an isocratic gradient 25% phosphate buffer (pH 7.4) and 75% methanol (run time: 15–40 min; flow: 1 mL min^{-1}). LRMS analyses were performed on a 4800 MALDI TOF/TOF™ analyzer (Applied Biosystems) or on an ESI Bruker Esquire 3000 plus. HRMS analyses were performed by LC-ESI on an LTQ Orbitrap XL mass spectrometer (Thermo Scientific). Quantitative γ-counting was performed on a COBRA II auto-gamma system (Model 5003; Packard Instruments).

Solid phase synthesis

Automated solid-phase peptide synthesis (SPPS; scale: 0.1–0.25 mmol) was run on a Pioneer synthesizer (Applied Biosystems) using standard Fmoc chemistry with TBTU–HOBt as coupling reagents and 20% piperidine in DMF as the deprotection reagent. The elongation was carried out using a 4-fold excess of protected amino acids and coupling reagents. For manual solid phase peptide synthesis, Fmoc-protected amino acids or azidoacetic acid (3 equiv.) were coupled onto the resin (scale: 0.03–0.1 mmol) in a syringe fitted with a polypropylene frit and a Teflon tap in the presence of HATU (3 equiv.) and DIPEA (5 equiv.) in DMF for 2 h. The completion of the reaction was verified by the Kaiser test and repeated if necessary. Elongation yields were determined by the UV-absorption of the fluorenylmethylpiperidine adduct after treatment of the resin with 5 mL of a 20% piperidine–DMF solution (3 × 3 min).

CuAAC on a solid support was carried out under argon in oxygen-free solvents by a modified procedure reported for CuAAC in solution.[42] In brief, the resin (loaded with 0.03 mmol peptide) was swollen several times in degassed DMF (5 mL). The solvent was drained off thoroughly and a solution of lysine derivatives **7** or **8** (0.06 mmol) and DIPEA (0.03 mmol) in

degassed DMF (2–3 mL) were added to the resin. To the suspension was added tetrakis(acetonitrile)copper(I) hexafluorophosphate ([Cu(CH$_3$CN)$_4$]PF$_6$) (0.015 mmol), tris[(1-benzyl-1H-1,2,3-triazol-4-yl)methyl]amine (TBTA) (0.015 mmol) and the mixture was vigorously shaken at rt overnight. The resin was washed with DMF and a solution of diethyldithiocarbamate (0.5% in DMF) to remove the remaining copper species. The completion of the reaction was verified by a colorimetric test for solid-supported azides.[43] The peptides were cleaved from the resin and deprotected using a solution of trifluoroacetic acid, phenol, water and triisopropylsilane (0.5–1 mL; 87.5/5/5/2.5%) as a cleavage cocktail at rt for 2 h. After precipitation in ice-cold diethyl ether (approx. 40 mL), the crude mixture of peptides was recovered by centrifugation and washed twice with cold diethyl ether. The precipitate was dissolved in water (5–10 mg mL^{-1}), purified by preparative HPLC, and lyophilized (Table 2).

In solution synthesis of building blocks and intermediates

Compounds **3** and **8** were prepared as previously described.[14]

Compound 6. The synthesis was accomplished according to a modified procedure reported by Leavens *et al.*[33] In brief, tris-(p-methoxy)phenylphosphine (501 mg, 1.42 mmol) and 3-bromopropionic acid (363 mg, 2.37 mmol) in toluene (15 mL) were stirred at reflux for 5 h and then cooled to rt. The mixture was centrifuged, the precipitate was washed with toluene (4 × 10 mL), and dried under reduced pressure. The crude product was dissolved in acetonitrile (2 mL) and precipitated at 4 °C by addition of diethyl ether (12 mL). After drying under reduced pressure, product **6** was isolated as a white solid (bromide salt, 702 mg, 98%); purity according to HPLC > 95%; ^{1}H NMR (MeOH-d$_4$): δ = 7.68 (dd, 6H, J_{H-H} = 9.0 Hz, J_{H-P} = 12.1 Hz), 7.27 (dd, 6H, J_{H-H} = 9.0 Hz, J_{H-P} = 2.6 Hz), 3.93 (s, 9H), 3.55–3.46 (m, 2H), 2.74–2.63 (m, 2H) ppm; ^{13}C NMR (MeOH-d$_4$): δ = 173.7, 166.6 (d, J_{C-P} = 3.0 Hz), 136.9 (d, J_{C-P} = 11.6 Hz), 117.3 (d, J_{C-P} = 13.8), 110.3 (d, J_{C-P} = 95.3 Hz), 56.6, 27.6 (d, J_{C-P} = 52.5 Hz), 20.1 (d, J_{C-P} = 57.8 Hz) ppm; ^{31}P NMR (MeOH-d$_4$): δ = 21.81 ppm (s); HRMS (ESI) m/z: 425.15119 [M]$^+$ (calcd for C$_{24}$H$_{26}$O$_5$P: 425.15124).

Compound 7. Compound **6** (bromide salt: 86.6 mg, 0.17 mmol) was dissolved under argon in CH$_2$Cl$_2$ (1.5 mL) and SOCl$_2$ (0.4 mL, 5.51 mmol) was added dropwise. The resulting solution was stirred at rt overnight. The excess of SOCl$_2$ was removed with a nitrogen stream and then evaporated to dryness under reduced pressure. The acid chloride of compound **6** was dissolved under argon in CH$_2$Cl$_2$ (2 mL) at −78 °C, Et$_3$N (0.4 mL, 2.87 mmol) and compound **3** (34 mg, 0.12 mmol) were added. The mixture was stirred for 4 h at −78 °C before quenching the reaction by the addition of water (2 mL) followed by warming to rt. The reaction mixture was washed with 0.1 M citric acid and water. The aqueous phases were extracted twice with CH$_2$Cl$_2$. The organic phases were combined, dried over Na$_2$SO$_4$, and concentrated under reduced pressure. The Boc-protected intermediate was directly deprotected by stirring it in a mixture of CH$_2$Cl$_2$–TFA (2 : 1; 6 mL) at rt for 5 h followed by drying under reduced pressure. Purification by preparative HPLC afforded compound **7** as a yellow oil (TFA salt; 50 mg; yield for

3 steps: 59%); purity according to HPLC >95%; ^{1}H-NMR (400 MHz, MeOH-d_4; recorded after completed H/D exchange): δ = 7.62 (dd, 6H, J_{H-H} = 9.0 Hz, J_{H-P} = 12.1 Hz), 7.21 (dd, 6H, J_{H-H} = 9.0 Hz, J_{H-P} = 2.5 Hz), 4.04 (dd, 1H, J_{H-H} = 6.6 Hz, J_{H-H} = 5.1 Hz), 3.99 (dd, 1H, J_{H-H} = 16.7 Hz, J_{H-H} = 2.6 Hz), 3.93 (dd, 1H, J_{H-H} = 16.7 Hz, J_{H-H} = 2.6 Hz), 3.88 (s, 9H), 3.49–3.38 (m, 2H), 3.16 (t, 1H, J_{H-H} = 2.6 Hz), 3.06 (t, 2H, J_{H-H} = 6.6 Hz), 2.60–2.50 (m, 2H), 2.00–1.83 (m, 2H), 1.50–1.23 (m, 4H) ppm; ^{13}C NMR (MeOH-d_4): δ = 171.7 (d, J_{C-P} = 13.6 Hz), 171.0, 166.6 (d, J_{C-P} = 3.0 Hz), 136.9 (d, J_{C-P} = 11.6 Hz), 117.3 (d, J_{C-P} = 13.8 Hz), 110.3 (d, J_{C-P} = 95.0 Hz), 79.7, 74.4, 60.1, 56.6, 55.0, 40.3, 36.5, 30.0 (d, J_{C-P} = 7.2 Hz), 29.2 (d, J_{C-P} = 2.8 Hz), 23.2, 20.2 (d, J_{C-P} = 57.8 Hz) ppm; ^{31}P NMR (MeOH-d_4): δ = 21.92 ppm (s); HRMS (ESI) m/z: 591.26208 [M]$^+$ (calcd for $C_{33}H_{40}O_6N_2P$: 591.26185).

(Radio)metal labeling of peptides

Na[^{99m}TcO$_4$] was eluted from a Mallinckrodt ^{99}Mo/^{99m}Tc generator (Tyco Healthcare, Petten, The Netherlands) using 0.9% NaCl. The precursor [^{99m}Tc(CO)$_3$(H$_2$O)$_3$]$^+$ was prepared according to published procedures.[44] In brief, [^{99m}TcO$_4$]$^-$ (1 mL, 1.5–2 GBq) in 0.9% NaCl was added to the IsoLink^{TM} kit (Mallinckrodt-Tyco, Petten, The Netherlands) and heated for 20 min at 100 °C. After the solution was cooled to rt, the pH was adjusted to pH 7 with a 1 : 2 mixture of 1 M phosphate buffer (pH 7.2) and 1 M HCl (final pH 1.4). Aliquots of 1 mM stock solutions of the peptides **9** or **10** in water (10–20 µL; 10–20 nmol) were added to a solution of [^{99m}Tc(CO)$_3$(H$_2$O)$_3$]$^+$ (90–180 µL; 100–250 MBq) to reach a final peptide concentration of 0.1 mM. The reaction mixture was heated at 100 °C for 30 min and the radiochemical yield and purity of [^{99m}Tc-(CO)$_3$(L)] (L = **9, 10**) was determined by HPLC.

Rhenium complexes were prepared by mixing aqueous stock solutions of peptides **9** or **10** (100 µL, 1 mM) with [Re(CO)$_3$Br$_3$]-[N(Et)$_4$]$_2$[34] (150 µL, 1 mM) and heating at 100 °C for 60 min. The products were purified by HPLC and analyzed by MS. [Re(CO)$_3$(**9**)]: quantitative conversion of peptide **9** (HPLC); purity >99%; MS (MALDI TOF) m/z: 2078.8 [M]$^+$ (calcd for $C_{91}H_{122}N_{21}O_{22}PRe$: 2078.84). [Re(CO)$_3$(**10**)]: quantitative conversion of peptide **10** (HPLC); purity >99%; MS (MALDI TOF) m/z: 1714.7 [M + H]$^+$ (calcd for $C_{69}H_{100}N_{21}O_{19}Re$: 1713.71).

Stability studies

The radiolabeled peptides [^{99m}Tc(CO)$_3$(L)] (L = **9, 10**) (100 µL; 100 pmol, 0.6 MBq) were incubated at 37 °C with 900 µL PBS (pH 7.4), NaCl (0.9%), or a cell culture medium (1% FBS) respectively. At different time points (1, 2, and 4 h), aliquots were analyzed by HPLC (n = 3). In the case of the cell culture medium, serum proteins were precipitated prior to HPLC analysis by the addition of aliquots to ethanol followed by centrifugation (2500g, 5 min).

Histidine challenge. Compounds [^{99m}Tc(CO)$_3$(L)] (L = **9, 10**) (100 µL; 200 pmol, 1.1 MBq) were incubated at 37 °C with 900 µL of a solution of histidine (1 mM in PBS; 4500-fold excess). Aliquots were analyzed by HPLC after 1, 4, and 24 h (n = 3).

Log D determination

Determination of log D values of radiotracers is usually accomplished by partitioning between n-octanol and PBS (pH 7.4) using the "shake flask method". However, the OECD guidelines for testing of chemicals (Nr. 117) recommend an HPLC method for the determination of log D values in the range of log D 0–6.[45] Applying this method also allows the evaluation of radioactive and non-radioactive species, $e.g.$, peptide precursors, and their radioactive and non-radioactive metal-labeled analogues. In brief, log D values of analytes were determined by correlating their retention time with those of standard compounds of known log D values using a calibration curve with at least six reference compounds. All measurements were done with a Bischoff HPLC system, column A and an isocratic mobile phase composed of methanol (75%) and phosphate buffer (pH 7.4; 25%) at a flow rate of 1 mL min^{-1}. Standard compounds (L-sodium ascorbate (t_0), aniline (log D = 0.9), benzaldehyde (log D = 1.5), anisole (log D = 2.1), bromobenzene (log D = 3.0), naphthalene (log D = 3.6), and dibenzyl (log D = 4.8); 0.1% in methanol)[45] and testing compounds were injected three times and analyzed either by UV or gamma detection. The differences in retention times (approx. 0.3 min) of radioactive analytes (^{99m}Tc-complexes) and the corresponding non-radioactive Re-compounds as a result of the serial arrangement of the UV/Vis and γ-detectors were corrected by analysis of co-injections. The calibration curve was calculated by linear regression analysis using GraphPad Prism 5.0 (see ESI†).

***In vitro* experiments**

Cell culturing. Human Caucasian prostate adenocarcinoma (PC-3) cells were obtained from HPA Culture Collections (Salisbury, UK) and cultured at 37 °C and 5% CO$_2$ in Dulbecco's modified Eagle's medium (DMEM, high glucose) containing 10% (v/v) heat-inactivated fetal bovine serum (FBS superior, OXOID, Pratteln, Switzerland), L-glutamine (200 mM), 100 IU mL^{-1} penicillin and 100 µg mL^{-1} streptomycin. All culture reagents, except FBS, were purchased from BioConcept (Allschwil, Switzerland). The cells were subcultured weekly after detaching them with a commercial solution of trypsin–EDTA (1 : 250) in PBS.

Saturation binding assay. On the day prior to the experiment PC-3 cells (10^6 cells per well) were plated in a six-well plate and incubated at 37 °C and 5% CO$_2$ overnight, allowing them to attach. The next day, the cell-culture medium (1% FBS) was changed (0.8 mL) and the cells were kept in the fridge for 30 min to stop cell activity prior to the start of the experiment. In order to reach receptor saturation, the cells were incubated with increasing concentrations (0.1, 0.5, 1, 5, 10, 20, 50, and 100 nM per well; each 100 µL) of the radiolabeled peptides [^{99m}Tc-(CO)$_3$(L)] (L = **9, 10**). Non-specific receptor binding was determined using an excess of natural bombesin (2.5 µM per well for concentrations of the radiopeptide <10 nM, and 10 µM per well for higher concentrations). After incubation at 4 °C for 2 h, the supernatant was removed and the cells were washed twice with 1 mL of ice-cold PBS (pH 7.4). The combined supernatants represent the free, unbound radiopeptide fraction. To determine the

receptor bound fraction, the cells were lysed with 1 M NaOH (1 mL) for 10 min at 37 °C and the wells were washed twice with 1 M NaOH (1 mL). The free and receptor bound fractions were measured in a gamma counter for quantification. Dissociation constants (K_d) were calculated from the data for specific binding with nonlinear regression using GraphPad Prism5, normalized to 10^6 cells ($n = 3$ in triplicate).

Internalization studies. On the day prior to the experiment, PC-3 cells (10^6 cells per well) were placed in six-well plates with a cell culture medium (1% FBS) and incubated at 37 °C, 5% CO_2 overnight to let them attach. On the day of the experiment, the medium was removed, and cells were incubated with fresh medium (1.3 mL) for 1 h. Radiolabeled peptides [^{99m}Tc-$(CO)_3$(L)] (L = **9**, **10**; per well: 100 µL; 0.25 pmol; 1.5 kBq) were added and the cells were incubated for different time points (10, 20, 30, 60, 90, and 120 min) in triplicate to allow binding and internalization. Non-specific receptor binding and internalization was determined in the presence of a 1000-fold excess of natural bombesin (250 pmol; 100 µL per well) as the receptor blocking agent. After each time point, the supernatant was collected, and the cells were washed twice with PBS (1 mL; pH 7.4). The combined supernatants represent the free, unbound radiopeptide fraction. Receptor-bound radioactivity was isolated by incubating the cells twice for 5 min with an acidic glycine solution (100 mM NaCl, 50 mM glycine, pH 2.8; 1 mL) on ice followed by removal of the supernatant. The internalized fraction was determined by cell lysis with 1 M NaOH (1 mL; 10 min; 37 °C, 5% CO_2) and the wells containing the cell lysate were washed twice with NaOH (1 M, 1 mL). All fractions were measured radiometrically in a gamma counter and calculated as percentage of applied dose normalized to 10^6 cells ($n = 3$ in triplicate).

Externalization studies. PC-3 cells (10^6 cells per well) were placed in six-well plates with a cell culture medium (1% FBS) and incubated at 37 °C and 5% CO_2 overnight to let them attach. On the day of the experiment, the medium was removed and cells were incubated with fresh medium (1.3 mL) for 1 h. Radiolabeled peptides [^{99m}Tc$(CO)_3$(L)] (L = **9**, **10**; per well: 100 µL; 0.25 pmol; 1.3 kBq or 2.5 pmol; 13.7 kBq) were added and the cells incubated for 1 h in triplicate to allow internalization into the cells. Non-specific receptor binding and internalization was determined in the presence of a 1000-fold excess of natural bombesin (250 pmol or 2500 pmol; 100 µL per well) as the receptor blocking agent. After 1 h, the supernatant was collected (free fraction) and receptor-bound radiopeptides were removed by washing the cells two times for 5 min with an acidic glycine buffer on ice (bound fraction). A fresh cell culture medium (1 mL) was added and the cells were incubated for 10, 20, 30, 60, 90, 120, 150, 180, 240, and 300 min. At each time-point, the supernatant was collected and cells were washed twice (1 mL PBS; pH 7.4). These fractions represent the externalized amount of radioactivity. The remaining internalized amount of radioactivity was recovered by cell lysis as described above. All fractions were measured in a gamma counter for quantification calculated as percentage of the total internalized fraction at $t = 0$ min ($n = 3$ in triplicate).

Mitochondria-binding experiments. Mitochondria were isolated from cultured PC-3 cells using the Thermo SCIENTIFIC mitochondria isolation kit for cultured cells according to the procedure described in the operating manual. Isolated mitochondria obtained by this procedure maintain their integrity.[46,47] Protein concentration was measured by the Bradford method using the Bio-Rad protein assay and BSA as a standard. Mitochondria binding experiments were performed following procedures published by Murphy *et al.*[38,39] In brief, isolated mitochondria were resuspended in KCl medium (120 mM KCl, 10 mM Hepes (pH 7.2), and 1 mM EGTA). The mitochondria (0.9 mL, 1 µg protein per mL) were incubated with 100 µL of each radiolabeled peptide [^{99m}Tc$(CO)_3$(L)] (L = **9**, **10**; 5 pmol; 11.5 and 15.3 kBq, respectively) at rt on a shaking plate for 30 min. To investigate the specificity of [^{99m}Tc$(CO)_3$(**9**)], mitochondria were preincubated with sodium succinate (10 mM), FCCP (0.5 µM) or sodium azide (20 mM)[40] respectively for 10–30 min prior to the addition of the radiolabeled conjugate. After the experiments, the mitochondria were pelleted (centrifugation at 12 000g for 5 min) and the supernatant was removed. The pellet was washed with KCl medium (1 mL), the supernatants combined and measured in a gamma counter; this fraction represents unbound radioactivity. The mitochondria precipitate was resuspended in 1 mL of triton X-100 (10% v/v) and measured in a gamma counter to quantify the amount of the radioactive peptide associated with the mitochondria relative to total added activity ($n = 4$ for all experiments).

Conclusion

In summary, we report the synthesis and *in vitro* evaluation of novel dual-targeting radiopeptide conjugates with the goal of improving the cellular retention of radioactivity in cancer cells after specific delivery. Starting from readily accessible building blocks, a tumor-targeting peptide ([Nle^{14}]BBS(7–14)), a ^{99m}Tc-based SPECT reporter probe ([^{99m}Tc$(CO)_3$]$^+$), and a mitochondria-seeking triphenylphosphonium (TPP) moiety were selectively and efficiently assembled into a trifunctional conjugate. With the exception of the radiometal labeling step, the assembly of the described multifunctional conjugates was accomplished conveniently on a solid support. While the first generation conjugate bound and internalized specifically into GRP receptor expressing PC-3 cells, it did not display specific accumulation in its intracellular target, the mitochondria, resulting in an overall unaltered externalization rate of radioactivity from PC-3 cells. Nevertheless, the combination of two different entities specific for an extra- and an intracellular target in the same radioconjugate is an attractive approach to improve the efficacy of radiotracers. We are currently employing the same modular synthetic strategy for the development of a simplified, second generation of dual-targeting radiopeptide conjugates in an effort to identify the features required for improving the retention time of radioactivity in cancer cells and tumors.

Acknowledgements

(Novartis, Basel, Switzerland) for assistance with NMR and MS analysis.

References

1 J. D. G. Correia, A. Paulo, P. D. Raposinho and I. Santos, *Dalton Trans.*, 2011, **40**, 6144–6167.
2 M. Schottelius and H.-J. Wester, *Methods*, 2009, **48**, 161–177.
3 J. C. Reubi and H. R. Mäcke, *J. Nucl. Med.*, 2008, **49**, 1735–1738.
4 W. A. P. Breeman, D. J. Kwekkeboom, E. de Blois, M. de Jong, T. J. Visser and E. P. Krenning, *Anti-Cancer Agents Med. Chem.*, 2007, **7**, 345–357.
5 J.-U. Kunstler, B. Veerendra, S. D. Figueroa, G. L. Sieckman, T. L. Rold, T. J. Hoffman, C. J. Smith and H.-J. Pietzsch, *Bioconjugate Chem.*, 2007, **18**, 1651–1661.
6 E. García-Garayoa, P. Bläuenstein, A. Blanc, V. Maes, D. Tourwé and P. A. Schubiger, *Eur. J. Nucl. Med. Mol. Imaging*, 2009, **36**, 37–47.
7 M. Ginj, K. Hinni, S. Tschumi, S. Schulz and H. R. Mäcke, *J. Nucl. Med.*, 2005, **46**, 2097–2103.
8 P. D. Raposinho, J. D. G. Correia, S. Alves, M. F. Botelho, A. C. Santos and I. Santos, *Nucl. Med. Biol.*, 2008, **35**, 91–99.
9 D. Wild, J. S. Schmitt, M. Ginj, H. R. Mäcke, B. F. Bernard, E. Krenning, M. de Jong, S. Wenger and J. C. Reubi, *Eur. J. Nucl. Med. Mol. Imaging*, 2003, **30**, 1338–1347.
10 E. García-Garayoa, C. Schweinsberg, V. Maes, L. Brans, P. Bläuenstein, D. A. Tourwé, R. Schibli and P. A. Schubiger, *Bioconjugate Chem.*, 2008, **19**, 2409–2416.
11 D. Wild, M. Béhé, A. Wicki, D. Storch, B. Waser, M. Gotthardt, B. Keil, G. Christofori, J. C. Reubi and H. R. Mäcke, *J. Nucl. Med.*, 2006, **47**, 2025–2033.
12 E. García-Garayoa, D. Rüegg, P. Bläuenstein, M. Zwimpfer, I. U. Khan, V. Maes, A. Blanc, A. G. Beck-Sickinger, D. A. Tourwé and P. A. Schubiger, *Nucl. Med. Biol.*, 2007, **34**, 17–28.
13 S. A. R. Naqvi, J. K. Sosabowski, S. A. Nagra, M. M. Ishfaq, S. J. Mather and T. Matzow, *Appl. Radiat. Isot.*, 2011, **69**, 68–74.
14 T. L. Mindt, H. Struthers, B. Spingler, L. Brans, D. Tourwé, E. García-Garayoa and R. Schibli, *ChemMedChem*, 2010, **5**, 2026–2038.
15 C. Schweinsberg, V. Maes, L. Brans, P. Bläuenstein, D. A. Tourwé, P. A. Schubiger, R. Schibli and E. García-Garayoa, *Bioconjugate Chem.*, 2008, **19**, 2432–2439.
16 S. Däpp, E. García-Garayoa, V. Maes, L. Brans, D. A. Tourwé, C. Müller and R. Schibli, *Nucl. Med. Biol.*, 2011, **38**, 997–1009.
17 K. Zelenka, L. Borsig and R. Alberto, *Org. Biomol. Chem.*, 2011, **9**, 1071–1078.
18 R. F. Vitor, T. Esteves, F. Marques, P. Raposinho, A. Paulo, S. Rodrigues, J. Rueff, S. Casimiro, L. Costa and I. Santos, *Cancer Biother. Radiopharm.*, 2009, **24**, 551–563.
19 K. Zelenka, L. Borsig and R. Alberto, *Bioconjugate Chem.*, 2011, **22**, 958–967.
20 F. L. Thorp-Greenwood and M. P. Coogan, *Dalton Trans.*, 2011, **40**, 6129–6143.
21 J. Kuil, T. Buckle, H. Yuan, N. S. van den Berg, S. Oishi, N. Fujii, L. Josephson and F. W. B. van Leeuwen, *Bioconjugate Chem.*, 2011, **22**, 859–864.

22 S. M. Okarvi and I. Al Jammaz, *Nucl. Med. Biol.*, 2010, **37**, 277–288.
23 S. S. Kelkar and T. M. Reineke, *Bioconjugate Chem.*, 2011, **22**, 1879–1903.
24 V. V. Rostovtsev, L. G. Green, V. V. Fokin and K. B. Sharpless, *Angew. Chem., Int. Ed.*, 2002, **41**, 2596–2599.
25 C. W. Tornøe, C. Christensen and M. Meldal, *J. Org. Chem.*, 2002, **67**, 3057–3064.
26 T. L. Mindt, C. Schweinsberg, L. Brans, A. Hagenbach, U. Abram, D. Tourwé, E. García-Garayoa and R. Schibli, *ChemMedChem*, 2009, **4**, 529–539.
27 R. Alberto, R. Schibli, A. Egli, A. P. Schubiger, U. Abram and T. A. Kaden, *J. Am. Chem. Soc.*, 1998, **120**, 7987–7988.
28 T. L. Mindt, H. Struthers, L. Brans, T. Anguelov, C. Schweinsberg, V. Maes, D. Tourwé and R. Schibli, *J. Am. Chem. Soc.*, 2006, **128**, 15096–15097.
29 T. Mindt, H. Struthers, E. García-Garayoa, D. Desbouis and R. Schibli, *Chimia*, 2007, **61**, 725–731.
30 R. P. J. Schroeder, W. M. van Weerden, C. Bangma, E. P. Krenning and M. de Jong, *Methods*, 2009, **48**, 200–204.
31 L. F. Yousif, K. M. Stewart and S. O. Kelley, *ChemBioChem*, 2009, **10**, 1939–1950.
32 Y. Zhou and S. Liu, *Bioconjugate Chem.*, 2011, **22**, 1459–1472.
33 W. J. Leavens, S. J. Lane, R. M. Carr, A. M. Lockie and I. Waterhouse, *Rapid Commun. Mass Spectrom.*, 2002, **16**, 433–441.
34 R. Alberto, A. Egli, U. Abram, K. Hegetschweiler, V. Gramlich and P. A. Schubiger, *J. Chem. Soc., Dalton Trans.*, 1994, 2815–2820.
35 R. Schibli, R. La Bella, R. Alberto, E. García-Garayoa, K. Ortner, U. Abram and P. A. Schubiger, *Bioconjugate Chem.*, 2000, **11**, 345–351.
36 C. C. Liolios, E. A. Fragogeorgi, C. Zikos, G. Loudos, S. Xanthopoulos, P. Bouziotis, M. Paravatou-Petsotas, E. Livaniou, A. D. Varvarigou and G. B. Sivolapenko, *Int. J. Pharm.*, 2012, **430**, 1–17.
37 L. Brans, V. Maes, E. García-Garayoa, C. Schweinsberg, S. Däpp, P. Bläuenstein, P. A. Schubiger, R. Schibli and D. A. Tourwé, *Chem. Biol. Drug Des.*, 2008, **72**, 496–506 (and references cited therein).
38 M. F. Ross, A. Filipovska, R. A. J. Smith, M. J. Gait and M. P. Murphy, *Biochem. J.*, 2004, **383**, 457–468.
39 R. A. J. Smith, G. F. Kelso, A. M. James and M. P. Murphy, *Methods Enzymol.*, 2004, **382**, 45–67.
40 P. Ludovico, F. Sansonetty and M. Côrte-Real, *Microbiology*, 2001, **147**, 3335–3343.
41 S. E. Abu-Gosh, N. Kolvazon, B. Tirosh, I. Ringel and E. Yavin, *Mol. Pharm.*, 2009, **6**, 1138–1144.
42 W. H. Binder, D. Gloger, H. Weinstabl, G. Allmaier and E. Pittenauer, *Macromolecules*, 2007, **40**, 3097–3107.
43 S. Punna and M. G. Finn, *Synlett*, 2004, 99–100.
44 R. Alberto, K. Ortner, N. Wheatley, R. Schibli and A. P. Schubiger, *J. Am. Chem. Soc.*, 2001, **123**, 3135–3136.
45 OECD Guideline for Testing of Chemicals, Nr. 117, Partition Coefficient, High Performance Liquid Chromatography (HPLC) Method, 1989, http://www.oecd.org/dataoecd/17/36/1948177.pdf (10.06.2011).
46 Q. Zhang, M. Raoof, Y. Chen, Y. Sumi, T. Sursal, W. Junger, K. Brohi, K. Itagaki and C. J. Hauser, *Nature*, 2010, **464**, 104–108.
47 L. J. Pagliari, T. Kuwana, C. Bonzon, D. D. Newmeyer, S. Tu, H. M. Beere and D. R. Green, *PNAS*, 2005, **102**, 17975–17980.

IV. A Bombesin-Shepherdin Radioconjugate Designed for Combined Extra- and Intracellular Targeting

Christiane A. Fischer, Sandra Vomstein, and Thomas L. Mindt[*]

Division of Radiopharmaceutical Chemistry, Clinic of Radiology and Nuclear Medicine, University of Basel Hospital, Petersgraben 4, 4031 Basel; Switzerland
([*]corresponding author)

(This article belongs to the Special Issue "Radiopharmaceutical Chemistry between Imaging and Radioendotherapy"; Guest Editor: Prof. Dr. Klaus Kopka)

Abstract: Radiolabeled peptides, which target tumor-specific membrane structures of cancer cells, represent a promising class of targeted radiopharmaceuticals for the diagnosis and therapy of cancer. A potential drawback of a number of radiopeptides reported is represented by a rapid washout of a substantial fraction of the initially delivered radioactivity from cancer cells and tumors. This renders the initial targeting effort in part futile and results in an imaging quality and efficacy of the radiotracer lower than achievable. We are investigating the combination of internalizing radiopeptides with molecular entities specific for an intracellular target. By enabling intracellular interactions of the radioconjugate, we aim at reducing/decelerating the externalization of radioactivity from cancer cells. Using the "Click-to-Chelate" approach, the ^{99m}Tc-tricarbonyl core as a reporter probe for single-photon emission computed tomography (SPECT) was combined with the binding sequence of bombesin for extracellular targeting of the gastrin-releasing peptide receptor (GRP-r) and peptidic inhibitors of the cytosolic heat shock 90 protein (Hsp90) for intracellular targeting. Receptor-specific uptake of the multifunctional radioconjugate could be confirmed, however, the cellular washout of radioactivity was not improved. We assume that either endosomal trapping or lysosomal degradation of the radioconjugate is accountable for these observations.

Keywords: multifunctional radioconjugates; intra- and extracellular targeting; tumor targeting; ^{99m}Tc-tricarbonyl; bombesin; shepherdin; gastrin-releasing peptide receptor; Hsp90; SPECT

Article

A Bombesin-Shepherdin Radioconjugate Designed for Combined Extra- and Intracellular Targeting

Christiane A. Fischer, Sandra Vomstein and Thomas L. Mindt *

University of Basel Hospital, Clinic of Radiology and Nuclear Medicine,
Division of Radiopharmaceutical Chemistry, Petersgraben 4, 4031 Basel, Switzerland; E-Mails: Christiane.Fischer@usb.ch; Sandra.Vomstein@usb.ch

*Author to whom correspondence should be addressed; E-Mail: Thomas.Mindt@usb.ch; Tel.: +41-61-556-5380; Fax: +41-61-265-5559.

Abstract: Radiolabeled peptides, which target tumor-specific membrane structures of cancer cells, represent a promising class of targeted radiopharmaceuticals for the diagnosis and therapy of cancer. A potential drawback of a number of reported radiopeptides is the rapid washout of a substantial fraction of the initially delivered radioactivity from cancer cells and tumors. This renders the initial targeting effort in part futile and results in a lower imaging quality and efficacy of the radiotracer than achievable. We are investigating the combination of internalizing radiopeptides with molecular entities specific for an intracellular target. By enabling intracellular interactions of the radioconjugate, we aim at reducing/decelerating the externalization of radioactivity from cancer cells. Using the "click-to-chelate" approach, the ^{99m}Tc-tricarbonyl core as a reporter probe for single-photon emission computed tomography (SPECT) was combined with the binding sequence of bombesin for extracellular targeting of the gastrin-releasing peptide receptor (GRP-r) and peptidic inhibitors of the cytosolic heat shock 90 protein (Hsp90) for intracellular targeting. Receptor-specific uptake of the multifunctional radioconjugate could be confirmed, however, the cellular washout of radioactivity was not improved. We assume that either endosomal trapping or lysosomal degradation of the radioconjugate is accountable for these observations.

Keywords: multifunctional radioconjugates; intra- and extracellular targeting; tumor targeting; ^{99m}Tc-tricarbonyl; bombesin; shepherdin; gastrin releasing peptide receptor; Hsp90; SPECT

1. Introduction

Regulatory peptides are known to display high specificity and affinity towards different G-protein coupled receptors (GPCRs) which are overexpressed on the cell membrane of various cancer cells [1]. On this account, a number of radiopharmaceuticals based on these peptides as tumor-targeting vectors are currently under preclinical and clinical evaluation or have already found application in nuclear medicine for the management of cancer [2–4]. However, after receptor-mediated uptake of radiolabeled regulatory peptides into tumors, a rapid washout of a significant fraction of radioactivity is often observed [5–9]. This not only renders the initial targeting efforts in part futile but may also impair imaging quality and the efficacy of radiopharmaceuticals where therapeutic radionuclides are employed. To overcome these limitations, new strategies are needed to enhance the cellular retention of radioactivity inside cancer cells and tumors. A possible approach to achieve this goal is represented by the application of radiolabeled conjugates which combine extra- and intracellular targeting. Such multifunctional radioconjugates have the promise to be recognized first by an extracellular target (e.g., a GPCR) that triggers cell internalization by endocytosis. Once inside the cell, the radioconjugate interacts with its intracellular target (e.g., an organelle or protein) by means of which the radioactive cargo is trapped [10]. Radioconjugates consisting of two molecular moieties, each of which specific for an extra- and intracellular target, respectively, have been reported; however, examples remain scarce. Ginj *et al.* have reported the combination of radiolabeled somatostatin derivatives with a nuclear localization sequence (NLS) to transport Auger electron emitting radionuclides to the cell nucleus. The reported conjugates target specifically the cell nucleus and display a decreased externalization rate *in vitro*; however, no *in vivo* data is available [6]. With the same goal, the groups of Alberto and Santos have combined a ^{99m}Tc-labeled bombesin (BBS) derivative with the DNA intercalator acridine orange, which simultaneously serves as a fluorescent probe for optical imaging. The *in vitro* results reported on the ability of the conjugates to target the cell nucleus are not consistent and data on the externalization of radioactivity from cells is not reported [11,12]. The Garrison group investigated the combination of a radiolabeled BBS derivative with 2-nitroimidazoles, a hypoxia-specific prodrug. Upon enzymatic reduction of the 2-nitroimidazole moiety, the radioconjugate gets covalently linked to intracellular proteins. While an enhancement of the retention of radioactivity in PC-3 cells as a result of 2-nitroimidazole moieties was demonstrated under hypoxic conditions *in vitro*, the effect was less pronounced in a mouse model [13]. Finally, we have recently reported a ^{99m}Tc-tricarbonyl-labeled, dual-targeting radiopeptide conjugate made of a modified amino acid sequence of BBS, [Nle^{14}]BBS(7-14) (QWAVGHLNle), for extracellular targeting of the gastrin-releasing peptide receptor (GRP-r) and a triphenylphosphonium (TPP) entity specific for mitochondria by its ability to accumulate electrophoretically driven in the energized membrane of the organelle [10]. While receptor-specific cell internalization of the conjugate could be confirmed, the cellular washout of radioactivity was not reduced. We tentatively ascribed our observations to the possibility of hindered passage of the TPP moiety through the membrane of mitochondria because of the peptide it is attached to; similar observations have been reported for cell penetrating peptide/TPP conjugates [14]. We therefore set out to investigate the utility of multifunctional radiopeptides, which target cytosolic proteins and thus, do not require multiple passages through intracellular membranes, a process considered as a major barrier for targeting intracellular epitopes [15]. With these considerations in mind, we chose the cytosolic chaperone, heat shock protein 90 (Hsp90), as a potential intracellular target for our purpose. Hsp90 is a ubiquitous protein important for, e.g., cell proliferation and survival. As such, it is found overexpressed by nearly all cancer cells in high concentrations [16–18]. Hsp90 assists and controls the non-covalent folding/unfolding of many client proteins, including the peptide survivin [17,19,20]. The group of Altieri has identified the binding sequence

of survivin(K79-L87), termed "shepherdin" as an inhibitor of the survivin-Hsp90 interaction and Hsp90 ATPase activity [21]. The high affinity and specificity towards Hsp90 and anticancer activities of shepherdin(79–87) (KHSSGCAFL) and its truncated form shepherdin(79–83) (KHSSG), respectively, have been demonstrated by different approaches [20–24]. However, applications of radiolabeled derivatives of shepherdin or its combination with tumor-targeting peptides for receptor-specific delivery have not yet been described. Herein, we wish to report the synthesis of BBS-shepherdin radioconjugates prepared by the previously reported modular "click-to-chelate" approach [25,26] (Figure 1) and their evaluation *in vitro*.

Figure 1. Assembly of multifunctional, ^{99m}Tc-tricarbonyl-labeled peptide conjugates by amide bond formation, CuAAC, and (radio)metal complexation; residues R^1 and R^2 represent two different entities of biological function (e.g., derivatives of BBS and shepherdin) to be combined in the final radioconjugate.
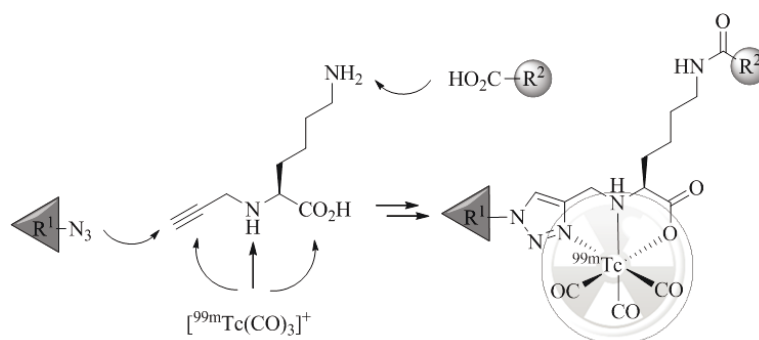
2. Experimental Section

2.1. General Procedures

General procedures, solvents, chemicals, synthesis equipment, analytic instruments (HPLC, MS, NMR, gamma counter) were previously described [10,27]. The "CRS Isolink kit" (Center for Radiopharmaceutical Science, Paul Scherrer Institute, Villigen, Switzerland) was used for the preparation of the precursor $[^{99m}Tc(CO)_3(H_2O)_3]^+$. For analytical separation, a C12 reversed-phase column Phenomenex Jupiter 4u Proteo 90 Å, 4 μm, 250 × 4.6 mm (column A) was used and preparative purification was performed on a Macherey Nagel Nucleodur C18 ISIS, 5 μm, 250 × 16 mm (column B). HPLC solvents were 0.1% trifluoroacetic acid (TFA) in water (A) and 0.1% TFA in acetonitrile (B). Quality control of (radio) metal-labeled peptides was performed using column A and a linear gradient from 80% A to 50% A in 20 min with a flow rate of 1.5 mL/min, or a linear gradient from 80% A to 60% A in
20 min. Peptide purification was performed using column B and different linear gradients with a flow rate of up to 8 mL/min. The observed *m/z* correspond to the monoisotopic ions. Chemical shifts are reported in parts per million (ppm) and coupling constants (*J*) in Hertz (Hz) from high to low field. Standard abbreviations indicating multiplicity are singlet (s), doublet (d), doublet of doublets (dd), triplet (t), and multiplet (m).

2.2. Synthetic Procedures

2.2.1. Organic Synthesis

$N(\alpha)$Boc-$N(\alpha)$propargyl-Lys(OMe) **1** was synthesized in five steps from commercial BocLysOMe according to published procedures [28]. Subsequently, succinic anhydride (2 equiv. 2.22 mmol) was coupled

to $N(\alpha)$Boc-$N(\alpha)$propargyl-Lys(OMe)*HCl (**1**, 370 mg, 1.11 mmol) *via* amide bond formation in CH2Cl2 under basic conditions (*i*-Pr$_2$NEt; 6 equiv.) for two hours at rt (Scheme 1). The reaction mixture was concentrated under reduced pressure and the crude product was dissolved in ethyl acetate. The organic phase was extracted with citric acid (0.1 M) and saturated sodium hydrogen carbonate. The organic layer was disposed. The hydrogen carbonate phase was acidified with hydrogen chloride (5%) under stirring and extracted twice with fresh ethyl acetate. The organic phases were combined, dried over magnesium sulfate, and concentrated under reduced pressure to yield compound **2a** as a pale yellowish oil (435.3 mg, 91%; see Scheme 1). For characterization purposes, the Boc protecting group of **2a** was removed (CH$_2$Cl$_2$/TFA, 2:1; 5 h; rt) and the product was analyzed as its TFA salt **2b**; ^{1}H-NMR (400 MHz, MeOH-d$_4$; recorded after completed H/D exchange): δ = 4.10 (dd, 1H, J = 7.0 Hz, J = 5.0 Hz), 3.96 (dd, 1H, J = 16.6 Hz, J = 2.5 Hz), 3.92 (dd, 1H, J = 16.6 Hz, J = 2.5 Hz), 3.79 (s, 3H), 3.18 (t, 1H, J = 2.5 Hz), 3.12 (m, 2H), 2.52 (t, 2H, J = 6.9 Hz), 2.38 (t, 2H, J = 6.9 Hz), 1.97–1.85 (m, 2H), 1.51–1.44 (m, 2H), 1.43–1.25 (m, 2H) ppm; ^{13}C-NMR (MeOH-d$_4$): δ = 176.42, 174.81, 170.19, 162.22 (TFA, q, JC-F: 35.7 Hz), 117.86 (TFA, q, JC-F: 290.7 Hz), 79.87, 74.28, 60.07, 54.05, 39.65, 36.61, 31.65, 30.39, 29.99, 29.92, 22.99 ppm; ESI-HRMS (C$_{14}$H$_{23}$N$_2$O$_5$): [M+H]$^+$ *m/z*: 299.16019 (calcd. 299.16013).

Scheme 1. Synthesis of central lysine-based precursor. (a) see reference [28]; (b) succinic anhydride, *i*-Pr$_2$NEt, CH$_2$Cl$_2$, 2 h, rt.
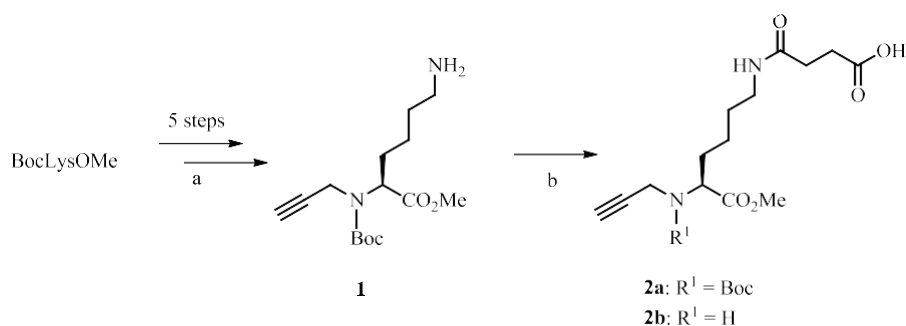
Solid-phase peptide synthesis (SPPS; scale: 0.03–0.25 mmol) was performed as described earlier [10,27]. Side-chain protected Fmoc-amino acids were Cys(Trt), Gln(Trt), His(Trt), Lys(Boc), Ser(tBu), and Trp(Boc). Azide-functionalized bombesin derivative **3** was synthesized according to the literature [10]. The different protected shepherdin peptide sequences [21,24] obtained by SPPS (**4–7**; 0.03–0.06 mmol) were subsequently coupled manually *via* selective amide bond formation to the central lysine precursor **2a** on solid support in the presence of HATU (2–3 equiv.) and *i*-Pr$_2$NEt (5–6 equiv.) in DMF for 2 h at rt. After the coupling was completed, removal of protecting groups and cleavage of the peptides were done with a solution of trifluoroacetic acid, phenol, water, and triisopropylsilane (0.5–1 mL; 87.5/5/5/2.5%) at rt for 2–8 h. The precipitated crude peptides were dissolved in water, purified by preparative HPLC, and lyophilized. Afterwards, selective methyl ester hydrolysis of intermediates was achieved with LiOH (0.5 M; 1–3 h, rt) following a procedure described by Reddy *et al.* [29]. After reactions were completed and the solutions were neutralized with HCl (0.5 M), the crude peptides **8–11** were obtained (see Scheme 2). Finally, the alkyne functionalized shepherdin derivatives **8–11** were reacted with the purified azidoacetic acid-functionalized bombesin sequence **3** according to published procedures [30] *via* the Cu(I)-catalyzed alkyne-azide cycloaddition (CuAAC) [31,32] in solution. In brief, stoichiometric amounts of alkyne-shepherdin peptides **8–11** and azido-BBS peptide **3** (2 µmol) were dissolved in DMSO (400 µL) under an argon atmosphere and a freshly prepared Cu(I) solution was added (60 µL; 3 equiv.), prepared by mixing a

CuSO$_4$ pentahydrate solution (0.2 M, 30 µL) with an sodium ascorbate solution (0.4 M, 30 µL) on ice. The reaction was allowed to stir for 1 h at rt and completion of the reaction was checked by analytical HPLC. The click products were purified by preparative HPLC and lyophilized to obtain the final peptide conjugates **12–15** (see Table 1 and Scheme 2). Reference compound **16** (see Scheme 2) was synthesized as described earlier [10].

Scheme 2. Synthesis of peptides and assembly of (radio)metal-labeled, multifunctional conjugates.
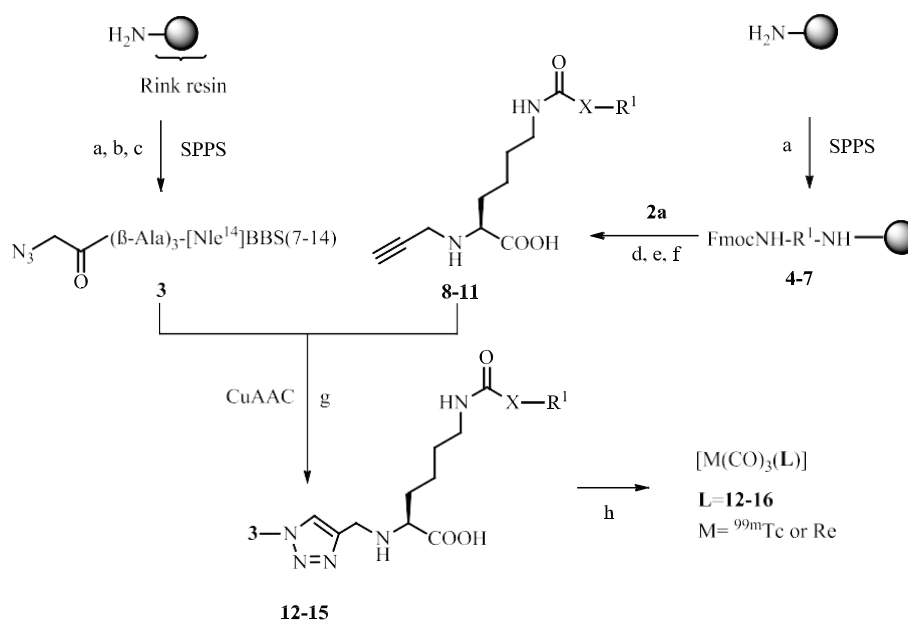
compound (*:protected AA)	X	R^1	
4*,8,12	-CH$_2$CH$_2$CO-	-KHSSGCAFL	shepherdin[79-87]
5*,9,13	-CH$_2$CH$_2$CO-	-SKLACFSHG	scrambled shepherdin[79-87]
6*,10,14	-CH$_2$CH$_2$CO-	-KHSSG	shepherdin[79-83]
7*,11,15	-CH$_2$CH$_2$CO-	-SGKHS	scrambled shepherdin[79-83]
16	-	CH$_3$	reference compound

(a) SPPS: (i) piperidine in DMF; (ii) Fmoc-amino acids, TBTU-HOBt, (b) azidoacetic acid, HATU; (c) cleavage solution: trifluoroacetic acid, phenol, water, triisopropylsilane (87.5/5/5/2.5%), 2–5 h, rt; (d) SPPS: **2a**, HATU, (e) cleavage solution, 2–8 h, rt; (f) LiOH (0.5 M), 1–3 h, rt; (g) CuAAC in solution; CuSO$_4$ (0.2 M), Na-ascorbate (0.4 M), 1 h, rt; (h) (radio)metal labeling; for M=^{99m}Tc: **12–16** (0.1 mM, aq.), [^{99m}Tc(CO)$_3$(H$_2$O)$_3$]$^+$, 100 °C, 30 min; for Re complexes: **12–16** (0.4 mM, aq.), [Et$_4$N]$_2$[Re(CO)$_3$(Br)$_3$], 100 °C, 60 min; AA = amino acid.

Table 1. Analytical data and yields of synthesized peptides and ^{nat}Re-complexes thereof.

Compound	MALDI-MS; m/z (observed)	Yield [%]	Purity [%][c]
12	[M+H]$^+$: 2432.23 (calcd.: 2432.24)	31[a]	92.9
13	[M+H]$^+$: 2432.18 (calcd.: 2432.24)	10[a]	95.3
14	[M+H]$^+$: 1998.01 (calcd.: 1998.04)	17[a]	98.3
15	[M+H]$^+$: 1998.03 (calcd.: 1998.04)	18[a]	97.5
16	[M+H]$^+$: 1458.75 (calcd.: 1458.80)	23[a]	97.6
[Re(CO)$_3$(12)]	[M+H]$^+$: 2700.10 (calcd.: 2700.17)	quant.[b]	>98
[Re(CO)$_3$(13)]	[M+H]$^+$: 2700.16 (calcd.: 2700.17)	quant.[b]	>98
[Re(CO)$_3$(14)]	[M+H]$^+$: 2265.95 (calcd.: 2265.97)	quant.[b]	>98
[Re(CO)$_3$(15)]	[M+H]$^+$: 2265.93 (calcd.: 2265.97)	quant.[b]	>98
[Re(CO)$_3$(16)]	[M+H]$^+$: 1712.7 (calcd.: 1712.71)	quant.[b]	>98

[a] overall yield of isolated conjugates; [b] conversion of starting material (HPLC); [c] determined by HPLC; for   reference compound **16** see reference [10].

2.2.2. (Radio)Metal Labeling of Peptides

Na[^{99m}TcO$_4$] was eluted from a Mallinckrodt ^{99}Mo/^{99m}Tc generator, and the precursor [^{99m}Tc(CO)$_3$(H$_2$O)$_3$]$^+$ was prepared by adding [^{99m}TcO$_4$]$^-$ (1.5–2 GBq) to the "CRS Isolink kit for tricarbonyl" and heating for 30 min at 100 °C. Aliquots of 1 mM stock solutions of peptides **12–16** in water (10 µL, 10 nmol) were added to a solution of [^{99m}Tc(CO)$_3$(H$_2$O)$_3$]$^+$ (~100 MBq; 0.1 mM final peptide concentration) and the reaction mixtures were heated at 100 °C for 30 min. Quality controls were performed by radio-HPLC to determine the radiochemical yield and purity of [^{99m}Tc(CO)$_3$(**L**)] (L = **12–16**). For characterization purposes, the peptides were labeled with cold ^{nat}Re. In brief, aliquots of aqueous stock solutions of peptides **12–16** (30–100 µL, 1 mM) were added to a solution of [Et$_4$N]$_2$[Re(CO)$_3$(Br)$_3$] [33] (50–150 µL, 1 mM) and heated for one hour at 100 °C [10]. The rhenium-complexes were purified by HPLC and analyzed by MS (see Table 1).

2.3. LogD Determinations

The hydrophilicity of the radiolabeled peptides **12–16** was evaluated by determination of their partition coefficient between *n*-octanol and phosphate buffered saline (PBS, pH 7.4) using the shake flask method [27]. In brief, 10 µL (1 µM) of radiolabeled peptides **12–16** were added to a pre-saturated solution of *n*-octanol and PBS (1:1, 1 mL) and the tubes were vortexed (1 min) and centrifuged (3,000 rpm, 10 min). Aliquots of 100 µL of each phase were radiometrically measured in a gamma counter and the logD values were calculated by the logarithm of the ratio between the radioactive counts in the octanol fraction and the radioactive counts in the PBS fraction. The experiment was performed 2–3 times, each in quintets, and results are reported by mean values ± standard deviation (SD).

2.4. In Vitro Experiments

Cell culturing of human Caucasian prostate adenocarcinoma (PC-3) cells and *in vitro* assays (internalization, receptor saturation binding, and externalization) were performed as previously   described [10,27] and are thus described only in brief.

2.4.1. Internalization Assay

For the determination of cellular uptake, PC-3 cells were incubated with the radiolabeled peptides $[^{99m}Tc(CO)_3(L)]$ (L = **14–16**; 0.25 pmol; 1.5–2.0 kBq/well) for different time points to allow binding and internalization. Non-specific receptor binding and internalization was determined by incubating the cells with excess of natural bombesin(1–14) as a receptor blocking agent. At each time point, the supernatant was collected, representing the free radiopeptide fraction. The cell surface receptor bound fraction was obtained by treating the cells with an acidic saline glycine buffer (100 mM NaCl, 50 mM glycine, pH 2.8; 2 times for 5 min, on ice). The internalized fraction was determined by cell lysis with 1 M NaOH (10 min). Fractions of free, receptor-bound, and internalized radiopeptide were radiometrically measured in the gamma counter and calculated as percentage of applied dose normalized to 10^6 cells for all time points (n = 2–3 in triplicates, reported by means ± SD) [10]. To verify whether specific uptake was influenced by the shepherdin sequence, internalization experiments were also conducted with excess shepherdin(79–87) (AnaSpec Inc., Fremont, CA, USA) as a blocking agent.

2.4.2. Receptor Saturation Binding Assay

PC-3 cells were incubated with increasing concentrations (0.1–100 nM/well) of the radiolabeled peptides $[^{99m}Tc(CO)_3(L)]$ (L = **14–16**) at 4 °C for 2 h. Non-specific binding was determined in the presence of excess of natural bombesin(1–14) as described above. Fractions of free and receptor-bound radioconjugates were radiometrically measured in the gamma counter for quantification and apparent binding dissociation constants ($K_{d, app}$) were calculated (n = 2–4 in triplicates, reported by means ± SD) [10].

2.4.3. Externalization Assay

PC-3 cells were incubated with the radiolabeled peptides $[^{99m}Tc(CO)_3(L)]$ (L = **14–16**; 2.5 pmol; 14–21 kBq/well) for one hour to allow cell internalization. The free and receptor-bound radiopeptide fractions were removed as described above, fresh cell culture medium was added, and the cells were incubated for different time points (10–300 min). At each time-point, the externalized fractions were collected and the medium replaced. The remaining internalized amount of radioactivity was recovered by cell lysis. All fractions were radiometrically measured and calculated as percentage of the total internalized fraction (n = 4–7 in triplicates, reported by means ± SD) [10].

3. Results and Discussion

The syntheses of building blocks and multifunctional conjugates are depicted in Schemes 1 and 2. $N(\alpha)$Boc-$N(\alpha)$propargyl-Lys(OMe) (**1**) was synthesized from commercial BocLysOMe in five steps according to previously published procedures [28]. Reaction of compound **1** with succinic anhydride provided intermediate **2a** appropriately functionalized with a carboxylic acid functionality for conjugation reactions *via* amide bond formation. Shepherdin derivatives **4–7** [21,24] were synthesized by automated solid-phase peptide synthesis (SPPS) using Fmoc-chemistry. Compounds **5** and **7** with a scrambled amino acid sequences were prepared for control experiments. Peptides **4–7** were coupled to the Lys precursor **2a** on solid support, cleaved from the resin, and fully deprotected under standard conditions.

Subsequent hydrolyses of the methyl ester of intermediates with LiOH provided alkyne-derivatized peptides **8**–**11**. The corresponding CuAAC reaction partner, N-terminally functionalized azido-(βAla)$_3$[Nle^{14}]BBS(7–14) **3**, was obtained by similar SPPS procedures [10]. A (β-Ala)$_3$ spacer was introduced at the N-terminus of peptide **3** in order to prevent potential interference between the different moieties of the final multifunctional conjugate [9,10]. Reaction of alkyne-bearing shepherdin derivatives **8**–**11** and azido-BBS **3** by CuAAC in solution afforded final peptide conjugates **12**–**15**. For a side-by-side comparison, reference conjugate **16**, identical in all respects but lacking a shepherdin moiety (replaced by a methyl group; Scheme 2) was used, the synthesis and characterization of which has been previously described [10]. For analytical data of products see Table 1.

Radiolabeling of the triazole-containing peptide conjugates with ^{99m}Tc-tricarbonyl was achieved following established procedures reported by us and others [10,28,34]. In brief, heating of aqueous solutions of 1,2,3-triazole containing peptide conjugates **12**–**16** with [^{99m}Tc(CO)$_3$(H$_2$O)$_3$]$^+$ yielded the corresponding radiolabeled compounds [^{99m}Tc(CO)$_3$(**L**)] (**L** = **12**–**16**) in >95% radiochemical yield and purity and with a specific activity of up to 100 GBq/µmol. As common practice for the identification and characterization of n.c.a. (no carrier added) ^{99m}Tc-labeled compounds, the corresponding non-radioactive analogous compounds [^{nat}Re(CO)$_3$(**L**)] (**L** = **12**–**16**) were also prepared by reaction of conjugates **12**–**16** with [Et$_4$N]$_2$[Re(CO)$_3$(Br)$_3$] [33] (for MS data see Table 1). Direct comparison of the UV-HPLC traces of the rhenium tricarbonyl complexes with the corresponding γ-HPLC traces of ^{99m}Tc-tricarbonyl complexes confirmed in each case their identity (see Supplementary Information).

Already at this stage we recognized a high and persistent unspecific binding of conjugate [^{99m}Tc(CO)$_3$(**12**)] containing the full length shepherdin(79–87) sequence to material used as well as cell surfaces. In particular, the unspecific binding of [^{99m}Tc(CO)$_3$(**12**)] impeded with *in vitro* assays regardless of precautions taken (e.g., using prelubricated disposables, the addition of solvents (e.g., DMSO or EtOH), or varying the composition and ionic strength of the media; data not shown). We therefore focused henceforth on radioconjugates containing the truncated shepherdin(79–83) sequence for which unspecific binding was not an issue. Thus, the physico-chemical properties of compounds [^{99m}Tc(CO)$_3$(**L**)] (**L** = **14**,**15**) were evaluated in comparison to reference compound [^{99m}Tc(CO)$_3$(**16**)].

The lipophilicity of the conjugates was determined by the shake flask method. LogD values obtained ranged from −1.70 ± 0.13 and −1.68 ± 0.08 for compounds [^{99m}Tc(CO)$_3$(**14**)] and [^{99m}Tc(CO)$_3$(**15**)], respectively, which indicates an improved hydrophilicity in comparison to the reference compound [^{99m}Tc(CO)$_3$(**16**)] (logD = −0.44 ± 0.07).

BBS-shepherdin conjugate [^{99m}Tc(CO)$_3$(**14**)], its analog with the scrambled amino acid sequence [^{99m}Tc(CO)$_3$(**15**)], and reference compound [^{99m}Tc(CO)$_3$(**16**)] exhibited similar cell internalization profiles into GRP-r overexpressing PC-3 cells in terms of extent and rate of uptake (Figure 2). Approximately 25%–30% of the applied radioactivity was internalized within 30–60 min, which is comparable to related bombesin derivatives labeled with the ^{99m}Tc-tricarbonyl core described by us and others [10,35]. Cell internalization was not influenced by the addition of shepherdin(79–87) and receptor-specific uptake was verified for all compounds by blocking experiments in the presence of excess natural bombesin(1-14) (data not shown).

Figure 2. Receptor specific internalization of radiometal conjugates in PC-3 cells, overexpressing GRP-receptor; [^{99m}Tc(CO)$_3$(**14**)] ($\square$, continuous line), [^{99m}Tc(CO)$_3$(**15**)] (Δ, dotted line), [^{99m}Tc(CO)$_3$(**16**)] ($\circ$, continuous line); normalized to 10^6 cells per well; n = 2–3 (in triplicates, reported by means ± SD, calculated by non-linear regression using GraphPad Prism 5.0).
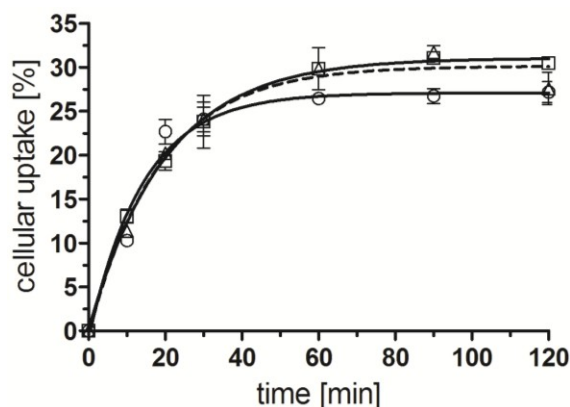
Binding affinities of radiolabeled conjugates [^{99m}Tc(CO)$_3$(**L**)] (**L** = **14**–**16**) towards the GRP-r were investigated by receptor binding saturation assays (Figure 3). All three derivatives showed high affinities towards GRP-r. Compared to reference compound [^{99m}Tc(CO)$_3$(**16**)] with an apparent dissociation constant ($K_{d,\ app}$) of 5.6 ± 0.8 nM, dual-targeting BBS-shepherdin conjugate [^{99m}Tc(CO)$_3$(**14**)] revealed a slightly decreased receptor binding affinity ($K_{d,\ app}$ = 10.9 ± 0.7 nM) as did its scrambled version [^{99m}Tc(CO)$_3$(**15**)] ($K_{d,\ app}$ = 11.3 ± 2.2 nM). K_d values of receptor-specific radiopeptides in the low two-digit nanomolar range are still considered appropriate for applications *in vivo* [36,37].

Figure 3. Specific receptor saturation binding to PC-3 cells; [^{99m}Tc(CO)$_3$(**14**)] ($\square$, continuous line), [^{99m}Tc(CO)$_3$(**15**)] (Δ, dotted line), [^{99m}Tc(CO)$_3$(**16**)] ($\circ$, continuous line); normalized to 10^6 cells per well; n = 2–3 (in triplicates, reported by means ± SD, and calculated by non-linear regression using GraphPad Prism 5.0).
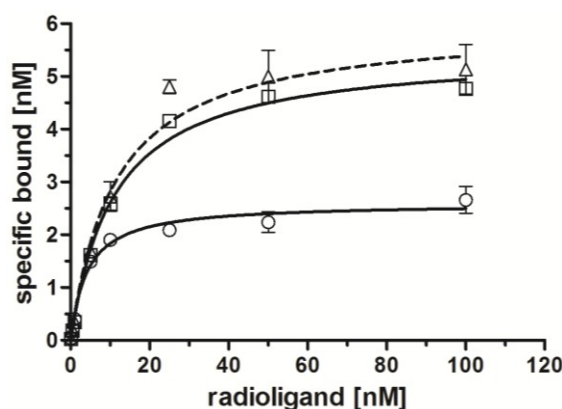
After having verified the specificity and affinity of the radioconjugates for their tumor-specific, extracellular target (GRP-r), we next set out to study the effect of the conjugated shepherdin moiety with regards to the cellular retention of radioactivity. Unexpectedly, the externalization profiles of the three radioconjugates [^{99m}Tc(CO)$_3$(**L**)] (**L** = **14**–**16**) were comparable (Figure 4). A washout of 50% of

the initially internalized radioactivity was observed within approximately 90 min for all conjugates. Thus, the additional shepherdin moiety of $[^{99m}Tc(CO)_3(14)]$ did not lead to an improved cellular retention of radioactivity in comparison to compounds $[^{99m}Tc(CO)_3(L)]$ (**L = 15–16**). These results were puzzling because of the reported high affinity (80 nM) and specificity of shepherdin(79–83) and peptide conjugates thereof towards Hsp90 [20,21], the expression of which in PC-3 cells was verified by western blot experiments (data not shown). A potential explanation for our findings might include the possibility of endosomal entrapment of the conjugate as a consequence of endocytotic cell internalization, which in turn would prevent interactions of $[^{99m}Tc(CO)_3(14)]$ with its cytosolic target Hsp90 [12,15,38]. Alternatively, enzymatic degradation of the peptidic radioconjugate within the intracellular endosome-lysosome cascade could result in the destruction of the shepherdin moiety and thus, loss of its specificity towards Hsp90 [15,38,39]. In either case, the intracellular fate of receptor-specific (radio)conjugates after cell internalization by endocytosis is generally not well understood in detail. There are recent reports suggesting solutions to overcome issues of endosomal entrapment including examples of the application of biomimetic peptides [40], cleavable linkers [41,42], and synthetic polymers [15]. In addition, reported non-peptidic inhibitors of Hsp90 [43] could be employed in order to address potential issues of the stability of the Hsp90-specific peptide moieties described herein. To address the challenging goal of improving the cellular retention of radioactivity after receptor-specific delivery to cancer cells by peptidic radiotracers, future research efforts will be directed towards the combination of our conjugates with the strategies outlined above.

Figure 4. Externalization of radiolabeled compounds $[^{99m}Tc(CO)_3(L)]$ (**L = 14–16**) from PC-3 cells; $[^{99m}Tc(CO)_3(14)]$ (□, continuous line), $[^{99m}Tc(CO)_3(15)]$ (Δ, dotted line), $[^{99m}Tc(CO)_3(16)]$ (○, continuous line); n = 4–7 (in triplicates, reported by means ± SD; calculated by non-linear regression using GraphPad Prism 5.0).
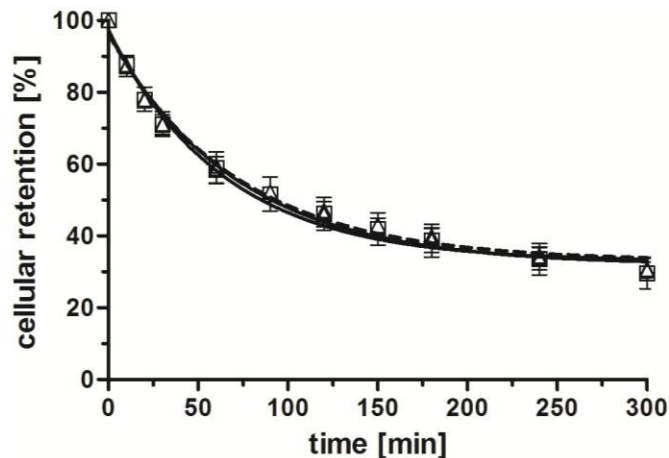
4. Conclusions

We herein report the synthesis and *in vitro* evaluation of bombesin-shepherdin conjugates radiolabeled with the ^{99m}Tc-tricarbonyl core by the "click-to-chelate" strategy. The multifunctional radioconjugates were designed for a combined extra- and intracellular targeting in order to improve the cellular retention of radioactivity after its receptor-specific delivery to cancerous cells. While the specificity of the radioconjugates towards the extracellular target (GRP-r) could be confirmed, the cellular externalization of radioactivity was not improved. The combination of extra- and intracellular targeting entities in a multifunctional radioconjugate represents a novel and innovative approach with potential to improve the efficacy of radiotracers provided that issues such as endosomal entrapment and lysosomal degradation can be addressed.

Acknowledgments

Author Contributions

Christiane A. Fischer carried out the syntheses, characterization, radiolabeling, and *in vitro* evaluations of the conjugates. Sandra Vomstein supported *in vitro* assays. Corresponding author Thomas L. Mindt supervised the project. The manuscript was written by Thomas L. Mindt and Christiane A. Fischer.

Conflicts of Interest

The authors declare no conflict of interest.

References

1. Reubi, J.C. Peptide receptors as molecular targets for cancer diagnosis and therapy. *Endocr. Rev.* **2003**, *24*, 389–427.
2. Correia, J.D.G.; Paulo, A.; Raposinho, P.D.; Santos, I. Radiometallated peptides for molecular imaging and targeted therapy. *Dalton Trans.* **2011**, *40*, 6144–6167.
3. Fani, M.; Mäcke, H.R.; Okarvi, S.M. Radiolabeled peptides: Valuable tools for the detection and treatment of cancer. *Theranostics* **2012**, *2*, 481–501.
4. Schottelius, M.; Wester, H.-J. Molecular imaging targeting peptide receptors. *Methods* **2009**, *48*, 161–177.
5. Raposinho, P.D.; Correia, J.D.G.; Alves, S.; Botelho, M.F.; Santos, A.C.; Santos, I. A ^{99m}Tc(CO)$_3$-labeled pyrazolyl-α-melanocyte-stimulating hormone analog conjugate for melanoma targeting. *Nucl. Med. Biol.* **2008**, *35*, 91–99.
6. Ginj, M.; Hinni, K.; Tschumi, S.; Schulz, S.; Mäcke, H.R. Trifunctional somatostatin-based derivatives designed for targeted radiotherapy using auger electron emitters. *J. Nucl. Med.* **2005**, *46*, 2097–2103.
7. García-Garayoa, E.; Bläuenstein, P.; Blanc, A.; Maes, V.; Tourwé, D.; Schubiger, P.A. A stable neurotensin-based radiopharmaceutical for targeted imaging and therapy of neurotensin receptor-positive tumours. *Eur. J. Nucl. Med. Mol. Imaging* **2009**, *36*, 37–47.
8. Kunstler, J.-U.; Veerendra, B.; Figueroa, S.D.; Sieckman, G.L.; Rold, T.L.; Hoffman, T.J.; Smith, C.J.; Pietzsch, H.-J. Organometallic ^{99m}Tc(III) '4+1' bombesin(7–14) conjugates: Synthesis, radiolabeling, and *in vitro/in vivo* studies. *Bioconjug. Chem.* **2007**, *18*, 1651–1661.
9. García-Garayoa, E.; Rüegg, D.; Bläuenstein, P.; Zwimpfer, M.; Khan, I.U.; Maes, V.; Blanc, A.; Beck-Sickinger, A.G.; Tourwé, D.A.; Schubiger, P.A. Chemical and biological characterization of new Re(CO)$_3$/[^{99m}Tc](CO)$_3$ bombesin analogues. *Nucl. Med. Biol.* **2007**, *34*, 17–28.
10. Kluba, C.A.; Bauman, A.; Valverde, I.E.; Vomstein, S.; Mindt, T.L. Dual-targeting conjugates designed to improve the efficacy of radiolabeled peptides. *Org. Biomol. Chem.* **2012**, *10*, 7594–7602.
11. Esteves, T.; Marques, F.; Paulo, A.; Rino, J.; Nanda, P.; Smith, C.J.; Santos, I. Nuclear targeting with cell-specific multifunctional tricarbonyl M(I) (M is Re, ^{99m}Tc) complexes: Synthesis, characterization, and cell studies. *J. Biol. Inorg. Chem.* **2011**, *16*, 1141–1153.

12. Zelenka, K.; Borsig, L.; Alberto, R. Metal complex mediated conjugation of peptides to nucleus targeting acridine orange: A modular concept for dual-modality imaging agents. *Bioconjug. Chem.* **2011**, *22*, 958–967.

13. Zhou, Z.; Wagh, N.K.; Ogbomo, S.M.; Shi, W.; Jia, Y.; Brusnahan, S.K.; Garrison, J.C. Synthesis and *in vitro* and *in vivo* evaluation of hypoxia-enhanced ^{111}In-bombesin conjugates for prostate cancer imaging. *J. Nucl. Med.* **2013**, *54*, 1605–1612.

14. Ross, M.F.; Filipovska, A.; Smith, R.A.J.; Gait, M.J.; Murphy, M.P. Cell-penetrating peptides do not cross mitochondrial membranes even when conjugated to a lipophilic cation: Evidence against direct passage through phospholipid bilayers. *Biochem. J.* **2004**, *383*, 457–468.

15. Cornelissen, B. Imaging the inside of a tumour: A review of radionuclide imaging and theranostics targeting intracellular epitopes. *J. Label. Compd. Radiopharm.* **2014**, *57*, 310–316.

16. Lindquist, S.; Craig, E.A. The heat-shock proteins. *Annu. Rev. Genet.* **1988**, *22*, 631–677.

17. Whitesell, L.; Lindquist, S.L. HSP90 and the chaperoning of cancer. *Nat. Rev. Cancer* **2005**, *5*, 761–772.

18. Li, Y.; Zhang, T.; Schwartz, S.J.; Sun, D. New developments in Hsp90 inhibitors as anti-cancer therapeutics: Mechanisms, clinical perspective and more potential. *Drug Resist. Update* **2009**, *12*, 17–27.

19. Altieri, D.C. Survivin, cancer networks and pathway-directed drug discovery. *Nat. Rev. Cancer* **2008**, *8*, 61–70.

20. Fortugno, P.; Beltrami, E.; Plescia, J.; Fontana, J.; Pradhan, D.; Marchisio, P.C.; Sessa, W.C.; Altieri, D.C. Regulation of survivin function by Hsp90. *Proc. Natl. Acad. Sci. USA* **2003**, *100*, 13791–13796.

21. Plescia, J.; Salz, W.; Xia, F.; Pennati, M.; Zaffaroni, N.; Daidone, M.G.; Meli, M.; Dohi, T.; Fortugno, P.; Nefedova, Y.; *et al.* Rational design of shepherdin, a novel anticancer agent. *Cancer Cell* **2005**, *7*, 457–468.

22. Xiaojiang, T.; Jinsong, Z.; Jiansheng, W.; Chengen, P.; Guangxiao, Y.; Quanying, W. Adeno-associated virus harboring fusion gene NT4-ant-shepherdin induce cell death in human lung cancer cells. *Cancer Invest.* **2010**, *28*, 465–471.

23. Siegelin, M.D.; Plescia, J.; Raskett, C.M.; Gilbert, C.A.; Ross, A.H.; Altieri, D.C. Global targeting of subcellular heat shock protein-90 networks for therapy of glioblastoma. *Mol. Cancer Ther.* **2010**, *9*, 1638–1646.

24. Gyurkocza, B.; Plescia, J.; Raskett, C.M.; Garlick, D.S.; Lowry, P.A.; Carter, B.Z.; Andreeff, M.; Meli, M.; Colombo, G.; Altieri, D.C. Antileukemic activity of shepherdin and molecular diversity of Hsp90 inhibitors. *J. Natl. Cancer I.* **2006**, *98*, 1068–1077.

25. Mindt, T.L.; Struthers, H.; Brans, L.; Anguelov, T.; Schweinsberg, C.; Maes, V.; Tourwé, D.; Schibli, R. "Click to chelate": Synthesis and installation of metal chelates into biomolecules in a single step. *J. Am. Chem. Soc.* **2006**, *128*, 15096–15097.

26. Kluba, C.A.; Mindt, T.L. Click-to-Chelate: Development of technetium and rhenium-tricarbonyl labeled radiopharmaceuticals. *Molecules* **2013**, *18*, 3206–3226.

27. Valverde, I.E.; Bauman, A.; Kluba, C.A.; Vomstein, S.; Walter, M.A.; Mindt, T.L. 1,2,3-Triazoles as amide bond mimics: Triazole scan yields protease-resistant peptidomimetics for tumor targeting. *Angew. Chem. Int. Ed.* **2013**, *52*, 8957–8960.

28. Mindt, T.L.; Struthers, H.; Spingler, B.; Brans, L.; Tourwé, D.; García-Garayoa, E.; Schibli, R. Molecular assembly of multifunctional ^{99m}Tc radiopharmaceuticals using "clickable" amino acid derivatives. *ChemMedChem.* **2010**, *5*, 2026–2038.

29. Reddy, D.S.; Vander Velde, D.; Aubé, J. Synthesis and conformational studies of dipeptides constrained by disubstituted 3-(aminoethoxy)propionic acid linkers. *J. Org. Chem.* **2004**, *69*, 1716–1719.

30. Valverde, I.E.; Lecaille, F.; Lalmanach, G.; Aucagne, V.; Delmas, A.F. Synthesis of a biologically active triazole-containing analogue of cystatin a through successive peptidomimetic alkyne–azide ligations. *Angew. Chem. Int. Ed.* **2012**, *51*, 718–722.

31. Rostovtsev, V.V.; Green, L.G.; Fokin, V.V.; Sharpless, K.B. A Stepwise huisgen cycloaddition process: Copper(I)-catalyzed regioselective "ligation" of azides and terminal alkynes. *Angew. Chem. Int. Ed.* **2002**, *41*, 2596–2599.

32. Tornøe, C.W.; Christensen, C.; Meldal, M. Peptidotriazoles on solid phase: [1,2,3]-Triazoles by

regiospecific copper(I)-catalyzed 1,3-dipolar cycloadditions of terminal alkynes to azides. *J. Org. Chem.* **2002**, *67*, 3057–3064.

33. Alberto, R.; Egli, A.; Abram, U.; Hegetschweiler, K.; Gramlich, V.; Schubiger, P.A. Synthesis and reactivity of [NEt$_4$]$_2$[ReBr$_3$(CO)$_3$]. Formation and structural characterization of the clusters [NEt$_4$][Re$_3$(μ_3-OH)(μ-OH)$_3$(CO)$_9$] and [NEt$_4$][Re$_2$(μ-OH)$_3$(CO)$_6$] by alkaline treatment. *J. Chem. Soc. Dalton Trans.* **1994**, *19*, 2815–2820.

34. Alberto, R.; Ortner, K.; Wheatley, N.; Schibli, R.; Schubiger, A.P. Synthesis and properties of boranocarbonate: A convenient in situ CO source for the aqueous preparation of [^{99m}Tc(OH$_2$)$_3$(CO)$_3$]$^+$. *J. Am. Chem. Soc.* **2001**, *123*, 3135–3136.

35. Schweinsberg, C.; Maes, V.; Brans, L.; Bläuenstein, P.; Tourwé, D.A.; Schubiger, P.A.; Schibli, R.; García-Garayoa, E. Novel glycated [Tc(CO)$_3$]-labeled bombesin analogues for improved targeting of gastrin-releasing peptide receptor-positive tumors. *Bioconjug. Chem.* **2008**, *19*, 2432–2439.

36. Smith-Jones, P.M.; Bischof, C.; Leimer, M.; Gludovacz, D.; Angelberger, P.; Pangerl, T.; Peck-Radosavljevic, M.; Hamilton, G.; Kaserer, K.; Kofler, A.; *et al.* DOTA-lanreotide: A novel somatostatin analog for tumor diagnosis and therapy. *Endocrinology* **1999**, *140*, 5136–5148.

37. Virgolini, I.; Angelberger, P.; Li, S.; Yang, Q.; Kurtaran, A.; Raderer, M.; Neuhold, N.; Kaserer, K.; Leimer, M.; Peck-Radosavljevic, M.; *et al. In vitro* and *in vivo* studies of three radiolabelled somatostatin analogues:^{123}I-octreotide (OCT), ^{123}I-Tyr-3-OCT and ^{111}In-DTPA-D-Phe-1-OCT. *Eur. J. Nucl. Med.* **1996**, *23*, 1388–1399.

38. Grady, E.F.; Slice, L.W.; Brant, W.O.; Walsh, J.H.; Payan, D.G.; Bunnett, N.W. Direct observation of endocytosis of gastrin releasing peptide and its receptor. *J. Biol. Chem.* **1995**, *270*, 4603–4611.

39. Delom, F.; Fessart, D. Role of phosphorylation in the control of clathrin-mediated internalization of GPCR. *Int. J. Cell Biol.* **2011**, *2011*, 246954.

40. Liang, W.; Lam, J.K.W. Endosomal escape pathways for non-viral nucleic acid delivery systems. In *Molecular Regulation of Endocytosis*; Ceresa, B., Ed., 2012; pp. 421–467.

41. Vlahov, I.R.; Leamon, C.P. Engineering folate–drug conjugates to target cancer: from chemistry to clinic. *Bioconjug. Chem.* **2012**, *23*, 1357–1369.

42. Leriche, G.; Chisholm, L.; Wagner, A. Cleavable linkers in chemical biology. *Bioorg. Med. Chem.* **2012**, *20*, 571–582.

43. Patel, H.J.; Modi, S.; Chiosis, G.; Taldone, T. Advances in the discovery and development of heat-shock protein 90 inhibitors for cancer treatment. *Expert Opin. Drug Discov.* **2011**, *6*, 559–587.

V. 1,2,3-Triazoles as Amide Bond Mimics: Triazole Scan Yields Protease-Resistant Peptidomimetics for Tumor Targeting

Ibai E. Valverde[1], Andreas Bauman[1], Christiane A. Kluba[1], Sandra Vomstein[1], Martin A. Walter[2], and Thomas L. Mindt[1*]

[1]Division of Radiopharmaceutical Chemistry, Clinic of Radiology and Nuclear Medicine, University of Basel Hospital, Petersgraben 4, 4031 Basel, Switzerland
[2]Institute of Nuclear Medicine, Bern University Hospital, Freiburgerstrasse 4, 3010 Bern, Switzerland
([*]corresponding author)

Abstract: The triazole makes the difference: Replacement of amide bonds in the backbone of peptides by 1,4-disubstituted 1,2,3-triazole isosteres affords peptidomimetics with retained receptor affinity and cell-internalization properties, enhanced proteolytic stability, and improved tumor targeting capabilities.

Keywords: click chemistry; drug delivery; metabolic stabilization; peptidomimetics; radiopharmaceuticals

Contributions:

Christiane A. Fischer supported *in vitro* experiments, organized, and conducted *in vivo* evaluation with Sandra Vomstein.

1,2,3-Triazoles as Amide Bond Mimics: Triazole Scan Yields Protease-Resistant Peptidomimetics for Tumor Targeting**
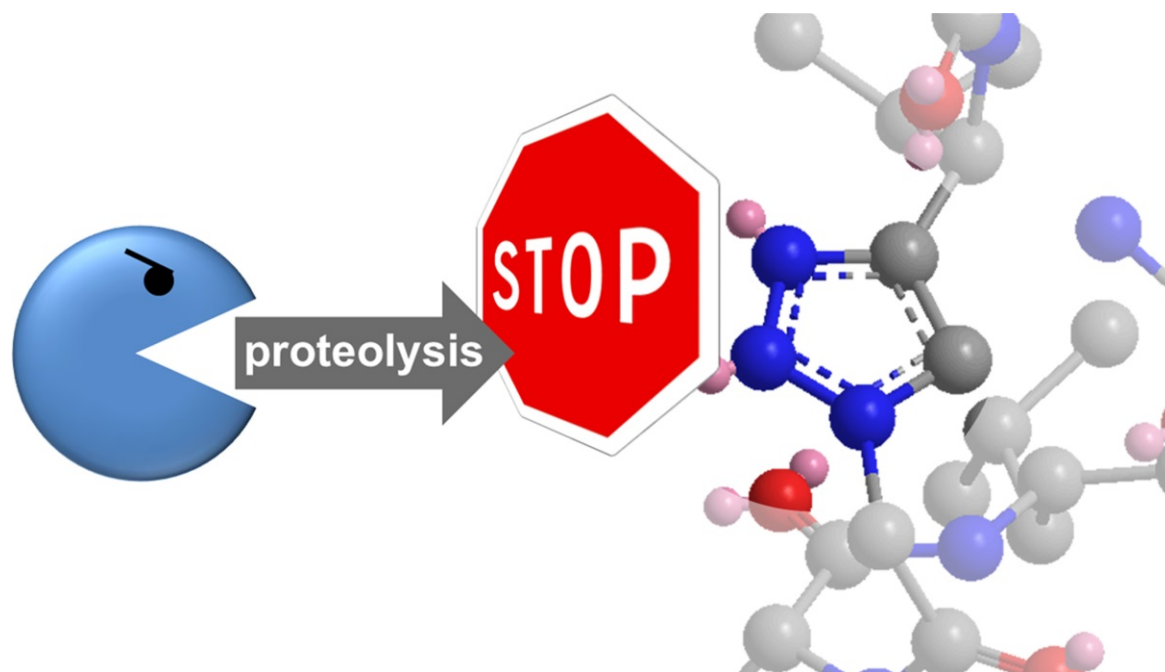
Ibai E. Valverde, Andreas Bauman, Christiane A. Kluba, Sandra Vomstein, Martin A. Walter, and Thomas L. Mindt*

The targeted delivery of diagnostic and therapeutic agents to tumors and metastases has emerged as a promising strategy for the management of cancer.[1] The functionalization of cytotoxic agents and imaging probes with targeting moieties (vectors) enables their specific delivery to tumors with an efficiency higher than in nonconjugated form and may thus reduce side effects and improve imaging, respectively.[2] Ideally, a vector should be readily synthesized, offer the possibility for conjugations, exhibit an appropriate stability, have a well-defined structure, and display nanomolar affinity towards a cell surface recognition element (e.g., receptors), which is overexpressed by tumors but not in nontargeted tissue.[3] Some naturally occurring, synthetically accessible small molecules fulfill these criteria and have found application in the clinic. For example, cyclic peptides (octreotide,[4] RGD[5]) labeled with diagnostic or therapeutic radionuclides are currently used in nuclear medicine. On the other hand, the employment of linear peptides (e.g., bombesin, neurotensin) in this context has been hampered despite their high potential in part due to their low stability in vivo.[6] Considerable research efforts have been made in the past in order to stabilize such peptides while not impacting their favorable biological properties, however, with varying degree of success.[6a] Therefore, new approaches for the metabolic stabilization of tumor-targeting peptides are needed.

It has previously been shown that 1,4-disubstituted 1,2,3-triazoles can effectively mimic *trans*-amide bonds because of their similar size, planarity, H-bonding capabilities, and dipole moment.[7] It has also been suggested that the replacement of an amide bond by a 1,2,3-triazole isostere could afford protease-resistant peptidomimetics.[7a,h,8] However, to the best of our knowledge, no study has yet reported the influence of such backbone modifications on the stability of the peptide. With the goal to develop a tumor-targeting peptidic vector with retained high receptor affinity but improved stability, we set out to replace systematically amide bonds of linear peptides with 1,4-disubstituted 1,2,3-triazoles by the Cu^I-catalyzed azide–alkyne cycloaddition (CuAAC)[7a,9] and study the effect of the structural changes. For proof of concept of the new methodology (termed a triazole scan), we chose the minimal binding sequence of the peptide bombesin (BBN(7-14)). This short octapeptide (H-QWAVGHLM-NH$_2$) is a high-affinity agonist of the gastrin-releasing peptide receptor (GRPr), which is overexpressed in a variety of clinically relevant tumors including, prostate and breast cancer.[10] BBN(7-14) undergoes cell internalization by endocytosis upon activation of the GRPr and thus is widely studied for applications in drug delivery and nuclear oncology.[11] BBN(7-14) represents not only a good model peptide to illustrate the potential of this novel stabilization technique but also a challenge as other backbone-modification strategies (e.g., cyclization, carbonyl reduction, N-methylation) have had only moderate success in providing bombesin analogues with maintained affinity towards GRPr.[12]

We are particularly interested in BBN(7-14) as a tumor-targeting vector for the development of novel radiopharmaceuticals using radioactive metals (radiometals) in a theranostic approach.[13] For this purpose, the peptide can be functionalized N-terminally through a spacer unit with an appropriate chelator for complexation of a radiometal. In this work, we used the universal macrocyclic chelator 1,4,7,10-tetraazacyclododecane-1,4,7,10-tetraacetic acid (DOTA), a short hydrophilic tetraethylene glycol (PEG$_4$) spacer, and lutetium-177 (^{177}Lu) as a clinically established therapeutic radionuclide with a concomitant γ-emission for imaging.[14] In addition, the methionine residue in position 14 of the amino acid sequence was replaced by norleucine to avoid the formation of oxidation side products during radiolabeling.[15] These modifications have all been reported to be tolerated by the peptide.[16]

The peptide analogues described herein were synthesized by a solid-phase approach, which includes the CuAAC reaction. Amino alkyne and azido acid building blocks were prepared following reported procedures (Scheme 1). In brief, chiral Fmoc-protected amino alkynes were obtained by reduction of amino acid derived Weinreb amides followed by a Seyferth–Gilbert homologation of the in situ generated α-amino aldehydes using the Bestmann–Ohira reagent.[17] The enantiomeric purity of the alkyne building blocks was verified in each case.[18] Azido acids were synthesized from amino acids with retention of chirality by diazo-transfer
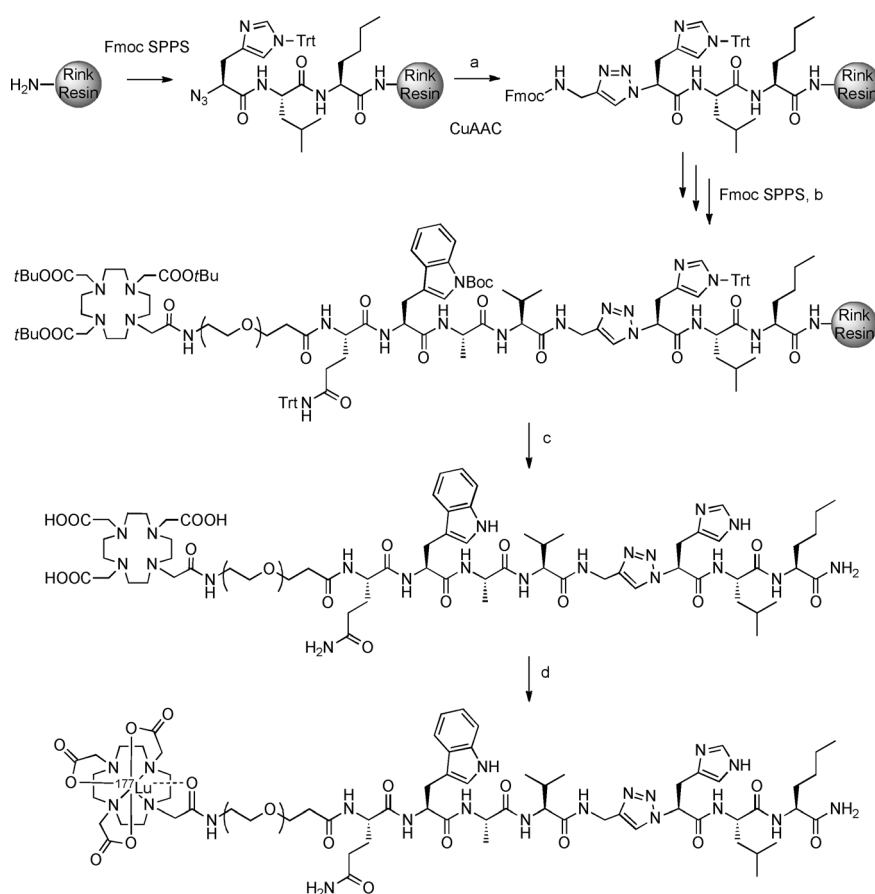
[*] Dr. I. E. Valverde, Dr. A. Bauman, C. A. Kluba, S. Vomstein,
Prof. Dr. T. L. Mindt
Department of Radiology and Nuclear Medicine
Division of Radiopharmaceutical Chemistry
University of Basel Hospital
Petersgraben 4, 4031 Basel (Switzerland)
E-mail: thomas.mindt@usb.ch

Dr. M. A. Walter
Institute of Nuclear Medicine, Bern University Hospital
Freiburgstrasse 4, 3010 Bern (Switzerland)

Scheme 1. Synthesis of radiolabeled peptidomimetics illustrated by the synthesis of **5**. Fmoc-SPPS: 1) 20% piperidine/DMF; 2) Fmoc-amino acid or azido acid, HATU, iPr$_2$NEt; DMF, a) (9H-fluoren-9-yl)methyl prop-2-yn-1-ylcarbamate, [Cu(CH$_3$CN)$_4$]PF$_6$, iPr$_2$NEt, DMF; b) DOTA($tris$-tBu), HATU, iPr$_2$NEt; DMF, c) trifluoroacetic acid/H$_2$O/PhOH/iPr$_3$SiH; d) ^{177}LuCl$_3$, 95 °C, ammonium acetate buffer (pH 5.0). Fmoc-SPPS: Fmoc-based solid-phase peptide synthesis, Fmoc: 9-fluorenylmethoxycarbonyl, tBu: $tert$-butyl, Trt: trityl, DMF: N,N-dimethylformamide, HATU: N-[(dimethylamino)-1H-1,2,3-triazolo[4,5-b]pyridin-1-yl-methylene]-N-methylmethanaminium-3-oxide.

reactions employing the reagent imidazole-1-sulfonyl azide[19] either in solution or on the solid support.[20] The introduction of the 1,2,3-triazole amide bond surrogate into the amino acid

sequence was achieved by CuAAC with the azide on the solid support and the corresponding amino alkynes using Cu-[CH$_3$CN]$_4$PF$_6$.[21] After completion of the amino acid sequence, the peptides were elongated N-terminally with a PEG$_4$ spacer and conjugated to the chelator DOTA. Cleavage from the support, subsequent deprotection, and purification by HPLC afforded the desired conjugates. Labeling of the bombesin analogues with ^{177}LuCl$_3$ using standard reaction conditions yielded radiolabeled compounds **1–10** in radiochemical yields and purities of > 95%.[16] The synthesis of compound **5** is shown as an example in Scheme 1.[18]

With radiotracers **1–10** in hand, we first studied their proteolytic stability by incubation in blood serum (Table 1). With the exception of compounds **2** and **10**, serum half-lives of backbone-modified compounds were significantly improved (by up to 20-fold) in comparison to the reference conjugate **1**. In general, we observed that the introduction of a 1,2,3-triazole in the C-terminal region of the peptide had the most pronounced effect on serum stability. Next, we investigated the influence of the backbone modifications on the biological properties of the targeting vector [Nle^{14}]BBN(7-14) in vitro using GRPr-overexpressing PC3 cells. Receptor-binding and cell-internalization characteristics of radiolabeled peptidomimetics **2–10** were assessed and compared with those of unmodified conjugate **1**.[18] In the case of compounds **3**, **4**, and **8–10**, receptor-specific cell binding and internalization was abolished, whereas conjugates **2**, **5**, and **7** displayed properties similar

Table 1: Structures and biological properties of radiolabeled compounds **1–10**.

Compound	Structure[a]	Half-life [h][b]	Uptake after 4 h[c,e]	K_D [nM][e,f]
1 (reference)	[^{177}Lu]DOTA-PEG$_4$-Gln-Trp-Ala-Val-Gly-His-Leu-Nle-NH$_2$	5	27.7	2.0 ± 0.6
2	[^{177}Lu]DOTA-PEG$_4$-Gln-Trp-Ala-Val-Gly-His-Leu-**Nleψ[Tz]-H**	6	29.1	3.0 ± 0.5
3	[^{177}Lu]DOTA-PEG$_4$-Gln-Trp-Ala-Val-Gly-His-**Leuψ[Tz]Nle**-NH$_2$	60	0.2	n.d.
4	[^{177}Lu]DOTA-PEG$_4$-Gln-Trp-Ala-Val-Gly-**Hisψ[Tz]Leu**-Nle-NH$_2$	>100	n.o.[d]	n.d.
5	[^{177}Lu]DOTA-PEG$_4$-Gln-Trp-Ala-Val-**Glyψ[Tz]His**-Leu-Nle-NH$_2$	17	28.3	3.1 ± 1.0
6	[^{177}Lu]DOTA-PEG$_4$-Gln-Trp-Ala-**Valψ[Tz]Gly**-His-Leu-Nle-NH$_2$	25	8.4	48.6 ± 11.5
7	[^{177}Lu]DOTA-PEG$_4$-Gln-Trp-**Alaψ[Tz]Val**-Gly-His-Leu-Nle-NH$_2$	16	24.5	5.9 ± 1.8
8	[^{177}Lu]DOTA-PEG$_4$-Gln-**Trpψ[Tz]Ala**-Val-Gly-His-Leu-Nle-NH$_2$	8	n.o.[d]	n.d.
9	[^{177}Lu]DOTA-PEG$_4$-**Glnψ[Tz]Trp**-Ala-Val-Gly-His-Leu-Nle-NH$_2$	14	n.o.[d]	n.d.
10	[^{177}Lu]DOTA-**PEG$_4\psi$[Tz]Gln**-Trp-Ala-Val-Gly-His-Leu-Nle-NH$_2$	5	0.5	n.d.

[a] ψ[Tz] represents the replacement of an amide bond by a 1,4-disubstituted [1,2,3]-triazole. [b] Determined in blood serum at 37 °C. [c] Ratio of specific receptor-bound and cell-internalized compound expressed in % of administered dose normalized to 10^6 cells. [d] n.o.: not observed; no specific binding or internalization was detected at a peptide concentration of 2.5 pmol/well. [e] All the values are means of at least two experiments performed in triplicate. [f] Determined by receptor saturation binding assay; n.d.: not determined.

to those of the reference compound **1**. Finally, compound **6** exhibited slower binding and internalization kinetics, indicating a decreased affinity for the GRPr. Receptor affinities (K_D) towards GRPr of conjugates **1**, **2**, and **5–7** were determined by receptor saturation binding assays. As expected, the compounds selected based on the receptor-binding and cell-internalization experiments all showed excellent affinities. Compounds **2**, **5**, and **7** exhibited single-digit nanomolar K_D values and a receptor affinity comparable to that of reference **1** and other reported bombesin-based radiotracers.[15–16,22] Notably, the triazole scan of [Nle[14]]BBN-(7-14) provided four novel peptidomimetic analogues with conserved biological activity, a screening result which is superior to that of other reported peptide bond substitution strategies.[12a]

Compound **5** with the most promising properties (retained GRPr affinity and 3.5-fold improved serum stability) was selected for evaluation in vivo and a side-by-side comparison with the parent compound **1** (Figure 1). Biodistribution studies were performed in athymic nude mice bearing PC3
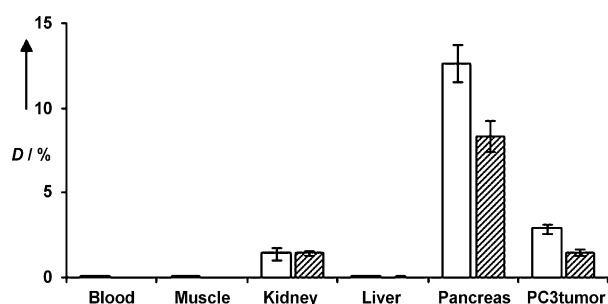

Figure 1. Biodistribution studies of compound **5** and reference compound **1** in PC3-xenografted athymic nude mice (only selected organs and tissue shown). Mice were sacrificed 4 h after intravenous injection of compound **5** (white bars) or reference **1** (dashed bars). Radioactivity in the organs is expressed as the percentage of injected dose per gram of tissue (*D*, mean ± standard deviation; *n* = 3 for each group). Receptor-specific uptake in GRPr-positive organs (e.g., pancreas) and tumors was verified by blocking experiments in the presence of excess natural BBS(1-14).

xenografts 4 h after injection of the radiotracers.[18] In general, both conjugates showed a similar biodistribution pattern. Accumulation in nontargeted tissue (e.g., muscle) was negligible for both compounds. Low levels of radioactivity were found in blood and in the liver, indicating fast blood clearance and the absence of hepatobiliary elimination, respectively. Unspecific uptake was observed in the kidneys as the result of renal excretion, a common feature of radiolabeled peptides. Strikingly, receptor-specific accumulation of radioactivity in receptor-positive organs (e.g., pancreas) was significantly enhanced for compound **5** and tumor uptake was doubled. Blocking experiments carried out by co-injection of natural bombesin suppressed GRPr-specific uptake, demonstrating that the triazole-modified peptide **5** retained its full in vivo specificity.[18] Thus, the introduction of a single 1,2,3-triazole heterocycle between Gly[11] and His[12] of

[Nle[14]]BBN(7-14) increased the peptide's proteolytic stability and led to an improved tumor uptake in vivo.[23]

In summary, we report for the first time a triazole scan of a biologically relevant peptide and its utility for the identification of novel peptidomimetics with improved properties. Application of the new strategy to the bombesin fragment [Nle[14]]BBN(7-14) led to the identification of a series of peptide-based radiotracers with retained nanomolar receptor affinity and an up-to-fivefold improved serum stability. In vivo evaluation of a backbone-modified peptide analogue demonstrated the enhanced stability of the vector and its improved tumor-targeting capability. Further optimization of our lead compounds and application of triazole scans to other peptides of medicinal interest are currently in progress. We expect that this new methodology for the stabilization of peptides will find broad application in the field of tumor targeting with small peptides for drug delivery, imaging, and peptide receptor radiotherapy.

[1] B. Wang, T. J. Siahaan, R. A. Soltero, *Drug Delivery: Principles and Applications*, Wiley, New York, **2005**.

[2] N. Krall, J. Scheuermann, D. Neri, *Angew. Chem.* **2013**, *125*, 1424–1443; *Angew. Chem. Int. Ed.* **2013**, *52*, 1384–1402.

[3] a) K. P. Koopmans, A. W. J. M. Glaudemans, *Eur. J. Nucl. Med. Mol. Imaging* **2012**, *39*, 4–10; b) J. C. Reubi, *Endocr. Rev.* **2003**, *24*, 389–427.

[4] A. Imhof, P. Brunner, N. Marincek, M. Briel, C. Schindler, H. Rasch, H. R. Mäcke, C. Rochlitz, J. Müller-Brand, M. A. Walter, *J. Clin. Oncol.* **2011**, *29*, 2416–2423.

[5] R. Haubner, W. A. Weber, A. J. Beer, E. Vabuliene, D. Reim, M. Sarbia, K.-F. Becker, M. Goebel, R. Hein, H.-J. Wester, H. Kessler, M. Schwaiger, *PLoS Med.* **2005**, *2*, 244–252.

[6] a) F. Buchegger, F. Bonvin, M. Kosinski, A. O. Schaffland, J. Prior, J. C. Reubi, P. Bläuenstein, D. Tourwé, E. García-Garayoa, A. Bischof Delaloye, *J. Nucl. Med.* **2003**, *44*, 1649–1654; b) K. E. Linder, E. Metcalfe, T. Arunachalam, J. Q. Chen, S. M. Eaton, W. W. Feng, H. Fan, N. Raju, A. Cagnolini, L. E. Lantry, A. D. Nunn, R. E. Swenson, *Bioconjugate Chem.* **2009**, *20*, 1171–1178.

[7] a) C. W. Tornøe, C. Christensen, M. Meldal, *J. Org. Chem.* **2002**, *67*, 3057–3064; b) W. S. Horne, M. K. Yadav, C. D. Stout, M. R. Ghadiri, *J. Am. Chem. Soc.* **2004**, *126*, 15366–15367; c) V. D. Bock, D. Speijer, H. Hiemstra, J. H. v. Maarseveen, *Org. Biomol. Chem.* **2007**, *5*, 971–975; d) Y. Q. Liu, L. H. Zhang, J. P. Wan, Y. S. Li, Y. H. Xu, Y. J. Pan, *Tetrahedron* **2008**, *64*, 10728–10734; e) S. W. Horne, C. A. Olsen, J. M. Beierle, A. Montero, R. M. Ghadiri, *Angew. Chem.* **2009**, *121*, 4812–4818; *Angew. Chem. Int. Ed.* **2009**, *48*, 4718–4724; f) M. R. Davis, E. K. Singh, H. Wahyudi, L. D. Alexander, J. B. Kunicki, L. A. Nazarova, K. A. Fairweather, A. M. Giltrap, K. A. Jolliffe, S. R. McAlpine, *Tetrahedron* **2012**, *68*, 1029–1051; g) M. Tischler, D. Nasu, M. Empting, S. Schmelz, D. W. Heinz, P. Rottmann, H. Kolmar, G. Buntkowsky, D. Tietze, O. Avrutina, *Angew. Chem.* **2012**, *124*, 3768–3772; *Angew. Chem. Int. Ed.* **2012**, *51*, 3708–3712; h) D. S. Pedersen, A. Abell, *Eur. J. Org. Chem.* **2011**, 2399–2411.

[8] H. C. Kolb, K. B. Sharpless, *Drug Discovery Today* **2003**, *8*, 1128–1137.

[9] V. V. Rostovtsev, L. G. Green, V. V. Fokin, K. B. Sharpless, *Angew. Chem.* **2002**, *114*, 2708–2711; *Angew. Chem. Int. Ed.* **2002**, *41*, 2596–2599.

[10] J. C. Reubi, S. Wenger, J. Schmuckli-Maurer, J.-C. Schaer, M. Gugger, *Clin. Cancer Res.* **2002**, *8*, 1139–1146.

[11] a) V. Sancho, A. Di Florio, T. W. Moody, R. T. Jensen, *Curr. Drug Delivery* **2011**, *8*, 79–134; b) S. Majumdar, T. J. Siahaan, *Med. Res. Rev.* **2012**, *32*, 637–658.

[12] a) D. C. Horwell, W. Howson, D. Naylor, S. Osborne, R. D. Pinnock, G. S. Ratcliffe, N. Suman-Chauhan, *Int. J. Pept. Prot. Res.* **1996**, *48*, 522–531; b) D. H. Coy, P. Heinz-Erian, N. Y. Jiang, Y. Sasaki, J. Taylor, J. P. Moreau, W. T. Wolfrey, J. D. Gardner, R. T. Jensen, *J. Biol. Chem.* **1988**, *263*, 5056–5060; c) D. H. Coy, N. Y. Jiang, S. H. Kim, J. P. Moreau, J. T. Lin, H. Frucht, J. M. Qian, L. W. Wang, R. T. Jensen, *J. Biol. Chem.* **1991**, *266*, 16441–16447.

[13] C. S. Cutler, H. M. Hennkens, N. Sisay, S. Huclier-Markai, S. S. Jurisson, *Chem. Rev.* **2013**, *113*, 858–883.

[14] B. L. R. Kam, J. J. M. Teunissen, E. P. Krenning, W. W. de Herder, S. Khan, E. I. van Vliet, D. J. Kwekkeboom, *Eur. J. Nucl. Med. Mol. Imaging* **2012**, *39 Suppl 1*, 103–112.

[15] B. A. Nock, A. Nikolopoulou, A. Galanis, P. Cordopatis, B. Waser, J.-C. Reubi, T. Maina, *J. Med. Chem.* **2005**, *48*, 100–110.

[16] H. Zhang, J. Schuhmacher, B. Waser, D. Wild, M. Eisenhut, J.-C. Reubi, H. Maecke, *Eur. J. Nucl. Med. Mol. Imaging* **2007**, *34*, 1198–1208.

[17] H. D. Dickson, S. C. Smith, K. W. Hinkle, *Tetrahedron Lett.* **2004**, *45*, 5597–5599.

[18] For more details, see the Supporting Information.

[19] E. D. Goddard-Borger, R. V. Stick, *Org. Lett.* **2007**, *9*, 3797–3800.

[20] M. B. Hansen, T. H. M. van Gurp, J. C. M. van Hest, D. W. P. M. Löwik, *Org. Lett.* **2012**, *14*, 2330–2333.

[21] a) W. H. Binder, D. Gloger, H. Weinstabl, G. Allmaier, E. Pittenauer, *Macromolecules* **2007**, *40*, 3097–3107; b) C. A. Kluba, A. Bauman, I. E. Valverde, S. Vomstein, T. L. Mindt, *Org. Biomol. Chem.* **2012**, *10*, 7594–7602.

[22] E. García Garayoa, D. Rüegg, P. Bläuenstein, M. Zwimpfer, I. U. Khan, V. Maes, A. Blanc, A. G. Beck-Sickinger, D. A. Tourwé, P. A. Schubiger, *Nucl. Med. Biol.* **2007**, *34*, 17–28.

[23] S. Good, M. A. Walter, B. Waser, X. J. Wang, J. Muller-Brand, M. P. Behe, J. C. Reubi, H. R. Maecke, *Eur. J. Nucl. Med. Mol. Imaging* **2008**, *35*, 1868–1877.

VI. Expression of Different Neurokinin-1 Receptor (NK$_1$R) Isoforms in Glioblastoma Multiforme: Potential Implications for Targeted Therapy

Dominik Cordier,[1,2*] **Alexandra Gerber,**[2] **Christiane Kluba,**[3] **Andreas Bauman,**[3] **Gregor Hutter,**[1,2] **Thomas L. Mindt,**[3*] **and Luigi Mariani**[1,2]

[1]Department of Neurosurgery and [3]Clinic of Radiology and Nuclear Medicine, Division of Radiopharmaceutical Chemistry, University Hospital Basel, Basel, Switzerland. [2]Department of Biomedicine, University Hospital Basel, Basel, Switzerland ([*]corresponding authors)

Abstract: In clinical trials, overexpression of neurokinin-1 receptors (NK$_1$R) in gliomas has been exploited by intratumoral injection of its radiolabeled ligand, substance P (SP). However, despite proven NK$_1$R expression, patients' response to the therapy was inhomogeneous. This study aims to identify the factors predicting response to NK$_1$R-targeted glioma therapy, thereby allowing the discrimination between potential "responders" and "nonresponders" and thus a personalized therapeutic approach. Four widely used glioblastoma cell lines were examined concerning their RNA levels of full-length and truncated NK$_1$R subtypes. Binding of SP to NK$_1$R and internalization into glioma cells was studied by three different approaches using radiolabeled SP (^{177}Lu-[DOTA,Thi^8,Met(O$_2$)^{11}]–SP), a fluorescence-labeled SP derivative (SP-FAM), and a toxin–SP conjugate (saporin-SP). While NK$_1$R RNA was detected in all cases, receptor subtype analysis revealed impressive differences between the cell lines; LN319 exhibited the highest level of full-length NK$_1$R RNA. Significant binding of SP conjugates to NK$_1$R, cell internalization, and specific cell killing were only observed with the cell line LN319. Thus, different NK$_1$R subtype profiles of glomerular basement membrane (GBM) cell lines appear to influence the binding of SP conjugates and their cell internalization properties. Both processes are crucial steps for NK$_1$R-based targeted therapy. Pre-therapeutic testing for NK$_1$R subtype expression may therefore be advisable before initiation of this generally promising therapeutic modality.

Keywords: Substance P; neurokinin-1 receptor (NK$_1$R); glioblastoma multiforme; targeted glioma therapy

Contributions:

Expression of Different Neurokinin-1 Receptor (NK$_1$R) Isoforms in Glioblastoma Multiforme: Potential Implications for Targeted Therapy

Dominik Cordier,[1,2] Alexandra Gerber,[2] Christiane Kluba,[3] Andreas Bauman,[3] Gregor Hutter,[1,2] Thomas L. Mindt,[3] and Luigi Mariani[1,2]

Abstract

In clinical trials, overexpression of neurokinin-1 receptors (NK1R) in gliomas has been exploited by intratumoral injection of its radiolabeled ligand, substance P (SP). However, despite proven NK1R expression, patients' response to the therapy was inhomogeneous. This study aims to identify the factors predicting response to NK1R-targeted glioma therapy, thereby allowing the discrimination between potential ''responders'' and ''nonresponders'' and thus a personalized therapeutic approach. Four widely used glioblastoma cell lines were examined concerning their RNA levels of full-length and truncated NK1R subtypes. Binding of SP to NK1R and internalization into glioma cells was studied by three different approaches using radiolabeled SP (^{177}Lu-[DOTA, Thi^8, Met(O$_2$)^{11}]–SP), a fluorescence-labeled SP derivative (SP-FAM), and a toxin–SP conjugate (saporin-SP). While NK1R RNA was detected in all cases, receptor subtype analysis revealed impressive differences between the cell lines; LN319 exhibited the highest level of full-length NK1R RNA. Significant binding of SP conjugates to NK1R, cell internalization, and specific cell killing were only observed with the cell line LN319. Thus, different NK1R subtype profiles of glomerular basement membrane (GBM) cell lines appear to influence the binding of SP conjugates and their cell internalization properties. Both processes are crucial steps for NK1R-based targeted therapy. Pretherapeutic testing for NK1R subtype expression may therefore be advisable before initiation of this generally promising therapeutic modality.

Key words: substance P, neurokinin-1 receptor (NK1R), glioblastoma multiforme, targeted glioma therapy

Introduction

Brain-intrinsic neoplasms represent the second most frequent cancer-related cause of death in the age group of 15 to 35 years after leukemias.[1] The prognosis of malignant gliomas has only slightly improved during recent decades.[2,3] Median survival for patients with glioblastoma multiforme (glomerular basement membrane [GBM], WHO IV) ranges from 10 to 18 months in patients 70 years old or younger[4–6] and is worse in older patients.[7] The currently accepted standard of care for high grade gliomas is surgical resection followed by combined radiotherapy and chemotherapy.[4,8,9] Several experimental therapeutic strategies are in development, of which the exploitation of glioma-specific antigens as target structures is one of the most promising approaches.[10–13]

The neurokinin-1 receptor (NK1R) is a surface structure molecule that has been described as consistently overexpressed in gliomas.[14,15] The physiological ligand of NK1R is substance P (SP).[16–18] In nude mice with U373 human glioma xenograft, an inhibitory effect on tumor growth by using SP antagonists was demonstrated, as was the reversal of this inhibitory effect by using SP agonists.[19] Another group

[1]Department of Neurosurgery and [3]Clinic of Radiology and Nuclear Medicine, Division of Radiopharmaceutical Chemistry, University Hospital Basel, Basel, Switzerland.
[2]Department of Biomedicine, University Hospital Basel, Basel, Switzerland.

Address correspondence to: Dominik Cordier; Department of Neurosurgery, University Hospital Basel; Spitalstrasse 21, 4031 Basel, Switzerland or Thomas L. Mindt; Clinic of Radiology and Nuclear Medicine, Division of Radiopharmaceutical Chemistry, University Hospital Basel; Petersgraben 4, 4031 Basel, Switzerland
E-mail: **Dominik.Cordier@usb.ch** *or* **Thomas.Mindt@usb.ch**

demonstrated glioma growth inhibition and apoptotic cell death by using the SP antagonist aprepitant in a concentration-dependent manner.[20] Aprepitant (Emend, Merck Pharmaceuticals) is FDA approved to treat chemotherapy-induced nausea. A clinical study to evaluate aprepitant as an adjunct to multimodal glioma therapy has been suggested.[21]

In clinical studies evaluating [90]Y- and [213]Bi-labeled SP radioconjugates in glioma therapy, the overexpression of NK1R was confirmed pretherapeutically in every patient without significant NK1R expression in surrounding brain tissue by local injection of ^{111}In-labeled SP derivative.[22–24] In the majority of study patients, a significant radiological and clinical response was observed. Despite confirmed NK1R expression, the response was not as pronounced as expected in several patients. Taking into account the sufficient intratumoral distribution as shown by the pretherapeutic test injection, we postulated that there might be specific features of these gliomas responsible for the variable response of patients to NK1R-targeted therapy.

Characterization of NK1R revealed that there are at least two distinct NK1R isoforms, differing in the length of the carboxyl terminus: (1) a full-length form with 407 amino acids (AAs), NK1R-Fl, and (2) a truncated variant with 311 AAs, NK1R-Tr. Both receptors have identical ligand-binding domains but differ in their cytoplasmic tails. Specifically, the cytoplasmic tail of NK1R-Tr lacks 96 amino acid residues, a region that functions as a substrate for phosphorylation by G protein–coupled receptor kinases in NK1R-Fl. Consequently, NK1R-Tr shows a reduced capacity to undergo SP-induced internalization and desensitization.[25,26] In contrast to NK1R-Fl, NK1R-Tr may play a role in tumor progression, as shown in breast cells transfected with NK1R-Tr.[27] Besides a potential role in tumorigenesis, NK1R-Tr has physiological functions (e.g., during monocyte/macrophage differentiation).[28]

In summary, NK1R overexpression in gliomas is a promising target structure for specific glioma therapy (e.g., peptide receptor radionuclide therapy [PRRT]). Therapeutics targeting NK1R are usually bifunctional molecules, consisting of a targeting domain (e.g., interleukins or antibodies)[29,30] and an effector domain (e.g., therapeutic radionuclides or toxins).[31,32]

Besides radionuclides, a promising candidate for conjugation with SP may be presented by saporin, an herbal toxin isolated from *Saponaria officinalis*.[33–35] The toxin is a potent member of the group of ribosome inactivating proteins (RIPs)[36] due to its N-glycosidase activity and has high intrinsic stability against denaturation and proteolysis. RIPs often contain a second protein strand that inserts the toxin into cells. Saporin does not exhibit such a structure; thus, it needs to be conjugated to a targeting molecule.[37–39]

In this work, we set out to study the mechanism of NK1R-based targeting of gliomas beyond the well documented overexpression of NK1R, in an effort to identify factors that may render some gliomas more responsive to NK1R-targeted therapy than others. The knowledge gained might help to evaluate whether or not NK1R is a worthwhile target for glioma therapy. Toward this goal, we analyzed four glioma cell lines routinely used preclinically in glioma research (LN71, LN229, LN319, LN405) for their RNA levels of the truncated isoform (NK1R-Tr) and the full-length isoform (NK1R-Fl). NK1R-specific binding of SP conjugates as well

as their internalization into these glioma cells was examined by using a radiolabeled SP and a fluorescence-labeled SP. The effect of saporin-labeled SP as a toxin-based targeted therapeutic was studied to evaluate the cell internalization in more detail.

Materials and Methods

In vitro experiments described henceforth were performed with $n = 2$-3 (in triplicates). The date shown in Figures 1, 3, and 5 are represented as mean values ± standard deviations (indicated by error bars) calculated using established software (e.g., GraphPad Prism 5.0).

Cell lines

Glioblastoma cell lines LN71, LN229, LN319, LN405 and chicken fibroblast DF1 cells were cultured at 37°C in 5% CO_2 atmosphere in DMEM medium (Sigma, St. Louis, MO) with 5% fetal bovine serum (FBS) and penicillin-streptomycin (Invitrogen Gibco, Paisley, UK, 100 units/mL). Cell lines were obtained from Monika Hegi, University Hospital of Lausanne, Lausanne, Switzerland.

RNA extraction

Total RNA was extracted from glioblastoma cell lines by using Tri-Reagent (Sigma). Phase separation was performed using chloroform. After centrifugation (12'000×G, 15 minutes), RNA-containing aqueous phase was mixed with 70% ethanol and transferred to spin columns of RNeasy Mini Kit (Qiagen, Hilden, Germany). Extractions were performed following the instructions of the supplier. Extracted RNA was subjected to genomic DNA digestion by TURBO DNase Kit (Ambion, Austin, TX).

Reverse transcription

Complementary DNA (cDNA) was synthesized from 1 μg of total RNA with QuantiTect Reverse Transcription Kit (Qiagen). Reverse transcription was maintained at 42°C for 15 minutes, and termination at 95°C for 3 minutes. Obtained cDNA was used as a template for real-time PCR amplification.

Real-time PCR primers

PCR primers for quantitative measurement of long and short isoforms of NK1R messenger RNA (mRNA) were previously published.[28,40] Sequences of primer pair for specific amplification of the full-length isoform were 5′-TCTTCTTCCTCCTGCCCTACATC-3′ (sense) and 5′-AGCACCGGA-AGGCATGCTTGAAGCCCA-3′ (antisense). Sequences of primer pair for truncated NK1R were 5′-TCTTCTTCCTCCTGCCCTACATC-3′ (sense) and 5′-TGGAGAGCTCATGGGGTTGGGATCCT-3′ (antisense). Primer pair for glyceraldehyde-3-phosphate dehydrogenase (GAPDH) was purchased from Qiagen. Primers were resuspended in Tris-EDTA buffer and stored at –20°C.

Real-time PCR assay

The CFX96 real-time cycler system (Bio-Rad, Hercules, CA) was used. For each PCR, 1 μl of cDNA template or 1 μl of corresponding non–reverse transcription (NRT) control

was mixed with 12.5 μl of QuantiFast SYBR Green PCR Master Mix (Qiagen) and a primer pair for either full-length or truncated NK1R (300 nM) or for GAPDH was added. Reaction efficiencies were monitored by standard curve on each plate. All amplifications were performed as duplicates. Threshold cycle (Ct) numbers of the duplicates were averaged and normalized to Ct values of endogenous GAPDH control. Standard comparative Ct method $2^{-\Delta Ct}$ was used to calculate relative mRNA expression levels of full-length and truncated NK1R.

The applied thermal cycling conditions were an initial denaturation (95°C, 5 minutes), followed by 40 cycles of 95°C for 10 seconds and 60°C for 30 seconds, finished by melting curve starting at 65°C, and increased for 0.5°C each 5 seconds until reaching 95°C. Fluorescent measurements were recorded during each annealing step and after each temperature increment during the melting process.

Radiolabeling of SP

^{177}Lu-[DOTA, Thi^8, Met(O$_2$)^{11}]–SP was prepared by reacting 20 μg per 20 μL (0.56 mM) [DOTA, Thi^8, Met(O$_2$)^{11}]–SP (M_w = 1772.06 g/mol) with $\sim$ 37 MBq ^{177}LuCl$_3$ in 300 μL 0.4 M NH$_4$OAc (pH 5.0) in prelubricated Eppendorf tubes for 30 minutes at 95°C. After adding 9 nmol of 0.1 mM ^{nat}LuCl$_3$ solution, the mixture was heated for additional 30 minutes (95°C). Quality control was performed by reversed phase high-phase liquid chromatography (HPLC) on Bischof system with HPLC pumps 2250, a λ-1010 UV detector, Berthold LB509 radioflow detector, and EC250/4.6 Nucleodur C$_{18}$ Isis 5-μm column (Macherey-Nagel, Düren, Germany). The column was eluted with mixtures of acetonitrile (solvent A) and water with 0.1% trifluoroacetic acid (TFA) (solvent B) at a flow rate of 0.75 mL per minute and a linear gradient (0 minutes 80% B, 20 minutes 60% B, 22 minutes 5% B, 25 minutes 5% B, 27 minutes 80% B, 30 minutes 80% B).

Binding and internalization studies with radiolabeled SP

LN71, LN229, LN319, and LN405 cells were seeded at a density of 0.8 to 1 million cells per well in a six-well plate and incubated (37°C, 5% CO$_2$) overnight in medium (1% FBS in DMEM medium, high glucose). On the day of the experiment, the medium was removed and cells were washed once with PBS (1 mL). Then 1.3 mL culture medium (1% FBS in DMEM medium) was added, plates were incubated at 37°C, 5% CO$_2$. Next, 0.25 pmol (100 μL, final concentration: 0.17 nM) of ^{177}Lu-[DOTA, Thi^8, Met(O$_2$)^{11}]– SP were added and incubated (37°C, 5% CO$_2$). For determination of nonspecific binding the cells were incubated in the presence of additional 250 pmol (1000-fold excess, final concentration 0.17 μM) of unlabeled [DOTA, Thi^8, Met(O$_2$)^{11}] –SP. Internalization was stopped by removal of medium and washing cells two times with ice cold PBS at four time points (0.5, 1, 2, and 4 hours). Cells were treated with glycine buffer (0.05 M, pH 2.8) twice for 5 minutes at 4°C to determine the cell surface–bound fraction. Internalized fraction was determined by cell lysis with 1 M NaOH. Fractions of free radioligand, receptor-bound fractions, and internalized fractions were measured radiometrically (γ-counter) and calculated as percentage of applied dose per 10^6 cells. Peptide concentration–dependent inter-

nalization was studied using two different concentrations of ^{177}Lu-[DOTA, Thi^8, Met(O$_2$)^{11}] –SP (0.17 nM and 1.7 nM).

SP-FAM internalization and immunohistochemistry

LN319, LN71, LN229, and LN405 cells were plated on 35-mm culture dishes (4 inner rings, Greiner Bio-One, Frickenhausen, Germany) and allowed to attach overnight. Cells were treated with 1 nM of either FAM-labeled SP, 5-FAM (AnaSpec, Fremont, CA), SP ([Sar^9, Met(O$_2$)^{11}]– substance P, Sigma) or left untreated. After 8 and 24 hours, cells were washed and stained with 5 μg/ml of CellMask Deep Red plasma membrane stain (Invitrogen) at 37°C for 5 minutes. Cells were washed two times with PBS and fixed with 4% formaldehyde (Thermo Scientific, Rockford, IL) for 10 minutes. After blocking with 10% donkey serum (Jackson Immuno Research Laboratories, Suffolk, UK) in PBS for 1 hour, rabbit anti-NK1R (Abcam, ab13133, 1:500) was incubated overnight in 5% donkey serum in PBS at 4°C. Cells were washed three times with PBS and incubated for 1 hour at room temperature with DAPI and the secondary antibody, DyLight 549-conjugated donkey anti-rabbit IgG (H + L, 1:300; Jackson Immuno Research Laboratories, West Grove, PA). Cells were washed again three times with PBS and mounted with Dako Fluorescent Mounting Medium (Dako, Glostrup, Denmark). Internalization of FAM and localization of NK1R was examined with confocal microscopy (Zeiss LSM 710, spectral type, laser lines at 405, 458, 488, 514, 543, 633 nm). Image analysis was performed with ZEN 2010 (Zeiss, Jena, Germany).

Cytotoxicity assay

SP–saporin (SP-SAP, conjugate of peptidase-resistant [Sar^9, Met(O$_2$)^{11}] SP–analogue and ribosome-inactivating protein saporin) was purchased from Advanced Targeting Systems (San Diego, CA).

LN71, LN229, LN319, LN405, and DF1 cells were plated at 2500 cells per 100 μl in triplicates on a 96-well plate. Cells were allowed to attach overnight and treated with SP-SAP at a concentration of 1 nM. After incubation for 72 hours, MTS and PMS (colorimetric CellTiter 96® AQueous Non-Radioactive Cell Proliferation Assay, Promega, Madison, WI) were added and the incubation was continued for 2 hours. Optical density was measured at 490 nm and mean values per standard deviations were calculated. The averaged data (in triplicates) were compared to those obtained from controls (PBS). Standard deviations of measured values were less than 10%.

Results

NK1R isoforms in glioma cell lines

With LN319, we detected a high level of NK1R mRNA, whereas the other three cell lines showed only moderate to low mRNA levels. Differentiating between the full-length and the truncated isoform of NK1R mRNA, LN319 showed a very high level of full-length NK1R mRNA, whereas the level of the truncated isoform was reduced by a factor of about 40 in comparison to the level of the full-length isoform. The level of full-length NKR1 mRNA of LN71 was less than 2% in comparison to that of LN319, while the level of the truncated isoform was found to be approximately 40%

of the full-length isoform. In contrast, LN405 and LN229 showed only very low levels of the full-length NK1R mRNA. Interestingly, the levels of truncated NK1R mRNA in LN405 and LN229 were higher than full-length NK1R mRNA in these cell lines (Fig. 1).

Radiolabeling of [DOTA, Thi^8, Met(O$_2$)^{11}]–SP (DOTA-SP) with ^{177}LuCl$_3$

Radiolabeling of DOTA-SP with Lu-177 was achieved in high radiochemical yield and purity (>99.5%) at a specific activity of 3.3 GBq/μmol (Fig. 2).

Internalization of radiolabeled SP

Internalization of ^{177}Lu-[DOTA, Thi^8, Met(O$_2$)^{11}]-SP was detected only in glioma cell line LN319 but not in LN71, LN229, and LN405. For a peptide concentration of 0.17 nM, the specific internalization for LN319 cells was 16.3%±0.2% of totally administered activity after 30 minutes, increasing to 31.4%±0.5% after 4 hours (Fig. 3). Applying the ten-fold peptide concentration (1.7 nM) resulted in 15.2%±0.6% after 30 minutes and 30.1%±0.9% after 4 hours. Nonspecific binding as determined by blocking experiments in the presence of 1000-fold excess of unlabelled DOTA-SP was less than 1% in all assays.

Internalization of FAM-labeled SP

Examinations with SP-FAM confirmed the results of experiments with radiolabeled SP. Only LN319 cells exhibited significant internalization of FAM–labeled SP. The highest amount of internalized SP-FAM was observed after 24 hours (Fig. 4).

Effect of saporin-labeled SP on glioma cell lines

LN319 cells were selectively killed by saporin–SP with a reduction of cell viability of approximately 40%. The viability of the other cell lines, LN71, LN229, and LN405, was not signif-
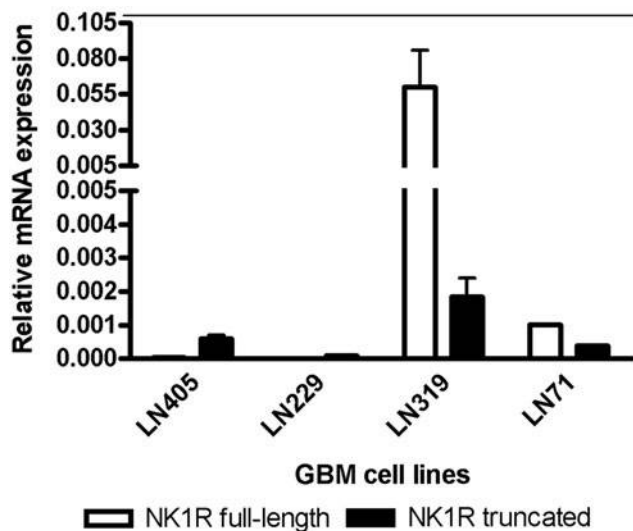

FIG. 2. Radio-HPLC chromatograph of ^{177}Lu-[DOTA, Thi^8, Met(O$_2$)^{11}]–SP.

icantly affected. The viability of the control cell line, DF1, was also not affected. Saporin and SP alone did not show a significant effect on cell viability in all examined cell lines (Fig. 5).

Discussion

The results of this work confirm previous findings of consistent overexpression of NK1R in gliomas,[15] as we could detect NK1R by quantitative reverse transcriptase (qRT) PCR in all cell lines. In previous clinical trials with radiolabeled SP,[22–24] the therapeutic response was difficult to predict

FIG. 1. Different endogenous mRNA expression levels of NK1R in glioma cell lines. qRT-PCR analysis of the full-length and the truncated variant of NK1R was used, and GAPDH was used as endogenous control.
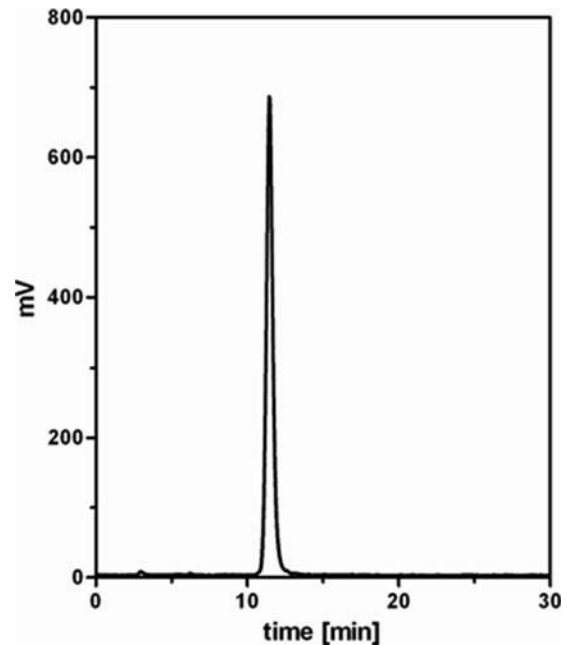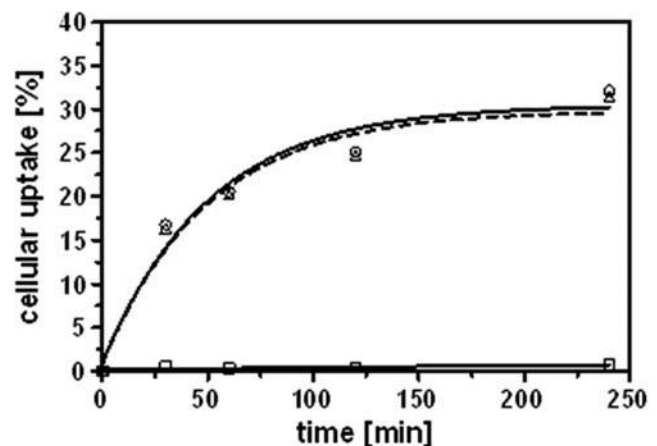

FIG. 3. Internalization of ^{177}Lu-[DOTA, Thi^8, Met(O$_2$)^{11}]–SP (0.25 pmol) in LN319 glioma cells, normalized to 10^6 cells per well. Data points include the following: Total internalized (○, continuous line); nonspecific binding (□, continuous line) as determined by blocking experiments in the presence of excess (1000×) [DOTA, Thi^8, Met(O$_2$)^{11}]–SP; and specific internalized (Δ, dotted line) as difference thereof.
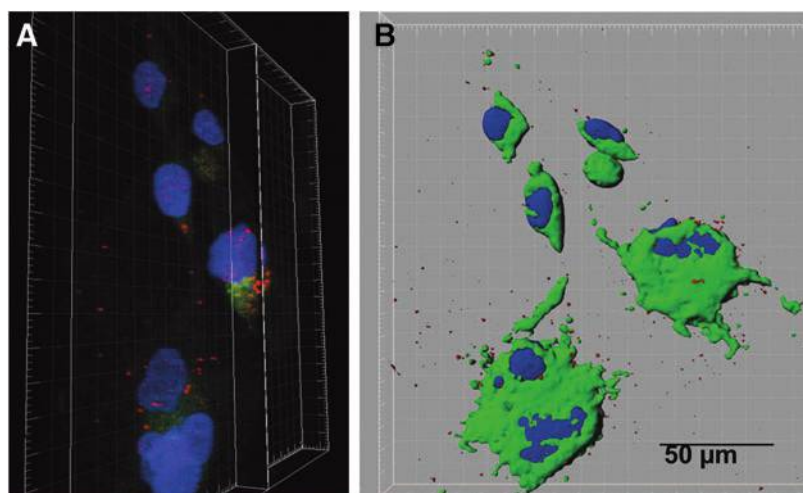
FIG. 4. Internalization of SP-FAM in LN319 glioma cells after 24 hours, shown using confocal microscopy: **(A)** 3-D tilted overview and **(B)** NK1R, nuclei, and cytoplasmatic SP-FAM as bodies. DAPI-nuclei (blue), SSP-FAM (green), and NK1R (red) are shown. Color images available online at www.liebertpub.com/cbr

despite confirmed NK1R expression and sufficient intratumoral distribution of radiolabeled SP. This observation raised the question whether or not there are other factors downstream in the NK1R pathway that may account for the variable response to therapies employing SP radioconjugates.

Hall et al. and Fong et al.[25,41] have reported two different variants of NK1R, a full-length (NK1R-Fl) and a truncated variant (NK1R-Tr), the latter of which also exhibits different functionalities. Our study using qRT-PCR confirms different levels of expression of the two receptor subtypes and suggests that the sole fact of NK1R expression may not be an adequate overall parameter to reliably predict the therapeutic response to NK1R–targeted therapy.[14,15]

We have investigated the correlation of NK1R-Fl expression for internalization of SP conjugates by three independent techniques, including the *in vitro* evaluation of a radiolabeled SP, a fluorescence-labeled SP derivative, and a toxin-SP conjugate. Of the cell lines tested, only the NK1R-Fl expressing LN319 was able to internalize the radiolabeled and fluorescence-labeled SP and, thus, showed a response to the toxin-SP conjugate. Our observations correlate well with previous reports depicting an NK1R-Tr association with a reduced capacity to undergo SP-induced internalization and desensitization.[25,26]

Consequently, NK1R-Fl expression could be considered a prerequisite for SP binding and internalization and, thus, the positive outcome of SP-based therapies. The findings of this work provide a possible explanation for the inconsistent therapeutic response observed in previous clinical studies using [90]Y- and [213]Bi-labeled SP conjugates for glioma therapy.[22–24] The observation of good responders and poor responders in these studies suggests that an examination of NK1R subtype expression of individual glioma patients may be advisable before initiation of NK1R-based targeted radiotherapy.

Conclusion

NK1R is a G protein–coupled membrane receptor consistently expressed by glioma cells and can therefore be considered a valuable target for peptide receptor–specific therapy. However, subclassification of the receptor into the two isoforms, the full-length and truncated variants, could be essential to predicting the functionality concerning cell internalization of its ligand and, hence, the efficacy of SP-based therapies. On the basis of our preclinical *in vitro* investigations reported herein, sufficient expression of the full-length NK1R appears to be required so that SP conjugates are internalized into glioma cells and the therapeutic effect of their cargo can be deployed. Thus, pretherapeutic screening for NK1R subtype expression may be advisable when considering this NK1R-specific therapeutic modality for the treatment of GBM.

Disclosure Statement
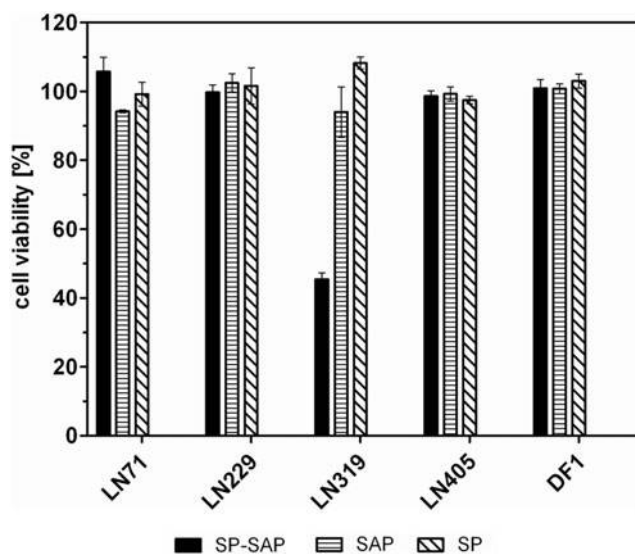
No competing financial interests exist.

FIG. 5. Viability of glioma cell lines LN71, LN229, LN319, and LN405 and control cell line DF1 exposed to saporin-SP (SP-SAP), saporin alone (SAP), and SP alone (SP).

References

1. Keene DL, Hsu E, Ventureyra E. Brain tumors in childhood and adolescence. Pediatr Neurol 1999;20:198.

2. Oertel J, von Buttlar E, Schroeder HW, Gaab MR. Prognosis of gliomas in the 1970s and today. Neurosurg Focus 2005;18:e12.

3. Cohen-Jonathan Moyal E. From bench to bedside: Experience of the glioblastoma model for the optimization of radiosensitization. Cancer Radiother 2012;16:25.

4. Stupp R, Mason WP, van den Bent MJ, et al. Radiotherapy plus concomitant and adjuvant temozolomide for glioblastoma. N Engl J Med 2005;352:987.

5. Walker MD, Green SB, Byar DP, et al. Randomized comparisons of radiotherapy and nitrosoureas for the treatment of malignant glioma after surgery. N Engl J Med 1980;303:1323.

6. Hegi ME, Diserens AC, Gorlia T, et al. MGMT gene silencing and benefit from temozolomide in glioblastoma. N Engl J Med 2005;352:997.

7. Kita D, Ciernik IF, Vaccarella S, et al. Age as a predictive factor in glioblastomas: Population-based study. Neuroepidemiology 2009;33:17.

8. Becker KP, Yu J. Status quo-standard-of-care medical and radiation therapy for glioblastoma. Cancer J 2012;18:12.

9. Villano JL, Letarte N, Bressler LR. Going past the data for temozolomide. Cancer Chemother Pharmacol 2012;69:1113.

10. Mrugala MM, Adair JE, Kiem HP. Outside the box-novel therapeutic strategies for glioblastoma. Cancer J 2012;18:51.

11. Castro MG, Candolfi M, Kroeger K, et al. Gene therapy and targeted toxins for glioma. Curr Gene Ther 2011;11:155.

12. Frankel AE, Kreitman RJ, Sausville EA. Targeted toxins. Clin Cancer Res 2000;6:326.

13. Dyba M, Tarasova NI, Michejda CJ. Small molecule toxins targeting tumor receptors. Curr Pharm Des 2004;10:2311.

14. Johnson CL, Johnson CG, Stauderman KA, Buck SH. Characterization of substance P receptors in human astrocytoma cells. Ann N Y Acad Sci 1991;632:410.

15. Hennig IM, Laissue JA, Horisberger U, Reubi JC. Substance-P receptors in human primary neoplasms: Tumoral and vascular localization. Int J Cancer 1995;61:786.

16. Dietl MM, Torrens Y, Beaujouan JC, Glowinski J. Substance P-induced reduction in the initial accumulation of cytosolic myo-[3H]inositol in rat parotid acinar cells mediated by the NK1 tachykinin receptor. J Neurochem 1989;53:1640.

17. Snider RM, Constantine JW, Lowe JA, 3rd, et al. A potent nonpeptide antagonist of the substance P (NK1) receptor. Science 1991;251:435.

18. Caioli S, Curcio L, Pieri M, et al. Substance P receptor activation induces downregulation of the AMPA receptor functionality in cortical neurons from a genetic model of Amyotrophic Lateral Sclerosis. Neurobiol Dis 2011;44:92.

19. Palma C, Maggi CA. The role of tachykinins via NK1 receptors in progression of human gliomas. Life Sci 2000;67:985.

20. Munoz M, Rosso M. The NK-1 receptor antagonist aprepitant as a broad spectrum antitumor drug. Invest New Drugs 2010;28:187.

21. Kast RE. Why cerebellar glioblastoma is rare and how that indicates adjunctive use of the FDA-approved anti-emetic aprepitant might retard cerebral glioblastoma growth: A new hypothesis to an old question. Clin Transl Oncol 2009;11:408.

22. Kneifel S, Cordier D, Good S, et al. Local targeting of malignant gliomas by the diffusible peptidic vector 1,4,7,10-tetraazacyclododecane-1-glutaric acid-4,7,10-triacetic acid-substance p. Clin Cancer Res 2006;12:3843.

23. Cordier D, Forrer F, Bruchertseifer F, et al. Targeted alpha-radionuclide therapy of functionally critically located gliomas with 213Bi-DOTA-[Thi8,Met(O2)11]-substance P: A pilot trial. Eur J Nucl Med Mol Imaging 2010;37:1335.

24. Cordier D, Forrer F, Kneifel S, et al. Neoadjuvant targeting of glioblastoma multiforme with radiolabeled DOTAGA-substance P–results from a phase I study. J Neurooncol 2010;100:129.

25. Fong TM, Anderson SA, Yu H, Huang RR, Strader CD. Differential activation of intracellular effector by two isoforms of human neurokinin-1 receptor. Mol Pharmacol 1992;41:24.

26. Maggi CA. The mammalian tachykinin receptors. Gen Pharmacol 1995;26:911.

27. Patel HJ, Ramkissoon SH, Patel PS, Rameshwar P. Transformation of breast cells by truncated neurokinin-1 receptor is secondary to activation by preprotachykinin-A peptides. Proc Natl Acad Sci USA 2005;102:17436.

28. Lai JP, Ho WZ, Kilpatrick LE, et al. Full-length and truncated neurokinin-1 receptor expression and function during monocyte/macrophage differentiation. Proc Natl Acad Sci USA 2006;103:7771.

29. Kawakami K, Kawakami M, Kioi M, Husain SR, Puri RK. Distribution kinetics of targeted cytotoxin in glioma by bolus or convection-enhanced delivery in a murine model. J Neurosurg 2004;101:1004.

30. Rand RW, Kreitman RJ, Patronas N, et al. Intratumoral administration of recombinant circularly permuted interleukin-4-pseudomonas exotoxin in patients with high-grade glioma. Clin Cancer Res 2000;6:2157.

31. Laske DW, Youle RJ, Oldfield EH. Tumor regression with regional distribution of the targeted toxin TF-CRM107 in patients with malignant brain tumors. Nat Med 1997;3:1362.

32. Mäcke HR. Radiolabeled peptides in nuclear oncology: influence of peptide structure and labeling strategy on pharmacology. Ernst Schering Res Found Workshop 2005:43.

33. Siena S, Lappi DA, Bregni M, et al. Synthesis and characterization of an antihuman T-lymphocyte saporin immunotoxin (OKT1-SAP) with in vivo stability into nonhuman primates. Blood 1988;72:756.

34. Siena S, Bregni M, Formosa A, et al. Evaluation of antihuman T lymphocyte saporin immunotoxins potentially useful in human transplantation. Transplantation 1988;46:747.

35. Flavell DJ, Cooper S, Morland B, Flavell SU. Characteristics and performance of a bispecific F (ab'gamma)2 antibody for delivering saporin to a CD7+ human acute T-cell leukaemia cell line. Br J Cancer 1991;64:274.

36. Kaur I, Gupta RC, Puri M. Ribosome inactivating proteins from plants inhibiting viruses. Virol Sin 2011;26:357.

37. Santanche S, Bellelli A, Brunori M. The unusual stability of saporin, a candidate for the synthesis of immunotoxins. Biochem Biophys Res Commun 1997;234:129.

38. Polito L, Bortolotti M, Pedrazzi M, Bolognesi A. Immunotoxins and other conjugates containing saporin-s6 for cancer therapy. Toxins 2011;3:697.

39. Quadros EV, Nakayama Y, Sequeira JM. Targeted delivery of saporin toxin by monoclonal antibody to the transcobalamin receptor, TCblR/CD320. Mol Cancer Ther 2010;9:3033.

40. Lai JP, Douglas SD, Wang YJ, Ho WZ. Real-time reverse transcription-PCR quantitation of substance P receptor (NK-1R) mRNA. Clin Diagn Lab Immunol 2005;12:537.

41. Hall JM, Mitchell D, Morton IK. Typical and atypical NK1 tachykinin receptor characteristics in the rabbit isolated iris sphincter. Br J Pharmacol 1994;112:985.

VII. Conclusions and Perspectives

Over the last two decades, the knowledge of molecular targets and their ligands, molecular and cell biology of malignancies, and structure-activity relationship of potential new radioligands has increased.[5,15a,37,55,58d,77] Also, advancements in combinatorial peptide chemistry, bioconjugation strategies, coordination chemistry of radiometals, radiolabeling protocols, and the availability of imaging instruments for small animals have expedited research in the fields of metal-based radiopharmaceutical chemistry and nuclear medicine.[2,8,15a,19a,59d,68] Nowadays, targeting peptides represent an integral part of research aimed at the development of novel radiotracers for molecular imaging and radionuclide therapy of cancer.[2,8,10,15a,c,19a,37,41,52-53,58d,83] Different approaches towards the optimization of radiolabeled, tumor targeting peptides to improve the quality of molecular imaging and to enhance the efficacy of radionuclide therapy of cancer were evaluated in this Ph.D. thesis. Conclusions and perspectives thereof will be discussed in the following sections.

Dual-targeting radioconjugates

Both, efficient internalization of radioactivity into tumor cells and prolonged retention are crucial features for the successful application of agonistic, radiolabeled peptides for targeted molecular imaging and therapy of cancer.[5,10,19a,37,41,52] We investigated dual-targeting bombesin radioconjugates to reduce rapid efflux of radioactivity from cancer cells after successful delivery. In a first step, we focused on developing new bifunctional, radiolabeled bombesin analogs for additional intracellular targeting of mitochondria, using TPP-derivatives. Starting from readily accessible building blocks, a dual-targeting BBS-TPP analog was assembled on solid support selectively and efficiently *via* an extended Click-to-Chelate[31c] strategy. Radiolabeling with the ^{99m}Tc-tricarbonyl core afforded stable complexation of the radionuclide. Dual-targeting BBS-TPP analog and a reference compound lacking the TPP moiety were evaluated *in vitro* using PC-3 cells. Attaching 3-tris(*p*-methoxyphenyl)-phosphonium propionic acid for mitochondria targeting did not alter the high affinity of the bombesin analog towards the GRP-r and specific receptor-mediated internalization into PC-3 cells was observed. Compared to the reference conjugate, the additional TPP moiety proved significant higher binding to isolated mitochondria *in vitro*. However, in intact PC-3 cells, dual-targeting TPP-BBS displayed an overall unaltered externalization rate of radioactivity from PC-3 cells. We speculate that hindered passage through the mitochondria membrane could have interfered with the intracellular targeting of the conjugate.[51c,139] Since the combination of two different entities specific for an extra- and intracellular target in the same radioconjugate is an attractive approach to reduce cellular washout of radioactivity, we decided to evaluate further this strategy with intracellular targets that do not require multiple trafficking through membranes.

In the next step, we simplified the system and developed bifunctional bombesin analogs for intracellular targeting of the ubiquitous, cytosolic chaperon protein Hsp90, which is found overexpressed in high concentrations by nearly all cancer cells.[129-130] For interaction with Hsp90, we covalently attached the peptidic Hsp90 inhibitor shepherdin[132-133] to a bombesin analog by the same synthetic approach. The attachment of the hydrophilic shepherdin[79-83] sequence did not interfere with specific receptor-mediated internalization into PC-3 cells, but reduced slightly the binding affinity towards the GRP-r. Compared to the reference conjugate lacking the shepherdin sequence, the dual-targeting BBS-shepherdin[79-83] conjugate did not result into a reduced efflux of radioactivity from PC-3 cells.

The fate of the radioligand after endocytosis and intracellular processes leading to externalization of the radiotracers is not fully understood in detail. Reasons for the observed lack of intracellular targeting of the conjugates described might include the enzymatic degradation of the shepherdin sequence or, alternatively, endosomal entrapment of the radioconjugate. Both scenarios would prevent the interaction with the cytosolic target.[49,51a,c,140] Potential issues of the stability of peptidic shepherdin sequences could be overcome by applying non-peptidic inhibitors of Hsp90.[141] Strategies to achieve endosomal release for intracellular delivery might include the combination of the radiopeptide conjugate described with cleavable linkers,[142] biomimetic peptides,[51a,140] or synthetic polymers.[51c,140,143] Different cleavable linkers including enzymatically degradable units, nucleophile/base- or electrophile/acid-sensitive, pH- or redox-sensitive entities, but also photo-cleavable linkers, and metal-assisted linker systems have been reported in the literature for various applications.[142] Amongst them, reduction-sensitive, disulfide-containing linkers have been most widely used in biochemistry.[142b] Disulfide bonds are known to be cleaved by glutathione *via* thiol/disulfide exchange and thus, are frequently used in the design of prodrugs for release of the pharmaceutical upon enzymatic reduction.[142a,144] Endosomal escape is also a crucial requirement for other drug delivery systems used, e.g., for the delivery of nucleic acids as potential therapeutic macromolecules for the prevention or treatment of several diseases, including cancer, cardiovascular diseases, infections, and genetic disorders.[51a,c,140] Reported strategies to enhance endosomal release of non-viral vectors for delivery of nucleic acids include, for example, the use of weak bases (e.g., chloroquine) that cause osmotic swelling and rupture of the endosomes.[51a,140] The possibility of endosomal membrane fusion, destabilization mechanisms, or the formation of pores in the membrane of endosomes have also been studied with e.g., cell penetrating peptides.[51a,140] Future research is directed towards the combination of the dual-targeting radiopeptides with the strategies outlined above.

In conclusion, endocytosis is a major route for cellular uptake of drugs and drug delivery systems.[51a,c,140] Further research towards the elucidation of the mechanism of the escape of drugs from the endosomes is needed in order to design efficient systems that ensure the release of the drug to the cytosol. Such novel drug delivery systems may also be used to increase the performance of radiolabeled, tumor targeting peptides.

1,2,3-Triazoles as protease-resistant peptidomimetics for tumor targeting

The metabolic stability of tumor targeting, radiolabeled peptides *in vivo* is crucial to extend their blood circulation time, which can increase tumor uptake.[15c,19a,26,42] We reported the systematic replacement of amide bonds of the bombesin derivative [Nle[14]]BBS(7-14) by isosteric 1,2,3-triazoles with the goal to improve the metabolic stability of the peptide while maintaining its high affinity towards the GRP-r.[30c,137-138] The triazole scan provided a series of novel peptidomimetics with an up to 3.5-fold improved serum stability and retained high binding affinity to the GRP-r in the low nanomolar range. Peptidomimetics with amide bonds substituted at the C-terminus and between positions Gly[11]-His[12], Val[10]-Gly[11], and Ala[9]-Val[10] exhibited internalization properties and specific affinity towards the GRP-r comparable to that of the unmodified reference peptide sequence. In addition, radioconjugates bearing the 1,2,3-triazole in positions Gly[11]-His[12], Val[10]-Gly[11], and Ala[9]-Val[10] showed significantly improved serum half-lives *in vitro*. The most promising ^{177}Lu-radiolabeled peptidomimetic bearing a triazole between Gly[11] and His[12] was compared side-by-side with the reference compound *in vivo* by biodistribution experiments in tumor-bearing mice. Metabolic stabilization of this peptide analog by the 1,2,3-triazole enhanced the uptake in GRP-receptor-positive organs (e.g., pancreas) and doubled the tumor uptake *in vivo*. Encouraged by these results, triazole scans of other peptides of medical interest are currently ongoing.[145] Further optimization of the lead compound(s) identified and the introduction of multiple 1,2,3-triazoles are also under evaluation. This new methodology for the

stabilization of peptides may allow broad applications for the development of novel, tumor targeting, radiolabeled peptides for molecular imaging and PRRT.

A pharmaceutical approach to increase the metabolic stability of radiopeptides administered *in vivo* is the utilization of enzyme inhibitors.[55,134,146] Nock *et al.* recently reported an efficient and promising strategy to increase metabolic stability of radiopeptides by co-administration of the neutral endopeptidase inhibitor phosphoramidon (PA).[146] They evaluated the co-administration of PA with radiolabeled derivatives of somatostatin, bombesin, and gastrin to tumor-bearing mice and observed significantly improved tumor uptake in all cases.[146] Thus, future research could also include the combination of co-administration of enzyme inhibitors and chemical stabilization of radiolabeled peptidomimetics.

Different NK$_1$R-isoforms overexpressed in glioblastoma multiforme

Several human cancers overexpress the NK$_1$-receptor that can be targeted with radiolabeled SP-derivatives for PRRT.[53,111b,114a,115] Intratumoral administration of radiolabeled SP analogs has previously been evaluated clinically in glioma patients.[118a-c] However, differences in the response of the patients that received local radionuclide therapy were observed.[118a,c] Reasons might be different concentrations of the NK$_1$R-*Fl* and NK$_1$R-*Tr* isoforms of the receptor in heterogeneous tumor tissues. Our preclinical *in vitro* evaluations suggested that confirmation of NK$_1$R expression alone might not be an adequate parameter to predict the therapeutic response to NK$_1$R-targeted therapy. Sufficient expression of the full-length NK$_1$R isoform appears to be essential for efficient binding and internalization of (radiolabeled) SP derivatives into glioma cells. The receptor expression of glioblastoma tissue may be different for multi-passaged glioma cell lines. Thus, future research should be directed towards the examination of NK$_1$R-subtypes in glioblastoma tissue samples. The expression of the different NK$_1$R isoforms should also be confirmed on the protein level by, e.g., western blot techniques. In conclusion, pre-therapeutic screening for the actual expression of the NK$_1$R-*Fl* isoform could improve the selection of glioma patients to benefit from NK$_1$R-specific radionuclide therapy and pave the way towards patient-individualized medicine in the future.

VIII.   References

1. Cutler, C. S.; Hennkens, H. M.; Sisay, N.; Huclier-Markai, S.; Jurisson, S. S. *Chemical Reviews* **2013**, *113*, 858.

2. Liu, S. *Advanced Drug Delivery Reviews* **2008**, *60*, 1347.

3. Saha, G. B. *Fundamentals of Nuclear Pharmacy, Sixth Edition*, Springer: New York **2010**.

4. Mankoff, D. A. *The Journal of Nuclear Medicine* **2007**, *48*, 18N.

5. Reubi, J.-C. *Endocrine Reviews* **2003**, *24*, 389.

6. Schubiger, P. A.; Alberto, R.; Smith, A. *Bioconjugate Chemistry* **1996**, *7*, 165.

7. Smith, S. V. *Journal of Inorganic Biochemistry* **2004**, *98*, 1874.

8. Ramogida, C. F.; Orvig, C. *Chemical Communications* **2013**, *49*, 4720.

9. Frischknecht, M. J. *Ph.D. thesis, University of Basel, Basel, Switzerland* **2011**.

10. Eberle, A. N.; Mild, G. *Journal of Receptors and Signal Transduction* **2009**, *29*, 1.

11. Liu, S. *Chemical Society Reviews* **2004**, *33*, 445.

12. Richards, P.; Tucker, W. D.; Srivastava, S. C. *International Journal of Applied Radiation and Isotopes* **1982**, *33*, 793.

13. Kassis, A. I.; Adelstein, S. J. *The Journal of Nuclear Medicine* **2005**, *46*, 4S.

14. a) Humm, J. L.; Howell, R. W.; Rao, D. V. *Medical Physics* **1994**, *21*, 1901; b) Tavares, A. A. S.; Tavares, J. M. R. S. *International Journal of Radiation Biology* **2010**, *86*, 261.

15. a) Correia, J. D. G.; Paulo, A.; Raposinho, P. D.; Santos, I. *Dalton Transactions* **2011**, *40*, 6144; b) Zoller, F.; Eisenhut, M.; Haberkorn, U.; Mier, W. *European Journal of Pharmacology* **2009**, *625*, 55; c) Fani, M.; Mäcke, H. R. *European Journal of Nuclear Medicine and Molecular Imaging* **2012**, *39 Suppl. 1.*, S11.

16. Liu, S.; Edwards, D. S. *Chemical Reviews* **1999**, *99*, 2235.

17. Liu, S.; Chakraborty, S. *Dalton Transactions* **2011**, *40*, 6077.

18. a) Sancho, V.; Di Florio, A.; Moody, T. W.; Jensen, R. T. *Current Drug Delivery* **2011**, *8*, 79; b) Alberto, R.; Braband, H. *Comprehensive Inorganic Chemistry II Second Edition.*; Elsevier: Amsterdam **2013**.

19. a) Müller, C.; Schibli, R. *Molecular Imaging in Oncology, Recent Results in Cancer Research;* Springer: Berlin Heidelberg **2013**, *187*, 65; b) Schibli, R.; Schubiger, P. A. *European Journal of Nuclear Medicine and Molecular Imaging* **2002**, *29*, 1529.

20. Abram, U.; Alberto, R. *Journal of the Brazilian Chemical Society* **2006**, *17*, 1486.

21. a) Nock, B. A.; Nikolopoulou, A.; Galanis, A.; Cordopatis, P.; Waser, B.; Reubi, J.-C.; Maina, T. *Journal of Medicinal Chemistry* **2005**, *48*, 100; b) Abiraj, K.; Mansi, R.; Tamma, M.-L.; Forrer, F.; Cescato, R.; Reubi, J.-C.; Akyel, K. G.; Mäcke, H. R. *Chemistry – A European Journal* **2010**, *16*, 2115.

22. Liu, S. *Contrast Agents III, Topics in Current Chemistry*; Springer: Berlin Heidelberg, **2005**, 252, 117.

23. Alberto, R.; Schibli, R.; Egli, A.; Schubiger, A. P.; Abram, U.; Kaden, T. A. *Journal of the American Chemical Society* **1998**, *120*, 7987.

24. Alberto, R.; Ortner, K.; Wheatley, N.; Schibli, R.; Schubiger, A. P. *Journal of the American Chemical Society* **2001**, *123*, 3135.

25. a) Alberto, R.; Schibli, R.; Waibel, R.; Abram, U.; Schubiger, A. P. *Coordination Chemistry Reviews* **1999**, *192*, 901; b) Morais, G. R.; Paulo, A.; Santos, I. *Organometallics* **2012**, *31*, 5693; c) Alberto, R.; Pak, J. K.; van Staveren, D.; Mundwiler, S.; Benny, P. *Biopolymers* **2004**, *76*, 324; d) Alberto, R. *Contrast Agents III, Topics in Current Chemistry,* Springer: Berlin Heidelberg **2005**, *252*, 1.

26. Okarvi, S. M. *Medicinal Research Reviews* **2004**, *24*, 357.

27. Schibli, R.; La, B. R.; Alberto, R.; García-Garayoa, E.; Ortner, K.; Abram, U.; Schubiger, P. A. *Bioconjugate Chemistry* **2000**, *11*, 345.

28. Bartholomä, M.; Valliant, J.; Maresca, K. P.; Babich, J.; Zubieta, J. *Chemical Communications* **2009**, 493.

29. Mindt, T. L.; Struthers, H.; Brans, L.; Anguelov, T.; Schweinsberg, C.; Maes, V.; Tourwé, D.; Schibli, R. *Journal of the American Chemical Society* **2006**, *128*, 15096.

30. a) Rostovtsev, V. V.; Green, L. G.; Fokin, V. V.; Sharpless, K. B. *Angewandte Chemie International Edition* **2002**, *41*, 2596; b) Tornøe, C. W.; Christensen, C.; Meldal, M. *Journal of Organic Chemistry* **2002**, *67*, 3057; c) Meldal, M.; Tornøe, C. W. *Chemical Reviews* **2008**, *108*, 2952.

31. a) Mindt, T. L.; Müller, C.; Melis, M.; de Jong, M.; Schibli, R. *Bioconjugate Chemistry* **2008**, *19*, 1689; b) Struthers, H.; Spingler, B.; Mindt, T. L.; Schibli, R. *Chemistry - a European Journal* **2008**, *14*, 6173; c) Mindt, T. L.; Struthers, H.; Spingler, B.; Brans, L.; Tourwé, D.; García-Garayoa, E.; Schibli, R. *ChemMedChem* **2010**, *5*, 2026.

32. Braband, H. *Chimia* **2011**, *65*, 776.

33. Pearlstein, R. M.; Davison, A. *Polyhedron* **1988**, *7*, 1981.

34. Braband, H.; Tooyama, Y.; Fox, T.; Alberto, R. *Chemistry - a European Journal* **2009**, *15*, 633.

35. Braband, H. *Journal of Labelled Compounds and Radiopharmaceuticals* **2014**, *57*, 270.

36. Braband, H.; Tooyama, Y.; Fox, T.; Simms, R.; Forbes, J.; Valliant, J. F.; Alberto, R. *Chemistry- a European Journal* **2011**, *17*, 12967.

37. Schottelius, M.; Wester, H.-J. *Methods* **2009**, *48*, 161.

38. Lyra, M.; Charalambatou, P.; Roussou, E.; Fytros, S.; Baka, I. *Hellenic Journal of Nuclear Medicine* **2011**, *14*, 49.

39. Galea, R.; Ross, C.; Wells, R. G. *Applied Radiation and Isotopes* **2014**, *87*, 148.

40. Dash, A.; Knapp Jr., F. F.; Pillai, M. R. A. *Nuclear Medicine and Biology* **2013**, *40*, 167.

41. Fani, M.; Mäcke, H. R.; Okarvi, S. M. *Theranostics* **2012**, *2*, 481.

42. Deepa, S.; Sai, K. V.; Gowrishankar, R.; Venkataramaniah, K. *The European Physical Journal A* **2012**, *48*, 126.

43. a) Kam, B. L. R.; Teunissen, J. J. M.; Krenning, E. P.; de Herder, W. W.; Khan, S.; van Vliet, E. I.; Kwekkeboom, D. J. *European Journal of Nuclear Medicine and Molecular Imaging* **2012**, *39*, S103; b) van Essen, M.; Krenning, E. P.; Kam, B. L. R.; de Jong, M.; Valkema, R.; Kwekkeboom, D. J. *Nature Reviews Endocrinology* **2009**, *5*, 382.

44. a) Lantry, L. E.; Cappelletti, E.; Maddalena, M. E.; Fox, J. S.; Feng, W.; Chen, J.; Thomas, R.; Eaton, S. M.; Bogdan, N. J.; Arunachalam, T.; Reubi, J.-C.; Raju, N.; Metcalfe, E. C.; Lattuada, L.; Linder, K. E.; Swenson, R. E.; Tweedle, M. F.; Nunn, A. D. *The Journal of Nuclear Medicine* **2006**, *47*, 1144; b) Bodei, L.; Ferrari, M.; Nunn, A.; Llull, J.; Cremonesi, M.; Martano, L.; Laurora, G.; Scardino, E.; Tiberini, S.; Bufi, G.; Eaton, S.; de Cobelli, O.; Paganelli, G. *European Journal of Nuclear Medicine and Molecular Imaging* **2007**, *34 Suppl 2.*, S221.

45. Forrer, F.; Oechslin-Oberholzer, C.; Campana, B.; Herrmann, R.; Mäcke, H. R.; Müller-Brand, J.; Lohri, A. *The Journal of Nuclear Medicine* **2013**, *54*, 1045.

46. Reubi, J.-C. *The Journal of Nuclear Medicine* **1995**, *36*, 1825.

47. Wolfe, B. L.; Trejo, J. *Traffic* **2007**, *8*, 462.

48. Aktories K., Förstermann U., Hofmann F., Starke K. *Allgemeine und spezielle Pharmakologie und Toxikologie,* 9th edition.; Elsevier München, **2005**.

49. Grady, E. F.; Slice, L. W.; Brant, W. O.; Walsh, J. H.; Payan, D. G.; Bunnett, N. W. *The Journal of Biological Chemistry* **1995**, *270*, 4603.

50.   a) Jean-Alphonse, F.; Hanyaloglu, A. C. *Molecular and Cellular Endocrinology* **2011**, *331*, 205; b) Delom, F.; Fessart, D. *International Journal of Cell Biology* **2011**, *2011*, 246954.

51.   a) Liang, W.; Lam, J. K. W. *Biochemistry, Genetics and Molecular Biology, Molecular Regulation of Endocytosis,* InTech **2012**, Chapter 17; b) Ginj, M.; Hinni, K.; Tschumi, S.; Schulz, S.; Mäcke, H. R. *The Journal of Nuclear Medicine* **2005**, *46*, 2097; c) Cornelissen, B. *Journal of Labelled Compounds and Radiopharmaceuticals* **2014**, *57*, 310.

52.   Reubi, J.-C.; Mäcke, H. R. *The Journal of Nuclear Medicine* **2008**, *49*, 1735.

53.   Reubi, J.-C.; Mäcke, H. R.; Krenning, E. P. *The Journal of Nuclear Medicine* **2005**, *46*, 67S.

54.   a) Wester, H.-J. *Clinical Cancer Research* **2007**, *13*, 3470; b) Tweedle, M. F. *Accounts of Chemical Research* **2009**, *42*, 958; c) Pool, S. E.; Krenning, E. P.; Koning, G. A.; van Eijck, C. H. J.; Teunissen, J. J. M.; Kam, B.; Valkema, R.; Kwekkeboom, D. J.; de Jong, M. *Seminars in Nuclear Medicine* **2010**, *40*, 209.

55.   Vlieghe, P.; Lisowski, V.; Martinez, J.; Khrestchatisky, M. *Drug Discovery Today* **2010**, *15*, 40.

56.   a) Nock, B.; Nikolopoulou, A.; Chiotellis, E.; Loudos, G.; Maintas, D.; Reubi, J.-C.; Maina, T. *European Journal of Nuclear Medicine and Molecular Imaging* **2003**, *30*, 247; b) Ginj, M.; Zhang, H.; Waser, B.; Cescato, R.; Wild, D.; Wang, X.; Erchegyi, J.; Rivier, J.; Mäcke, H. R.; Reubi, J.-C. *Proceedings of the National Academy of Sciences of the United States of America* **2006**, *103*, 16436.

57.   Schroeder, R. P. J.; van Weerden, W. M.; Bangma, C.; Krenning, E. P.; de Jong, M. *Methods* **2009**, *48*, 200.

58.   a) Newton, J.; Deutscher, S. L. *Handbook of Experimental Pharmacology, Molecular Imaging II*; **2008**; *185*, 145; b) Brown, K. C. *Current Opinion in Chemical Biology* **2000**, *4*, 16; c) Benedetti, E.; Morelli, G.; Accardo, A.; Mansi, R.; Tesauro, D.; Aloj, L. *BioDrugs* **2004**, *18*, 279; d) Lee, S.; Xie, J.; Chen, X. *Chemical Reviews* **2010**, *110*, 3087.

59.   Rösch, F.; Baum, R. P. *Dalton Transactions* **2011**, *40*, 6104.

60.   a) Baum, R. P.; Kulkarni, H. R.; Carreras, C. *Seminars in Nuclear Medicine* **2012**, *42*, 190; b) Baum, R. P.; Kulkarni, H. R. *Theranostics* **2012**, *2*, 437.

61.   Kubicek, V.; Rudovsky, J.; Kotek, J.; Hermann, P.; Vander Elst, L.; Muller, R. N.; Kolar, Z. I.; Wolterbeek, H. T.; Peters, J. A.; Lukes, I. *Journal of the American Chemical Society* **2005**, *127*, 16477.

62.   a) Liu, S.; Edwards, D. S. *Bioconjugate Chemistry* **2001**, *12*, 7; b) Lattuada, L.; Barge, A.; Cravotto, G.; Giovenzana, G. B.; Tei, L. *Chemical Society Reviews* **2011**, *40*, 3019.

63.   Vincent, J. B.; Love, S. *Biochimica et Biophysica Acta* **2012**, *1820*, 362.

64.   Zeglis, B. M.; Lewis, J. S. *Dalton Transactions.* **2011**, *40*, 6168.

65.   a) Deri, M. A.; Zeglis, B. M.; Francesconi, L. C.; Lewis, J. S. *Nuclear Medicine and Biology* **2013**, *40*, 3; b) Fischer, G.; Seibold, U.; Schirrmacher, R.; Wängler, B.; Wängler, C. *Molecules* **2013**, *18*, 6469.

66.   Good, S. *Ph.D. thesis, University of Basel, Basel, Switzerland* **2006**.

67.   Zeng, D.; Zeglis, B. M.; Lewis, J. S.; Anderson, C. J. *The Journal of Nuclear Medicine* **2013**, *54*, 829.

68.   Jewett, J. C.; Bertozzi, C. R. *Chemical Society Reviews* **2010**, *39*, 1272.

69.   Mindt, T. L.; Jungi, V.; Wyss, S.; Friedli, A.; Pla, G.; Novak-Hofer, I.; Grünberg, J.; Schibli, R. *Bioconjug Chemistry* **2008**, *19*, 271.

70.   García-Garayoa, E.; Schweinsberg, C.; Maes, V.; Brans, L.; Bläuenstein, P.; Tourwé, D. A.; Schibli, R.; Schubiger, P. A. *Bioconjugate Chemistry* **2008**, *19*, 2409.

71.   García-Garayoa, E.; Rüegg, D.; Bläuenstein, P.; Zwimpfer, M.; Khan, I. U.; Maes, V.; Blanc, A.; Beck-Sickinger, A. G.; Tourwé, D. A.; Schubiger, P. A. *Nuclear Medicine and Biology* **2007**, *34*, 17.

72.   Hosseinimehr, S. J.; Tolmachev, V.; Orlova, A. *Drug Discovery Today* **2012**, *17*, 1224.

73.   a) Esteves, T.; Marques, F.; Paulo, A.; Rino, J.; Nanda, P.; Smith, C. J.; Santos, I. *Journal of Biological Inorganic Chemistry* **2011**, *16*, 1141; b) Zelenka, K.; Borsig, L.; Alberto, R. *Bioconjugate Chemistry* **2011**, *22*, 958.

74.   a) Schweinsberg, C.; Maes, V.; Brans, L.; Bläuenstein, P.; Tourwé, D. A.; Schubiger, P. A.; Schibli, R.; García-Garayoa, E. *Bioconjugate Chemistry* **2008**, *19*, 2432; b) Schottelius, M.; Wester, H. J.; Reubi, J.-C.; Senekowitsch-Schmidtke, R.; Schwaiger, M. *Bioconjugate Chemistry* **2002**, *13*, 1021; c) Wester, H. J.; Schottelius, M.; Poethko, T.; Bruus-Jensen, K.; Schwaiger, M. *Cancer Biotherapy and Radiopharmaceuticals* **2004**, *19*, 231.

75.   Mier, W.; Graham, K. A. N.; Wang, Q.; Krämer, S.; Hoffend, J.; Eisenhut, M.; Haberkorn, U. *Tetrahedron Letters* **2004**, *45*, 5453.

76.   Zhang, H.; Schuhmacher, J.; Waser, B.; Wild, D.; Eisenhut, M.; Reubi, J.-C.; Mäcke, H. R. *European Journal of Nuclear Medicine and Molecular Imaging* **2007**, *34*, 1198.

77.   Schally, A. V.; Nagy, A. *European Journal of Endocrinology* **1999**, *141*, 1.

78.   Mansi, R.; Fleischmann, A.; Mäcke, H. R.; Reubi, J.-C. *Nature Reviews Urology* **2013**, *10*, 235.

79.   Reubi, J.-C.; Körner, M.; Waser, B.; Mazzucchelli, L.; Guillou, L. *European Journal of Nuclear Medicine and Molecular Imaging* **2004**, *31*, 803.

80.   Tofilon, P. J.; Saxman, S.; Coleman, N. C. *Clinical Cancer Research* **2003**, *9*, 3518.

81.   Kwekkeboom, D. J.; Müller-Brand, J.; Paganelli, G.; Anthony, L. B.; Pauwels, S.; Kvols, L. K.; O'Dorisio, T. M.; Valkema, R.; Bodei, L.; Chinol, M.; Mäcke, H. R.; Krenning, E. P. *The Journal of Nuclear Medicine* **2005**, *46*, 62S.

82.   Kwekkeboom, D.; Krenning, E. P.; de Jong, M. *The Journal of Nuclear Medicine* **2000**, *41*, 1704.

83.   Ambrosini, V.; Fani, M.; Fanti, S.; Forrer, F.; Mäcke, H. R. *The Journal of Nuclear Medicine* **2011**, *52 Suppl 2*, 42S.

84.   Reubi, J.-C.; Schär, J. C.; Waser, B.; Wenger, S.; Heppeler, A.; Schmitt, J. S.; Mäcke, H. R. *European Journal of Nuclear Medicine* **2000**, *27*, 273.

85.   Reubi, J.-C.; Krenning, E.; Lamberts, S. W. J.; Kvols, L. *Metabolism* **1992**, *41*, 104.

86.   a) Anastasi, A.; Erspamer, V.; Bucci, M. *Experientia* **1971**, *27*, 166; b) Erspamer, V.; Erspamer, G. F.; Inselvin.M *Journal of Pharmacy and Pharmacology* **1970**, *22*, 875.

87.   Szczepanek, M. *http://en.wikipedia.org/wiki/European_fire-bellied_toad*, 06.05.2014.

88.   McDonald, T. J.; Jörnvall, H.; Nilsson, G.; Vagne, M.; Ghatei, M.; Bloom, S. R.; Mutt, V. *Biochemical and Biophysical Research Communications* **1979**, *90*, 227.

89.   Jensen, R. T.; Battey, J. F.; Spindel, E. R.; Benya, R. V. *Pharmacological Reviews* **2008**, *60*, 1.

90.   Wada, E.; Way, J.; Shapira, H.; Kusano, K.; Lebacq-Verheyden, A. M.; Coy, D.; Jensen, R.; Battey, J. *Neuron* **1991**, *6*, 421.

91.   Spindel, E. R.; Giladi, E.; Brehm, P.; Goodman, R. H.; Segerson, T. P. *Molecular Endocrinology* **1990**, *4*, 1956.

92.   Fathi, Z.; Corjay, M. H.; Shapira, H.; Wada, E.; Benya, R.; Jensen, R.; Viallet, J.; Sausville, E. A.; Battey, J. F. *Journal of Biological Chemistry* **1993**, *268*, 5979.

93.   Nagalla, S. R.; Barry, B. J.; Creswick, K. C.; Eden, P.; Taylor, J. T.; Spindel, E. R. *Proceedings of the National Academy of Sciences of the United States of America* **1995**, *92*, 6205.

94.   Reubi, J.-C.; Wenger, S.; Schmuckli-Maurer, J.; Schaer, J. C.; Gugger, M. *Clinical Cancer Research* **2002**, *8*, 1139.

95.   Reile, H.; Armatis, P. E.; Schally, A. V. *The Prostate* **1994**, *25*, 29.

96.   Van de Wiele, C.; Dumont, F.; Vanden Broecke, R.; Oosterlinck, W.; Cocquyt, V.; Serreyn, R.; Peers, S.; Thornback, J.; Slegers, G.; Dierckx, R. A. *European Journal of Nuclear Medicine and Molecular Imaging* **2000**, *27*, 1694.

97.   Smith, C. J.; Gali, H.; Sieckman, G. L.; Higginbotham, C.; Volkert, W. A.; Hoffman, T. J. *Bioconjugate Chemistry* **2003**, *14*, 93.

98. Mindt, T. L.; Schweinsberg, C.; Brans, L.; Hagenbach, A.; Abram, U.; Tourwé, D.; García-Garayoa, E.; Schibli, R. *ChemMedChem* **2009**, *4*, 529.

99. Wild, D.; Frischknecht, M.; Zhang, H.; Morgenstern, A.; Bruchertseifer, F.; Boisclair, J.; Provencher-Bolliger, A.; Reubi, J.-C.; Mäcke, H. R. *Cancer Research* **2011**, *71*, 1009.

100. Lindner, S.; Michler, C.; Wängler, B.; Bartenstein, P.; Fischer, G.; Schirrmacher, R.; Wängler, C. *Bioconjugate Chemistry* **2014**, *25*, 489.

101. Pradhan, T. K.; Katsuno, T.; Taylor, J. E.; Kim, S. H.; Ryan, R. R.; Mantey, S. A.; Donohue, P. J.; Weber, H. C.; Sainz, E.; Battey, J. F.; Coy, D. H.; Jensen, R. T. *European Journal of Pharmacology* **1998**, *343*, 275.

102. Zhang, H. W.; Chen, J. H.; Waldherr, C.; Hinni, K.; Waser, B.; Reubi, J.-C.; Mäcke, H. R. *Cancer Research* **2004**, *64*, 6707.

103. Schuhmacher, J.; Zhang, H. W.; Doll, J.; Mäcke, H. R.; Matys, R.; Hauser, H.; Henze, M.; Haberkorn, U.; Eisenhut, M. *The Journal of Nuclear Medicine* **2005**, *46*, 691.

104. Dimitrakopoulou-Strauss, A.; Hohenberger, P.; Haberkorn, U.; Mäcke, H. R.; Eisenhut, M.; Strauss, L. G. *The Journal of Nuclear Medicine* **2007**, *48*, 1245.

105. a) Cescato, R.; Maina, T.; Nock, B.; Nikolopoulou, A.; Charalambidis, D.; Piccand, V.; Reubi, J.-C. *The Journal of Nuclear Medicine* **2008**, *49*, 318; b) Schroeder, R. P. J.; Müller, C.; Reneman, S.; Melis, M. L.; Breeman, W. A. P.; Blois, E.; Bangma, C. H.; Krenning, E. P.; Weerden, W. M.; Jong, M. *European Journal of Nuclear Medicine and Molecular Imaging* **2010**, *37*, 1386.

106. Abiraj, K.; Mansi, R.; Tamma, M.-L.; Fani, M.; Forrer, F.; Nicolas, G.; Cescato, R.; Reubi, J.-C.; Mäcke, H. R. *The Journal of Nuclear Medicine* **2011**, *52*, 1970.

107. Wieser, G.; Mansi, R.; Grosu, A. L.; Schultze-Seemann, W.; Dumont-Walter, R. A.; Meyer, P. T.; Mäcke, H. R.; Reubi, J.-C.; Weber, W. A. *Theranostics* **2014**, *4*, 412.

108. Honer, M.; Mu, L.; Stellfeld, T.; Graham, K.; Martic, M.; Fischer, C. R.; Lehmann, L.; Schubiger, P. A.; Ametamey, S. M.; Dinkelborg, L.; Srinivasan, A.; Borkowski, S. *The Journal of Nuclear Medicine* **2011**, *52*, 270.

109. Kähkönen, E.; Jambor, I.; Kemppainen, J.; Lehtiö, K.; Grönroos, T. J.; Kuisma, A.; Luoto, P.; Sipilä, H. J.; Tolvanen, T.; Alanen, K.; Silén, J.; Kallajoki, M.; Roivainen, A.; Schäfer, N.; Schibli, R.; Dragic, M.; Johayem, A.; Valencia, R.; Borkowski, S.; Minn, H. *Clinical Cancer Research* **2013**, *19*, 5434.

110. Kroll, C.; Mansi, R.; Braun, F.; Dobitz, S.; Mäcke, H. R.; Wennemers, H. *Journal of the American Chemical Society* **2013**, *135*, 16793.

111. a) Maggi, C. A. *General Pharmacology* **1995**, *26*, 911; b) Steinhoff, M. S.; von Mentzer, B.; Geppetti, P.; Pothoulakis, C.; Bunnett, N. W. *Physiological Reviews* **2014**, *94*, 265.

112. Fong, T. M.; Anderson, S. A.; Yu, H.; Huang, R. R.; Strader, C. D. *Molecular Pharmacology* **1992**, *41*, 24.

113. a) Hökfelt, T.; Pernow, B.; Wahren, J. *Journal of Internal Medicine* **2001**, *249*, 27; b) Mantyh, P. W. *Journal of Clinical Psychiatry* **2002**, *63*, 6.

114. a) Harford-Wright, E.; Lewis, K. M.; Vink, R. *Recent Patents on CNS Drug Discovery* **2013**, *8*, 13; b) Łazarczyk, M.; Matyja, E.; Lipkowski, A. *Folia Neuropathologica* **2007**, *45*, 99.

115. Hennig, I. M.; Laissue, J. A.; Horisberger, U.; Reubi, J.-C. *International Journal of Cancer* **1995**, *61*, 786.

116. van Hagen, P. M.; Breeman, W. A. P.; Reubi, J.-C.; Postema, P. T. E.; van den Anker-Lugtenburg, P. J.; Kwekkeboom, D. J.; Laissue, J.; Waser, B.; Lamberts, S. W. J.; Visser, T. J.; Krenning, E. P. *European Journal of Nuclear Medicine* **1996**, *23*, 1508.

117. Gniazdowska, E.; Koźmiński, P.; Fuks, L. *Journal of Radioanalytical and Nuclear Chemistry* **2013**, *298*, 1171.

118. a) Cordier, D.; Forrer, F.; Bruchertseifer, F.; Morgenstern, A.; Apostolidis, C.; Good, S.; Müller-Brand, J.; Mäcke, H.; Reubi, J.-C.; Merlo, A. *European Journal of Nuclear Medicine and Molecular Imaging* **2010**, *37*, 1335; b) Cordier, D.; Forrer, F.; Kneifel, S.; Sailer, M.; Mariani, L.; Mäcke, H.; Müller-Brand, J.; Merlo, A. *Journal of Neuro-Oncology* **2010**, *100*, 129; c) Kneifel, S.; Cordier, D.; Good, S.; Ionescu, M. C. S.; Ghaffari, A.; Hofer, S.; Kretzschmar, M.; Tolnay, M.; Apostolidis, C.; Waser, B.; Arnold, M.; Müller-Brand, J.; Mäcke, H. R.; Reubi, J.-C.; Merlo, A. *Clinical Cancer Research* **2006**, *12*, 3843; d) Merlo, A.; Hausmann, O.; Wasner, M.; Steiner, P.; Otte, A.; Jermann, E.; Freitag, P.; Reubi, J.-C.; Müller-Brand, J.; Gratzl, O.; Mäcke, H. R. *Clinical Cancer Research* **1999**, *5*, 1025; e) Schumacher, T.; Hofer, S.; Eichhorn, K.; Wasner, M.; Zimmerer, S.; Freitag, P.; Probst, A.; Gratzl, O.; Reubi, J.-C.; Mäcke, H. R.; Müller-Brand, J.; Merlo, A. *European Journal of Nuclear Medicine and Molecular Imaging* **2002**, *29*, 486.

119. Louis, D. N.; Ohgaki, H.; Wiestler, O. D.; Cavenee, W. K.; Burger, P. C.; Jouvet, A.; Scheithauer, B. W.; Kleihues, P. *Acta Neuropathologica* **2007**, *114*, 97.

120. a) Belda-Iniesta, C.; de Castro Carpeño, J.; Sáenz, E. C.; Guerrero, P. C.; Perona, R.; Barón, M. G. *Clinical and Translational Oncology* **2006**, *8*, 635; b) Westphal, M.; Lamszus, K. *Nature Reviews Neuroscience* **2011**, *12*, 495; c) Becker, K. P.; Yu, J. *The Cancer Journal* **2012**, *18*, 12.

121. Hochberg, F. H.; Pruitt, A. *Neurology* **1980**, *30*, 907.

122. a) Kunstler, J.-U.; Veerendra, B.; Figueroa, S. D.; Sieckman, G. L.; Rold, T. L.; Hoffman, T. J.; Smith, C. J.; Pietzsch, H.-J. *Bioconjugate Chemistry* **2007**, *18*, 1651; b) García-Garayoa, E.; Bläuenstein, P.; Blanc, A.; Maes, V.; Tourwé, D.; Schubiger, P. A. *European Journal of Nuclear Medicine and Molecular Imaging* **2009**, *36*, 37; c) Raposinho, P. D.; Correia, J. D. G.; Alves, S.; Botelho, M. F.; Santos, A. C.; Santos, I. *Nuclear Medicine and Biology* **2008**, *35*, 91 d) Wild, D.; Schmitt, J. S.; Ginj, M.; Mäcke, H. R.; Bernard, B. F.; Krenning, E.; de, J. M.; Wenger, S.; Reubi, J.-C. *European Journal of Nuclear Medicine and Molecular Imaging* **2003**, *30*, 1338; e) Wild, D.; Béhé, M.; Wicki, A.; Storch, D.; Waser, B.; Gotthardt, M.; Keil, B.; Christofori, G.; Reubi, J.-C.; Mäcke, H. R. *The Journal of Nuclear Medicine* **2006**, *47*, 2025.

123. Zhou, Z.; Wagh, N. K.; Ogbomo, S. M.; Shi, W.; Jia, Y.; Brusnahan, S. K.; Garrison, J. C. *The Journal of Nuclear Medicine* **2013**, *54*, 1605.

124. Goodsell, D. S. *RCSB Protein Data Bank* **2008**, doi: 10.2210/rcsb_pdb/mom_2008_12.

125. Kim, Y.-S.; Yang, C.-T.; Wang, J.; Wang, L.; Li, Z.-B.; Chen, X.; Liu, S. *Journal of Medicinal Chemistry* **2008**, *51*, 2971.

126. a) Murphy, M. P.; Smith, R. A. J. *Annual Review of Pharmacology and Toxicology* **2007**, *47*, 629; b) Smith, R. A. J.; Hartley, R. C.; Murphy, M. P. *Antioxidants & Redox Signaling* **2011**, *15*, 3021; c) Yousif, L. F.; Stewart, K. M.; Kelley, S. O. *ChemBioChem* **2009**, *10*, 1939.

127. Zhou, Y.; Liu, S. *Bioconjugate Chemistry* **2011**, *22*, 1459.

128. a) Gurm, G. S.; Danik, S. B.; Shoup, T. M.; Weise, S.; Takahashi, K.; Laferrier, S.; Elmaleh, D. R.; Gewirtz, H. *JACC: Cardiovascular Imaging* **2012**, *5*, 285; b) Yuan, H.; Cho, H.; Chen, H. H.; Panagia, M.; Sosnovik, D. E.; Josephson, L. *Chemical Communications* **2013**, *49*, 10361.

129. a) Lindquist, S.; Craig, E. A. *Annual Review of Genetics* **1988**, *22*, 631; b) Whitesell, L.; Lindquist, S. L. *Nature Reviews Cancer* **2005**, *5*, 761.

130. Li, Y.; Zhang, T.; Schwartz, S. J.; Sun, D. *Drug Resistance Updates* **2009**, *12*, 17.

131. a) Fortugno, P.; Beltrami, E.; Plescia, J.; Fontana, J.; Pradhan, D.; Marchisio, P. C.; Sessa, W. C.; Altieri, D. C. *Proceedings of the National Academy of Sciences of the United States of America* **2003**, *100*, 13791; b) Altieri, D. C. *Nature Reviews Cancer* **2008**, *8*, 61.

132. Plescia, J.; Salz, W.; Xia, F.; Pennati, M.; Zaffaroni, N.; Daidone, M. G.; Meli, M.; Dohi, T.; Fortugno, P.; Nefedova, Y.; Gabrilovich, D. I.; Colombo, G.; Altieri, D. C. *Cancer Cell* **2005**, *7*, 457.

133. a) Gyurkocza, B.; Plescia, J.; Raskett, C. M.; Garlick, D. S.; Lowry, P. A.; Carter, B. Z.; Andreeff, M.; Meli, M.; Colombo, G.; Altieri, D. C. *Journal of the National Cancer Institute* **2006**, *98*, 1068; b) Siegelin, M. D.; Plescia, J.; Raskett, C. M.; Gilbert, C. A.; Ross, A. H.; Altieri, D. C. *Molecular Cancer Therapeutics* **2010**, *9*, 1638; c) Xiaojiang, T.; Jinsong, Z.; Jiansheng, W.; Chengen, P.; Guangxiao, Y.; Quanying, W. *Cancer Investigation* **2010**, *28*, 465.

134. Rawlings, N. D.; Barrett, A. J. *Handbook of Proteolytic Enzymes, Introduction: Metallopeptidases and Their Clans, 3ʳᵈ Edition*, Elsevier Amsterdam, **2013**, 325.

135. Lelais, G.; Seebach, D. *Peptide Science* **2004**, *76*, 206.

136. Wiegand, H.; Wirz, B.; Schweitzer, A.; Camenisch, G. P.; Rodriguez Perez, M. I.; Gross, G.; Woessner, R.; Voges, R.; Arvidsson, P. I.; Frackenpohl, J.; Seebach, D. *Biopharmaceutics & Drug Disposition* **2002**, *23*, 251.

137. Valverde, I. E.; Mindt, T. L. *Chimia* **2013**, *67*, 262.

138. a) Pedersen, D. S.; Abell, A. *European Journal of Organic Chemistry* **2011**, *2011*, 2399; b) Kolb, H. C.; Sharpless, K. B. *Drug Discovery Today* **2003**, *8*, 1128.

139. Ross, M. F.; Filipovska, A.; Smith, R. A. J.; Gait, M. J.; Murphy, M. P. *Biochemical Journal* **2004**, *383*, 457.

140. Varkouhi, A. K.; Scholte, M.; Storm, G.; Haisma, H. J. *Journal of Controlled Release* **2011**, *151*, 220.

141. Patel, H. J.; Modi, S.; Chiosis, G.; Taldone, T. *Expert Opinion on Drug Discovery* **2011**, *6*, 559.

142. a) Vlahov, I. R.; Leamon, C. P. *Bioconjugate Chemistry* **2012**, *23*, 1357; b) Leriche, G.; Chisholm, L.; Wagner, A. *Bioorganic & Medical Chemistry* **2012**, *20*, 571.

143. Haag, R.; Kratz, F. *Angewandte Chemie International Edition* **2006**, *45*, 1198.

144. a) Saito, G.; Swanson, J. A.; Lee, K.-D. *Advanced Drug Delivery Reviews* **2003**, *55*, 199; b) Bauhuber, S.; Hozsa, C.; Breunig, M.; Göpferich, A. *Advanced Materials* **2009**, *21*, 3286; c) Góngora-Benítez, M.; Tulla-Puche, J.; Albericio, F. *Chemical Reviews* **2014**, *114*, 901.

145. Valverde, I. E.; Huxol, E.; Mindt, T. L. *Journal of Labelled Compounds and Radiopharmaceuticals* **2014**, 57, 275.

146. Nock, B. A.; Maina, T.; Krenning, E. P.; de, J. M. *The Journal of Nuclear Medicine* **2014**, 55, 121.

Danke!

Ein herzliches Dankeschön an alle, die mich in den letzten Jahren während meiner Dissertation in verschiedenster Weise unterstützt haben und damit zum Gelingen dieser Doktorarbeit beigetragen haben.

Ein besonderer Dank gebührt zunächst Herrn Prof. Dr. Thomas L. Mindt für die Möglichkeit in der Radiopharmazeutischen Chemie am Universitätsspital in Basel zu promovieren, für die interessanten Projekte, die ich bearbeiten durfte, und das entgegengebrachte Vertrauen. Vielen Dank für die Unterstützung und das Feedback beim Erstellen dieser Arbeit, der Publikationen, wissenschaftlicher Vorträge und Postern. Danke auch für die Möglichkeit der Teilnahme an nationalen und internationalen Kongressen, sowie an diversen Fort- und Weiterbildungen.

Prof. Dr. Roger Schibli danke ich für die Übernahme des Korreferates und dafür, dass ich zu Beginn meiner Dissertation an der Vorlesung „Radiopharmazeutische Chemie" (ETH) teilnehmen durfte, die als wunderbare Grundlage für die Einarbeitung in die Fachgebiete Radiopharmazie und Nuklearmedizin diente.

Prof. Dr. Edwin Constable danke ich, dass er die Funktion des Fakultätsvertreters übernommen hat. Ihm und Prof. Dr. Catherine Housecroft danke ich ebenso dafür, dass ich aktiv an den Forschungssitzungen der Arbeitsgruppe und wissenschaftlichen Diskussionen teilnehmen durfte.

Prof. Dr. Jörg Huwyler danke ich für die Übernahme des Vorsitzes meiner Dissertationsprüfung.

Danke an alle, mit denen ich in externen Kooperationen zusammenarbeiten durfte: Dr. Dominik Cordier (Neurochirurgie, Universitätsspital Basel) und seinen KollegInnen im Rahmen des Substanz P Projektes, Prof. Dr. Matthias Wymann und Mirjam Zimmermann (Departement Biomedizin, Universität Basel) für ihre Unterstützung bei biochemischen Fragestellungen und Prof. Dr. Jörg Huwyler, Dr. Pascal Detampel und Dominik Witzigmann (Pharmazeutische Technologie, Pharmacenter, Universität Basel) im Rahmen der hier nicht beschriebenen Liposomen-Projekte.

Bei allen Mitgliedern der Forschungsgruppe Mindt, den MitarbeiterInnen der Radiopharmazeutischen Chemie und der Nuklearmedizin (Universitätsspital Basel) bedanke ich mich für die Zusammenarbeit, die Unterstützung, die schöne Zeit und die super Events, die wir miteinander erlebt haben. Besonderer Dank gebührt hier Dr. Andreas Bauman und Dr. Ibai Valverde für ihre Unterstützung beim Erlernen diverser (radio)chemischer Arbeitstechniken, für die Zusammenarbeit in unterschiedlichen Projekten und wissenschaftliche Diskussionen. Ebenfalls ein besonderes Dankeschön an Sandra Vomstein für ihre tatkräftige Unterstützung bei der Zellkultur, den Zell-, und Tierversuchen. Allen Damen des „Routine"-Teams danke ich für die Einarbeitung im „Hotlabor" und ihre Unterstützung bei den Radiomarkierungen.

Allen MitarbeiterInnen der Medizintechnik und Informatik (Radiologie), vor allem Philippe Schwald, Florian Hoffmann und Julien Albuquerque danke ich für ihre Unterstützung bei technischen Problemen, die immer schnell behoben werden konnten.

Dieter Staab, Kayhan Akyel, Dr. Christian Guenat und Dr. Ingo Muckenschnabel (Novartis Institute for BioMedical Research, Basel) danke ich für ihre Unterstützung bei der NMR und MS Analytik.